K_V7 potassium channels: A focus on human intra-pulmonary arteries

A thesis submitted to the University of Manchester for the degree of Doctor of Philosophy in the Faculty of Life Sciences

2015

Sean Brennan

List of contents

List of figures

List of tables

Abstract

Name of the University: The University of Manchester

Candidate's name: Sean Brennan

Degree Title: Pharmacology PhD

Date: 30/09/2013

Pulmonary arterial hypertension (PAH) is a disease in which pulmonary vascular resistance increases. The cell membrane of pulmonary artery smooth muscle cells (PASMC) in PAH patients is depolarised, resulting in disrupted Ca^{2+} signalling leading to smooth muscle constriction and PASMC proliferation and migration.

In rat pulmonary artery (PA) smooth muscle the K_V7 K^+ channels, encoded by the *KCNQ* genes, have been proposed to contribute to the resting K^+ current, promoting low resting tone by maintaining a negative membrane potential and low intracellular Ca^{2+}. K_V7 channel activating drugs have the potential to counteract the dysfunctional signalling during PAH by causing hyperpolarisation. This study set out to determine if the K_V7 channels are expressed in human PA and if so whether they can alter vascular tone, PASMC proliferation and/or migration due to their ability to reduce intracellular Ca^{2+} indirectly. The effects of K_V7 K^+ channel modulators on human PA tone were measured using myography, while *KCNQ* gene expression was examined with quantitative PCR. Markers of proliferation (5-bromo-2'-deoxy-uridine (BrdU) and Ki67 antigen), were used to measure PASMC proliferation, while migration was assessed using the scratch-wound assay. Human PASMCs express all *KCNQ* genes, except *KCNQ2*. The K_V7 channel blockers XE991, linopirdine and (-)chromanol 293B, constricted PAs. The K_V7 channel activators retigabine and zinc pyrithione (ZnPy) relaxed PAs pre-constricted with agonists. The retigabine response was enhanced in PAs constricted with Bay K 8644, abolished in ionomycin constricted PAs and reduced in the presence of 90 mM K^+, suggesting inhibition of voltage-gated Ca^{2+} influx. Similar experiments on rat PAs suggest that only part of the ZnPy-induced relaxation can be attributed to K_V7 channel activation. The *KCNQ5* gene remained in cultured PASMCs while no K_V7 channel modulator altered proliferation or migration. Thus $K_V7.5$ channels could possibly be a marker of differentiated PASMCs and/or be involved in the regulation of cell phenotype. The results imply that K_V7 channels play a role in regulating PA tone and Ca^{2+} signalling in PA smooth. It is concluded that although *KCNQ5* transcripts are preserved in proliferating PASMC, it is unlikely they play a role in PASMC proliferation or migration. In summary, K_V7 channel activators may be useful in the treatment of PAH since they can prevent vasoconstriction.

Declaration

No portion of the work referred to in the thesis has been submitted in support of an application for another degree or qualification of this or any other university or other institute of learning. The results chapters submitted as part of this thesis are presented as scientific papers. The contributions of each author are listed alongside the description of each paper.

Copyright statement

Acknowledgments

I would like to express my deepest gratitude to my PhD supervisor Professor Alison Gurney for the all her support and guidance over the duration of my PhD as well as providing me the opportunity to pursue a career in pharmacological research. I would also like to thank my advisor Dr Jason Bruce and Dr Paolo Tammaro for all their advice during my project. I would like to thank the postgraduate tutor, Dr Donald Ward, for his support and guidance in the latter stages of my PhD.

I would also like to express my thanks to all past and present members of the Gurney and Tammaro labs especially; Katie Smith, Roberta Oliveira Roberts, Leonie Diffly, Andrew Chadburn, Rebecca Brookfield and Hannah Garnet. The PhD would not have been as enjoyable without all of you.

I am particularly grateful to my current supervisor Dr Richard Rainbow, University of Leicester, for his guidance and generosity with his time until thesis submission. I cannot imagine many supervisors would have been as understanding and helpful. Also from the University of Leicester I would like to thank Professor John Challiss, Dr Dave Lodwick and Dr Noel Davies for their support and words of encouragement.

I would also like to thank all my house mates Nikki Paul, Christopher Logie, Nick Rooney, William Ripley and Tom Dimambro.

Finally, I would like thank my parents and brother for all their support and encouragement throughout my time in Manchester. My only regret is that my Nan was not able to see me graduate, I never envisaged it would take so long to complete the thesis.

I am also grateful to the Medical Research Council for funding my project.

Abbreviations

The following abbreviations have been used in this thesis:

$[ATP]_i$	intracelular ATP concentration
$[Ca^{2+}]_i$	intracelular Ca^{2+} concentration
$[K^+]_o$	extracellular K^+ concentration
4-AP	4-aminopyridine
5-HT	serotonin
ADP	adenosine diphosphate
ATP	adenosine triphosphate
AVD	apoptotic volume decrease
cAMP	cyclic adenosine monophosphate
cGMP	cyclic guanosine monophosphate
Ct	threshold cycle
DAG	diacylglycerol
EC_{50}	half maximal effective concentration
EDTA	ethylenediaminetetraacetic acid
ET-1	endothelin-1
GAPDH	glyceraldehyde-3-phosphate dehydrogenase
HEPES	(4-(2-hydroxyethyl)-1-piperazineethanesulfonic acid
HPV	hypoxic pulmonary vasoconstriction
IC_{50}	half maximal inhibitory concentration
I_{KM}	neuronal M-current
I_{Kr}	cardiac rapid delayed rectifier K^+ current
I_{KS}	cardiac slow delayed rectifier current
IP_3	inositol 1,4,5-trisphosphate
iPA	intra-pulmonary artery
NCX	Na^+/Ca^{2+} exchanger
NO	nitric oxide
PA	pulmonary artery
PASMC	Pulmonary artery smooth muscle cell
PCR	polymerase chain reaction
pEC_{50}	negative log of half maximal effective concentration (Molar)

PH	pulmonary hypertension
pIC_{50}	negative log of half maximal inhibitory concentration
PSS	physiological salt solution
qRT-PCR	quantitative reverse transcriptase-polymerase chain reaction
RIN	RNA integrity number
RIPA	radioimmunoprecipitation (lysis buffer)
RMP	resting membrane potential
ROC	receptor-operated channel
RT-PCR	reverse transcriptase-polymerase chain reaction
SAC	stretch-activated channel
SERCA	sarcoplasmic-endoplasmic reticulum Ca^{2+}-ATPase
SERT	serotonin transporter
siRNA	small interfering RNA
SOC	store-operated channel
SOCE	store-operated calcium entry
SR	sarcoplasmic reticulum
STIM	stromal interaction molecule
TEA	tetraethylammonium
TM	transmembrane
$V_{0.5}$	voltage of half-maximal channel activation
VGCC	voltage-gated calcium channel
ZnPy	zinc pyrithione

Chapter 1 : Introduction

1.1 Anatomy and physiology of the lungs

The lungs are responsible for gas exchange, allowing oxygen to diffuse into capillaries surrounding the alveoli with simultaneous removal of carbon dioxide. To carry out the role of gaseous exchange efficiently, the lungs must be ventilated and supplied with an adequate blood supply.

The oxygenated blood received by the lungs accounts for approximately 1% of the lung's total blood supply and is provided via the bronchial arteries. The main blood supply, which is deoxygenated, travels from the right side of the heart through the pulmonary artery (PA) towards the lungs. The PA bifurcates into the right and left branch, which bifurcate further so that each lobe has a blood supply. The lobar arteries further divide into irregular branches that closely follow the route of the bronchial tree. Branching of the intra-pulmonary arteries (iPAs) results in capillaries where the blood is oxygenated and returned to the left side of the heart, via the pulmonary vein, for systemic distribution. The importance of the relationship between ventilation and perfusion is underlined by the proximity of the PAs and airways (Charan et al. 1987).

1.2 Pulmonary artery structure

The PA wall, like systemic arteries, is comprised of three layers: an adventitia, a muscular media with internal and external elastic laminae and also an intima containing a single layer of endothelium cells. The structure of the media layer differs when travelling distally down the vessel and these changes can be correlated with the external diameter (Figure 1.1) (Hislop and Reid, 1978; Meyrick et al., 1978):

1) Elastic arteries (≥2 mm): Contain ≥4 central elastic laminae with layers of smooth muscle cells between the laminae.

2) Muscular arteries (100 μm – 2 mm): The artery has a complete layer of circularly orientated muscle.

3) Partially muscular artery (50 μm – 150 μm): The media layer thins and the complete muscular layer gives way to a spiral of muscle, which when examined under cross-section gives the appearance of a partially muscular artery.

4) Non-muscular arteries (≤120 µm): The spiral of muscle disappears completely at the distal end of the artery rendering it non muscular.

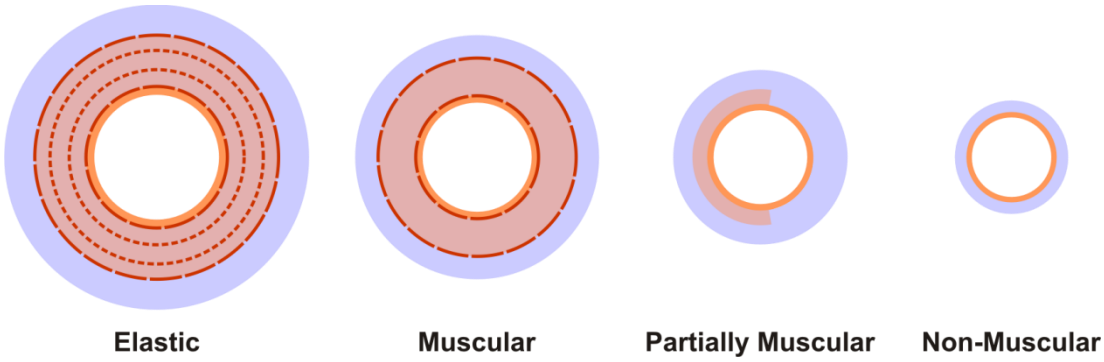

Figure 1.1: Transverse illustration of the elastic, muscular, partially muscular and non-muscular segments of the pulmonary artery tree. Proximal arteries have circularly orientated muscle (pink), bounded by an internal and external elastic lamina (broken lines). Distally, the spiralling of muscle leads to arteries appearing partially muscular. Finally, the muscle disappears rendering the arteries non-muscular. The adventitia and endothelial layers are shown in blue and orange respectively (Ellis et al., 1952; Marchand et al., 1950).

1.3 Pulmonary hypertension

1.3.1 Definition

Pulmonary hypertension (PH) is a complex and multi-faceted disorder characterised by an increase in PA pressure within the lungs. Pulmonary arterial hypertension (PAH), a specific subgroup of pulmonary hypertension (PH), is caused by pathophysiological changes of the small PAs (> 150 µm) themselves. PAH is a haemodynamic and pathophysiological condition defined as an increase in mean pulmonary arterial pressure ≥ 25 mmHg at rest. This definition is based on the following:

1) 20 mmHg is 2 standard deviations above the “normal” mean pressure of 14 mmHg, so that ≥ 25 mmHg is convincingly above the distribution of values likely to be considered “normal”.

2) The value of 25 mmHg has, by consensus, been used to identify candidates for participation in clinical drug studies.

3) A pulmonary artery occlusion pressure ≤15 mmHg and a pulmonary vascular resistance above 3 Wood units (Galiè et al., 2009a, 2009b; McLaughlin et al., 2011).

1.3.2 Characteristics

PAH has an estimated prevalence of 15-50 cases per million of the population (Humbert et al., 2006; Peacock et al., 2007) and is 2-4 times more prevalent in women (Badesch et al., 2010; Gaine and Rubin, 1998). Various histopathological features are associated with PAs from PAH patients, including: vasoconstriction, medial thickening due to smooth muscle cell hypertrophy and hyperplasia, concentric thickening of PAs resulting from intimal proliferation, plexiform and / or thrombotic lesions and muscularization of non-muscularized arteries. This results in the obliteration of the lumen in small and medium-sized arteries, followed by weakened right-heart function due to increased right ventricular afterload. Death usually occurs due to right-heart failure and without treatment the median survival time is 2.8 years in adults and 10 months in children (Bjornsson and Edwards, 1985; D'Alonzo et al., 1991; Pietra et al., 1989; Sandoval et al., 1995; Tuder et al., 2007).

1.3.3 Classification

As there are numerous underlying causes associated with PAH, the most suitable therapy can differ between patients. Therefore, accurate classification of the disease is required to aid clinicians. Improvements in PAH diagnosis, understanding of the pathophysiology and therapy has led to changes of the clinical classification system, most recently at the 5th world symposium on PH (Simonneau et al., 2013). The most recent clinical classification is shown in Table 1.1. An appreciation of the previous classification categories can, however, be useful when reading older literature on PAH. The first classification contained 2 categories, Primary or Secondary PAH. Each patient was categorised into one of these groups depending on the presence or absence of known causes and risk factors. The term "secondary pulmonary hypertension" described a range of conditions associated with pulmonary vascular disease that displayed comparable pathological features to primary PAH, but was abandoned in 1998 as it was considered confusing and did not help diagnosis or treatment. The term "primary pulmonary hypertension" has been replaced by the more descriptive terms "Idiopathic PAH" and "Familial PAH" (Simonneau et al., 2004, 2009).

Group	Clinical Classification
1	Pulmonary arterial hypertension 1.1. Idiopathic PAH 1.2.Heritable 1.2.1. Bone morphogenetic protein receptor type 2 1.2.2. Activin receptor-like kinase 1 gene, endoglin (with or without hemorrhagic telangiectasia) 1.2.3. Unknown 1.3. Drug- and toxin-induced 1.4. Associated with: 1.4.1. Connective tissue diseases 1.4.2. Human immunodeficiency virus infection 1.4.3. Portal hypertension 1.4.4. Congenital heart disease 1.4.5. Schistosomiasis 1.5. Persistent pulmonary hypertension of the newborn
1’	Pulmonary veno-occlusive disease and/or pulmonary capillary haemangiomatosis
1’ ’	Persistent pulmonary hypertension of the newborn
2	Pulmonary hypertension due to left heart disease 1.2. Systolic dysfunction 1.3. Diastolic dysfunction 2.3. Valvular disease 2.4. Congenital/acquired left heart inflow/outflow tract obstruction and congenital cardiomyopathies
3	Pulmonary hypertension due to lung diseases and/or hypoxemia 3.1. Chronic obstructive pulmonary disease 3.2. Interstitial lung disease 3.3. Other pulmonary diseases with mixed restrictive and obstructive pattern 3.4. Sleep-disordered breathing 3.5. Alveolar hypoventilation disorders 3.6. Chronic exposure to high altitude 3.7. Developmental abnormalities
4	Chronic thromboembolic pulmonary hypertension
5	PH with unclear multifactorial mechanisms 5.1. Haematological disorders: myeloproliferative disorders, splenectomy 5.2. Systemic disorders: sarcoidosis, pulmonary Langerhans cell histiocytosis, lymphangioleiomyomatosis, neurofibromatosis, vasculitis 5.3. Metabolic disorders: glycogen storage disease, Gaucher disease, thyroid disorders 5.4. Others: tumoral obstruction, fibrosing mediastinitis, chronic renal failure on

Table 1.1: The Clinical Classification of Pulmonary Hypertension. Adapted from (Simonneau et al., 2013)

1.3.4 Treatment

It is common for clinicians to measure a PAH patient's response to a short-acting vasodilator agent delivered via right heart catheterisation to determine suitability for therapeutic intervention (Palevsky et al., 1990; Rozkovec et al., 1988). Patients that respond well to this are known as "responders" and prescribed a voltage-gated calcium channel blocker such as nifedipine, diltiazem or amlodipine. Fewer than 10 % of PAH patients respond well long term to such treatment (McLaughlin et al., 2009). Currently, three major drug classes are used in the treatment of PAH for patients who do not respond well to calcium channels blockers (Palmer, 2009; Patel et al., 2012).

It is only in the last 30 years that treatments targeted more directly at the pathology of PAH have become available. Epoprostenol (prostacyclin) administered intravenously was the first treatment studied and has since been investigated in numerous clinical trials. It is the only treatment that has been shown to offer a survival advantage while also improving quality of life (Herner and Mauro, 1999; Higenbottam et al., 1984; Rhodes et al., 2009). Due to the short half-life, chemical instability and complex delivery of epoprostenol, a number of chemically stable analogues have been synthesised including: treprostinil, iloprost and beraprost. Like prostacyclin, its analogues are potent inhibitors of platelet aggregation and cause relaxation of PAs (Coleman et al., 1994; Ichida et al., 1997; Kaukinen et al., 1984; Narumiya et al., 1999; Olschewski et al., 1999; Takeo, 1992; Clapp et al., 2002).

The biological responses to prostacyclin (IP) and its analogues have mainly been associated with prostacyclin receptor activation. These receptors are known to couple to and activate adenylyl cyclase, resulting in enhanced levels of cyclic adenosine monophosphate (cAMP) (Coleman et al., 1994; Narumiya et al., 1999). This is consistent with the observations that IP receptor agonists increase cAMP in smooth muscle and IP receptors are expressed in human PAs (Falcetti et al., 2010; Holzmann et al., 1980; Turcato and Clapp, 1999). Various studies, however, have observed biological responses to prostacyclin analogues independent of raised cAMP levels. Prostacyclin analogues inhibit proliferation of pulmonary artery smooth muscle cells (PASMCs) isolated from PAH patients (Clapp et al., 2002; Falcetti et al., 2010) via a peroxisome proliferator-activated receptor-γ dependent mechanism (Falcetti et al., 2010). Furthermore, the adenylyl cyclase inhibitor SQ22536 prevents iloprost-induced elevation of cAMP but did not prevent relaxation (Turcato and Clapp, 1999). The protective role for prostacyclin against PAH has been demonstrated in

various studies. There is a decrease in prostacyclin metabolite levels, as measured by 2,3-dinor-6-keto-prostaglandin F1 alpha levels, and IP receptor protein levels in PASMCs from PAH patients (Christman et al., 1992; Falcetti et al., 2010). Additonally, mice overexpressing prostacyclin synthase are protected against hypoxia-induced PAH (Christman et al., 1992; Geraci et al., 1999)

Endothelin-1 (ET-1), a 21-amino acid polypeptide, exhibits potent vasoconstrictor and pro-proliferative properties in systemic and pulmonary arteries (Davie et al., 2002; McCulloch et al., 1996; Yanagisawa et al., 1988; Zamora et al., 1993). Raised levels of ET-1 and enhanced receptor density have been associated with PAH (Cernacek and Stewart, 1989; Davie et al., 2002; Eddahibi et al., 1991; Stewart et al., 1991). Two distinct G-protein–coupled receptors, ET_A and ET_B, mediate the effects of ET-1 in the pulmonary vasculature (Davie et al., 2002). Both receptor types are present in the medial layer and cause constriction. Only ET_B receptors were considered to be expressed in the endothelium until Hall et al., (2011) demonstrated that ET_A receptors are also expressed (LaDouceur et al., 1993; Migneault et al., 2005; Milara et al., 2010; Yu et al., 2013), and can stimulate the release of vasodilators such as nitric oxide and prostacyclin (Hirata et al., 1993; Lal et al., 1996). ET_A receptors mediate the response in proximal arteries, whereas both receptors are implicated in ET-1-induced contraction of distal human pulmonary resistance arteries (Fukuroda et al., 1994; McCulloch et al., 1996). Treatment with ET-1 receptor antagonists has been shown to be beneficial in animal models of PAH by attenuating or reversing the vascular remodelling and right ventricular hypertrophy (Chen et al., 1995; Jasmin et al., 2001). Currently, the ET-1 receptor antagonists, bosentan and ambrisentan, are used in the treatment of PAH (Palmer, 2009). The presence and function of ET_B receptors has caused debate as to whether selective ET_A antagonists offer advantages in efficacy over dual ET_A and ET_B receptor antagonists.

Phosphodiesterase 5 inhibitors, such as sildenafil, prevent the metabolism of cyclic guanosine monophosphate (cGMP) in smooth muscle cells, resulting in raised cGMP levels and enhanced nitric oxide (NO) synthesis. This leads to PA relaxation and inhibition of PASMC proliferation (Pauvert et al., 2003; Rabe et al., 1994; Wharton et al., 2005). Phosphodiesterase 5 levels are naturally high in PAs and are raised in the lung of PAH patients (Corbin et al., 2005; Pauvert et al., 2002; Rabe et al., 1994; Wharton et al., 2005). Decreased NO bioavailability has also been associated with PAH, and this may contribute to PA constriction in PAH (Klinger et al., 2013). Although phosphodiesterase 5 is known to be

expressed in various cell types including non-vascular and vascular smooth muscle cells (Lin, 2004), sildenafil has been reported to cause only a small drop in systemic blood pressure that caused no adverse effects (Ghofrani et al., 2002; Kloner, 2004). Orally administered sildenafil taken by PAH patients improved the 6 minute walking distance and also decreased mean PA pressure (Galiè et al., 2005).

These treatments offer hope to PAH patients by slowing time to clinical worsening of symptoms, due to their anti-proliferative and dilation of PAs. However, none of the treatments available cures PAH and progression of the disease is currently unavoidable (Rhodes et al., 2009). This underlines the need to discover novel targets and treatments for PAH.

1.4 Regulation of the pulmonary vasculature

PAs have low resting tone that is regulated by both active and passive factors. Active factors include autonomic nerves, humoral substances (as listed in Table 1.2) and respiratory gases, all of which can modify vascular tone and resistance via contraction or relaxation of pulmonary vascular smooth muscle. Passive factors alter pulmonary vascular resistance and/or blood flow independently of alterations in vascular tone and include cardiac output, left atrial pressure, airway and interstitial pressure, gravitational force and vascular obstruction (Barnes and Liu, 1995).

1.4.1 Neuronal regulation

Parasympathetic innervation is generally considered not present in human, mouse or rat intra-pulmonary arteries (iPAs) as they do not contain acetylcholinesterase-positively stained nerve fibres (Barnes and Liu, 1995; Partanen et al., 1982). PAs are, however, innervated by sympathetic nerves although there are substantial differences between species (Barnes and Liu, 1995).

Catecholamines exert their effects on the pulmonary circulation by acting on α- and β-adrenoreceptors. Human iPAs are heavily innervated with adrenergic nerve fibres extending to arterioles of < 60 μm outer diameter. Stimulation of α_1-adrenoceptors on PA muscle by neuronally released noradrenaline results in vasoconstriction (Barnes and Liu, 1995). In contrast, activation of endothelial α_2-adrenoceptors evokes vasodilatation (Pepke-Zaba et al., 1993). Also, α_2-adrenoceptors expressed on pre-synaptic nerve terminals

provide a negative feedback loop towards the release of noradrenaline (Langer, 1980; Langer and Hicks, 1984). Activation of β1 or β2-adrenoceptors by circulating catecholamines or neutrally released noradrenaline results in dilation (Boe and Simonsson, 1980; Carstairs et al., 1985).

Non-adrenergic, non-cholinergic responses have been observed in rat (Gümüşel et al., 2001) and human (Scott et al., 1996) PAs. These are defined as neuronal pathways present after the inhibition of adrenergic and cholinergic pathways (Barnes and Liu, 1995). In the presence of guanethidine and atropine, to block adrenergic and cholinergic neurotransmitter pathways, respectively, electrical field stimulation of human PA rings caused relaxation (Scott et al., 1996). Furthermore, half of the relaxation induced by electrical field stimulation occurred in the presence of L-nitro-arginine methyl ester (L-NAME), indicating that NO was only partly responsible for the relaxation observed (Scott et al., 1996).

1.4.2 Humoral regulation

Humoral agents, such as ET-1 and prostacyclin, released either locally or systemically, are known to regulate pulmonary vascular tone by interaction with receptors on the smooth muscle and endothelial layers. The regulation of PA tone by humoral agents is complex and can vary according to species, age, and pre-existing tone. Barnes & Lu (1995) provided an extensive review on the regulation of PA tone. Table 1.2 displays the established humoral responses in PAs.

Humoral agent	Effect	Receptor
Angiotensin II	Contraction	AT_1
Bradykinin	Dependent on species and pre-existing vascular tone	B_2/B_1 (Species dependent)
Vasopressin	Dependent on pre-existing tone	V_1 mediates relaxation
Endothelins	Dependent on pre-existing tone. Baseline tone= contraction, elevated tone= relaxation	ET_A on smooth muscle= relaxation ET_B on endothelium= contraction
Substance P	Dependent on pre-existing tone. Baseline tone= contraction, elevated tone= relaxation	NK_2 on Smooth Muscle NK_1 on Vascular Endothelial
Histamine (released by mast cells)	Dependent on pre-existing tone. Baseline tone= contraction, elevated tone= relaxation[1,2]	H_1 on Smooth muscle= contraction H_2 on smooth muscle and H_1 on endothelial cells
Serotonin (produced by platelets)	Both (Species dependent) Potent contraction in human PA. [3,4,5]	5-HT_1 and 5-HT_2 involved in contraction 5-HT_{1C} receptors in the endothelium
Prostaglandins PGD_2, PGE_2 $PGF_{2\alpha}$	Contraction by $PGF_{2\alpha}$, PGD_2 and PGE_2 Relaxation by PGI_2, PGE_2	prostanoid receptors
Lipoxygenase metabolites of arachidonic acid	Contraction by Leukotriene B4, Leukotriene C4 and Leukotriene D4	Specific Leukotriene receptors
Purines	Both. Adenosine and ATP Baseline tone= contraction, elevated tone= relaxation	A_1 and/or P_{2x} on smooth muscle= contraction A_2 and/or P_{2y}= relaxation

Table 1.2: The humoral mechanisms involved in the regulation of pulmonary artery tone. Pre-existing tone can occur either naturally (as in the foetus) or artificially (by adding a vasoconstrictor agent). Information taken from Barnes and Liu, 1995; [(1)] Ortiz et al., 1992; [(2)] Mikkelsen et al. 1983; [(3)] Houghton and Phillips, 1973; [(4)] Gruetter et al., 1981; [(5)] Freeman et al., 1981.

1.4.3 Respiratory gases and the pulmonary artery

PAs respond to hypoxia by constricting. This pulmonary hypoxic vasoconstriction (HPV) response has been demonstrated in multiple species (Dumas et al., 1999). HPV is the physiological mechanism that maintains the optimal balance between ventilation and perfusion and reduces the perfusion of blood to under-ventilated parts of the lung, thus directing blood to well-ventilated regions. Prolonged hypoxia also causes significant structural remodelling of the PAs: people living at high altitude display a chronic elevation in PA pressure and a greater increase during exercise compared to sea-level subjects (Stenmark et al., 2006). The main site for HPV is considered to be the small PAs and arterioles (internal diameter 100-500 μm) (Staub, 1985, Shirai et al., 1986; Hillier et al., 1997). Although larger PAs have been shown to constrict in response to hypoxia (Demiryurek et al., 1991; Leach et al., 1994; Yuan et al., 1990) others have observed relaxation (Kovitz et al., 1993; Madden et al., 1985). The underlying mechanisms are likely to reside within the medial layer of the arteries themselves, since the response to hypoxia occurs in isolated PASMCs (Madden et al., 1985), however, the precise signalling pathway remains unclear (Evans and Ward, 2009). A number of reports concluded that the endothelium is responsible (Demiryurek et al., 1991; Holden and McCall, 1984; Jin et al., 1992; Kovitz et al., 1993; Leach et al., 1994; Wadsworth, 1994) while other reports suggest the smooth muscle is responsible (Murray et al., 1990; Madden et al., 1992; Marshall and Marshall, 1992; Wang et al., 1995). There is little evidence to support a role for the endothelium in initiating the hypoxia-induced rise in intracellular Ca^{2+} concentration ($[Ca^{2+}]_i$) in PASMCs, as endothelium denuded iPAs constrict in response to hypoxia (Yuan et al., 1990) as do isolated PASMCs (Madden et al., 1992; Cornfield et al., 1993;Aaronson et al., 2002; Evans and Ward, 2009). There is wide, but not universal, acceptance that the oxygen sensor responsible for the initiation of HPV resides in the mitochondria of PASMCs, while the downstream signalling pathways remain elusive (Evans and Ward, 2009; Ward, 2007). Evidence supporting the mitochondria as the O_2 sensor in PASMCs has been supported by studies demonstrating that inhibitors of the mitochondrial electron transport chain specifically block HPV (Evans and Ward, 2009).

1.5 Calcium and contraction

A rise in $[Ca^{2+}]_i$ within a PASMC is the major trigger for contraction in PA (Casteels et al., 1977a). At rest, $[Ca^{2+}]_i$ is maintained at approximately 100 nM, creating a large chemical gradient with the extracellular environment, which contains around 1.8 mM Ca^{2+} (Yuan, 1995). When $[Ca^{2+}]_i$ increases, a Ca^{2+}/calmodulin complex is formed which then activates myosin light chain kinase to phosphorylate the myosin light chain (MLC). MLC phosphorylation leads to cross-bridge formation between the myosin heads and the actin filaments, resulting in muscle contraction. There are several pathways that coordinate the control of $[Ca^{2+}]_i$ in PASMCs, as illustrated in Figure 1.2.

Membrane depolarisation can cause Ca^{2+} influx via the opening of voltage-gated calcium channels (VGCCs). Both L-type and T-type VGCC currents have been recorded in human PASMCs, however, Ca^{2+} influx is mainly driven through L-type VGCCs (Firth et al., 2011; Shimoda et al., 2000). Ca^{2+} influx can also occur by voltage-independent mechanisms, via receptor-operated (ROCs), store-operated (SOCs) and stretch activated channels (SACs), which are thought to be encoded by the transient receptor potential channel genes (TRP). These channels are non-selective cation channels that produce a depolarising current when activated and can therefore contribute to the contraction through the opening of VGCCs. ROCs are defined as channels residing in the plasma membrane that open when an agonist binds to a receptor. The receptor and channel may be the same protein, as is the case for P2X receptors. However, the majority of ROCs are activated via G-protein coupled receptors and downstream signalling proteins, such as diacylglycerol (DAG) and inositol 1,4,5-trisphosphate (IP_3) (Guibert et al., 1996; Hamada et al., 1997; Ko et al., 2005; McDaniel et al., 2001; Tang et al., 2009). As well as the IP_3 sensitive channels, the sarcoplasmic reticulum (SR) also contains ryanodine receptors, which are activated by increased $[Ca^{2+}]_i$ (Jabr et al., 1997; Janiak et al., 2001).

SOCs are activated by depletion of the SR Ca^{2+} store, but are not Ca^{2+}-gated (Guibert et al., 2008). Studies on PASMCs show that sufficient Ca^{2+} influx to cause contraction can occur by depletion of the SR Ca^{2+} store (Ng and Gurney, 2001). It is generally accepted that this form of Ca^{2+} influx allows refilling of the SR. The molecular components of store-operated calcium entry (SOCE) are still disputed (Ng et al., 2009, 2010; Ogawa et al., 2012; Song et al., 2011). Coupling of stromal interacting molecule (STIM-1), a Ca^{2+} sensor residing in the SR membrane, with a pore-forming protein (Orai) in the plasma membrane or TRPC1 channels,

have been shown to contribute to SOCE in PASMCs. STIM-1 senses a decrease in $[Ca^{2+}]_i$ in the SR when IP_3 -mediated activation of IP_3 receptors results in Ca^{2+} release from the SR to the cytosol. STIM1 then clusters in the SR membrane and translocates to the plasma membrane. There STIM-1 stimulates Orai1 (Ng et al., 2010; Ogawa et al., 2012; Song et al., 2011) or TRPC1 (Ng et al., 2009) channels, allowing Ca^{2+} influx through tetrameric Orai1 or TRPC1 channels in the cell membrane (Ng et al., 2009, 2010; Ogawa et al., 2012; Song et al., 2011).

SACs are defined as mechanotransducers due to their ability to convert physical force into a biological response. The major characteristic of SACs is that their open probability increases, leading to Ca^{2+} influx, when pressure is applied to the tissue (Guibert et al., 2008). Stretch-activated currents have been recorded in PASMC (Bialecki et al., 1992; Ducret et al., 2010; Park et al., 2006), with TRPC channels the likely molecular component responsible. This is because the current is inhibited (a) in the absence of external Ca^{2+}, (b) in the presence of the TRP channel blocker, gadolinium (Alexander et al., 2011) or (c) by the selective SAC blocker GsMTx-4, a peptide toxin isolated from spider venom (Suchyna et al., 2000). In a separate study, GsMTx-4 was shown to inhibit currents generated in cells heterologously expressing TRPC1 or TRPC6 (Bowman et al., 2007).

There is evidence that the large-conductance Ca^{2+}-activated K^+ (BK_{Ca}) channels (described on page 37) can also respond to stretch in PASMCs (Kirber et al., 1992). The effect of stretch activation would be to pass a hyperpolarising K^+ current, which would act to limit PASMC contraction.

Human PASMCs express a variety of Ca^{2+} transporters that allow the movement of Ca^{2+} with or against its electrochemical gradient. The Na^+/Ca^{2+} exchanger (NCX) transports Ca^{2+} across the membrane with the direction of movement dependent on the electrochemical gradients for Na^+ and Ca^{2+} (Zhang et al., 2005). When the $[Na^+]_i$ increases or the membrane depolarises, the exchanger can operate in reverse mode, thus increasing $[Ca^{2+}]_i$. Studies have proposed that the NCX transporter is localised in close proximity to the sarco/endoplasmic reticulum $Ca2^+$-ATPase (SERCA). The NCX transporter could therefore cause a higher concentration of Ca^{2+} to be present in the SR (Zhang et al., 2007).

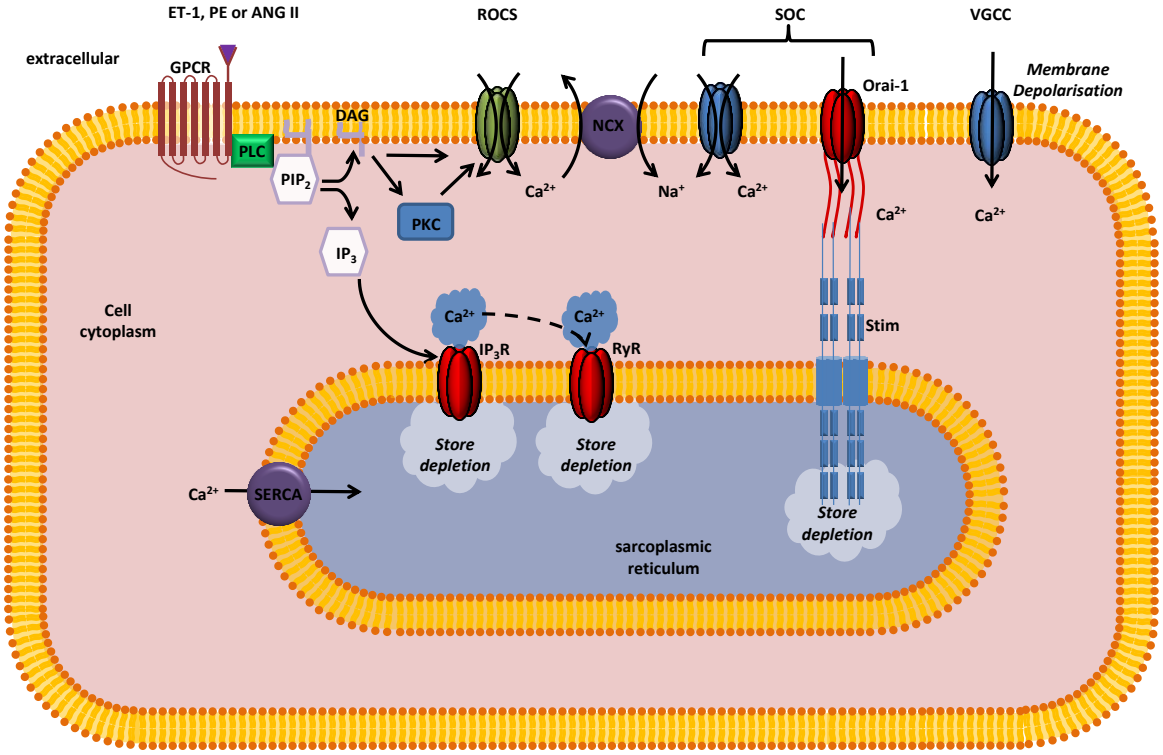

Figure 1.2: Ion channels and transporters involved in regulating PASMC $[Ca^{2+}]_i$. A number of mechanisms lead to an increase in PASMC $[Ca^{2+}]_i$. G-protein-coupled receptor (GPCR) activation leads to receptor-operated channel (ROC) opening. Store depletion leads to calcium entry via store-operated channel (SOC) activation in order to refill the stores. VGCC opening occurs in response to membrane depolarisation. Transporters such as the Na^+/Ca^{2+} exchanger (NCX) remove Ca^{+2} from the cytosol (Zhang et al., 2005). The sarcoplasmic endoplasmic reticulum Ca^{2+}-Mg^{2+} ATPase (SERCA) removes Ca^{+2} from the cytoplasm into the SR against the electrochemical gradient. The molecular structure of SOC and ROC are thought to involve members of the transient receptor potential (TRP) family of proteins, although activation of SOC is also thought to result from Orai-1 channels. Phospholipase C, PLC; phosphatidylinositol 4,5-biphosphate, PIP_2; inositol 1,4,5-triphosphate, IP_3; diacylglycerol, DG; protein kinase C, PKC. endothelin-1, ET-1; phenylephrine, PE; angiotensin II; ANG II; inositol 1,4,5-triphosphate receptor, IP_3R; ryanodine receptor, RyR .

1.6 Pulmonary artery smooth muscle cells and membrane potential

The low basal tone of the PA is due, in part, to the electrical quiescence of PASMCs at rest (Su et al., 1964; Suzuki and Twarog, 1982). PAs can, however, respond to various pharmacological and electrical stimuli. There are 2 types of excitation-contraction coupling mechanisms that have been described in PAs.

Su et al. (1964) described noradrenaline-induced contraction of SMCs from the main rabbit PA without causing depolarisation or eliciting action potentials in these cells. In a subsequent study, Somlyo & Somlyo (1968) reported that noradrenaline depolarised and provoked oscillations of the membrane potential. Due to the limited correlation between the tension and depolarisation, and because drug-induced contractions also occurred in depolarized tissues, this type of excitation-contraction coupling was termed pharmacomechanical coupling.

In 1977, two papers demonstrated that membrane potential was an important regulator of PA tone, occurring via a process termed electromechanical coupling (Casteels et al., 1977a; 1977b). These two studies demonstrated that increasing the extracellular K^+ concentration ($[K^+]_o$) depolarised the PASMCs and caused Ca^{2+} influx. Altering $[K^+]_o$ can alter the membrane potential and mechanical response. The minimal depolarisation of 4 mV required to cause contraction of PASMC occurred at 9 mM KCl, with maximum contraction achieved by 58 mM KCl. Furthermore, noradrenaline-induced contraction was decreased when the membrane was hyperpolarised, caused by decreasing $[K^+]_o$. These results show that electromechanical coupling is also of importance in the excitation-contraction coupling in PA (Casteels et al., 1977a). This is also consistent with there being a very steep relationship between membrane potential and Ca^{2+} influx around the resting membrane potential (RMP) of smooth muscle cells, with a 3-4 mV change being enough to double Ca^{2+} entry (Nelson et al, 1990).

Electromechanical coupling requires a change in membrane potential to alter vascular tone. The RMP of PASMCs lies between -45 mV and -60 mV (Casteels et al., 1977b; Clapp and Gurney, 1992; Osipenko et al., 1997; Platoshyn et al., 2004; Smirnov et al., 1994). In healthy PASMCs, the RMP is predominantly determined by a basal level of transmembrane K^+ current, which is driven by K^+ efflux through K^+ channels (Mandegar and Yuan, 2002; Moudgil et al., 2006; Yuan et al., 1998b). Since the RMP is not equal to the K^+ equilibrium potential (-80 mV) other cation (e.g., Na^+ and Ca^{2+}) and anion (e.g. Cl^-) channels must also

contribute to regulating the RMP of PASMCs (Mandegar and Yuan, 2002; Moudgil et al., 2006).

1.7 Pulmonary artery smooth muscle cell proliferation.

The arterial media is often wrongly depicted as a phenotypically homogeneous population of differentiated, quiescent, contractile SMCs. Vascular smooth muscle performs functions other than contraction, especially in physiological and pathophysiological conditions where vascular remodelling occurs, for example pregnancy, vasculogenesis, atherosclerosis, hypertension and PAH (Frid et al., 1997; Owens, 1995; Schwartz et al., 1986). In such conditions, SMCs produce increased amounts of extracellular matrix components and display higher rates of proliferation and migration. SMCs can provide a diverse range of functions due to their plasticity, and various phenotypes, ranging from quiescent contractile SMCs to proliferative synthetic SMCs, representing the two ends of a spectrum with intermediate phenotypes (Rensen et al., 2007). Phenotype diversity has been shown in various systemic arteries by investigating cell morphology, expression of SMC marker proteins and the proliferation rate (Frid et al., 1993; Giuriato et al., 1992; Mironov et al., 1995; Osborn et al., 1981; Skalli et al., 1986; Zanellato et al., 1990). Four distinct SMC phenotypes within the bovine PA have also been described (Durmowicz et al., 1996; Frid et al., 1994, 1997).

Under normal physiological conditions, mature PASMCs have the ability to control contraction and exhibit a low proliferation rate. During PAH, the PASMC phenotype appears to change and loses the ability to control contraction, while the rate of proliferation is increased. PASMCs taken from patients diagnosed with PAH have a significantly higher proliferation rate in culture compared to PASMCs from control subjects (Limsuwan et al., 2001; Marcos et al., 2004; Falcetti et al., 2010; Ikeda et al., 2010).

A rise in $[Ca^{2+}]_i$ is a key event for PASMC proliferation, with a higher resting $[Ca^{2+}]_i$ found in proliferating cells compared with quiescent cells (Golovina, 1999; Platoshyn et al., 2000). $[Ca^{2+}]_i$ can induce cell proliferation by activating proliferation-related signal transduction proteins, such as MAP kinases, due to phosphorylation (Berridge, 1993; Chao et al., 1992). A rise in $[Ca^{2+}]_i$ is also associated with an increase in $[Ca^{2+}]$ within the nucleus, which can lead to proliferation via modulation of the cell cycle, presumably by activation of calcium-dependent transcription factors, such as Nuclear factor of activated T-cells (NFAT) (Bading

et al., 1997; Rodrigues et al., 2007). Hypoxia and PAH are also associated with a decrease in the Ca^{2+} buffering capacity of mitochondria in PASMCs, which results in raised $[Ca^{2+}]i$ (Kang et al., 2003; Toth et al., 2011).

Membrane depolarisation has been implicated in the proliferation of various cell types (Dalle Lucca et al., 2000; Platoshyn et al., 2000; Seo et al., 2006; Starikova et al., 2000). In animal models and humans, PASMCs are depolarised in PAH compared with controls (Evans et al., 1998; Hong et al., 2004; Smirnov et al., 1994; Suzuki and Twarog, 1982; Yuan et al., 1998a). Furthermore, proliferating cells are more depolarised, display reduced K^+ current and have raised $[Ca^{2+}]_i$ compared to growth arrested cells (Cui et al., 2002). Growth of the proliferating cells is abolished in the presence of 2 mM EGTA in media containing approximately 525 nM free Ca^{2+}, underlining the importance of membrane depolarisation and Ca^{2+} influx for PASMC proliferation (Platoshyn et al., 2000).

1.8 Pulmonary artery smooth muscle cell migration.

Migration of PASMCs also contributes to the pathophysiological changes that occur to the architecture of the walls of iPAs during PAH. PASMCs migrate from the media to the intima in PAH patients (Aiello et al., 2003; Jones et al., 1997) while migration of PASMCs has also been attributed to disease progression in experimental models of PAH (Sarkar et al., 2010; Ye and Rabinovitch, 1991). Furthermore, elevated levels of chemical mediators such as ET-1 and serotonin, which are associated with disease progression in PAH (Cernacek and Stewart, 1989; Davie et al., 2002; Eddahibi et al., 1991; Stewart et al., 1991), can induce PASMC migration (Day et al., 2006; Feng et al., 1996). Raised $[Ca^{2+}]_i$ is required for PASMC migration to occur (Kuhr et al., 2012), because many Ca^{2+}-dependent protein kinases that phosphorylate effector proteins involved in regulating actin, microtubule or intermediate filament function are involved in mediating the response (Gerthoffer, 2007). Moreover, Ca^{2+} enhances the expression of proteins (e.g. aquaporin) and activity of pathways (e.g. ERK1/2 MAP kinase) necessary for migration to occur (Leggett et al., 2012; Meoli and White, 2010). In addition, TRPV1 and TRPV4 channels have been implicated in causing rat PASMC migration, due to increasing $[Ca^{2+}]_i$ (Martin et al., 2012).

1.9 Potassium ion channels in pulmonary artery smooth muscle

Mammals have more than 75 genes coding for K^+ channel subunits, making it the most diverse of all the ion channel families. Further diversity is added by different members of the same α-subunit sub-family co-assembling to form functional channels, in association with auxiliary subunits and alternative splicing (Jenkinson, 2006). This diversity makes K^+ channels perfect to fine tune the membrane potential in numerous different cells types.

Grouping the K^+ channel α-subunits by the number of trans-membrane (TM) regions each possesses, divides the channels into three sub-families (Figure 1.3), which can be further sub-divided. The 2TM family (inward-rectifier) α-subunits contain a single pore domain between the two TM regions (Figure 1.3A) with four of these α-subunits required to form a functional channel (Alexander et al., 2011; Jenkinson, 2006). Inward rectifiers conduct K^+ and can carry large inward currents at membrane potentials negative to E_K and outward currents at potentials positive to E_K (Figure 1.3B), even with equal K^+ concentrations on both sides of the cell membrane (Nichols and Lopatin, 1997). The physiological role of K^+ inward rectifier channels depends critically on their degree of rectification. A strong inward rectifier current, I_{K1}, is required for the stable resting potential and long plateau phase in cardiac myocytes (Lopatin and Nichols, 2001). The molecular basis for this current has now been attributed to members of the $K_{ir}2$ sub-family (Lopatin and Nichols, 2001). The inward rectification of these channels ensures little current flows through them at voltages positive to approximately −40 mV. A large current at negative voltages maintains a stable resting potential with the small conductance at positive voltages preventing short-circuiting of the action potential (Nichols and Lopatin, 1997). PASMC, which do not require this control for AP firing, lack this channel.They do, however, express $K_{ir}6.1$ (K_{ATP} channel), which differs from other K_{ir} channels in that it is sensitive to the intracellular ATP concentration (Cui et al, 2002). K_{ATP} channels form protein complexes containing 4 pore-forming Kir6 α-subunits and 4 accessory sulfonylurea receptor (SUR) subunits. Functional expression of the K_{ATP} channel requires co-expression with the SUR subunit (Ammälä et al., 1996). There are 2 main SUR genes, SUR1 and 2, with SUR2A and B subtypes. SUR2B is the main one distributed in smooth muscle tissues (Shi et al., 2012).

The name of the 4TM sub-family of K^+ channels, “two-pore domain” (K_{2P}) channels, was given on the basis of the distinctive topology of the α-subunits. Each α-subunit contains two K^+ channel pore loop forming (P) domains (Figure 1.3B). K_{2P} α-subunits dimerize to

form one functional K^+ channel containing four pore loop domains, a structure characteristic for all other K^+ channels (Enyedi and Czirják, 2010). The K_{2P} channel family can be divided into six distinct sub-families on the basis of both their structural and their functional properties, as shown in Figure 1.4. The K_{2P} channels are open across the physiological voltage range (Figure 1.3B) and have been implicated in the 'background' or leak conductance, which regulates the resting membrane potential and excitability of many mammalian cells. K_{2P} channels are regulated by a number of neurotransmitters and biochemical mediators which alter channel open probability and underpin the role of K_{2P} channels in numerous physiological systems and also their role in several diseases, including pulmonary vasoconstriction (Enyedi and Czirják, 2010). Knockdown of TASK-1 using siRNA in human PASMCs resulted in membrane depolarisation and a loss of responsiveness to hypoxia (Olschewski et al., 2006) while knockdown of TASK-2 in rat PASMCs has been shown to cause membrane depolarisation (Gönczi et al., 2006).

The vertebrate α-subunit of the voltage-gated K_V channels is by far the largest family, the earliest discovered and the best characterised. Each K_V α-subunit contains 6TM domains and 1 pore forming domain (Figure 1.3C); thus functional K_V channels require a minimal tetrameric structure (González et al., 2012; Robbins, 2001). Typically, the fourth TM region of each K_V α-subunit contains positively charged amino acids which play an essential role in the K_V channels ability to detect changes in membrane potential (Figure 1.3C).

In basic terms, K_V currents can be classified into showing either inactivating (A-type) or non-inactivating (delayed rectifier) behaviour (González et al., 2012). The biophysical properties of the channel current determine the physiological role of the channel. Inactivating K_V channels activate after a positive voltage pulse and then inactivate (10s of ms), producing a transient response. K_V channels that display fast inactivation could determine action potential frequency in excitable cells. K_V channels that are non-inactivating can not only terminate the action potential, they can also set the resting membrane potential by maintaining a K^+ efflux if they can activate at the RMP (González et al., 2012).

The properties of the currents produced by K_V channels display huge diversity due to three main reasons (González et al., 2012):

1) Heterotetramers in which different gene products belonging to the same family form channels that have different biophysical properties compared to homotetramers. This can be seen with members of the K_V1, K_V7, and K_V10 families.

(2) Heterotetramers with silent subunit families. For example, the K_V5, K_V6, and K_V8 α-subunits do not form functional channels as homotetramers but can alter the biophysical properties of the K_V2 family (Patel et al., 1997).

(3) Association of auxiliary subunits (β-subunits) with K_V α-tetramers. For example, the MinK-related peptides, encoded by the *KCNE* (*1-5*) genes (McCrossan and Abbott, 2004) , interact with K_V7 family α-subunits and modulate channel pharmacology and biophysical properties as discussed in section 1.14.2.

As illustrated in Figure 1.4, many K^+ channel α-subunits, have been reported to be expressed in PASMCs. The majority of the 6TM K_v channels have been shown to be expressed (Davies and Kozlowski, 2001; Moudgil et al., 2006), including the K_V7 family members (Joshi et al., 2009). Members of the 4TM family are also expressed in the PA, including the TASK-1 channel (Gardener et al., 2004; Gurney, 2002). The K_{ATP} channel (Clapp and Gurney, 1992; Clapp et al., 1993) and the 7TM spanning BK_{Ca} channel (Peinado et al., 2008) are also expressed. As illustrated in Figure 1.4, the presence of membrane protein has yet to be confirmed for a number of the K channel α-subunits identified at the mRNA level. Since K^+ channel expression in PASMCs can alter during tissue culture, data included in Figure 1.4 were from expression studies on freshly isolated PAs or PASMCs only. Less is known about the β-subunits present in PASMCs, but they include the KCNB1, KCNB2 and KCNB3 genes encoding $K_V\beta1$-3 (Yuan et al, 1998b), which interact with K_V1 and K_V2 α-subunits to influence channel expression and function.

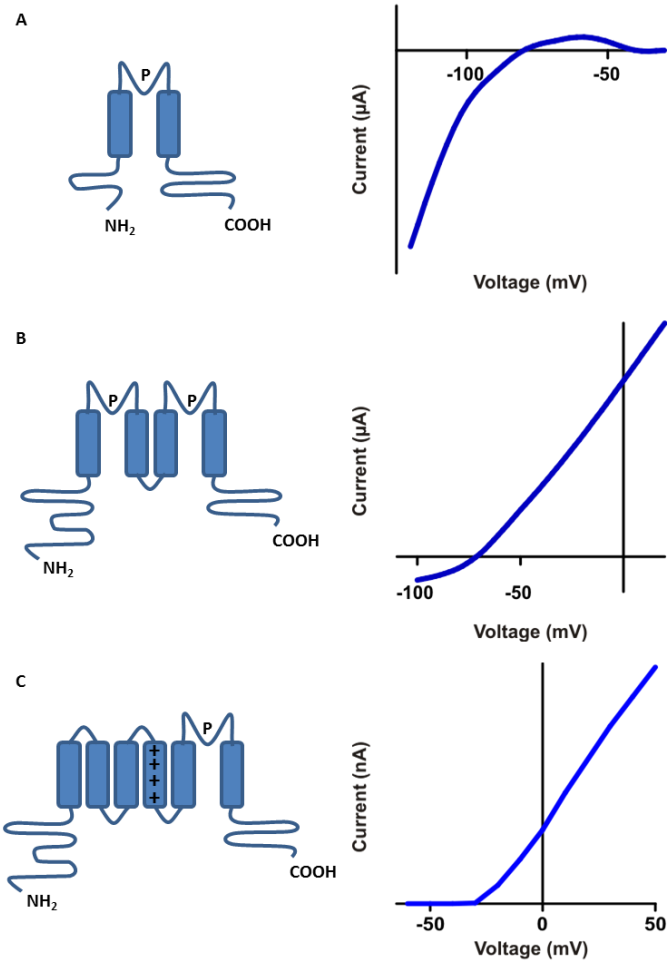

Figure 1.3: Potassium channels: structure and current-voltage relationships of the 3 main sub-families. A) Inwardly- rectifying K^+ channel α-subunits have one pore (P) domain and two transmembrane segments. K_{ir} channels pass small outward currents due to blockade by intracellular cations; large inward currents pass when voltage is negative to E_K and the pore is unblocked. B) The α-subunit of the four transmembrane channel family contains 2 pore loops, thus dimerisation of 2 α-subunits forms one functional channel. These channels are considered open rectifiers as they allow the passage of large outward currents under physiological conditions. C) Voltage-gated K^+ channel (K_V) α-subunits have one pore loop each and six transmembrane domains, with 4 α-subunits forming one functional pore. The fourth transmembrane segment, which contains positively charged (+) amino acids, acts as a sensor to changes in membrane potential. Therefore, they are closed at negative potentials and open to conduct current as the membrane depolarises beyond a certain threshold, which varies among different members of the Kv superfamily. Current-voltage relationship examples reproduced from McKay & Worley, 2001; and Plaster et al., 2001; Enyedi and Czirják, 2010.

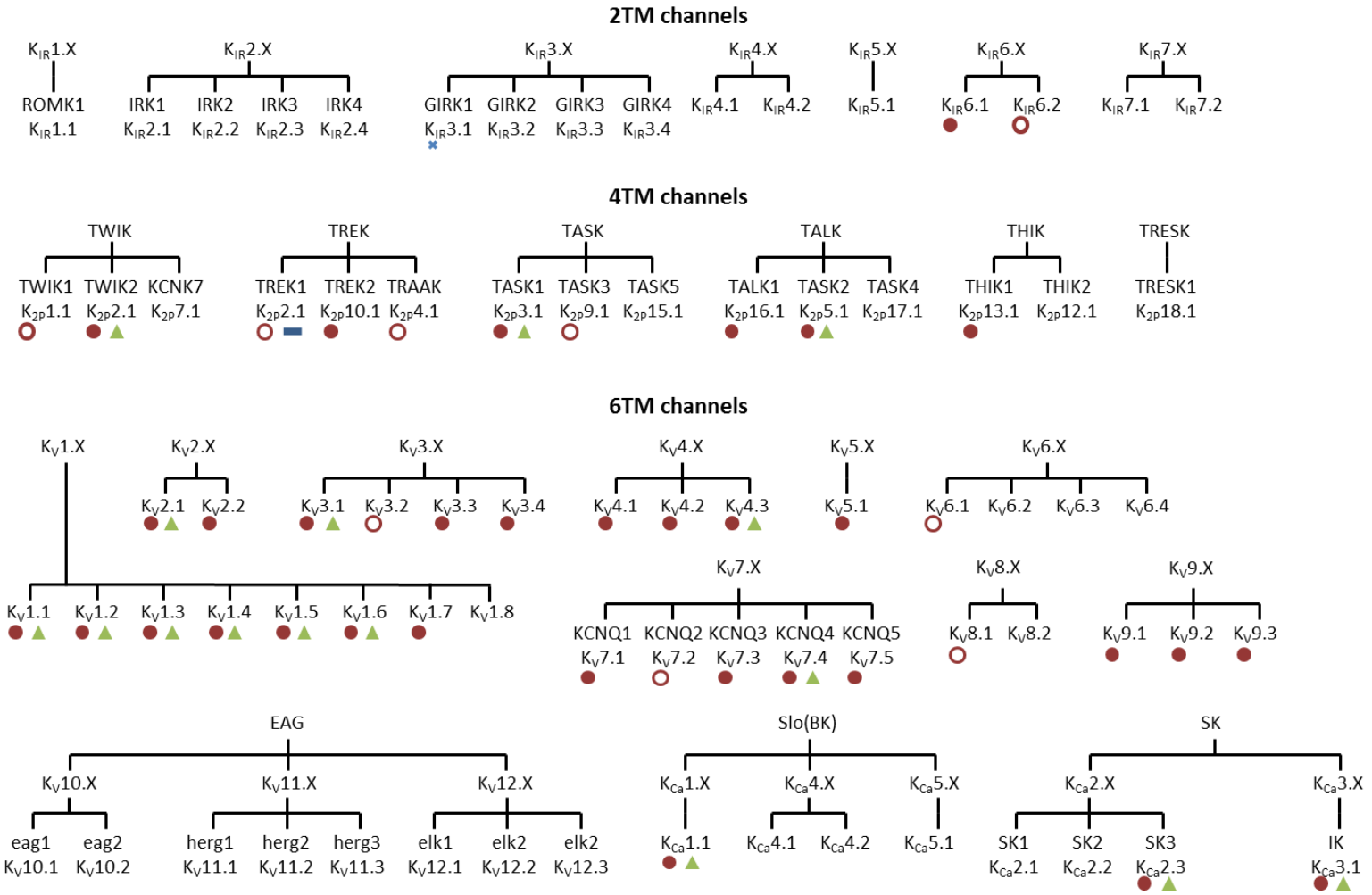
2TM channels
$K_{IR}1.X$
ROMK1
$K_{IR}1.1$
$K_{IR}2.X$
IRK1 IRK2 IRK3 IRK4
$K_{IR}2.1$ $K_{IR}2.2$ $K_{IR}2.3$ $K_{IR}2.4$
$K_{IR}3.X$
GIRK1 GIRK2 GIRK3 GIRK4
$K_{IR}3.1$ $K_{IR}3.2$ $K_{IR}3.3$ $K_{IR}3.4$
$K_{IR}4.X$
$K_{IR}4.1$ $K_{IR}4.2$
$K_{IR}5.X$
$K_{IR}5.1$
$K_{IR}6.X$
$K_{IR}6.1$ $K_{IR}6.2$
$K_{IR}7.X$
$K_{IR}7.1$ $K_{IR}7.2$
4TM channels
TWIK
TWIK1 TWIK2 KCNK7
$K_{2P}1.1$ $K_{2P}2.1$ $K_{2P}7.1$
TREK
TREK1 TREK2 TRAAK
$K_{2P}2.1$ $K_{2P}10.1$ $K_{2P}4.1$
TASK
TASK1 TASK3 TASK5
$K_{2P}3.1$ $K_{2P}9.1$ $K_{2P}15.1$
TALK
TALK1 TASK2 TASK4
$K_{2P}16.1$ $K_{2P}5.1$ $K_{2P}17.1$
THIK
THIK1 THIK2
$K_{2P}13.1$ $K_{2P}12.1$
TRESK
TRESK1
$K_{2P}18.1$
6TM channels
$K_V1.X$
$K_V1.1$ $K_V1.2$ $K_V1.3$ $K_V1.4$ $K_V1.5$ $K_V1.6$ $K_V1.7$ $K_V1.8$
$K_V2.X$
$K_V2.1$ $K_V2.2$
$K_V3.X$
$K_V3.1$ $K_V3.2$ $K_V3.3$ $K_V3.4$
$K_V4.X$
$K_V4.1$ $K_V4.2$ $K_V4.3$
$K_V5.X$
$K_V5.1$
$K_V6.X$
$K_V6.1$ $K_V6.2$ $K_V6.3$ $K_V6.4$
$K_V7.X$
KCNQ1 KCNQ2 KCNQ3 KCNQ4 KCNQ5
$K_V7.1$ $K_V7.2$ $K_V7.3$ $K_V7.4$ $K_V7.5$
$K_V8.X$
$K_V8.1$ $K_V8.2$
$K_V9.X$
$K_V9.1$ $K_V9.2$ $K_V9.3$
EAG
$K_V10.X$
eag1 eag2
$K_V10.1$ $K_V10.2$
$K_V11.X$
herg1 herg2 herg3
$K_V11.1$ $K_V11.2$ $K_V11.3$
$K_V12.X$
elk1 elk2 elk2
$K_V12.1$ $K_V12.2$ $K_V12.3$
Slo(BK)
$K_{Ca}1.X$
$K_{Ca}1.1$
$K_{Ca}4.X$
$K_{Ca}4.1$ $K_{Ca}4.2$
$K_{Ca}5.X$
$K_{Ca}5.1$
SK
$K_{Ca}2.X$
SK1 SK2 SK3
$K_{Ca}2.1$ $K_{Ca}2.2$ $K_{Ca}2.3$
$K_{Ca}3.X$
IK
$K_{Ca}3.1$

Figure 1.4: K^+ channel α-subunits and their expression in pulmonary artery. K^+ channel α-subunits arranged by the number of TM domains. ●, mRNA detected; ○, mRNA not detected; ▲, protein detected; ▬, protein not detected by western blot; ✖, protein not detected by electrophysiology. Compiled using data from Archer et al., 1998; Osipenko et al., 2000; Davies and Kozlowski, 2001; Platoshyn et al., 2001; Reichenberger et al., 2001; Cui et al., 2002; Gurney et al., 2003; Gardener et al., 2004; Wang et al., 2005; Gönczi et al., 2006; Moudgil et al., 2006; Peinado et al., 2008; Kroigaard et al., 2013.

1.10 Potassium channel involvement in regulating the membrane potential of pulmonary artery smooth muscle

The background K^+ efflux is the major determinant of the RMP in PASMCs (Casteels et al., 1977a). A number of studies have shown that block of K^+ channels leads to Ca^{2+} influx through L-type VGCCS and PASMCs contraction (Post et al., 1992; Yuan et al., 1993a). It is still not agreed what K^+ channels control the RMP in PASMC, but a number have been investigated to determine whether they play a key role in setting or maintaining the RMP in PASMC.

1.10.1 K_{ATP} ($K_{IR}6.1$) channels

ATP-sensitive potassium (K_{ATP}) channels are voltage-insensitive, but show weak inward rectification due to block by cytoplasmic polyamines (Seino, 1999). In many tissues they are inhibited by intracellular ATP at normal physiological concentrations and link metabolism to membrane excitability. The vascular smooth muscle, pore-forming subunit, Kir6.1, shows a relatively low sensitivity to ATP, but is activated by ADP. This property is imparted by interactions with the auxiliary subunit (predominantly SUR2B) (Seino, 1999; Nichols et al., 2013) and has led to the description of Kir6.1-containing channels as nucleoside diphosphate dependent (NDPs). $K_{ATP}/_{NDP}$ channels are exquisitely sensitive to PKA (stimulatory) and PKC (inhibitory), so are modulated by GPCR-mediated vasodilators and constrictors. Pharmacologically, these channels are inhibited by the sulphonylurea, glibenclamide, and activated by a number of agents, including levcromakalim (Seino, 1999).

The presence of K_{ATP} channels in PASMC was first demonstrated by the finding that reducing the cytoplasmic ATP concentration induced a K^+ current and hyperpolarised the membrane, both responses being inhibited by glibenclamide (Clapp and Gurney, 1991a,

1992). Under physiological conditions, when the intracellular concentration of ATP ($[ATP]_i$) is high, K_{ATP} channels are closed. Since glibenclamide (10 μM) failed to alter the RMP of PASMCs or increase $[Ca^{2+}]_i$ under physiological conditions (Clapp and Gurney, 1992; Yuan, 1995), it is unlikely that K_{ATP} channels are involved in setting the RMP. Also, hypoxic inhibition of whole cell K^+ current is not dependent on the $[ATP]_i$ (Post et al., 1992) and hypoxia does not raise $[ATP]_i$ (Yuan et al., 1993a), again suggesting that K_{ATP} channels are unlikely to be responsible for hypoxic PASMC contraction either. This implies that K_{ATP} channels can regulate, but not set the PASMC membrane potential. Furthermore, drugs that open K_{ATP} channels, such as levcromakalim, have been shown to relax pre-constricted PAs and hyperpolarise PASMCs (Clapp et al., 1993; Wiener et al., 1991). K_{ATP} channel openers have also been shown to be potentially useful in the treatment of HPV and PAH (Sahara et al., 2012; Xie et al., 2004), most likely because of their enhanced responsiveness under these conditions.

1.10.2 Large-conductance Ca^{2+}-activated K^+ (BK_{Ca}) channels

BK_{Ca} α-subunits contain 7 TM domains, the first 6 being analogous to K_V channels with a voltage sensor at TM4 (Nelson and Quayle, 1995). The additional TM domain renders the N-terminal peptide on the extracellular side of the membrane (Wallner et al., 1996). The C-terminal region of the α-subunit contains a calcium/calmodulin binding domain, often referred to as a 'calcium bowl', which confers calcium sensitivity to the channel (Chalmers et al., 2007). Additionally, there are four β-subunit isoforms (β1-4), which have two TM domains and may associate with the α-subunits in a 1:1 ratio (Wallner et al., 1995). The β1-subunit is considered the predominant β-subunit in vascular smooth muscle cells (Jiang et al., 1999; Tanaka et al., 2004).

BK_{Ca} channels are activated in a voltage-and time-dependent manner (Clapp and Gurney, 1991a). They activate in PASMCs in response to depolarising stimuli and rises in $[Ca^{2+}]_i$ (Albarwani et al., 1994; Clapp and Gurney, 1991a). BK_{Ca} channels are normally closed at the RMP of PASMCs and are unlikely to set RMP since inhibitors of the BK_{Ca} channel, such as tetraethylammonium ions (TEA), charybdotoxin (Yuan, 1995) and iberiotoxin (Osipenko et al., 1997), do not cause PASMC membrane depolarisation when applied at a sufficient concentration to maximally block the BK_{Ca} channels. Block of BK_{Ca} channels with charybdotoxin does, however, enhance the rise in $[Ca^{2+}]_i$ measured in response to depolarisation stimuli (Yuan, 1995). This implies that BK_{Ca} channels can regulate PASMC

membrane potential by counteracting depolarisation. It is more likely that the BK_{Ca} channels act as a negative feedback mechanism, causing repolarisation by opening in response to increased $[Ca^{2+}]_i$, thereby enabling these channels to regulate Ca^{2+} influx and PASMC contraction (Brayden and Nelson, 1992).

Initially BK_{Ca} channels were considered responsible for the attenuation of the K^+ current that occurs in response to hypoxia (Post et al., 1992). Evidence against the involvement of BK_{Ca} channels in HPV was provided by the finding that hypoxia significantly depolarised primary cultured PASMCs bathed in either physiological salt solution (PSS) or with Ca^{2+}-free PSS. Furthermore, complete removal of extracellular Ca^{2+} while maintaining a low Ca^{2+} -intracellular solution with 10 mM EGTA in the recording pipette (to prevent BK_{Ca} channels from opening due to Ca^{2+} release from intracellular stores), did not impede the hypoxia-induced inhibition of the outward K^+ current in primary cultured PASMCs (Yuan et al., 1993a).

1.10.3 Voltage-gated K^+ (K_V) channels

As the K_{ATP} and BK_{Ca} channels play little role in setting the RMP in PASMC, attention turned towards two other known K^+ currents of the voltage-gated (K_V) family of ion channels. The I_{KA}, or A-like current, is transient with rapid activation: it peaks within 5 ms of a depolarising voltage step and is completely inactivated within 100 ms (Clapp and Gurney, 1991a). The I_{KV} current activates and inactivates more slowly with respect to the I_{KA} current, reaching peak activation within 100 ms of a depolarising step (Smirnov et al., 1994; Yuan, 1995). I_{KA} and I_{KV} can be distinguished pharmacologically from other K^+ currents in PASMCs by their relative insensitivity to TEA and glibenclamide (Clapp and Gurney, 1991a; McCulloch et al., 2000). The pharmacology of I_{KA} and I_{KV} are similar in that both are sensitive to high concentrations of 4-AP (Clapp and Gurney, 1991a; McCulloch et al., 2000), but can be separated based on their different kinetics. Of the K^+ channel α-subunits present in PASMC (see Figure 1.4) $K_V1.4$, K_V4 and some K_V3 family members are all capable of forming an A-type current (Pawson et al, 2014), but their contributions have not yet been established. The main candidates proposed to mediate I_{KV} are $K_V1.5$ and $K_V2.1$, either as homotetramer or heterotetramer of $K_V1.5/1.2$ (Hulme et al, 1999) and $K_V2.1/9.3$ (Patel et al, 1997).

K_V7 channels expressed in PASMC activate with time constants of 100 ms or more, so are too slow to mediate I_{KA} or I_{KV}. They have however been proposed to play a role in regulating

the resting membrane potential of PASMC. The K_V7 family of K^+ channel α-subunits consists of five subtypes that are encoded by five separate genes (*KCNQ1-5*). In general, K_V7 channels activate positive to -60 mV with little or no inactivation (Robbins, 2001), so they could be active at the RMP. K_V7 channels form the primary molecular basis of a number of established and diverse K^+ currents, including the cardiac slow delayed rectifier current I_{KS} ($K_V7.1$; Noble and Tsien, 1968), the neuronal M-current, I_{KM} ($K_V7.2/K_V7.3$ and $K_V7.2/K_V7.5$ heteromers; Brown and Adams, 1980; Constanti and Brown, 1981), and a low threshold K^+ current in cochlear outer hair cells, I_{KN} ($K_V7.4$; Housley and Ashmore, 1992). A low threshold, non-inactivating current that is inhibited by the K_V7 blocker, linopirdine, and enhanced by the K_V7 activator, flupirtine, has been described in PASMC (Joshi et al, 2009). The molecular composition of the underlying channels are not yet known, but the *KCNQ4* gene appears to be the most strongly expressed in PASMC, with *KCNQ1* and *KCNQ5* also expressed, but not *KCNQ2* or *KCNQ3* (Joshi et al., 2009).

1.10.4 Two-pore domain channels

The two-pore domain channel TASK-1 has also been implicated in the regulation RMP in human, rabbit and rat PASMC (Gurney et al., 2003; Gardener et al., 2004; Olschewski et al., 2006; Manoury et a.l, 2011). PASMC were shown to express the *KCNK3* gene, which encodes TASK-1 (two-pore domain acid-sensitive K^+ channel), and to display a K^+ current with properties consistent with this channel type. The current was active at membrane potentials negative to -60 mV, inhibited by acidosis, Zn^{2+} ions and anadamide and enhanced by halothane (Gurney et al., 2003). It was recently reported that six heterozygous missense mutations in the *KCNK3* gene, which result in a loss of function in the TASK-1 channel, were found in patients with familial and idiopathic PAH (Ma et al., 2013). This suggests an important physiological role for TASK-1 in PA.

1.10.5 Two alternative hypotheses to explain the resting potential of PASMC.

Today, there is reasonable agreement that non-inactivating, voltage-gated K^+ channels with a low voltage threshold for activation and sensitivity to high (≥10 mM) concentrations of 4-aminopyridine (4-AP) contribute to setting the RMP of PASMC (Evans et al., 1996; Post et al., 1992; Yuan, 1995). Reducing the outward current causes membrane depolarisation and Ca^{2+} influx via VGCCs (Yuan et al., 1993a), thus resulting in PASMC contraction. However,

this is where the agreement ends with two separate hypotheses on what channel(s) are actually responsible for setting the RMP in PASMCs.

1.10.5.1 Hypothesis 1- K_V1.5 and K_V2.1 set the resting membrane potential in pulmonary artery smooth muscle cells.

The proposed contribution of K_V1.5 and K_V2.1 α-subunits in setting the RMP in PASMCs, is partly based on the finding that antibodies against either subunit partially, but rapidly inhibited the outward K^+ current (Archer et al., 1998). Rat PAs exposed to hypoxia, compared to normoxia controls, show significantly reduced expression of K_V1.5 and K_V2.1 while the RMP of PASMCs was more depolarised (Platoshyn et al., 2001). There are flaws to this theory however. The IC_{50} value for 4-AP inhibition of K_V1.5 and K_V2.1 channels lies between 0.1 and 4.5 mM (Coetzee et al., 1999), yet 10 mM 4-AP was required to depolarise rat PASMCs with 1 mM 4-AP failing to alter membrane potential or PA tone (Osipenko et al., 1998). Furthermore, K_V1.5 and K_V2.1 channels are activated at voltages that are depolarised (Coetzee et al., 1999) with respect to the RMP of PASMC, so they are unlikely to be open at the RMP (Figure 1.5) (Evans et al., 1996; Osipenko et al., 1997). Furthermore, prolonged depolarisation at 0 mV inactivates I_{KA} and I_{KV}, but does not affect the RMP of the PASMC (Coetzee et al., 1999; Osipenko et al., 1997), suggesting that these channels are not responsible for setting the RMP. Alternatively, it has been suggested that K_V1.5 and K_V2.1 channels act as depolarisation detectors and reduce excitation by causing enhanced K^+ efflux in response to membrane depolarisation, so that decreased expression could increase excitability (Gurney et al., 2010). Heteromeric K_V1.5/K_V1.2 and K_V2.1/K_V9.3 channels have, however, been shown to activate within the RMP range in PASMCs (Figure 1.5) and could therefore contribute to the background K^+ efflux (Hulme et al., 1999; Patel et al., 1997).

1.10.5.2 Hypothesis 2: The K_V7 sub-family and TASK channels set the resting membrane potential in pulmonary artery smooth muscle cells.

Evans et al. (1996) reported a current, denoted I_{KN}, which was present in PASMC when I_{KA} and I_{KV} currents were inactivated by clamping PASMCs at 0 mV, and K_{ATP} and BK_{Ca} channels were blocked in the presence of glibenclamide and TEA. At least part of I_{KN} was voltage-gated, had a threshold of activation between -80 and -65 mV, activated on a time scale of seconds, and was non-inactivating during depolarisation (Osipenko et al., 1997; Patel et al.,

1997). The I_{KN} current could be distinguished from I_{KA} and I_{KV} by its voltage-dependence, kinetics and pharmacology (Osipenko et al., 1997).

The original paper by Evans et al. (1996) outlined similarities and differences between I_{KN} and the M-current (I_{KM}) in neuronal cells. I_{KM} was so called as original studies in frog sympathetic ganglion showed that the current was inhibited by muscarinic receptor agonists (Brown and Adams, 1980; Constanti and Brown, 1981). I_{KM} has a threshold for gating at approximately -65 mV, activates slowly and is non-inactivating, hence it has similar properties to I_{KN} in PASMCs. The kinetics of the two currents are however different, with the time constant of activation varying between them: I_{KM} usually below 200 ms at -60 mV, compared to 1.6 s for I_{KN}. I_{KN} displays asymmetric activation and deactivation kinetics whereas I_{KM} exhibits symmetric kinetics of activation and deactivation. Pharmacological discrepancies between the two currents include: first, I_{KN} is not inhibited by the muscarinic agonist carbachol whereas muscarinic activation suppressed I_{KM}-like current in toad gastric smooth muscle (Sims et al., 1985) and the neuronal I_{KM} (Marrion et al., 1987); second, Ba^{2+} blocks I_{KM} in the millimolar range but has no effect on I_{KN} (Evans et al ., 1996).

The reason K_V7 channels are attractive candidates for regulating RMP in PASMC is because the channels would be active at that potential (Figure 1.5) (Osipenko et al., 1997). There is also growing pharmacological evidence from the actions of K_V7 channel modulating drugs on PASMC and intact vessels (Joshi et al., 2006, 2009). To date there are no studies to consolidate the role of K_V7 channels in regulating the RMP of PASMCs, although a study using small interfering RNA (siRNA) in systemic arteries suggests that $K_V7.4$ channels may contribute to RMP in smooth muscle (Chadha et al., 2012).

I_{KN} contains voltage-dependent and voltage-independent components (Gurney and Joshi, 2006; Joshi et al., 2006). While K_V7 channels might contribute to RMP, they cannot account for the voltage-independent component of I_{KN}. TASK-1 channels do not have a positively charged TM4 region and consequently lack voltage sensitivity, but display open rectification and therefore are open at RMP (Lesage and Lazdunski, 2000). The TASK-1 channels are thought to contribute to I_{KN} due to similar pharmacological and biophysical properties, including low sensitivity to the classical K^+ channel-blocking drugs TEA, quinine, glibenclamide, 4-AP and Ba^{2+} (Robbins 2001). However, mouse PASMC lack functional TASK-1 channels and I_{KN}, implying there are differences between species (Manoury et al., 2011). TASK-1 channels appear to be important in humans, because knockdown of TASK-1 using

siRNA in human PASMCs resulted in loss of I_{KN}, membrane depolarisation and a loss of responsiveness to hypoxia, which was also shown to inhibit TASK-1 current (Olschewski et al., 2006). Knockdown of TASK-2 by siRNA in rat PASMCs has also been shown to cause membrane depolarisation (Gönczi et al., 2006), thus TASK1 and TASK2 may both contribute to RMP. .

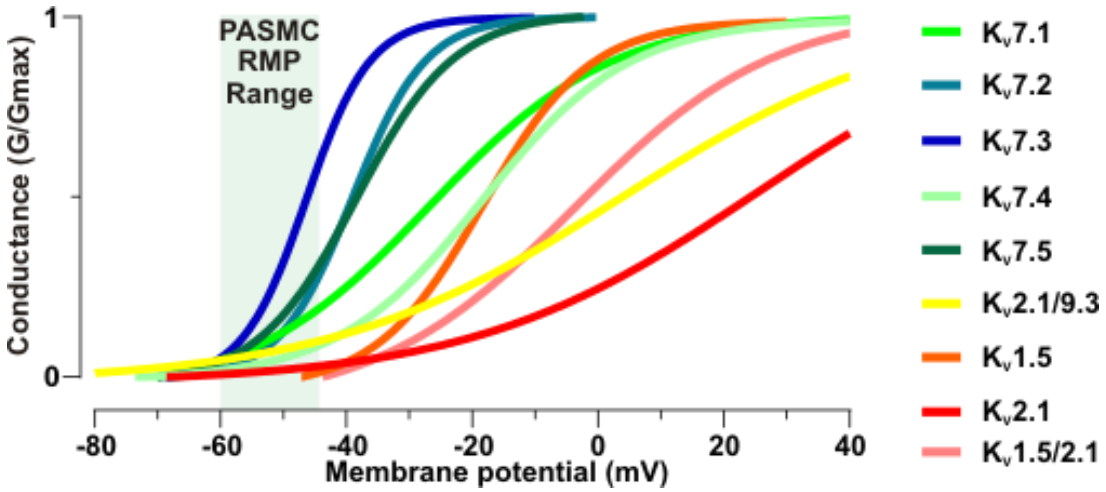

Figure 1.5: Voltage dependence of candidate K^+ channels considered to set the RMP in PAMCs. Relative conductance of K^+ channels against cell membrane potential. $K_V1.5$ and $K_V2.1$ channels are only activated at potentials that are positive with respect to the PASMC RMP, thus they cannot set the RMP. Data from the following papers were used to produce this figure: Patel et al., 1997; Hulme et al., 1999; Vicente et al., 2006; Shamgar et al., 2008; Jindal et al., 2008; Miceli et al., 2009; Gofman et al., 2012; Ruscic et al., 2013. Co-expression of K_V7 auxiliary subunits KCNE1 and 2 may shift $V_{0.5}$ more positive, however co-expression of KNCE3-5 largely have no effect on the activation kinetics (See Table 1.3).

1.11 K^+ channels and pulmonary artery smooth muscle cell proliferation, apoptosis and migration.

K^+ channels have been implicated in the proliferation of a vast number of different cell types, including PASMCs (Burg et al., 2008; Wonderlin and Strobl, 1996). K^+ channel inhibition is associated with increased proliferation in PASMCs (Platoshyn et al., 2000), however, K^+ efflux has been linked with increased proliferation in other cell types (Wonderlin and Strobl, 1996). Thus, the effect K^+ flux has on the proliferation rate is cell specific. The whole-cell voltage-gated K^+ current amplitude is significantly smaller and

inactivates faster in PASMCs cultured in growth medium, compared to PASMCs in basal medium (Platoshyn et al., 2000; Cui et al., 2002). Reduced K^+ current amplitude has also been implicated in primary (idiopathic) PAH (Yuan et al., 1998a) and HPV (Post et al., 1992; Wang et al., 1997; Yuan et al., 1993a). The proliferation rate of PASMCs was significantly reduced in the presence of valinomycin (K^+ ionophore), presumably because the K^+ efflux prevented membrane depolarisation and subsequent Ca^{2+} influx (Platoshyn et al., 2000).

Further complexity exists concerning the role of K^+ channels in regulating cell proliferation as follows: 1) freshly isolated PASMCs may express a K^+ channel profile different from the cells in culture (Moudgil et al., 2006); 2) different segments of the PA tree express K^+ channels to varying degrees; 3) different PASMC phenotypes may have a different K^+ channel profile (Archer, 1996; Archer et al., 1996; Smirnov et al., 2002).

Any alteration in the proliferation rate of cells might be associated with the inverse response in the rate of apoptosis. Given their role in proliferation, it is not surprising that K^+ channels have also been implicated in both early and late stages of apoptosis. An apoptotic volume decrease, leading to cell shrinkage, is generally considered a universal characteristic of apoptotic cells and occurs early on in the course of apoptosis (Núñez et al., 2010). By hyperpolarising the cell, an increase in K^+ efflux will increase the electrochemical gradient for Cl^- and cause Cl^- efflux. This ion efflux results in water leaving the cell via aquaporins in an attempt to maintain osmolality, though ultimately this leads to cell shrinkage. The "prerequisite" of K^+ efflux for PASMC apoptosis has been demonstrated. A high extracellular K^+ concentration ($[K^+]_o$) or block of K_V channels with 4-aminopyridine markedly decreased the staurosporine-mediated apoptosis of PASMCs (Krick et al., 2001a). High $[K^+]_o$ also inhibited valinomycin induced apoptosis of PASMCs, presumably by reducing K^+ efflux as E_K and the membrane potential are brought closer together at a more depolarised level (Krick et al., 2001b). Staurosporine induced apoptosis was also associated with an increase in the concentration of the pro-apoptotic enzyme, caspase-3. The increase in caspase-3 was attributed to low cytosolic $[K^+]$ since normal cytosolic levels are considered to prevent caspase activation (Krick et al., 2001a).

The K_V7 channels have been implicated in cell migration in various other cells types. For example, $K_V7.1$ and the accessory subunit KCNE1 are asymmetrically localized during the first few cleavages of frog embryo development and are required for normal left-right asymmetry (Morokuma et al., 2008). Inhibition of K_V7 channels promotes the motility of the

oligodendrocyte lineage cells, this movement of which is physiologically vital in the development of the nervous system (Wang et al., 2011).

1.12 Molecular diversity in K_V7 channels

The K_V7 α-subunits share 40–60% amino acid homology, which is particularly high throughout the TM regions and the conserved pore domain region between TM segments 5 and 6, which has a TxxtxGYG sequence and determines K^+ selectivity, (Figure 1.6) (Lerche et al., 2000a; Schroeder et al., 2000a). The C-terminus length varies amongst the K_V7 α-subunits following the order; $K_V7.5$> $K_V7.2$> $K_V7.3$> $K_V7.4$> $K_V7.1$. The C-terminus of each α-subunit member shares a region of highly conserved amino acids; this is termed the A-domain (Schwake et al., 2000). The $K_V7.1$, $K_V7.2$ and $K_V7.5$ α-subunits contain intracellular protein kinase A phosphorylation sites. $K_V7.1$ α-subunits have also been reported to contain a glycosylation site on the loop between TM5 and TM6 (Barhanin et al., 1996; Wang et al., 1996).

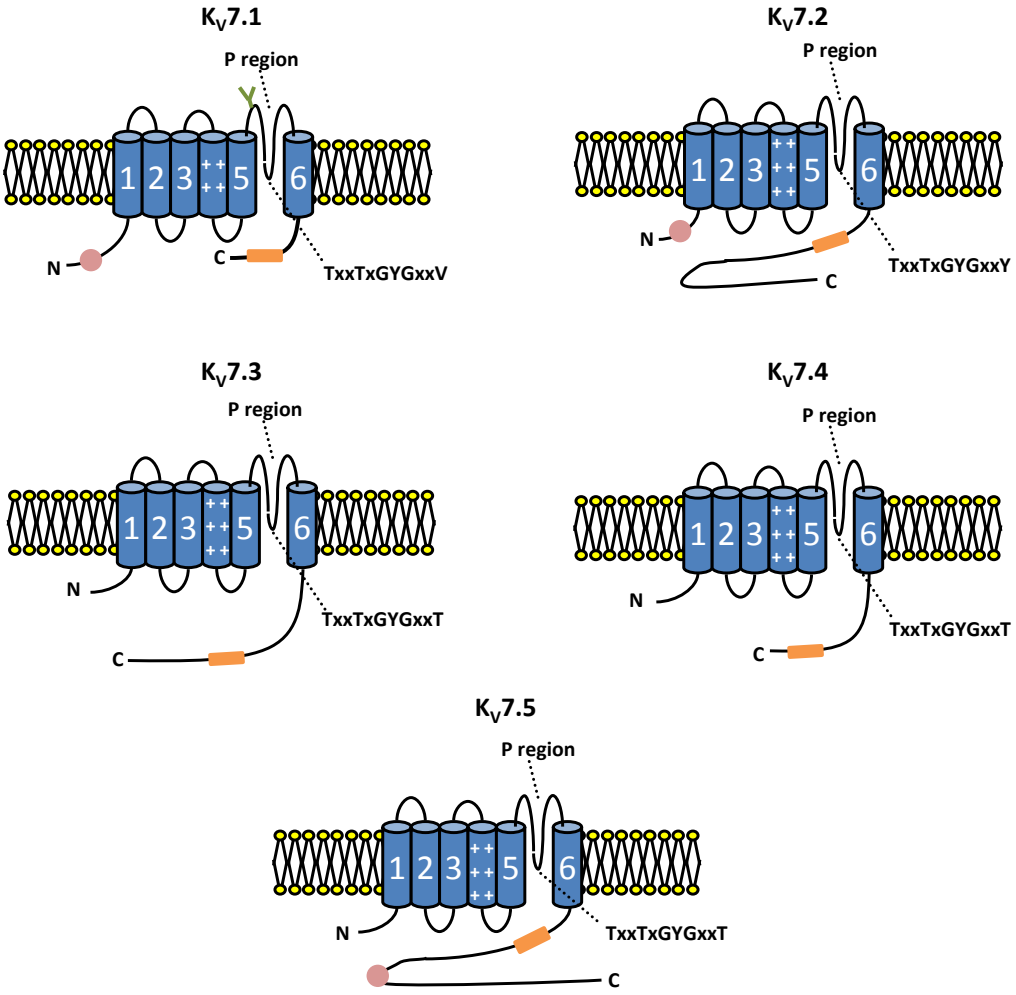

Figure 1.6: Structural characteristics of the K_V7 potassium channel α-subunits. The six TM regions (1-6), the pore region (P region) amino acids, A-domains (orange rectangle), glycosylation site (Green Y) locations and protein kinase A phosphorylation sites (pink circle) for $K_V7.1$-5 α-subunits are shown. Diagrams and/or information adapted from: (Howard et al., 2007; Robbins, 2001; Robertson, 1997).

In order to understand the biophysical properties of the K_V7 channel sub-family, the channels have been expressed in a variety of different expression systems. The currents produced by homomultimers differ from those produced by heteromultimers and also differ from channels associated with auxiliary subunits. The current characteristics of $K_V7.1$ homotetramers include a half activation voltage ($V_{0.5}$) between -10 and -29 mV (Barhanin et al., 1996; Shamgar et al., 2008). Activation kinetics are sigmoidal and activate in the order of 100-200 ms to achieve 90%, with a threshold at approximately -53 mV. The current reaches a steady state within 1 s at +40 mV when expressed in African green monkey kidney fibroblast (COS) cells (Sanguinetti et al., 1996; Yang et al., 1997). $K_V7.1$ does not form functional heteromultimers with other members of the K_V7 family (Haitin and Attali, 2008), but it can co-assemble with members of the KCNE family (Table 1.3). $K_V7.1$ co-expressed with the auxiliary subunit KCNE1 is the molecular correlate of I_{KS} in cardiac myocytes (Barhanin et al., 1996; Sanguinetti et al., 1996).

$K_V7.2$ homotetramers have been shown to be functionally active in a variety of expression systems, including oocytes (Yang et al., 1998), human embryonic kidney (HEK) cells (Shapiro et al., 2000) and COS cells (Tinel et al., 2000a). The currents activate at potentials positive to -60 mV and exhibit a rapidly activating delayed rectifier current phenotype, similar to the $K_V7.1$ current in oocytes (Yang et al., 1998). In contrast other studies have shown $K_V7.2$ homotetramers cause a large, slowly activating outward current in the same expression system (Main et al., 2000; Wang et al., 1998). The biophysical properties of $K_V7.2$ homotetramers seem to depend on the expression system and/or the protocol used to study the current. An example of this is the $V_{0.5}$, which ranges from -14 to -38 mV, depending on the expression system used (Wang et al., 1998). $K_V7.2$ can form functional heteromultimer channels with $K_V7.3$ subunits, which have distinct properties from either $K_V7.2$ or $K_V7.3$ homotetramer channels (Main et al., 2000; Wang et al., 1998). $K_V7.2$/ $K_V7.3$ channels have an activation threshold around -60 mV. Single channel conductance values differed significantly for $K_V7.2$/$K_V7.3$ channels, suggesting that different stoichiometries give rise to channels of different current amplitudes (Schwake et al., 2000). $K_V7.2$ cannot form functional channels with $K_V7.4$ or $K_V7.5$. This is because a dominant negative mutation in *KCNQ2* did not significantly change the current amplitude when expressed with $K_V7.4$ or $K_V7.5$ homotetramers (Kubisch et al., 1999; Schroeder et al., 2000a).

The kinetic properties of homotetramer $K_V7.4$ channels depend on the expression system used for the investigations. In Chinese hamster ovary (CHO) cells, the $V_{0.5}$ for $K_V7.4$ was −18 mV, with an activation threshold of approximately -60 mV (Selyanko et al., 2000). $K_V7.4$ did not inactivate at positive membrane potentials in CHO cells. In contrast, the activation voltage for $K_V7.4$ homotetramer channels expressed in oocytes was reported to be between -10 mV and -11 mV (Kubisch et al., 1999; Strutz-Seebohm et al., 2006). Dominant negative mutants of *KCNQ1* and *KCNQ2* were shown to be incapable of altering the current amplitude of $K_V7.4$, thus $K_V7.1$ or $K_V7.2$ do not form functional heterotetramer channels with $K_V7.4$ (Kubisch et al., 1999). Recently, $K_V7.4/K_V7.5$ heterotetramer channels were reported to be expressed in mesenteric and cerebral arteries (Brueggemann et al., 2014; Chadha et al., 2014). Expression in A7r5 smooth muscle cells of $K_V7.5$, $K_V7.4$, or both produced currents with similar densities but the voltage-dependencies of activation for the heterotetramer was intermediate to either homotetramer (Brueggemann et al., 2010).

In oocytes, $K_V7.5$ homotetramer channels have a $V_{0.5}$ value between -46 and -48 mV, depending on the splice variant, and activate slowly upon depolarisation. Since the $V_{0.5}$ for native I_{KM} is approximately -45 mV, the $K_V7.5$ channels have kinetics similar to I_{KM} (Schroeder et al., 2000).

Given that in rodent PAMSC the K_V7 subunit expression is predominantly $K_V7.1$, $K_V7.4$ and $K_V7.5$ (Joshi et al., 2006), it is likely that there will be a heterogeneous population of channels expressed. Although $K_V7.1$ is predicted to form only homotetramer, $K_V7.4$ and $K_V7.5$ could be subject to heteromultimerisation, as reported in systemic arteries (Brueggemann et al., 2014; Chadha et al., 2014). Distinguishing such expression profiles would be difficult pharmacologically due to a lack of subunit specific modulators. Electrophysiological studies to assess the biophysical properties of the K_V7 currents in PASMC, combined with molecular silencing approaches, will be needed to elucidate the precise molecular composition of the functional channels.

1.12.1 *KCNQ* Splice Variants

Another source of diversity in K_V7 channels derives from alternative gene splicing. All *KCNQ* transcripts have at least one splice variant, except *KCNQ3*. A truncated splice variant of *KCNQ1* in rat suppresses the current caused by $K_V7.1$ channels when expressed alone or with KCNE1 (Yamada et al., 2002). Co-transfection of a short variant of KCNQ2 with a long *KCNQ2* splice variant, *KCNQ3*, or the *KCNQ2* long/*KCNQ3* heterotetramer profoundly alters functional expression by shifting the voltage dependence of activation to more depolarized potentials and/or producing overall suppression of K^+ conductance (Smith et al., 2001). Beisel et al, (2005) described 4 splice variants of *KCNQ4* and although not investigated, hypothesised that homotetramer and heterotetramer channels may have important electrophysiological implications. *KCNQ5* splice variants have been reported to alter the biophysical properties of the $K_V7.5$ channels (Yeung et al., 2008).

1.12.2 KCNE1-5 auxiliary subunits

There are various auxiliary proteins (β-subunits) that interact with and alter the biophysical properties of K^+ channel α-subunits. One particular group, the KCNE gene family (MinK-related peptides) has been shown to interact with and alter the biophysical properties of all K_V7 channels and also other ion channels (Abbott and Goldstein, 2002). The KCNE family comprises of five proteins (KCNE1 to 5) that span the cell membrane once. Each member has been shown to associate with K_V7 channels in heterologous expression systems. Table 1.3 summarises the effects of KCNE subunits on the electrophysiological properties of the K_V7 channels when heterologously co-expressed.

	$K_V7.1$	$K_V7.2$	$K_V7.3$	$K_V7.4$	$K_V7.5$
KCNE1	Increased current amplitude Activated at more positive potentials. No inactivation [2,3,4,5].	Attenuated current and slowed activation in $K_V7.2$ / $K_V7.3$ heterotetramer channels [8].		Increased current and shit $V_{0.5}$ toward 0 mV [12]	Increased current and slowed activation[10]
KCNE2	Constitutively active with small current [1] Reduced current when co-expressed with $K_V7.1$ /KCNE1 [2]	Decreased time constant of activation and deactivation [9]	Interact but no change [9]	Increased current and shifts $V_{0.5}$ to -6.9mV [12]	No effect[10]
		$V_{0.5}$ shifted to the right. Time constant for activation and deactivation reduced in $K_V7.2$ / $K_V7.3$ heterotetramer channels [9]			
KCNE3	Constitutively active and slowly activated at potentials ≥ -40 mV [6] Increased current density when co-expressed with $K_V7.1$ /KCNE1 channels			Decreased current [6,12]	Current inhibited [10]
KCNE4	Small current in physiological range [7,13]	No effect in oocytes [11]	No effect in oocytes [11]	Increased current and modulate channel selectivity [11, 12]	No effect in oocytes[10, 11]
KCNE5	Small current in physiological range [7]			Current not altered [12]	No effect[10]

Table 1.3: Effects of *KCNE1-5* auxiliary subunits on K_V7 channel properties. The *KCNE* subunits alter the properties of K_V7 homomultimeric and heteromultimeric channels. $V_{0.5}$, half maximal activation voltage. [1] Tinel et al., 2000b; [2] Wu et al., 2006; [3] Barhanin et al., 1996; [4] Sanguinetti et al., 1996; [5] Tristani-Firouzi and Sanguinetti, 1998; [6] Schroeder et al., 2000b; [7] Bendahhou et al., 2005; [8] Yang et al., 1998; [9] Tinel et al., 2000a; [10] Roura-Ferrer et al., 2012; [11] Grunnet et al., 2002; [12] Strutz-Seebohm et al., 2006; [13] Grunnet et al., 2005.

1.13 Expression and the physiological roles of K_V7 channels

The expression and physiological function of K_V7 channels has been widely studied. Since studies demonstrated that the K_V7 channels play crucial physiological roles in the heart and brain, their role in various other tissue has been reported. $K_V7.1$ channels are known to play a crucial physiological role in the heart, their expression and function in various other tissues, including smooth muscle, has been investigated as listed in Table 1.4.

Tissue (Species)	Function
Heart (Human and horse) [1, 2]	Repolarisation of the cardiac action potential
Stria vascularis of the cochlea (Mouse) [3]	Endolymph homeostasis
Thyroid gland (Human and mouse) [1, 4, 5, 6]	Thyroid I^- accumulation, required for thyroid hormone production
Pancreas (Human, mouse and rat) [1, 7, 8, 9]	Exocrine Cl^- secretion
Adrenal gland (Human and mouse) [1, 10]	Aldosterone production
Small intestine and Colon crypt cells (Human and Mouse) [1,7, 11, 12]	Cl^- secretion
Kidney (Human) [1, 13, 14]	Counteract membrane depolarisation caused by electrogenic transfer of Na^+ into the Proximal tubule
Stomach parietal cells (Mouse) and antrum SMCs (Rat) [15, 16]	Replenish luminal K^+, allowing H^+-K^+-ATPase to pump H^+ into the lumen. Possible role in controlling RMP in antrum SMCs

Table 1.4: $K_V7.1$ channel expression and function in different tissues. [(1)]Yang et al., 1997; [(2)]Finley et al., 2002; [(3)]Neyroud et al., 1997; [(4)]Roepke et al., 2009; [(5)]Fröhlich et al., 2011; [(6)]Purtell et al., 2012; [(7)]Warth et al., 2002; [(8)]Köttgen et al., 1999; [(9)]Kim and Greger, 1999; [(10)]Sarzani et al., 2006; [(11)]Matos et al., 2007; [(12)]Schroeder et al., 2000b; [(13)]Sugimoto et al., 1990; [(14)]Vallon et al., 2001; [(15)]Heitzmann and Warth, 2007; [(16)]Ohya et al., 2002.

$K_V7.2$ and $K_V7.3$ channels are almost exclusively expressed in the nervous system and their expression overlaps considerably (Schroeder et al., 1998). High expression of *KCNQ2* and *KCNQ3* occurs in anterior olfactory nuclei, neocortex, frontal olfactory cortex, the cerebellar granular layer and hippocampus (Tinel et al., 2000a). The I_{KM} recorded from central neurones is produced by heteromeric $K_V7.2/K_V7.3$ channels and regulates neuronal excitability, thus preventing repetitive firing of neurones (Prole and Marrion, 2004; Robbins, 2001; Wang et al., 1998). $K_V7.2$ and $K_V7.3$ channels are also expressed in human brachial biceps and are reported to regulate skeletal muscle proliferation and dedifferentiation (Iannotti et al., 2010).

K_V7.4 is expressed in outer hair cells, but not inner hair cells, of the organ of Corti and in type I vestibular hair cells. K_V7.4 channels are absent from most brain areas, yet expressed in many regions involved with hearing, such as the brainstem (Kharkovets et al., 2000; Kubisch et al., 1999). K_V7.4 expression has been shown in many regions of the gastrointestinal tract, including stomach, jejunum, ileum and colon, with a potential role for K_V7.4 channels to limit contractile activity in the gastrointestinal tract reported (Jepps et al., 2009).

Messenger RNA for *KCNQ5* can be found within the cerebral cortex, occipital, frontal and temporal lobes, putamen and the hippocampus (Lerche et al., 2000a; Schroeder et al., 2000a). Expression of *KCNQ5* mRNA is also found in the colon, hypothalamus, lung and uterus whereas low expression is observed in whole embryo, heart, kidney and skeletal muscle (Jensen et al., 2005). *KCNQ5*, along with *KCNQ4*, is expressed in a number of areas along the gastrointestinal tract (Jepps et al., 2009).

1.13.1 K_V7 channels in vascular smooth muscle

The first reported expression of K_V7 channels in vascular smooth muscle was 10 years ago, when the expression of the *KCNQ1* gene and K_V7.1 protein was found in mouse portal vein myocytes (Ohya et al., 2003). In the same study, a component of the outward K^+ current recorded from mouse portal vein myocytes was inhibited by the K_V7 channel blocker linopirdine, presenting the first functional evidence for K_V7 channels in vascular myocytes. The K_V7 channel blockers, XE991 and linopirdine, were later shown to induce membrane depolarization in mouse portal vein myocytes and increase the excitability of isolated portal veins (Yeung and Greenwood, 2005). Since this work on mouse portal vein myocytes, a number of studies have implicated K_V7 channels in the regulation of vascular tone. The main evidence is that K_V7 channel modulators alter vascular tone in a number of blood vessels, including aorta, mesenteric, cerebral, carotid, femoral and pulmonary arteries (Joshi et al., 2006, 2009; Mackie et al., 2008; Yeung et al., 2007; Zhong et al., 2010). Electrophysiological studies showed that K_V7 channel modulators alter membrane potential in mouse portal vein, rat mesenteric and PA myocytes, as well as in aorta-derived, A7r cultured smooth muscle cells (Brueggemann et al., 2007; Joshi et al., 2009; Mackie et al., 2008; Yeung and Greenwood, 2005). Together, the investigations provide strong evidence that K_V7 channels are expressed, regulate membrane potential and alter vascular tone in various vascular beds.

In mouse aorta and rat PAs, contraction induced by the K_V7 channel blockers, XE991 and linopiridine, was abolished by blocking VGCC directly with an L-type VGCC blocker (nicardipine or nifedipine) or indirectly by inducing membrane hyperpolarization with a K_{ATP} channel opener (pinacidil or levcromakalim) (Joshi et al., 2006; Yeung et al., 2007). Also, K_V7 channel block induced contraction that remained in the presence of a α1-adrenoceptor blocker (prazosin or phentolamine). Thus, contraction was not due to the depolarization of sympathetic nerves and subsequent release of noradrenaline (Joshi et al., 2006; Yeung et al., 2007).

The literature provides good evidence that K_V7 channel modulators are likely to be acting directly on vascular smooth muscle cells and subsequently altering vascular tone indirectly by altering Ca^{2+} influx through VGCC. Figure 1.7 illustrates the proposed physiological role of K_V7 channels in vascular smooth muscle. A decrease in the open probability of K_V7 channels by channel blockers, such as linopirdine and XE991, leads to membrane depolarisation and Ca^{2+} influx through opened VGCC, with subsequent contraction. Conversely, if the K_V7 channels are opened by activators, such as retigabine, flupirtine or Zinc Pyrithione (ZnPy), the cell membrane remains polarised (or hyperpolarised) and VGCC close, preventing Ca^{2+} influx and contraction.

Joshi et al. (2009) demonstrated that the mean PA pressure in isolated perfused lungs significantly increased in the presence of 1–10 μM linopirdine. In the same study, *in vivo* measurements showed that linopirdine (at 6–11 mg/kg) significantly increased PA pressure but had no effect on systemic blood pressure. This is consistent with the finding that PAs are more sensitive to the constrictor effects of K_V7 blockers (Joshi et al., 2009)

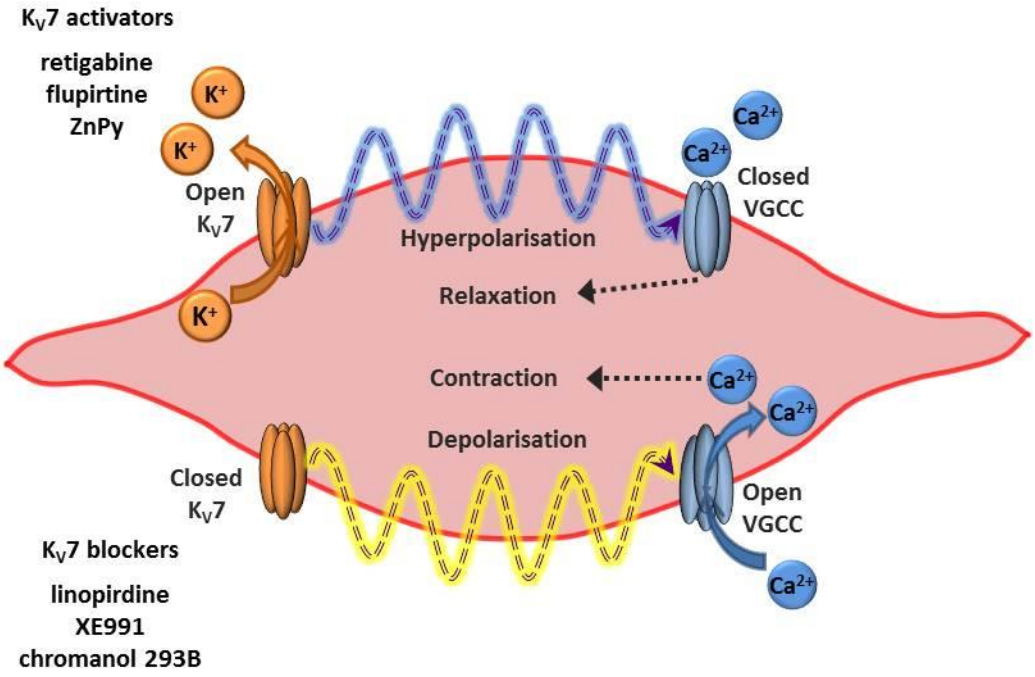

Figure 1.7: K_V7 channels in the regulation of vascular tone.

1.14 K_V7 channel Pharmacology

Much of our understanding of K_V7 channels in vascular muscle has come from studies employing drugs that selectively modulate K_V7 channel activity. A range of K_V7 channel blockers and activators are available,

1.14.1 K_V7 channel blockers

The phenylindolinone derivative, linopirdine (Figure 1.8) (DuP 996; 1,3-Dihydro-1-phenyl-3,3-bis(4-pyridinylmethyl)-2H-indol-2-one), was synthesised in the 1980s. It inhibits K_V7 channels with pIC_{50} (negative log of the half maximal molar inhibitory concentration) values of 5.32 ($K_V7.2$= $K_V7.3$)> 5.05 ($K_V7.1$) > 4.80/4.29 ($K_V7.5$) <3.69/4.85 ($K_V7.4$) (Lerche et al., 2000a; Robbins, 2001; Schroeder et al., 2000a; Wang et al., 1998). The two values for $K_V7.5$ reflect a three-fold difference in potency reported in two separate studies (Lerche et al., 2000a; Schroeder et al., 2000a). For $K_V7.4$ one study found that 200 µM linopirdine did not cause significant block (Robbins, 2001), whereas a different study reported an IC_{50} of 14 µM (Søgaard et al., 2001). Heterotetramer channels also show different pIC_{50} values for linopirdine: 5.46/5 ($K_V7.2$/ $K_V7.3$)> 4.8 ($K_V7.3$/ $K_V7.5$)>> >3.70 ($K_V7.3$/ $K_V7.4$) (Lerche et al., 2000a; Robbins, 2001).

Second generation functional analogues of linopirdine, such as XE991 (10,10-bis(4-pyridinylmethyl)-9(10H)-anthracenone), have an anthracenone structure (Figure 1.8). The compounds are widely used in research to reduce the I_{KM} or I_{KM}-like currents during *in vitro* and *in vivo* experiments (Miceli et al., 2008). The pIC_{50} values for the K_V7 homotetramers is slightly different for XE991 compared to linopirdine. XE991 inhibits K_V7 channels with pIC_{50} values of 6.12 ($K_V7.1$)= 6.15 ($K_V7.2$)> 5.62 ($K_V7.4$)> 4.19 ($K_V7.5$) = >4.30 ($K_V7.3$) (Robbins, 2001; Søgaard et al., 2001; Wang et al., 1998). Both linopirdine and XE991 show selectivity for K_V7 channels against other voltage-gated outward rectifiers, such as $K_V1.2$ and $K_V4.3$ (Wang et al., 1998). However, linopirdine and XE991 show minimal selectivity between the K_V7 channel subunits, hence the suggestion by Miceli *et al* (2008) that future drugs should have improved subunit-specificity to avoid side effects. Although selective for the K_V7 channels, linopirdine and XE991 are relatively non-selective between the different K_V7-subunits. Although these compounds can help to determine the role of K_V7 channels in vascular tissue, they cannot distinguish the function of specific subunits.

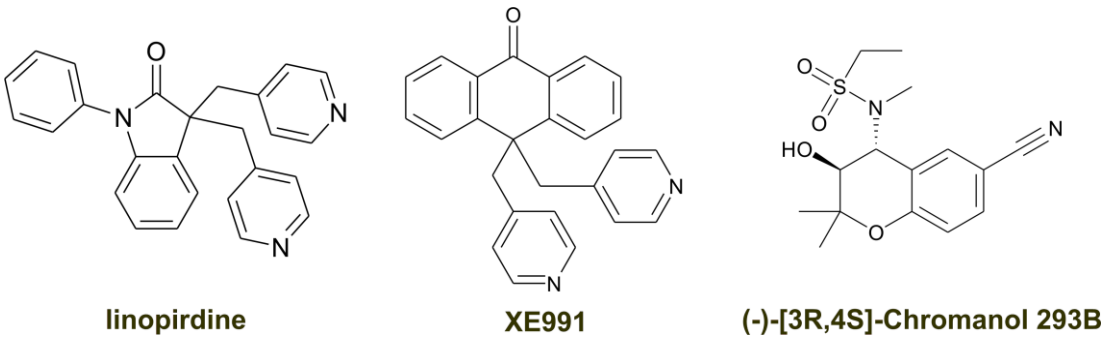

Figure 1.8: Chemical structure of K_V7 channel blockers.

Chromanol 293B (N-[(3R,4S)-6-Cyano-3,4-dihydro-3-hydroxy-2,2-dimethyl-2H-1-benzopyran-4-yl]-N-methylethanesulfonamide; Figure. 1.8) has been shown to block $K_V7.1$ channels selectively, with the (-)293B enantiomer significantly more potent than (+)293B (Lerche et al., 2000b; Seebohm et al., 2001; Yang et al., 2000). (-)Chromanol 293B is often described as a selective $K_V7.1$ blocker and experiments have shown that chromanol has negligible effects on guinea pig I_{Kr} and no significant effect on HERG channels expressed in *Xenopus* oocytes (Busch et al., 1996). However, 30 µM (-)chromanol 293B blocked $K_V7.1$/KCNE1 current by 90%, $K_V1.5$ by 52% and $K_V4.3$ by 37%. The other K_V7 channels are relatively insensitive, 100 µM chromanol 293 blocks $K_V7.5$ channels by (40%) while all other K_V7 channels are blocked by 10% or less (Lerche et al., 2007). Table 1.5 simplifies the

potency prolife of the K_V7 channel blockers used in this study. This selectivity of chromanol 293B can be used to investigate the role of $K_V7.1$ channels in the vasculature.

Pore Blocker	$K_V7.1$	$K_V7.2$	$K_V7.3$	$K_V7.4$	$K_V7.5$
chromanol 293B	90% block at 30 µM	>10% block at 100 µM			
linopirdine	8.91 µM	4.79 µM	4.79 µM	14 – 200 µM	15.8 – 51.3 µM
XE991	0.76 µM	0.71 µM	50 µM	2.4 µM	64.9 µM

Table 1.5: Selectivity profile of the K_V7 channel blockers for K_V7 channel isoforms. Block of homomeric K_V7 channels listed as EC_{50}, where available, or % block at the highest concentration reported.

All the K_V7 channel blockers used in this study are considered to prevent K^+ efflux by blocking the channel pore via the extracellular side of the membrane. Linopirdine only inhibits M-current in intact cells or excised outside-out membrane patches, but not in inside-out patches, thus supporting the notion that linopirdine directly blocks channels from the extracellular side (Costa and Brown; Lamas et al., 1997). While reviewing the literature no studies investigating the site of action for XE991 were found. As XE991 is an anthracenone analogue of linopirdine (Zaczek et al., 1998), it is likely to also block channels from the extracellular side. Using a chimera and single-point mutational approach, amino acid residues in the TM6 and lower selectivity filter of the $K_V7.1$ channel have been shown to determine chromanol 293B sensitivity (Lerche et al., 2007).

1.14.2 K_V7 channel activators

Retigabine (N-[2-amino-4-(4-fluorobenzylamino)-phenyl] carbamic ethyl ester; Figure 1.9) activates all K_V7 channels, except $K_V7.1$ (Main et al., 2000). Retigabine has recently been approved as a treatment for epilepsy by the European Medicines Agency and the United States Food and Drug Administration, with the respective trade names of Trobalt® and Potiga®. Several different modes of action of retigabine, other than K^+ channel activation, have been reported, including augmenting gamma-aminobutyric acid (GABA) activity and blocking Na^+ and Ca^{2+} channels. However, these effects only occurred at concentrations at least one order of magnitude greater than the concentration needed for K^+ channel

activation (Rundfeldt and Netzer, 2000a). Main et al., (2000) reported that the action of retigabine on $K_V7.2$/ $K_V7.3$ channels altered the channel properties in three distinct ways. First, retigabine caused a hyperpolarizing shift of the threshold for activation, towards -80 from -60 mV. Second, retigabine altered the kinetics of channel activation such that time-to-half-maximal activation was reduced from 317 ms to 174 ms. Finally, retigabine prevented channel deactivation at positive potentials (+30 mV) and slowed the deactivation at more negative potentials (Main et al., 2000). In a separate study the actions of retigabine on $K_V7.3/K_V7.5$ heterotetramer channels were found to be similar to those on $K_V7.2/K_V7.3$ channels (Wickenden et al., 2001). It is now generally accepted that the principal effect of retigabine on K_V7 channels is to increase the open probability, rather than increase the single channel conductance (Blackburn-Munro et al., 2005). The pEC_{50} (negative log of the half maximal effective molar concentration) values of retigabine for homotetramers are in the order 6.22 ($K_V7.3$) > 5.60 ($K_V7.2$) > 5.28 ($K_V7.4$) > 3.99 ($K_V7.1$) (Tatulian et al., 2001). Retigabine also activates $K_V7.5$ channels in the sub-micromolar range, but an EC_{50} value was not reported (Dupuis et al., 2002). The pEC_{50} values for $K_V7.2$/ $K_V7.3$ and $K_V7.3$/ $K_V7.5$ channels were 7.72 and 5.85 respectively in CHO cells (Blackburn-Munro et al., 2005).

Flupirtine (N-[2-Amino-6-[[4-fluorophenyl)methyl]amino]-3-pyridinyl]carbamic acid ethyl ester), a structural analogue of retigabine (Figure 1.9), has been used as a non-opioid analgesic since the 1980's and marketed as a selective neuronal K^+ channel opener (Kornhuber et al., 1999; Szelenyi, 2013). Application of flupirtine shifts channel activation in a hyperpolarizing direction with recombinant $K_V7.2$ or $K_V7.2/K_V7.3$ channels (Klinger et al., 2012; Martire et al., 2004), as well as native K_V7 channels in rat nodose ganglion neurons (Wladyka and Kunze, 2006). In order to demonstrate selectivity for K_V7 channels, flupirtine has been tested on a number of other ion channels or currents associated with pain perception. Na^+ and Ca^{2+} channel currents tested in dorsal root ganglion and in hippocampal neurons were unaffected by flupirtine at concentrations up to 10 μM, but current amplitude was reduced by < 30 % at 30 μM. NMDA receptors and recombinant $\alpha 3\beta 4$ nicotinic acetylcholine receptors were blocked by 30 μM, but not by 10 μM flupirtine. Flupirtine was also shown to be ineffective against non-NMDA, ionotropic glutamate receptors, inhibitory glycine receptors, and TRPV1 channels (Klinger et al., 2012). Similar to the pan-K_V7 blockers linopirdine and XE991, retigabine and flupirtine are useful pharmacological tools for identifying K_V7 channel function, but cannot distinguish the role of a particular K_V7 channel subunit.

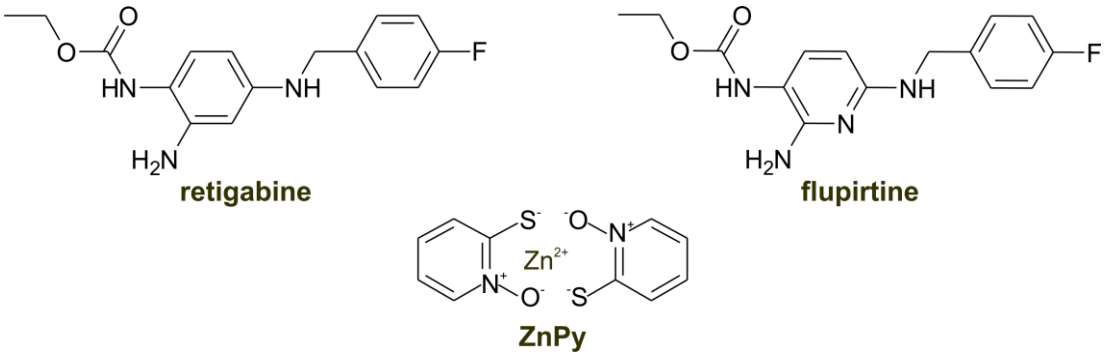

Figure 1.9: The chemical structure of the K_V7 channel activators.

ZnPy (1-Hydroxypyridine-2-thione zinc salt; Fig. 1.9) is a small molecule that is commonly used in anti-dandruff shampoos and in the treatment of psoriasis (Sadeghian et al., 2011; Schwartz et al., 2013). Recently, ZnPy was reported to potentiate K_V7 channels and the native I_{KM}, with several properties distinguishing it from retigabine (Xiong et al., 2007, 2008a). Firstly, ZnPy potentiated current mediated by all K_V7 isoforms ($K_V7.5$> $K_V7.4$> $K_V7.2$> $K_V7.1$), except $K_V7.3$, when the channels were heterologously expressed. Like retigabine, ZnPy caused a hyperpolarizing shift in the conductance-voltage relationship, as well as markedly increasing overall current amplitude. The current produced by retigabine and ZnPy was found to be larger than the sum of the effects when the compounds were added separately, thus suggesting distinct binding site for ZnPy and retigabine (Xiong et al., 2007, 2008a). These differences make ZnPy a promising unique molecular probe for investigating the function of K_V7 channels. The different mechanism of action and selectivity profile of ZnPy compared to retigabine and flupirtine, suggest it could be a useful tool in dissecting which K_V7 channel subunits are important within the vasculature. Table 1.6 shows the potency profiles of the K_V7 channel activators used in this study.

Activator	$K_V7.1$	$K_V7.2$	$K_V7.3$	$K_V7.4$	$K_V7.5$
retigabine	Weak Inhibition	2.51 µM	0.6 µm	5.25 µM	Ec50 in µM range
flupirtine		µM range on I_{KM}	µM range on I_{KM}		
Zinc Pyrithione	Current potentiation	Current potentiation	No effect	Current potentiation	Current potentiation

Table 1.6: Selectivity profile for the K_V7 channel activators. Activation of homomeric K_V7 channels are listed as EC_{50} where available.

A number of studies have been carried out to determine what parts of the channel are important in the interaction with K_V7 activators. Using a chimera approach, substitution of either the TM5 or TM6 domain in the $K_V7.2$ channel, with the equivalent parts of the $K_V7.1$ channel, rendered it insensitive to retigabine (Wuttke et al., 2005). The same study found that mutating either the Trp236 residue in the cytoplasmic part of the TM5, or the conserved Gly301 in the TM6 domain, considered as the gating hinge, prevented the effect of retigabine in $K_V7.2$ channels or restored it partially in $K_V7.1/K_V7.2$ chimera channels. The absence of the Trp236 residue in $K_V7.1$ channels thus explains the lack of sensitivity to retigabine (Gunthorpe et al., 2012). The binding site for flupirtine has not been studied in as much depth. Given that flupirtine is a structural analogue of retigabine, it is likely that the same residues are important.

Given the evidence that ZnPy, unlike retigabine, potentiates $K_V7.1$ activity and has additive effects with retigabine, it probably potentiates K_V7 activity via a residue other than the retigibine-sensing Trp236 on TM5. Mutagenesis studies on $K_V7.2$ channels revealed that the amino acid residues Leu249, Leu275 and Arg306, located in TM5 and TM6 are important for ZnPy pharmacology, since mutations in these residues affected the voltage required for half-maximal activation and maximum conductance (Xiong et al., 2007). Using the assumption that the structure of the $K_V7.2$ channel is similar to the solved crystal structure of the $K_V1.2$ channel, the residues Leu249 and Leu275 should be on separate α-helices, but facing the same side. The linear distance between the two residues would be large enough to allow interaction with ZnPy. Residue Arg306, however, would reside deeper in the channel structure and between Gly301 and the conserved Pro-Ala-Gly bend of the TM6. Both are required for voltage-dependent gating in K_V7 channels (Xiong et al., 2007).

1.15 Project aims

Evidence suggests that K_V7 channels are expressed and play a functional role in setting vascular tone in rodent iPAs. In other cell types, K^+ channels in general have been shown to alter the rate of proliferation and migration. Along with the finding that flupirtine was beneficial in two independent mouse models of PAH, Morecroft et al. (2009) suggest that the K_V7 channels could be a novel target to treat PAH. The hypothesis of this study is that K_V7 channels will be expressed and functional in human intra-pulmonary arteries and play an important role in pulmonary artery smooth muscle contraction, proliferation and migration. Below are the aims of the project all of which are addressed in the three result chapters:

1) Establish the profile of expression of the *KCNQ* (K_V7 alpha subunits) mRNA transcripts in human iPAs (Chapter 2).

2) To determine if K_V7 channel modulators alter human iPA tone and investigate their underlying mechanism (Chapter 2).

3) To reveal the expression profile of the *KCNQ* mRNA transcripts in cultured PASMCs (Chapter 3).

4) To ascertain if K_V7 channel modulators alter the rate of proliferation and/or migration of cultured human PASMCs (Chapter 3).

5) To examine the effect and ascertain the mechanism of action of the recently reported K_V7 channel activator, ZnPy, on rat iPAs (Chapter 4).

1.16 Alternative format

This thesis is being presented in the alternative format, in accordance with the rules and regulations of the University of Manchester. The three results chapters are presented in manuscript form in the style suitable for their intended journal of submission. Some elements have, however, been reformatted to deliver a cohesive body of work. Below are the details of each manuscript, its intended journal and the contributions of each author.

Human tissues were provided by Prof Dave Singh, University Hospital of South Manchester Foundation Trust. They were obtained from patients following written informed consent and with approval of the local research ethics committee (South Manchester Research Ethics Committee, reference: 03/SM/396).

Chapter 2: Functional role for K_V7 potassium channels in human pulmonary artery

Authors: Sean Brennan, Katie Smith, Roberta Oliviera, Paolo Tammaro, Alison M Gurney

Intended journal: American journal of respiratory and critical care medicine

Contribution of authors: Sean Brennan contributed to almost all experiments described in this manuscript. Sean Brennan was responsible for the tissue collection, experimental design, data analysis, and for the construction of all the figures presented in the paper. As second author, Katie Smith (Postdoctoral Researcher) was responsible for the experiments using systemic arteries. As third author, Roberta Oliviera (Research Technician) finished a small number of experiments that were initially set up by Sean Brennan to investigate the underlying mechanism of linopirdine. It allowed us to obtain the maximum data from the limited supply of human tissue, as additional experiments were carried out in parallel. Dr Paolo Tammaro provided helpful discussion on data presentation and the manuscript text. Prof Alison Gurney provided advice and guidance on all experimental work. As first author on this paper, the initial draft of the manuscript text was produced by Sean Brennan. The co-authors then reviewed the manuscript and provided comments. The initial draft was edited for manuscript submission by Prof Alison Gurney. The version intended for publication was then altered by Sean Brennan into the version presented here.

Chapter 3: Loss of K_V7 channel expression and function in proliferating human pulmonary artery smooth muscle cells

Authors: Katie Smith, Sean Brennan, Neil Bodagh, Paolo Tammaro, Alison M Gurney

Intended journal: Pulmonary Circulation

Contribution of authors: This manuscript is representative of experiments to which Sean Brennan contributed significantly. This work would not, however, have been possible without the work of Katie Smith (Postdoctoral Researcher) who also contributed significantly to the experiments presented. As second author on this paper, Sean Brennan was heavily involved in initiating cultures of human pulmonary artery smooth muscle cells and the experimental design, while also executing and analysing proliferation and migration experiments. Sean Brennan also produced a macro for use with the image analysis programme ImageJ, which was used by me and Katie Smith to analyse the proliferation experiments. As first author Katie Smith was fully responsible for the RT-PCR and whole-cell patch clamp experiments while also making the largest contribution to the proliferation and migration experiments. However RT-PCR work on cells built on previous work conducted by Sean Brennan with human arteries, which established conditions for measuring *KCNQ* mRNA by RT-PCR. As third author, Neil Bodagh (undergraduate project student) helped to execute some of the proliferation experiments under the supervision of Katie Smith. Paolo Tammaro provided helpful discussion on data presentation and manuscript text. Prof Alison Gurney provided advice and guidance on all experimental work. The preliminary draft of the paper text was produced by Prof Alison Gurney and Sean Brennan, including figures prepared by Sean Brennan and Katie Smith. The co-authors then reviewed the manuscript and provided comments, which were edited accordingly by Prof Gurney. These comments were then synthesised by Sean Brennan into the final version presented here.

Chapter 4: Mechanisms of vasodilation by the K_V7 channel activator zinc pyrithione

Authors: Sean Brennan, Basma Eid, Alison Gurney

Intended journal: Britsh Journal of Pharmacology.

Contribution of authors: This manuscript presents experiments that I contributed to substantially, however, Dr Eid along with Prof Alison Gurney provided the majority of data presented within this chapter. Due to an error in the concentration of the stock solution of zinc pyrithione, the final concentration of zinc pyrithione used in the experiments was inaccurate in the initial experiments carried out by Sean Brennan. In the interests of scientific rigour, despite the trend in the data being consistent with the reported findings, these data were excluded. Data were only excluded where it varied significantly from previous control data when analysed by Sean Brennan, with agreement from Prof Alison Gurney. All data was analysed, and figures prepared, by Sean Brennan.

Sean Brennan was responsible for the initial experiments showing a dilator effect of ZnPy on rat iPAs and for the experiments investigating the effect of endothelium removal, pre-constriction with high potassium and calcium free conditions on the dilator effect of ZnPy. Most of these experiments were done twice by Sean Brennan to ensure the reported range of zinc pyrithione concentrations was correct. Sean Brennan was also responsible, along with Prof Alison Gurney, for the experimental design used to investigate the mechanism of action of ZnPy. This work was done by Dr Eid, but it follows the protocols established by Sean Brennan for investigating retigabine activation, as presented in chapter 2. As joint first author, Dr Eid was responsible for executing most of the experiments in figures 2-4. Sean Brennan was responsible for the construction of all figures, analysis and writing the initial draft of the manuscript text. Prof Gurney then reviewed and provided comments. These comments were then synthesised by me into the final version presented here.

Chapter 2 : Functional role for K_V7 potassium channels in human pulmonary artery

Sean Brennan, Katie Smith[1], Roberta Oliviera, Paolo Tammaro[2], Alison M Gurney*

Faculty of Life Sciences

University of Manchester

Manchester

M13 9NT

[1]Current address:

UCL Ear Institute, University College London, Gower Street, London WC1E 6BT

[2]Current address:

Department of Pharmacology, University of Oxford, Mansfield Road, Oxford OX1 3QT

Intended journal: American journal of respiratory and critical care medicine

*Author for correspondence

2.1 Abstract

K_V7 potassium channels encoded by *KCNQ* genes help to regulate arterial constriction. In rat pulmonary artery (PA) smooth muscle they contribute to the resting K^+ conductance, which promotes low resting tone by maintaining a negative membrane potential. The membrane is depolarised in pulmonary arterial hypertension (PAH), resulting in disrupted Ca^{2+} signalling, vasoconstriction and cell proliferation. K_V7 activating drugs have the potential to counteract this dysfunctional signalling by causing hyperpolarisation. Pulmonary selectivity is further suggested by the greater expression and activity of K_V7 channels found in rodent PAs compared with systemic vessels. We therefore investigated the functional expression of K_V7 channels in human intra-pulmonary artery (iPA) in comparison with omental artery, as a representative human systemic resistance vessel. The effects of K_V7 channel modulators on distal arteries from human lung and omentum were measured using small vessel myography, while *KCNQ* subunit expression was investigated with qRT-PCR and Western blotting. Both types of artery expressed all *KCNQ* subunits, except *KCNQ2*. Human iPAs also expressed K_V7 channel β-subunits (*KCNE1-5*), but not the cardiac specific *KCNE1b* isoform. The pan-K_V7 channel blockers, XE991 and linopirdine, as well as the $K_V7.1$-selective blocker, (-)chromanol 293B, constricted iPAs at micromolar concentrations, by activating voltage-gated Ca^{2+} influx. K_V7 channels are therefore active at the resting membrane potential of human PA smooth muscle and contribute to resting tone. The K_V7 channel activators retigabine, flupirtine and zinc pyrithione dilated agonist pre-constricted pulmonary and omental arteries with similar potency. The retigabine response was enhanced in pulmonary vessels constricted with Bay K 8644, an L-type Ca^{2+}-channel activator, abolished when constricted with ionomycin, a Ca^{2+} ionophore and reduced when constricted with 90 mM K^+. These data suggest that both direct and indirect inhibition of voltage-gated Ca^{2+} influx was largely responsible for retigabine-induced relaxation. The results suggest that K_V7 channels, including $K_V7.1$, play a major role in regulating the membrane potential and Ca^{2+} signalling in PA smooth muscle and could be exploited therapeutically to cause pulmonary vasodilation. Although systemic effects are predicted, they have not been evident in epileptic patients treated with K_V7 channel activators.

2.2 Introduction

There is increasing evidence for the involvement of the K_V7 family of K^+ channels in the regulation of blood vessel tone (Greenwood and Ohya, 2009; Ng et al., 2011). Three of the

genes coding for K_V7 channel α-subunits, *KCNQ1*, *KCNQ4* and *KCNQ5*, are expressed in rodent iPAs (Joshi et al., 2009). *KCNQ4* is the most strongly implicated in rodent iPA, where its expression was found to be higher than in mesenteric artery (Joshi et al., 2009) and reduced in rodent models of pulmonary arterial hypertension (PAH), which was associated with suppressed pulmonary vasoconstriction in response to K_V7 channel blocking drugs (Morecroft et al., 2009; Sedivy et al., 2014). The studies on PAH in rodents predict an effect at doses equivalent to those used clinically in man to treat pain (Szelenyi, 2013). Flupirtine prevented the development of hypoxia-induced PAH in mice and rats and reversed spontaneous PAH in mice over expressing the serotonin transporter (Morecroft et al., 2009; Sedivy et al., 2014). The potential for a pulmonary-selective effect of K_V7 channel activators is suggested by the preferential expression of *KCNQ4* in rat iPA and the lack of systemic cardiovascular side effects noted in clinical studies of humans treated with flupirtine or the newer K_V7 channel activator, retigabine (Devulder, 2010; French et al., 2011; Szelenyi, 2013).

Animal models of PAH do not fully replicate the human condition so that drugs effective in the models often fail in the clinic. Moreover, treatments are often instigated in animals at an earlier time point in disease progression, so therapies may be more effective than in human disease (Shimoda and Laurie, 2013; Stenmark et al., 2009). In man PAH is often a co-morbidity and therefore early identification is not always achieved. As a minimum, any proposed drug target must be demonstrated to serve the expected function in humans as well as animals. We have therefore assessed the potential of K_V7 channel activators in the treatment of PH by investigating the functional expression of K_V7 channels and the actions of K_V7 modulating drugs in human distal PAs. The drugs used were the $K_V7.1$ selective blocker, chromanol 293B, the pan-K_V7 blockers, linopirdine and XE991, and the K_V7 channel activators, retigabine, flupirtine and zinc pyrithione (Robbins 2001; Xiong et al., 2007). Comparisons were made with human systemic resistance arteries, using the omental artery as a model. Similar expression profiles of *KCNQ* mRNAs were found in pulmonary and omental arteries and both vessels dilated in response to K_V7 activating drugs. The results demonstrate a similar role for K_V7 channels in human and rodent arteries, although species differences were apparent in the K_V7 channel subunits expressed and their pharmacology. By promoting smooth muscle cell hyperpolarisation, K_V7 activating drugs could rectify the depolarised condition that is commonly found in the smooth muscle cells of diseased PAs from both humans and animals (Osipenko et al., 1998; Smirnov et al., 1994; Suzuki and

Twarog, 1982; Yuan et al., 1998a), thereby suppressing Ca^{2+} signalling and downstream pathways.

2.3 Methods

2.3.1 Human Tissue samples

The use of human tissue for this study was approved by the South Manchester Research Ethics Committee (Reference 03/SM/396). Samples were collected with informed consent in compliance with the Helsinki Declaration (World Medical Association., 2013).

Normal lung samples were obtained from patients undergoing surgical resection for suspected or confirmed lung cancer and stored at 4°C until collection. A pathologist confirmed that no cancerous tissue was present. All collected samples were used for the study, without prior knowledge of the patient demographics, which are listed in Table 2.1. Tissue was transferred to the laboratory on ice and placed in ice-cold physiological salt solution (PSS) containing 122 mM NaCl, 5 mM KCl, 1 mM $MgCl_2$, 0.5 mM NaH_2PO_4, 0.5 mM KH_2PO_4, 10 mM (4-(2-hydroxyethyl)-1-piperazineethanesulfonic acid (HEPES), 11 mM glucose, and 1 mM $CaCl_2$, pH 7.3. Distal PAs were dissected from lung samples within 24 hr of tumour resection and connective tissue removed. Some vessels were used immediately for studies of vessel function with wire myography. All functional studies were completed no later than 48 h after tissue collection as vessel viability deteriorated beyond this time. For studies of gene and channel protein expression, other vessels were cut open longitudinally, then into small segments and submerged in RNA*later*® solution (Invitrogen, UK), according to the manufacturer's instructions, or snap frozen in liquid nitrogen and stored at -80°C for later analysis.

Biopsies of omentum were obtained from women with uncomplicated pregnancies undergoing elective Cesarean section at term and placed in ice-cold PSS. Small arteries (150-400 μm diameter) were dissected and used immediately for myograph studies. Some arteries were opened longitudinally and stored in RNA*later*® solution (Invitrogen, UK) for subsequent mRNA analysis. As each biopsy provided only a small amount of arterial tissue, samples from 3 patients were pooled for each RNA extraction.

Characteristic	Number	%
Age	64 ± 1 (range 44-80)	
Gender		
Male	22	50
Female	21	48
Undefined	1	2
Smoking & disease status		
Non smoker	4	9
Ex-smoker		
No other disease	11	25
COPD	8	18
Current smoker		
No other disease	12	27
COPD	6	14
Asthma	2	5
Undefined	1	2
Lobectomy Position		
Upper Right	11	25
Middle Right	3	7
Lower Right	6	14
Upper Left	11	25
Lower Left	6	14
Undefined	7	16
Medication		
None	32	73
SABA	1	2
MA	1	2
SABA + GC	2	5
LABA + GC	2	5
SABA + LABA + GC	3	7
MA + LABA + GC*	2	5
SABA + LABA + MA + GC	1	2

Table 2.1: Patient demographics. Medications at the time of recruitment included combinations of short acting β2 agonists (SABA), long acting β2 agonists (LABA), muscarinic antagonists (MA) and glucocorticoids (GC). * one patient also took pholedrine.

2.3.2 Rat pulmonary arteries

Male Sprague-Dawley rats (200-300g) were sacrificed via cervical dislocation. Experiments met the regulations outlined in the UK Scientific Procedures (Animals) Act 1986. Lungs were rapidly excised from the carcass and submerged in ice cold physiological salt solution (PSS). Intra-pulmonary arteries were dissected out from the lungs with all connective tissue removed before mounting a vessel on to the myograph.

2.3.3 Measurement of mRNA Expression

2.3.3.1 RNA isolation

Total RNA was isolated from tissue preserved in RNA*later* using an RNeasy Micro or Mini kit (Qiagen Cat # 74004 & 74104, UK), following their animal tissues protocol. Human iPA, stabilised in RNA*later*, was thawed at room temperature and transferred into a 2 ml tube containing 150 µl RLT lysis buffer with 1% β-mercaptoethanol and 295 µl nuclease-free water (Qiagen, UK. Cat #129114). β-mercaptoethanol irreversibly denatures RNases, thus inhibiting their ability to breakdown RNA. Tissue was then homogenised, 7 µl of proteinase K (Qiagen, UK. Cat #19131) was added and the homogenate incubated for 10 min at 55°C. Proteinase K rapidly inactivates DNA and RNA nucleases which may be released in the homogenisation step. The homogenate was then transferred to a QIAshredder column (Qiagen, UK. Cat #79654) followed by centrifugation at 16000 xg for 3 min. The supernatant was collected from the QIAshredder collection column and transferred to a new tube containing 0.5 volume of ethanol (Sigma Aldrich, UK. Cat #E7025). The mixture was transferred into an RNeasy column sitting in a 2 ml collection tube and centrifuged at 16000 xg for 45 sec. This process leaves the RNA bound to the silica-gel membrane contained within the spin RNeasy column. The spin column was washed by addition of 350 µl RW1 wash buffer and centrifuged at 16000 xg for 45 sec. On-Column DNase digestion was then performed to remove any genomic DNA using the RNase-free DNase kit (Qiagen, UK. Cat #79254). To perform DNase digestion, 80 µl of DNase I incubation mix (10 µl of DNase I stock solution in 70 µl of proprietary RDD buffer) was applied directly onto the spin column membrane and incubated at room temperature for 15 min. The spin column was then washed again with 350 µl RW1 wash buffer and centrifuged at 16000 xg for 45 sec. 500 µL RPE wash buffer was added to the spin column and centrifuged at 16000 xg for 45 sec followed by another addition of 500 µL RPE wash buffer to the spin column and centrifuged

at 16000 xg for 3 min. The RNeasy column was then placed in to a fresh 2 ml collection tube and centrifuged at 16000 xg for 2 min to ensure the membrane is completely dry. It is essential to remove all RPE wash buffer from the membrane as this contains ethanol which may interfere with downstream reactions. The RNeasy column was then transferred to a fresh 1.5 ml collection tube. Nuclease-free water (30-50 µl) was added directly to the spin column membrane and then the RNA is eluted into the water by centrifuging at 16000 xg for 1.5 min. The concentration of eluted RNA was quantified by the ND-1000 spectrophotometer (Thermo Scientific). The ratio of absorbance 260 nm/280 nm and 260 nm /230 nm ratios were recorded, as well as the concentration of the sample, as a measure of RNA purity. It is generally accepted that a 260 nm /280 nm ratio of ~2.0 corresponds to a "pure" RNA sample while a 260 nm /230 nm ratio lower than 2.0 indicates the presence of contaminants that absorb at 230 nm (Thermo Scientific Technical Bulletin).

2.3.3.2 RNA integrity

Although isolating RNA from cell cultures is fairly straightforward, harvesting RNA from tissues, particularly human tissues, is more challenging. RNA is thermodynamically stable, however, it can be rapidly degraded, which compromises its integrity. RNA integrity depends on the time to preservation, the metabolic profiles of the tissues, endogenous ribonuclease activity and natural RNA degradation (Schroeder et al., 2006). RNA samples that are not preserved efficiently will contain shorter RNA fragments, which can compromise results of downstream applications such as qRT-PCR (Fleige and Pfaffl, 2006; Fleige et al., 2006; Imbeaud et al., 2005).

The Agilent 2100 Bioanalyzer (Agilent Technologies, UK) was used to determine RNA integrity. The Bioanalyzer uses capillary electrophoresis to separate small samples of RNA (>5 ng) by molecular weight and subsequently detects the RNA sample via laser-induced fluorescence (Mueller et al., 2000; Schroeder et al., 2006). Samples were visualised as electrophoretic traces where the amount of measured fluorescence correlated with the amount of RNA of a given molecular weight. Analysis of the electrophoretic traces using a software algorithm permits the calculation of the RNA Integrity Number (RIN). The RIN is a value between 1 and 10, with 1 meaning the sample is completely degraded and 10 indicating the RNA sample is intact (Schroeder et al., 2006). Samples with an RIN >5 are recommended by Fleige & Pfaffl (2006). The Agilent 2100 Bioanalyzer used in this study

belongs to the Genomic Technologies Core Facility, University of Manchester. A special thanks goes to Michal Smiga for running the samples on the Bioanalyzer.

2.3.3.3 cDNA synthesis

Only samples with an RIN >5 were used for mRNA analysis. To reverse transcribe the RNA to cDNA, 100 ng or 150 ng of total RNA was mixed with 1 µl random hexamers (50 µM, Roche, UK. Cat #N12470), 0.5 µl dNTPs (10 mM, Invitrogen, UK. Cat #18427-013) and nuclease-free water to make the volume up to 13 µl. The reaction mixture was heated to 65 °C, using the thermal cycler, for 5 min to enable the random hexamers to bind and then incubated on ice for 1 min. Next, 4 µl of first strand buffer, 1 µl dithiothreitol (DTT, 0.1 M) and 1 µl RNAseout (Invitrogen, UK. Cat #100000840) were added to the reaction mixture. The reducing agent DTT and RNAseout serve to inhibit the activity of ribonucleases, which would degrade the RNA if left untreated. The reverse transcriptase enzyme, Superscript III (Invitrogen, UK. Cat #18080-044; 1 µl), was then added to the reaction mixture, followed by incubation at 42 °C for 5 min in the thermal cycler. For reverse transcription (RT) negative controls, the reaction was carried out without reverse transcriptase (RT-) and instead 1 µl nuclease-free water was added to make the reaction up to volume. The RT- reactions control against genomic DNA contamination in the RNA. The reaction mixture, including RT- controls, was then incubated at 55°C for 1 hr, followed by enzyme inactivation by increasing the temperature to 70 °C for 15 min. The cDNA synthesised was used as a template for amplification in the PCR.

2.3.3.4 End-point PCR

End-point polymerase chain reaction (PCR) was used to detect the presence of channel subunit mRNAs. First-strand cDNA (5 µl), or its respective negative control, was used as the template in a PCR reaction also including forward and reverse primers (MWG Biotech, Ebersberg, Germany, 0.5 µM each) and 1 µl Hotstart Taq polymerase mastermix (Qiagen) in a reaction volume of 20 µl. The reaction mix was heated to 95°C for 15 min followed by 32 or 36 repetitions of the following cycle: denaturation (95°C, 20 s), annealing and extension (60 °C, 70 s). PCR products were analysed using 1.5% agarose gel electrophoresis and visualised with ethidium bromide under untraviolet illumination, using a GelDoc2000 system to capture the images (Bio-Rad, Hercules, CA, USA). The specificity of the reaction

was confirmed by sequencing products of the expected size (DNA sequencing facility, University of Manchester).

2.3.3.5 Quantitative RT-PCR

SYBR Green detection was used to quantify expression levels of *KCNQ* mRNAs by real-time, quantitative PCR (qPCR). Reactions were carried out in 20 µl volumes containing 5 µl template, 4 µl water, 10 µl SYBR Green master mix and 7.5 pmol each primer, using an Applied Biosystems 7500 PCR instrument (Foster City, CA), according to the manufacturer's instructions. Cycling parameters were 95°C for 15 min followed by 40 cycles at 95°C for 1 min and 60°C for 1 min. A dissociation step was routinely performed for melt curve analysis, with a single peak representing specificity. Primer efficiency was corrected using the comparative quantitation method described by Pfaffl (2001). Each reaction was performed in duplicate and repeated on 9 pulmonary artery samples and 3 pooled omental artery samples.

2.3.3.6 Primers

The primers used to amplify mRNAs coding for subunits of K_V7 channels are listed in Table 2.2. The primers for *KCNQ2*, *KCNQ4* and *KCNQ5* were from Primer Design (Southampton, UK). Primers for *KCNQ1* and *KCNQ3* were designed using Primer 3 software (v.0.4.0; Whitehead Institute and Howard Hughes Medical Institute, http://primer3.sourceforge.net/) so as to amplify intron-spanning sequences. The primers for *KCNE 1-5* genes (Table **2.3**) were as described previously (Lundquist et al., 2005).

Gene	Accession Number	Primer (5'-3')	Product length (bp)
*KCNQ*1	NM_000218	For: ATTCGACGCATGCAGTACTT	122
		Rev: AACCTCATGGTGCGCATCAA	
*KCNQ*2	NM_172107	For: CCACCATCAAGGAGTATGAGAAG	102
		Rev: TACTTCGTGCGGATCTGGG	
*KCNQ*3	NM_004519	For: AGGTGGATGCACAAGGAGAG	159
		Rev: AGGTGGATGCACAAGGAGAG	
*KCNQ*4	NM_004700	For: CGCCTCCTTCCTGGTCTAC	104
		Rev: ATTACATTGACAACCATCGGCT	
*KCNQ*5	NM_019842	For: AGCAGAACATGAGACCACCAGA	124
		Rev: CATCTATCAACAGGTCCTTCGG	

Table 2.2: *KCNQ1-5* Primers for RT-PCR. Forward (For) and reverse (Rev) primers for genes with the indicated accession numbers to amplify transcripts with the base pair (bp) length indicated.

Gene	Accession Number	Primer (5'-3')	Product length (bp)
*KCNE*1a	NM_000219.4	For: GGAGGAAGGCATTATCTGTATCCA	99
		Rev: TCCTGGGCATTAAGGTTCCA	
*KCNE*1b	NM_001127670.2	For: TCACTGTGCAAGCTACAAAAGCT	142
		Rev: TCACCGCTGTGGTGTTAGACA	
*KCNE*2	NM_172201.1	For: CAGAACAGCCTGGCTTTGGA	99
		Rev: TCCAGCGTCTGTGTGAAATTG	
*KCNE*3	NM_005472.4	For: ACTGAGAGCCAGTGGATTTGC	99
		Rev: AGGTCTCCGTTCCATTGGTAGTC	
*KCNE*4	NM_080671.3	For: AACCCTCTTGGACTGGACGAT	99
		Rev: AGGCTCCATTTTCAGCATTGA	
*KCNE*5	NM_012282.2	For: CCCCTACCCCGCACATC	107
		Rev: TTGGACGTGTTGGATTCAGTTC	

Table 2.3: *KCNE1-5* Primers for RT-PCR. Forward (For) and reverse (Rev) primers for genes with the indicated accession numbers to amplify transcripts with the base pair (bp) length indicated.

2.3.3.7 Primer Efficiency

Primer efficiency is an important factor in qRT-PCR. In theory, primers with 100% efficiency would double the amount of amplicon (product) with every cycle. Threshold cycle (Ct) values for serial template dilutions in water are correlated to the logarithm of the dilution factor, and the gradient (Equation 1) is a measure of primer efficiency. Primer efficiency was verified by constructing standard curves, which plot Ct as a function of the log copy number of the gene. A standard curve slope of –3.32 indicates 100% PCR efficiency. A slope more negative than –3.32 indicates PCR efficiency below 100% efficiency, while a slope more positive than –3.32 may indicate poor sample quality or a pipetting error.

Equation 1 $$Primer\ efficiency\ (\%) = \left(10^{\frac{-1}{slope}} - 1\right) x\ 100$$

At the end of each qRT-PCR, a dissociation step was performed to determine if only one product was amplified during the reaction. Here the temperature of the reaction was raised while fluorescence was measured. As the temperature increases, double-stranded cDNA (with attached SYBR green) dissociates into single strands, thus decreasing the fluorescence. The data obtained from this were used to produce a dissociation (or melting) curve, visualised as the change in fluorescence/change in temperature on the y-axis against temperature on the x-axis. If the reaction only amplified one product, then the fluorescence should be reduced dramatically at one temperature, whereas if two or more products of different base pair length were present, the fluorescence would be reduced at multiple temperatures.

2.3.3.8 qRT-PCR normalisation

The use of housekeeping genes , also referred to as reference genes, is the preferred way of normalising qRT-PCR data to correct for differences in RNA load between samples (Suzuki et al., 2000; Thellin et al., 1999). They provide an internal control that is affected by the same sources of variation during experimental procedures as the genes of interest. For housekeeping genes to be valid, ideally they should not vary in the samples under investigation. However, the drawback is that there is extensive evidence demonstrating that the expression of frequently used housekeeping genes can be highly variable between samples in some circumstances (Dheda et al., 2004; Eskesen et al., 2007; Foss et al., 1998; Glare et al., 2002; Schmittgen and Zakrajsek, 2000; Tricarico et al., 2002). To overcome this problem, stable expression of housekeeping genes used within an experiment must be verified before using them to normalise. Mathematical algorithms have been developed to verify the stability of candidate housekeeping genes. The most commonly used algorithms are geNorm (Vandesompele et al., 2002) and BestKeeper (Pfaffl et al., 2004); both were used in this study.

GeNorm is based on the principle that ideal housekeeping genes would have consistent expression across all samples. For each candidate housekeeping gene, the pairwise variation with all other candidate housekeeping genes is calculated as the standard deviation of the logarithmic transformed expression ratios. In theory, two ideal housekeeping genes would have an expression ratio of 1, therefore the further away values

are from 1 the more unstable the expression is between those 2 candidate housekeeping genes. The M-value for each candidate housekeeping gene a measure of gene stability, is calculated as the average pairwise variation of a particular candidate housekeeping gene with all other tested candidate housekeeping genes. The lowest M indicates the candidate housekeeping gene with the most stable expression. GeNorm also determines the optimal number of housekeeping genes for normalisation, since using one housekeeping gene can still lead to significant error (Vandesompele et al., 2002). The software calculates the normalisation factor as the pairwise variation Vn/n+1, were Vn is the normalisation factor for the two housekeeping genes with the lowest M-value. The software includes more candidate housekeeping genes in a stepwise manner until the addition of a gene has no significant effect on the calculated normalisation factor.

BestKeeper is based on the principle that true housekeeping genes should display a similar expression pattern and so their expression levels should be highly correlated. BestKeeper calculates a Pearson correlation coefficient (r) for each pair of candidate housekeeping genes and determines the probability that the correlation is significant. All highly correlated candidate housekeeping genes are combined to form an index value (normalisation factor) by calculating the geometric mean. The relationship between the index and the contributing housekeeping gene is described by the Pearson correlation coefficient, the coefficient of determination (r2) and the p-value. The Pearson correlation coefficient measures the strength and the direction of a linear relationship between the index and the contributing housekeeping gene. The coefficient of determination indicates the proportion of the variance of one candidate housekeeping gene that is predictable from the index.

Pulmonary artery expression was compared to either heart (*KCNQ1*), or brain (*KCNQ3-5*), using human heart and brain cDNAs supplied by Primer Design (UK), or omental arteries (*KCNQ1*, *3-5*). The candidate housekeeping genes used were β-actin (*ACTB*), glyceraldehyde-3-phosphate dehydrogenase (*GAPDH*), phospholipase A2 (*YWHAZ*), topoisomerase I (*TOP1*) and hypoxanthine phosphoribosyltransferase 1 (*HRTP1*), β2-microglobulin (*B2M*). The primers were supplied by Primer Design (UK) as part of their human GeNorm kit (Cat #: ge-PP-6).

2.3.4 Western blot

Human iPAs were snap frozen in liquid nitrogen and stored at −80 °C until required for lysis. Protein was extracted from arteries using a manual glass homogeniser (Wheaton industries, from VWR, UK) with ice cold radioimmunoprecipitation (RIPA) lysis buffer (80 µL) comprising: 25 mM Tris-HCl pH 7.5, 150 mM NaCl, 1% NP-40 (v/v), 0.5% sodium deoxycholate (w/v), 1 mM ethylenediaminetetraacetic acid (EDTA), 1% sodium dodecyl sulfate (SDS) (w/v) and 1x protease inhibitor cocktail (cOmplete, Mini, Ethylenediaminetetraacetic acid (EDTA)-free, Roche, UK). To isolate proteins from cells, the cells were washed in phosphate buffered saline (PBS) and lysed on ice using 150 µL RIPA lysis buffer, while using a cell scraper to remove cells from the bottom of the culture dish. Lysates were passed through a 22-gauge syringe needle several times to shear genomic DNA and then placed in a test-tube rotor for 30 min at 4°C to aid lysis. Samples were centrifuged at 1000 g for 2 min with the resulting supernatant frozen at -80°C. The same method was employed on rat iPA and heart samples to obtain lysates. The total protein concentration was determined using a bicinchoninic acid (BCA) protein assay kit (Thermo Scientific Pierce, UK), according to the manufacturer's instructions. The total protein concentration of each lysate was determined by measuring the absorbance of each sample mixture in triplicate at 570 nm, using a PowerWave 340 microplate spectrophotometer (BioTek) and comparing it with a standard curve constructed with known concentrations of bovine serum albumin (BSA).

Supernatants were incubated at 95°C for 7 min with 1x laemmli loading buffer composed of 25 mM Tris-HCl, 2% SDS (w/v), 10% glycerol, 5% (w/v) β-mercaptoethanol, 0.04% (w/v) bromophenol blue, pH 6.8. Protein samples were separated by 10% SDS-PAGE for 2.5 hr at 100 V using the Mini-PROTEAN® 3 Cell electrophoresis apparatus (Bio-Rad, UK). Protein samples were then transferred by electrophoresis for 1 hr at 110 V, using the Trans-blot® Cell apparatus (Bio-Rad, UK), onto an immobilon-P PVDF membrane (Millipore, UK).

Following protein transfer, membranes were washed 3x (5 min per wash) in Tris-buffered saline (TBS), containing 25 mM Tris-HCl and 150 mM NaCl (pH 7.3) with 0.1% Tween-20 (v/v; TTBS), before being incubated at room temperature for 1 hr with blocking solution containing 5% milk powder (w/v) in TTBS. Following another 3x 5 min washes in TTBS, membranes were incubated overnight at 4°C with the appropriate primary antibody, diluted in 1% milk powder (w/v) in TTBS. Primary antibodies used in this study were anti-

KCNQ4 mouse (Cat# 75-082, NeuroMab, CA), anti-β-tubulin (Sigma) and anti-α-actin (Cat# A3853, Sigma). Following overnight incubation, membranes were washed 3x in TTBS for 5 min per wash and then incubated at room temperature for 2 hr with the appropriate horseradish peroxidase-conjugated secondary antibody, diluted in 1% milk powder (w/v) in TTBS. The secondary antibody used in this study was anti-mouse raised in goat (Jackson ImmunoResearch, UK) Membranes were then washed 6x in TTBS for 10 min per wash before being treated with SuperSignal West Pico or Femto Chemiluminescent Substrate kit (Thermo Scientific, UK). Immunoreactive proteins were detected using the ChemiDoc™ system (Bio-Rad, UK).

To generate a source of $K_V7.4$ protein, complementary DNA (cDNA) for the human *KCNQ4* gene was transfected into HEK-293T cells. Untransfected cells served as a negative control. A plasmid encoding human *KCNQ4* (GenBank accessionnumber: AF105202) was kindly provided by Dr Nikita Gamper (University of Leeds, UK). *KCNQ4* was subcloned into pcDNA3.1zeo- (Invitrogen) using XhoI–HindIII. Human Embryonic Kidney 293T (HEK-293T) cells were cultured in 100 mm tissue culture dishes using Dulbecco's modified Eagle's medium (DMEM; Sigma) supplemented with 10% fetal bovine serum (FBS; Sigma), L-glutamine (Invitrogen) and Gentamicin (Sigma). Once cells reached ~50% confluency they were transfected with *KCNQ4* pcDNA3.1zeo using X-tremeGENE9 DNA transfection reagent (Roche, UK) according to the instructions of the manufacturer.

2.3.5 Myography

2.3.5.1 Mounting vessels

Artery segments (~2 mm long), were cleaned of surrounding connective tissue and threaded through parallel fixed and adjustable mounting pins in a small vessel myograph (Danish Myo Technology, Model 610M). Figure 2.1 displays the experimental set up used for myograph experiments. One pin is attached to a micrometer, allowing the researcher to control vessel diameter. The other pin is fixed in position and attached to a force transducer capable of measuring changes in vessel tension of 0.01 mN. The force transducer is connected to a computer via an analogue to digital interface (National Instruments USB-6221-BNC). The data produced by the force transducer was displayed and recorded using the software program Chart (J.Dempster, University of Strathclyde, Glasgow). In the myograph chamber the vessel was submerged in pre-warmed

physiological salt solution and maintained at 37°C for the entire experiment. The suction allows vessels to be washed by completely replacing the bath solution. Room air can also be bubbled into the chamber solution to ensure the concentration of drugs remains homogenous. The myograph used in this investigation contained 4 separate 5 ml chambers, thus enabling 4 investigations to be carried out concurrently.

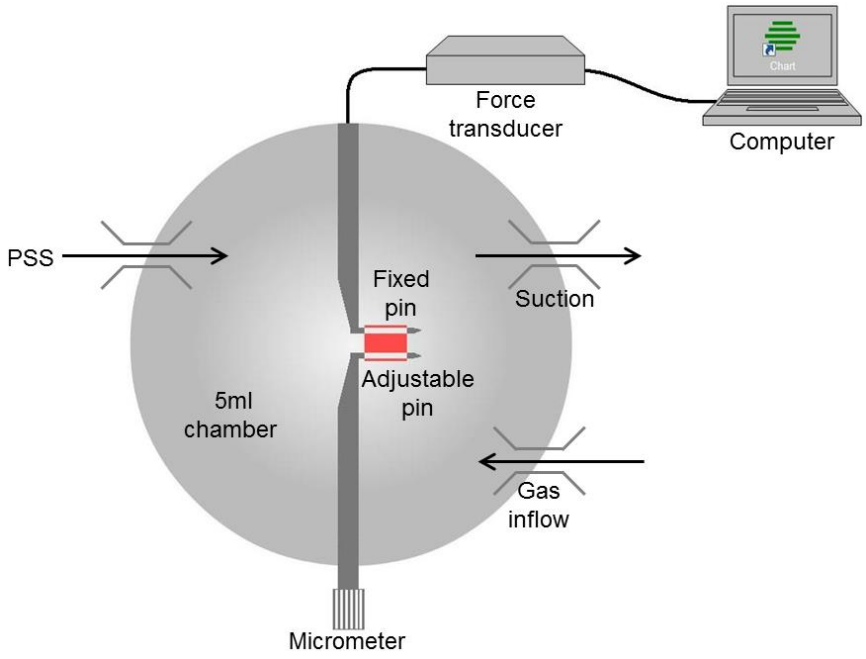

Figure 2.1:Schematic demonstrating the myograph set-up. A vessel is mounted between two parallel pins. One pin is connected to a micrometer, which is used to apply tension at the start of experiments, and the other to an isometric force transducer that measures vessel wall tension. Inflow tubes allow the addition of solution and bubbling with air. Suction provided by a vacuum pump removes solution from the chamber. Tension is continually recorded and saved on a computer running the Chart software.

2.3.5.2 Normalisation protocol

At the start of all myograph experiments, a basel level of tension must be applied to the vessel. Without this basel tension it would be impossible to measure any alterations in vascular tone. Since the response of a vessel to agonists is dependent on the degree of stretch, it is important that the amount of applied tension is clearly defined (Mulvany 1998). Also, since the active response of a vessel is dependent on the extent of stretch, it is useful to set vessels to an internal circumference that gives the maximum response.

At the beginning of the normalisation procedure the preparation was subjected to a small load (~2 mN) and challenged with 50 mM KCl until the contraction plateaued. Using the micrometer, the vessel was then challenged with 50 mM KCl at increasing increments of tension until the maximum response to 50 mM KCl was achieved. The ring preparation was maintained at this tension and experiments proceeded under isometric conditions. The tension required to produce the maximum response to 50 mM KCl is heavily dependent on the vessel properties (e.g. species and morphology), thus the normalisation protocol was performed for each type of vessel to be investigated.

In experiments investigating the effects of K_V7 channel blocking drugs on human PA, a basal tension of 5 mN was applied, before leaving the vessels to equilibrate for 30 min. In preliminary experiments this level of tension appeared to result in the maximum response to 50 mM KCl: it is estimated to give an equivalent wall pressure of around 10 mmHg in a 600 μm diameter artery. In these conditions, agonists of α-adrenergic, endothelin and serotonin receptors failed to cause substantial or sustained constriction, precluding experiments designed to investigate the effects of K_V7 channel activators. For the latter studies a higher basal tension of 7 mN, equivalent to 14 mmHg in a 600 μm artery, was applied and resulted in more consistent and sustained agonist-induced constriction.

2.3.5.3 Vessel validation protocol

Once the ring preparation was under optimum isometric conditions, vessel integrity was validated by challenging the vessel with 50 mM KCl for 6 min, followed by washing with fresh PSS. This procedure was repeated a further two times. Arterial ring preparations with good integrity reached peak contraction within 5 min of KCl application and also maintained a constant basal tone between applications. Before using the ring preparation for an experiment, vessels that responded well to the validation protocol were given fresh PSS and left undisturbed for 15 min to ensure baseline tone remained stable.

2.3.5.4 Endothelium integrity

The myograph presents researchers with the opportunity to study the tension developed by vessels of various sizes, from small resistance arterioles to arteries as large as 1 mm diameter (Mulvany 1998)). However, poor dissection of the vessels can cause disruption to the integrity and structure of the preparation. The most likely way vessel structure could be

altered during dissection is by accidental removal of the endothelial layer when mounting the preparation on to the myograph. Initial experiments set out to determine if the endothelial layer from rat iPAs was damaged during dissection. To investigate this, acetylcholine and carbachol were applied to induce endothelium-depended relaxation to agonist pre-constricted rat iPAs. Previous studies have shown that 10 µM acetylcholine or carbachol cause male Sprague-Dawley rat PAs to relax by at least 77% (Karamsetty et al., 2001; Yamaguchi et al., 1989). In contrast, endothelium-denuded PAs produce negligible relaxation to 10 µM acetylcholine (Yamaguchi et al., 1989). The vasorelaxation is dependent upon the activation of M_1 and M_3 muscarinic receptors present on the endothelial cells, which initiate a rise in the intracellular Ca^{2+} concentration and release of relaxing factors (Norel et al., 1996). If the dissection compromised the integrity of the endothelial layer, the relaxation produced by acetylcholine or carbachol would be substantially reduced.

For experiments on human iPAs, where indicated, endothelium was disrupted by gently rubbing the vessel lumen with a roughened wire or by inhibiting the release of endothelium-derived nitric oxide with 300 µM L-nitro-arginine methyl ester (L-NAME) added to the myograph chamber.

2.3.5.5 Experimental protocols for K_V7 blockers

The effects of the K_V7 channel blocking drugs linopirdine, XE991 and (-)chromanol 293B were tested by applying them to vessels at resting tone. The drugs were applied in a cumulative manner at 20-30 min intervals, at concentrations ranging from 1 nM to 100 µM, with increments being made after artery tone achieved a plateau. The L-type VGCC antagonist, nifedipine (100 nM), was used to inhibit voltage-gated Ca^{2+} influx and determine its role in the constrictor response.

2.3.5.6 Experimental protocols for K_V7 activators

To assess the vasodilator ability of K_V7 activating drugs (retigabine, flupirtine and zinc pyrithione), vessels were pre-constricted with phenylephrine (1 or 10 µM), endothelin-1 (1 or 10 nM) or serotonin (10 µM). When constriction reached a plateau, a K_V7 channel activator was applied cumulatively at concentrations from 1 nM to 200 µM. Resulting relaxation was measured as percent reduction of the agonist induced tone present before adding the drug.

The role of membrane hyperpolarisation and loss of voltage-gated Ca^{2+} entry in the vasodilation evoked by retigabine was addressed by comparing its ability to dilate arteries under conditions that either enhanced or by-passed Ca^{2+} entry through L-type VGCCs. To deplete the K^+ gradient across the smooth muscle cell membrane and prevent K^+ efflux in response to K^+ channel opening, vessels were pre-constricted with PSS in which the K^+ concentration was raised to 90 mM by equimolar substitution of KCl for NaCl. Raising the K^+ concentration evokes constriction by activating voltage-gated Ca^{2+} entry. Pre-constriction was alternatively induced with Bay K 8644 (1 μM), a direct activator of Ca^{2+} entry through L-type VGCCs or the Ca^{2+} ionophore, ionomycin (3 μM), which was used to induce constriction as a consequence of voltage-independent Ca^{2+} entry.

2.3.6 Drugs

Phenylephrine hydrochloride (PE), serotonin creatinine sulfate (5-HT), endothelin-1 (ET-1), L-nitro-arginine methyl ester (L-NAME), zinc pyrythione (ZnPy), nifedipine and ionomycin were from Sigma-Aldrich (Poole, UK). Linopirdine dihydrochloride, XE991 dihydrochloride, racemic chromanol 293B, (-)-[3R,4S]-chromanol 293B and flupirtine maleate were from Tocris Bioscience (Bristol, UK). Retigabine dihydrochloride was supplied by Toronto Research Chemicals Inc. (Toronto, Canada) and (±) BayK 8644 by R&D Systems Europe (Abingdon, UK).

PE, 5-HT, L-NAME, linopirdine, XE991 and retigabine were dissolved in water to provide 10 or 100 mM stock solutions. ET-1 was prepared as a 100 μM stock solution in water. Nifedipine, flupirtine, ZnPy, ionomycin and Bay K 8644 were prepared as 10 or 100 mM stock solutions in dimethylsulphoxide (DMSO). All drugs were diluted to the working concentration in PSS so that the vehicle volume did not exceed 1% of the final bath volume.

2.3.7 Data analysis

Data handling and statistical analysis were performed in Microsoft Excel and GraphPad Instat (GraphPad Software Inc., La Jolla, CA, USA) software. Data in text and figures are represented as means ± SEM. For EC_{50} calculations, concentration–response curves were fitted using the Hill equation. Normality of data was assessed using the Shapiro–Wilk test and parametric or non-parametric statistical tests applied accordingly. Groups of data were compared using the Student's t-test or Mann–Whitney U test. Data samples were considered as significantly different if $P< 0.05$.

2.4 Results

2.4.1 RNA quality

Figure 2.2 shows the output of the Bioanalyzer analysis of RNA samples from each of 9 patients. The average RIN value was 7.77 ± 0.15 (n=9).

2.3.2.8 Primer Efficiency and specificity

The data represented in Figure 2.3 indicate the efficiencies and specificities of the primers used in qPCR to amplify the *KCNQ* genes present in human PA. The single peak in each dissociation curve indicates that, for each gene, a single DNA species was amplified. The correlation co-efficient for each standard curve was close to 1, indicating a linear relationship between Ct value and template concentration for all the *KCNQ* primer pairs. The slopes of the standard curves constructed for the *KCNQ* primers all lay within the range -3.3 to -3.6, equating to efficiencies of 97% for *KCNQ1* and *KCNQ3*, 88% for *KCNQ4* and 98% for *KCNQ5*.

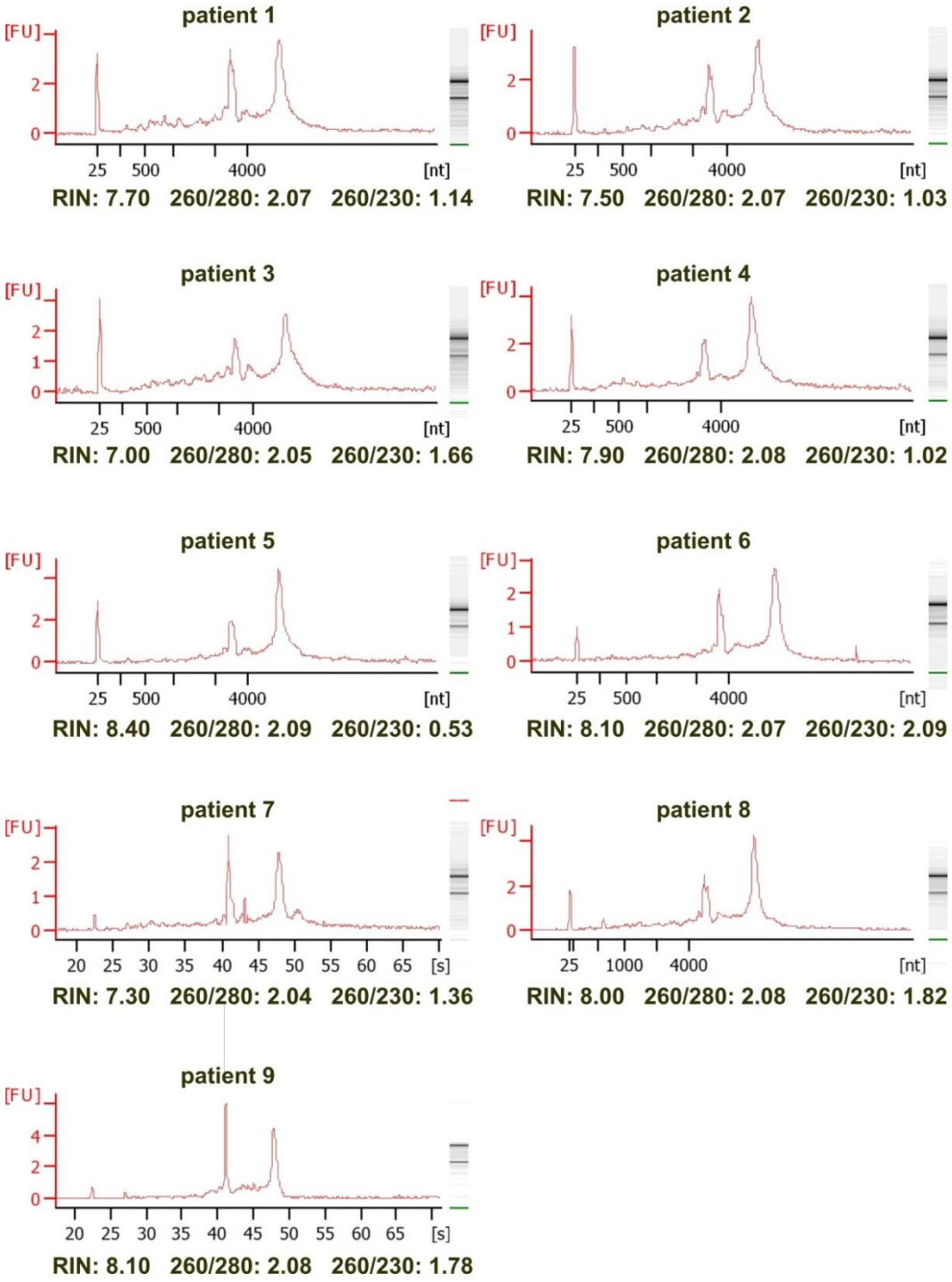

Figure 2.2: Human intra-pulmonary artery mRNA preparations analysed by the Agilent 2100 bioanalyzer. Data displayed as electropherograms as well as gel-like images. The RIN calculated by the Agilent 2100 bioanalyzer are displayed, plus the 260 nm/280 nm and 260 nm/230 nm ratios assessed by a spectrophotometer. Graphs show arbitrary fluorescence vs time of detection which is an indication of molecular size. RIN and ratios for each RNA sample shown below each plot.

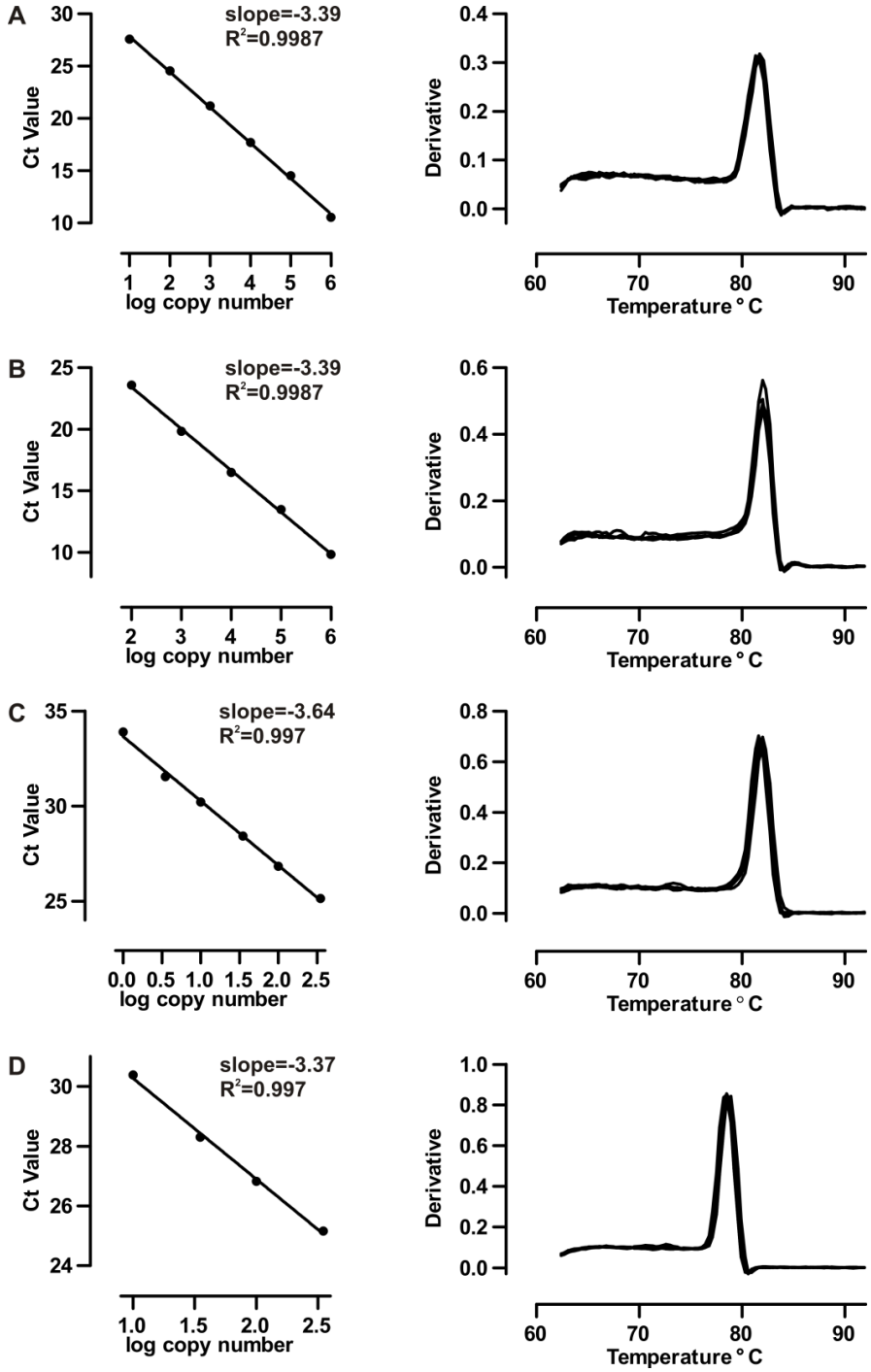

Figure 2.3: qRT-PCR standard and dissociation curves for *KCNQ1*, *KCNQ3*, *KCNQ4* and *KCNQ5* primers. The standard curves (left) were generated using serial dilutions (log copy number) of DNA templates for *KCNQ1* (A), *KCNQ3* (B) *KCNQ4* (C) and *KCNQ5* (D). Dissociation curves (right) are plotted as the fluorescence derivative (change in fluorescence/change in temperature) against temperature.

2.4.2 Housekeeping gene selection

The variation of 6 candidate housekeeping genes are shown in whisker plots (Figure 2.4), demonstrating the clear difference between the genes. Dheda et al (2004) proposed that a standard deviation of less than one Ct value from the mean expression level is a requirement for any candidate housekeeping gene. BestKeeper software calculated that the only candidate housekeeping gene that did not fulfil this criterion was *B2M* with a Ct standard deviation of 1.14. When excluding the heart Ct values, *GAPDH* had a standard deviation of 0.74 but this was increased to 0.98 when including the heart sample, this demonstrated that *GAPDH* was not stably expressed in heart and PA samples. This variation can be seen by comparing *GAPDH* in Figure 2.4A and Figure 2.4C.

BestKeeper software calculated that all candidate housekeeping genes, except GAPDH, had a strong Pearson correlation coefficient ($r > 0.6$) and coefficient of determination ($r2 > 0.52$) with the normalisation index. Thus, BestKeeper demonstrated that all candidate housekeeping genes except B2M (due to the large standard deviation) were acceptable to use when comparing the expression between iPA and brain. However, since the expression of *GAPDH* is considerably higher in the heart compared to iPA, it was deemed a poor housekeeping gene to use when comparing heart and iPA expression.

geNorm software obtained similar results to BestKeeper. This program calculated that the geometric mean of *YWHAZ*, *HRTP*, *TOPI*, *ACTB* and *GAPDH* should be used when comparing iPA with brain samples (V=0.157), but that the geometric mean of *YWHAZ*, *HRTP*, *TOPI* and *ACTB* should be used when comparing iPA with heart samples (V=0.194). Expression in pulmonary and omental arteries was compared after normalising each *KCNQ* gene to the geometric mean of 3 housekeeping genes (*B2M*, *HRTP*, *TOPI*).

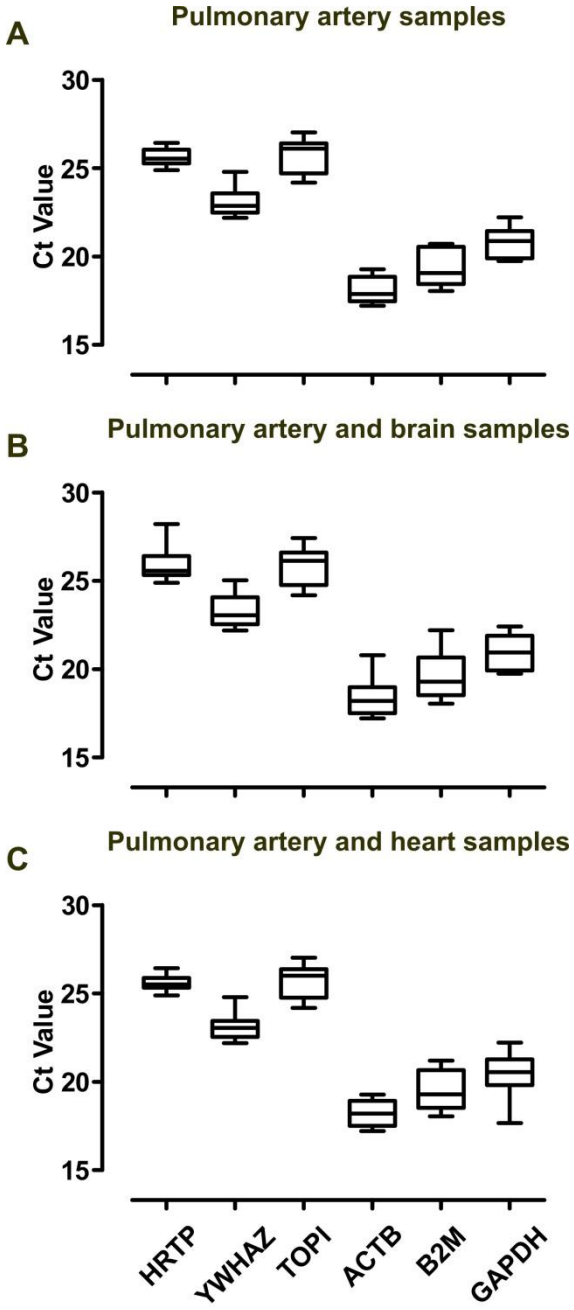

Figure 2.4: Real-time PCR candidate housekeeping gene cycle threshold values. Variation in Ct value of candidate housekeeping genes in 9 iPA samples (A), 9 iPA and 1 brain samples (B) and 9 iPA and 1 heart samples (C) are presented as box-whisker plots. *HPRT*, hypoxanthine phosphoribosyltransferase; *YWHAZ*, tyrosine 3-monooxygenase/tryptophan 5-monooxygenase activation protein zeta polypeptide; *TOPI*, topoisomerase I; *ACTB*, β-actin; *B2M*, β2-microglobulin; *GAPDH*, glyceraldehyde-3-phosphate dehydrogenase.

2.4.3 K_V7 channel expression in human intra-pulmonary and omental arteries

The expression of *KCNQ* subunit mRNAs was initially investigated in whole iPAs. End-point RT-PCR showed that the arteries express mRNA for *KCNQ1*, *KCNQ3*, *KCNQ4* and *KCNQ5*, but not *KCNQ2* (Figure 2.5A). To determine if the expression was localised in smooth muscle cells, RT-PCR was also performed on the isolated smooth muscle layer, obtained by carefully stripping off the adventitia, opening up the vessel and rubbing off the endothelium. As shown in Figure 2.5A, the muscle layer showed the same pattern of mRNA expression as the intact vessels. Since we previously found a difference in *KCNQ4* expression between pulmonary and mesenteric arteries in rats (Joshi et al., 2009), a similar comparison was carried out in human tissue, using the omental artery as a representative example of systemic resistance arteries. Omental artery was found to express the same transcripts as PA (Figure 2.5A). Figure 2.5B shows the results of qPCR analysis of RNA isolated from human pulmonary and omental arteries. The iPAs from 9 patients expressed all 4 transcripts with similar relative expression. A similar profile of *KCNQ* mRNAs was apparent in both arteries, although there may be higher expression of *KCNQ5* in the iPAs. The expression of *KCNQ1* mRNA in iPAs was also compared with heart, where it is highly expressed and forms a K^+ channel that contributes to repolarisation of the cardiac action potential (Charpentier et al., 2010). Figure 2.5D shows that *KCNQ1* mRNA expression in iPA was about a quarter of that in the heart sample tested. *KCNQ3* and *KCNQ5* contribute to the neuronal I_{KM} and are expressed in many areas of the brain (Jensen et al., 2005; Tinel et al., 1998). *KCNQ4* is also expressed in the brain, but especially the auditory pathway (Kubisch et al., 1999). The iPA expression of *KCNQ3*, *4* and *5* was therefore compared with brain and appeared to be more highly expressed in the artery (Figure 2.5C).

Functional K_V7 channels may also contain auxiliary subunits, which modify their properties. Five human genes, denoted *KCNE1-5*, give rise to proteins that play this role (Cai et al., 2006). We therefore explored the expression profile of *KCNE* mRNAs in human iPA as illustrated in Figure 2.5B. The *KCNE1b* transcript is thought to be a cardiac specific isoform (Lundquist et al., 2005) and it was absent from the iPA samples, but primers designed to detect the *KCNE1a* isoform did detect the presence of the *KCNE1* subunit. All 4 iPAs tested also showed expression of *KCNE2*, *KCNE3* and *KCNE5*, while *KCNE4* expression was detected in 2 out of 3 samples.

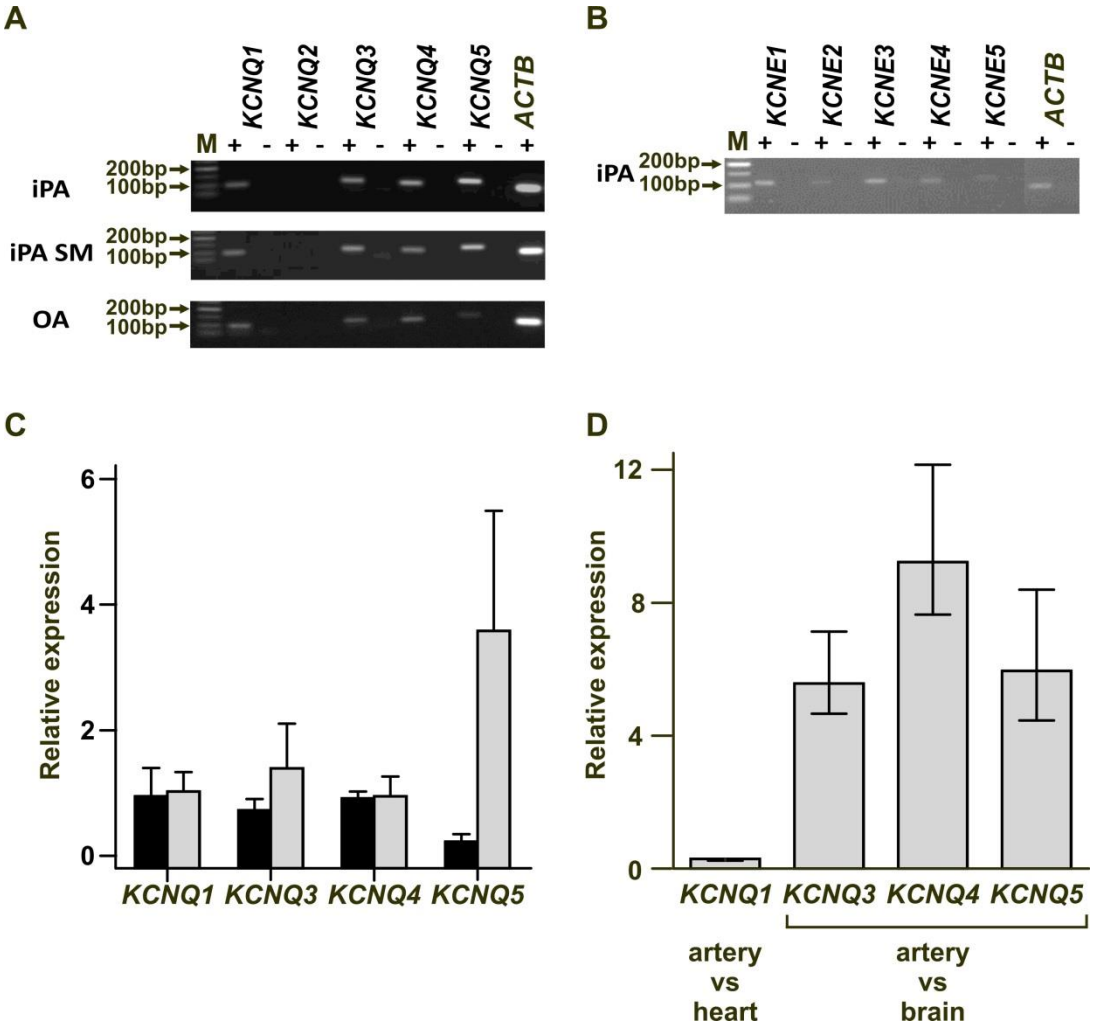

Figure 2.5: K_V7 channel subunit expression in human intra-pulmonary and omental arteries. (A) End point RT-PCR using primers for *KCNQ* subunits 1-5 in iPAs (n=3), a iPA sample denuded of endothelium and adventitia (IPA SM) and omental arteries (n=3). *ACTB* is shown as a loading control. (B) End point RT-PCR with primers for *KCNE* (*1-5*) subunits and *ACTB* on iPAs (n=4). (C) *KCNQ* gene expression measured by qPCR in human iPA (grey bars) and omental (black bars) arteries and expressed relative to the geometric mean of 3 housekeeping genes. Bars show mean + s.e.m. (D) qRT-PCR measurement of *KCNQ* mRNA in iPA expressed relative to human heart (*KCNQ1*) or brain (*KCNQ3-5*) after normalizing to the geometric mean of 4 (heart: *ACTB, YWHAZ, TOP1, HRTP1*) or 5 (brain: + *GAPDH*) housekeeping genes. Bars represent mean and confidence intervals. The experiments on omental arteries were done by the post-doctoral researcher Katie Smith.

Out of three human iPA lysates used for detection of $K_V7.4$, a band at the expected molecular weight (77 kDa) was only detected in one lysate (Figure 2.6A). No band was detected in non-transfected HEK cells while in cells transfected with *KCNQ4*, a positive band at the expected molecular weight for $K_V7.4$ was observed. Bands for $K_V7.4$ were also detected in rat iPA and whole heart lysates. Staining for β-tubulin (Figure 2.6B) yielded no bands in any of the three human iPA lysates while a band at the correct molecular weight (51 kDa) was detected in all other lysates. Staining for α-actin (Figure 2.6C) yielded a band at the expected molecular weight (42 kDa) in two of the human iPA lysates, although the band in one of these lysates was particularly faint. The rat iPA and heart lysates also stained positive for α-actin while the HEK cells (both non-transfected and transfected) did not. When using ponceau (Figure 2.6D) to stain the membrane, no bands were detected in any of the HEK cell lysates which is most likely due to the small amount of total protein used within those lanes. The ponceau stain provided a smudged appearance in the human artery lysates, while distinct bands (of various sizes) were detected in the rat iPA and heart lysates.

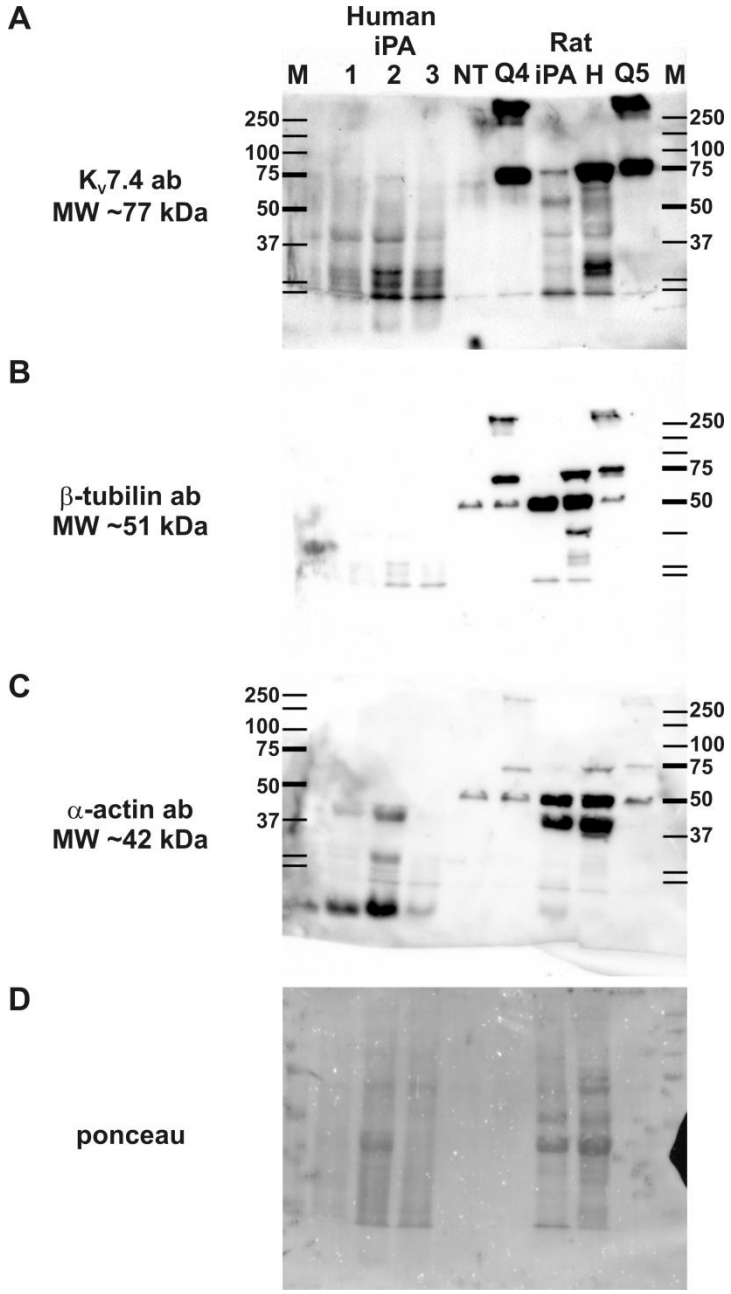

Figure 2.6: Expression of the K_V7.4 α-subunit in human intra-pulmonary artery. Immunoblots showing bands for K_V7.4 (A), β-tubulin (B) and α-actin (C) antibodies with molecular weight markers shown at the two ends of the blots. Ponceau protein staining is shown in D. Samples were from 3 different human iPAs, rat iPA, rat heart (H), HEK-293 cells transfected with K_V7.4 (Q4) or K_V7.5 (Q5) and non-transfected HEK-293 cells (NT).

2.4.4 Endothelium integrity

The muscarinic receptor agonists, acetylcholine and carbachol, produced concentration-dependent relaxation of rat iPAs pre-constricted with phenylephrine. The magnitude of the relaxation produced was often large enough to abolish the constriction evoked by 1 µM phenylephrine (Figure 2.7A,B). Figure 2.7C displays the mean concentration-response curves for acetylcholine and carbachol (n=5). Increasing drug concentrations were applied to vessels after the response to the previous concentration reached a steady state. Vessel tension was measured immediately before the application of the higher concentration. The mean negative log of the half maximal effective concentration (values in Molar; pEC_{50}) values for acetylcholine and carbachol, estimated by fitting the Hill equation to the concentration-response curves, were 6.3 ± 0.3 and 6.5 ± 0.1, respectively (2-tailed unpaired *t*-test P>0.05). Maximum response values, also calculated by the Hill equation, were 94 ± 3% and 92 ± 3% for acetylcholine and carbachol respectively (2-tailed unpaired *t*-test P>0.05). These data show that the endothelium remained intact after mounting the vessel on to the myograph.

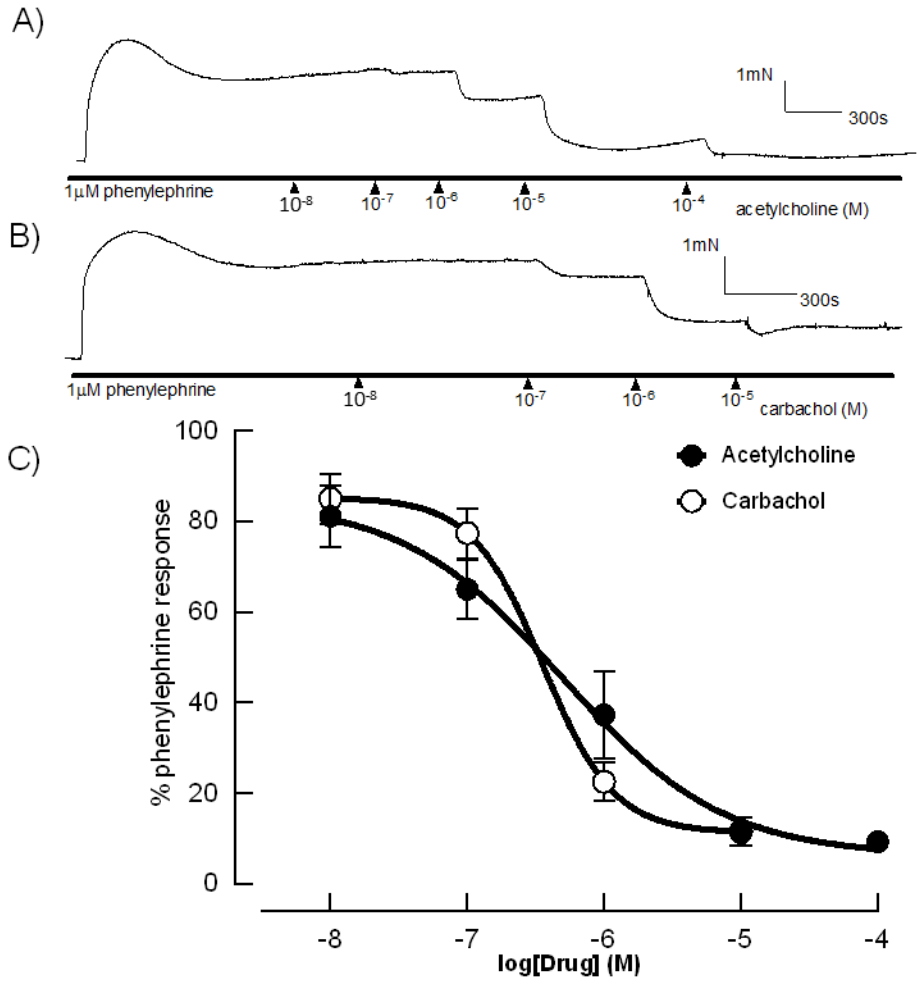

Figure 2.7:Muscarinic receptor agonists acetylcholine and carbachol evoke vasorelaxation of rat intra-pulmonary artery. Original recordings of tension displaying the constriction induced by 1 μM phenylephrine and relaxation following cumulative application of acetylcholine (A) or carbachol (B) at the concentrations stated. Log concentration-response curves for rat iPA relaxation induced by acetylcholine and carbachol. Relaxation responses were measured in each vessel as a percentage of the constriction induced by 1 μM phenylephrine. Each data point represents the mean ± S.E.M of 4-5 experiments.

2.4.5 Effects of K_V7 channel blockers on human intra-pulmonary artery tone

When applied to human iPAs XE991, linopirdine and (-)chromanol 293B produced concentration-dependent constriction (Figure 2.8A-C). The three drugs showed similar concentration-response relationships (Figure 2.8D), approaching the maximal effect above 10 μM. XE991 evoked a maximum constriction that amounted to 61 ± 7 % (n=11) of the response to 50 mM KCl, compared with 84 ± 17 % (n=8) with linopirdine and 67 ± 17 % (n=8) with (-)chromanol 293B. At higher concentrations there was often a loss of constriction, especially with linopirdine (Figure 2.8B). The concentrations producing 50% of the maximal effect (EC_{50}) were determined by fitting the data obtained from each vessel to the Hill equation then calculating the mean value. This gave pEC_{50} values of 5.52 ± 0.21 for XE991, 5.96 ± 0.18 for linopirdine and 5.74 ± 0.48 for (-)chromanol 293B. Chromanol 293B is a selective inhibitor of $K_V7.1$ channels, but its effects are stereospecific (Yang et al, 2000). The results shown in Figure 2.8C were obtained with the 7-fold more potent (-)chromanol 293B enantiomer. Over the same concentration range chromanol 293B failed to cause constriction of rat iPAs, while 10 μM XE991, resulted in pronounced constriction as previously reported by Joshi et al. (2006). These results suggest that K_V7 channels are open at rest, since channel blockade induced contraction, presumably as a consequence of depolarisation.

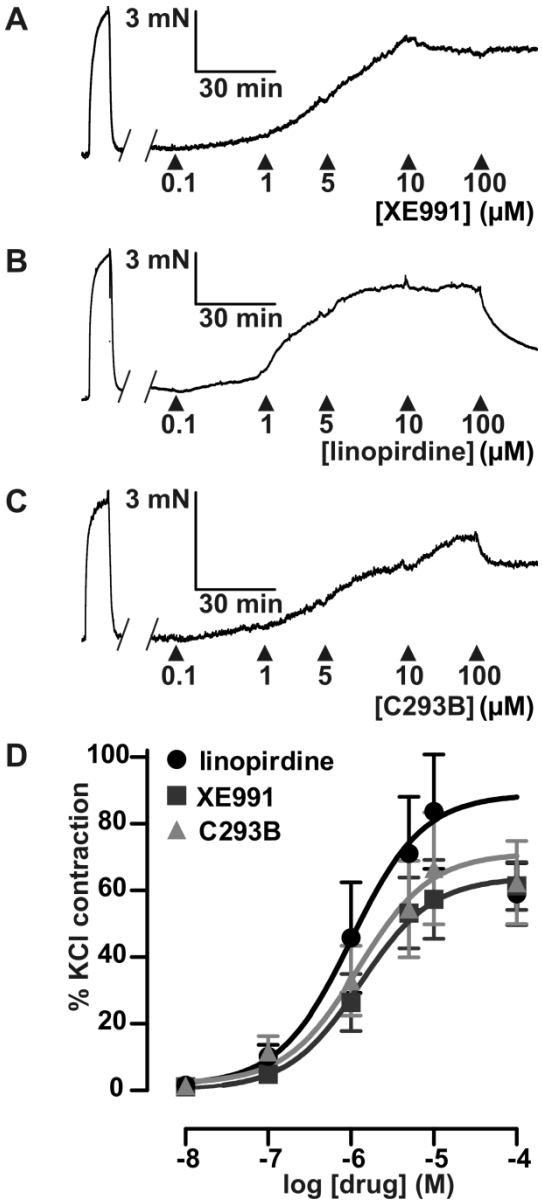

Figure 2.8: K_V7 channel blockers constrict human intra-pulmonary arteries. (A) Original records of tension developed in response to brief application of 50mM KCl, followed by cumulative addition of linopirdine at 10 nM-100 μM (A), XE991 (B) or (-)chromanol 293B (C). Concentration dependence of the contraction induced by linopirdine, XE991, and (-)chromanol 293B is shown in (D). Responses were measured in each vessel as a percentage of the contractile response to 50 mM KCl. Each point represents the mean ± SEM of 7–12 experiments.

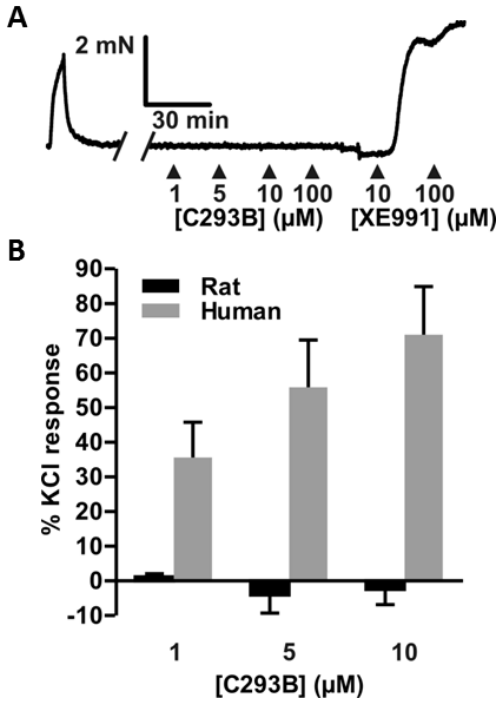

Figure 2.9: Chromanol 293B constricts human but not rat intra-pulmonary arteries. (A) Original record of tension developed in rat iPA in response to brief application of 50 mM KCl, followed by cumulative addition of chromanol 293B and XE991. (B) Constriction responses to chromanol 293B in human or rat iPAs. Each point represents the mean ± SEM of 3-7 experiments.

2.4.6 Constriction induced by K_V7 channel blockers requires voltage-gated Ca^{2+} influx.

The ability of the selective L-type VGCC antagonist, nifedipine, to inhibit constriction evoked by linopirdine or XE991 was investigated to establish the contribution played by Ca^{2+} entry through voltage-gated Ca^{2+} channels. Vessels pre-exposed to nifedipine (100 nM) for 30 min failed to constrict when either 5 μM linopirdine (Figure 2.10A) or 1 μM XE991 was applied. Following a washout period (approximately 1 hr) to remove nifedipine from the myograph chamber, both drugs, applied at the same concentrations, caused pronounced vessel constriction. Re-applying nifedipine to the constricted vessels caused artery tone to decrease rapidly towards baseline. Figure 2.10B compares the mean amplitudes of constrictor responses to each of the drugs, in the presence of nifedipine and then following its removal. Pre-exposure to nifedipine essentially abolished the response. Figure 2.10C shows that nifedipine was able to reverse around 80% of the constriction pre-

induced by linopirdine or XE991. Thus, voltage-gated Ca^{2+} influx is essential for the constriction induced by K_V7 channel blockers.

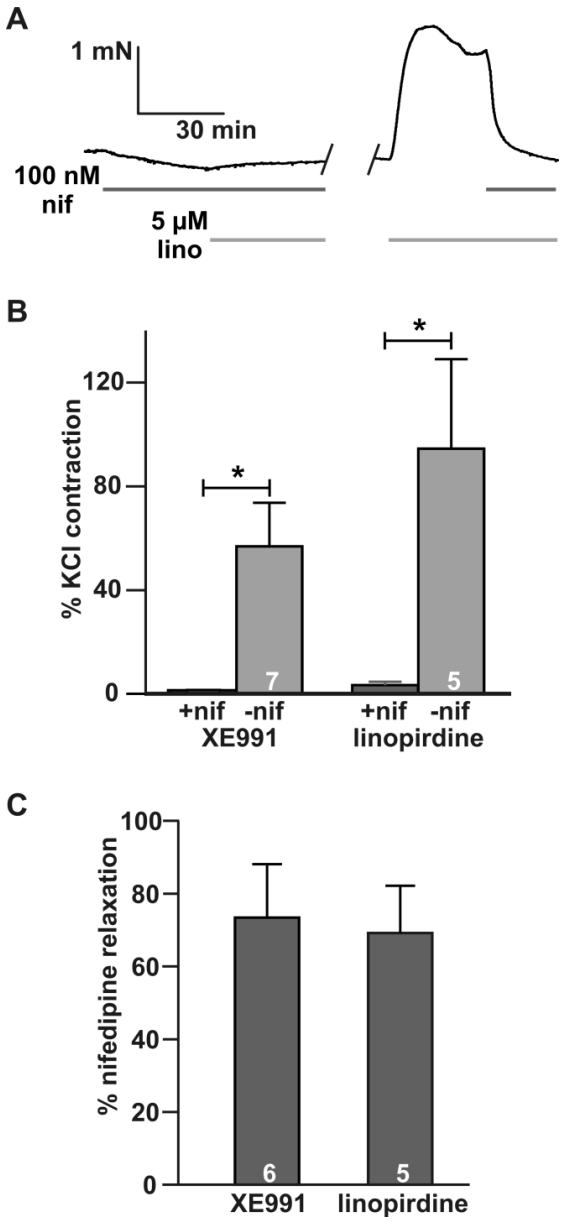

Figure 2.10: Constriction to K_V7 channel blockers requires activation of voltage-gated Ca^{2+} channels. (A) Original record of tension in a human iPA following application of linopirdine (lino, 5 μM) in the presence and absence of nifedipine (nif, 100 nM), with a 1 hr wash-out period in between. (B) Mean (± s.e.m.) constriction responses to linopirdine and XE991 when applied in the absence (-) or presence (+) of nifedpine. (C) Mean (± s.e.m.) relaxation induced by nifedipine in vessels contracted with either K_V7 channel blocker. (*paired t-test $P < 0.05$).

2.4.7 Dilator effects of K_V7 channel activators on human intra-pulmonary and omental arteries.

Pulmonary and omental arteries pre-constricted with ET-1 (1 or 10 nM) relaxed in a concentration-dependent manner when exposed to the K_V7 channel activators retigabine or ZnPy Figure 2.11. The dilator effect of retigabine was tested against arteries that had been pre-constricted with ET-1 (1 nM), phenylephrine (1 μM) or serotonin (5-HT; 10 μM), with similar results obtained in each case Figure 2.11. When vessels were pre-constricted with ET-1 (1-10 nM) retigabine induced a significantly larger maximal relaxation in omental than pulmonary arteries Figure 2.11. It inhibited the endothelin-induced tone by up to 78 ± 4% (n= 5) in omental artery compared with 44 ± 7 % (n= 4, $p<0.01$) in iPA, but with a similar pEC_{50} in each case (pulmonary 5.3 ± 0.1, omental 5.0 ± 0.1). Flupirtine, an analogue of retigabine, also dilated pulmonary vessels with pEC_{50} = 4.9 ± 0.3 (n=6) and maximum relaxation of 50 ± 10 %, (Figure 2.12). ZnPy dilated pulmonary arteries with pEC_{50} = 5.7 ± 0.2 (n=7) and omental arteries with pEC_{50} = 5.54 ± 0.09 (n=5), showing significantly higher potency than retigabine ($p = 0.01$). ZnPy was also the most effective dilator, with only 20 ± 11% of the induced tone remaining in iPAs at a concentration of 10 μM, and complete relaxation of omental arteries achieved (Figure 2.11). These data show that K_V7 activation can induce relaxation of agonist pre-constricted pulmonary and omental arteries.

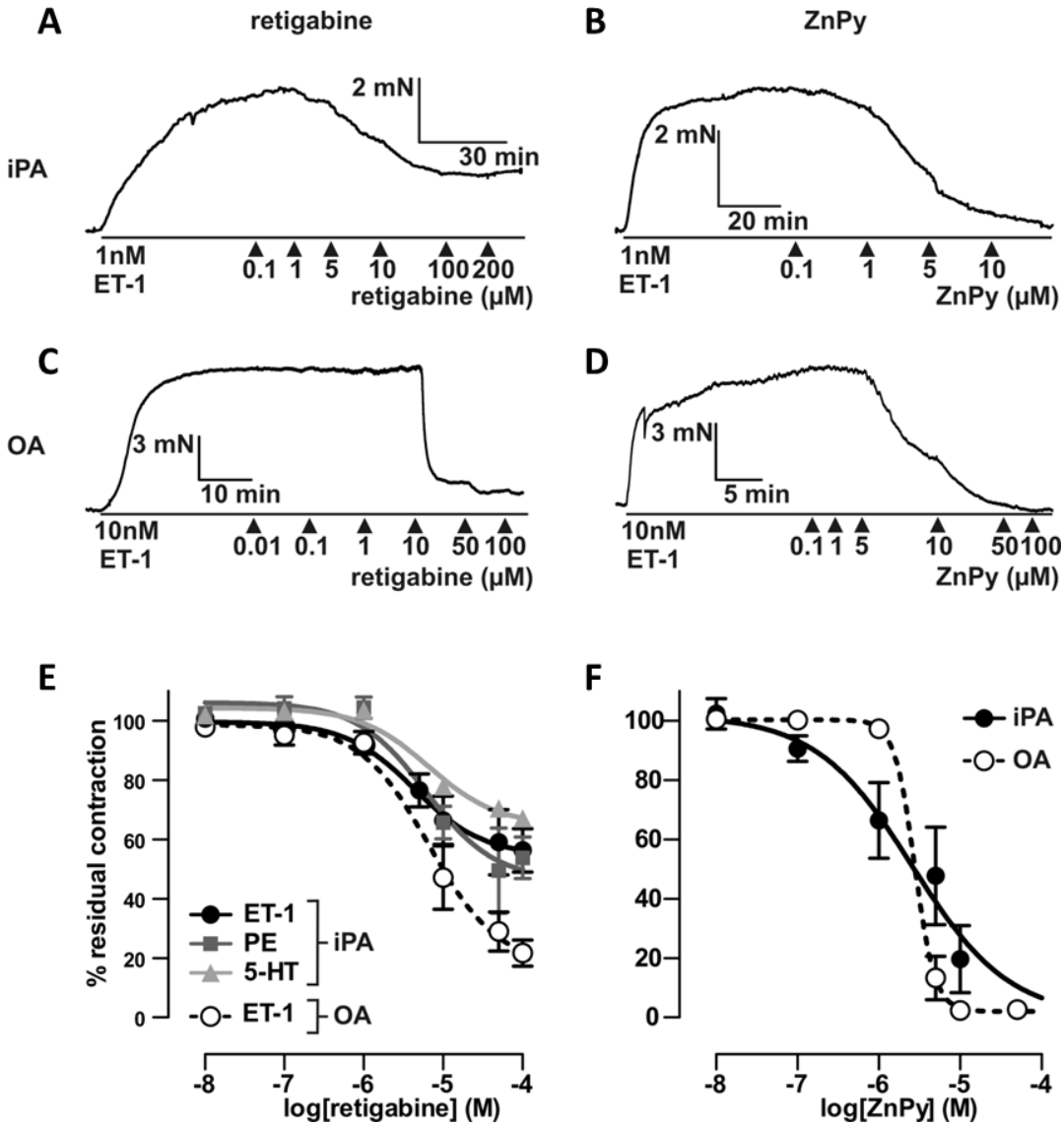

Figure 2.11: K_V7 channel activators dilate human intra-pulmonary and omental arteries. Original records of tension developed in response to endothelin-1 (ET-1) and subsequent cumulative addition of 0.1 nM – 100 μM retigabine (A & C) or ZnPy (B & D) in pulmonary (A & B) and omental (C & D) arteries. (E) Concentration-response curves for retigabine induced dilation of pulmonary arteries pre-constricted with 1 nM ET-1, 1 μM phenylephrine (PE) or 10 mM 5-HT and omental artery constricted with ET-1. (F) Log-concentration response curves for ZnPy induced dilation of pulmonary and omental arteries pre-constricted with ET-1. Responses measured as the residual agonist-induced contraction. Each point represents the mean ± SEM of 3–8 experiments. The experiments on omental arteries were done by the post-doctoral researcher Katie Smith.

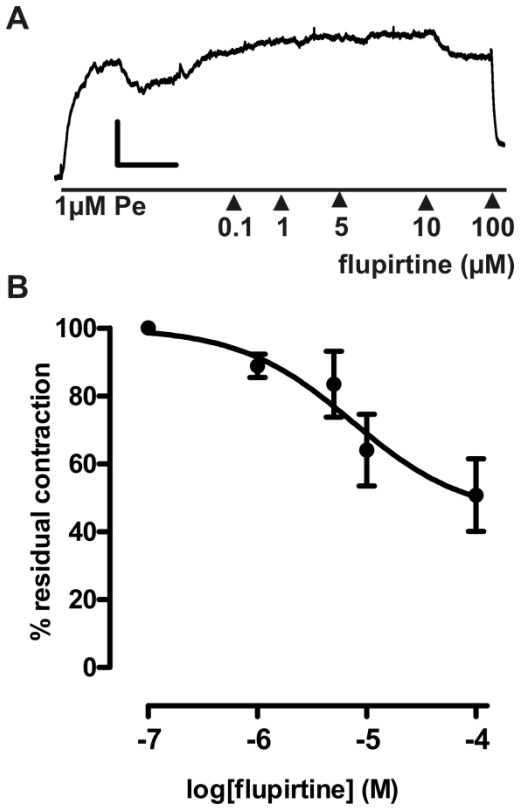

Figure 2.12: Flupirtine dilates human intra-pulmonary artery. A) Original recording of tension developed in response to phenylephrine (Pe) and subsequent effect of cumulative addition of 0.1- 100 µM flupirtine. B) Log-concentration response curve for flupirtine induced relaxation of human iPAs pre-constricted with 1 µM PE. Each point represents the mean ± SEM of 6 experiments, except at 100 nM flupirtine where n=2. Calibration bars: 2 mN (vertical) and 30 min (horizontal).

2.4.8 Retigabine acts via membrane hyperpolarisation and inhibition of voltage-gated Ca^{2+} influx

Although retigabine is widely regarded as a K_V7 channel activator it was found to possess weak voltage-gated Na^+ and Ca^{2+} channel blocking activity and to affect some neuronal ligand-gated ion channels (Rundfeldt and Netzer, 2000a). Inhibition of Ca^{2+} channels was seen in cerebral artery smooth muscle cells at only 10 µM retigabine (Mani et al., 2013). To investigate the mechanisms by which retigabine brings about vasodilation, we measured its ability to dilate iPAs under a range of conditions designed to produce constriction by either promoting or avoiding voltage-gated Ca^{2+} entry into the smooth muscle cells. The effect of applying retigabine was compared when vessels were pre-constricted with 10 nM ET-1 (Figure 2.13A), 1 µM Bay K 8644 (Figure 2.13B) to directly activate L-type VGCC, 90 mM K^+

PSS (Figure 2.13C) to evoke depolarization and voltage-gated Ca^{2+} entry while depleting the trans-membrane K^+ gradient or 3 µM ionomycin (Figure 2.13D), which acts as a Ca^{2+} ionophore to evoke voltage-independent Ca^{2+} entry. Figure 2.13E shows the mean relaxations induced by 25 µM retigabine in each of these conditions. The experiments were performed on pairs of artery segments, with ET-1 constricted vessels acting as a positive control in each case. Retigabine caused significantly larger relaxation of arteries pre-constricted with Bay K 8644 (75 ± 12 %, n=4) when compared with artery segments from the same vessels constricted with ET-1 (21 ± 2 %, n=4). In contrast, the relaxation was significantly smaller when the arteries were pre-constricted with 90 mM K^+PSS (14 ± 5 %, n=9) compared with ET-1 in matched vessels, or with Bay K 8644. Provided the endothelium was removed from vessels exposed to ionomycin, vasoconstriction occurred. Retigabine had little effect or even caused a small increase in contraction. Thus the effectiveness of retigabine was lost when constriction developed independently of voltage-gated Ca^{2+} influx and enhanced when it was promoted.

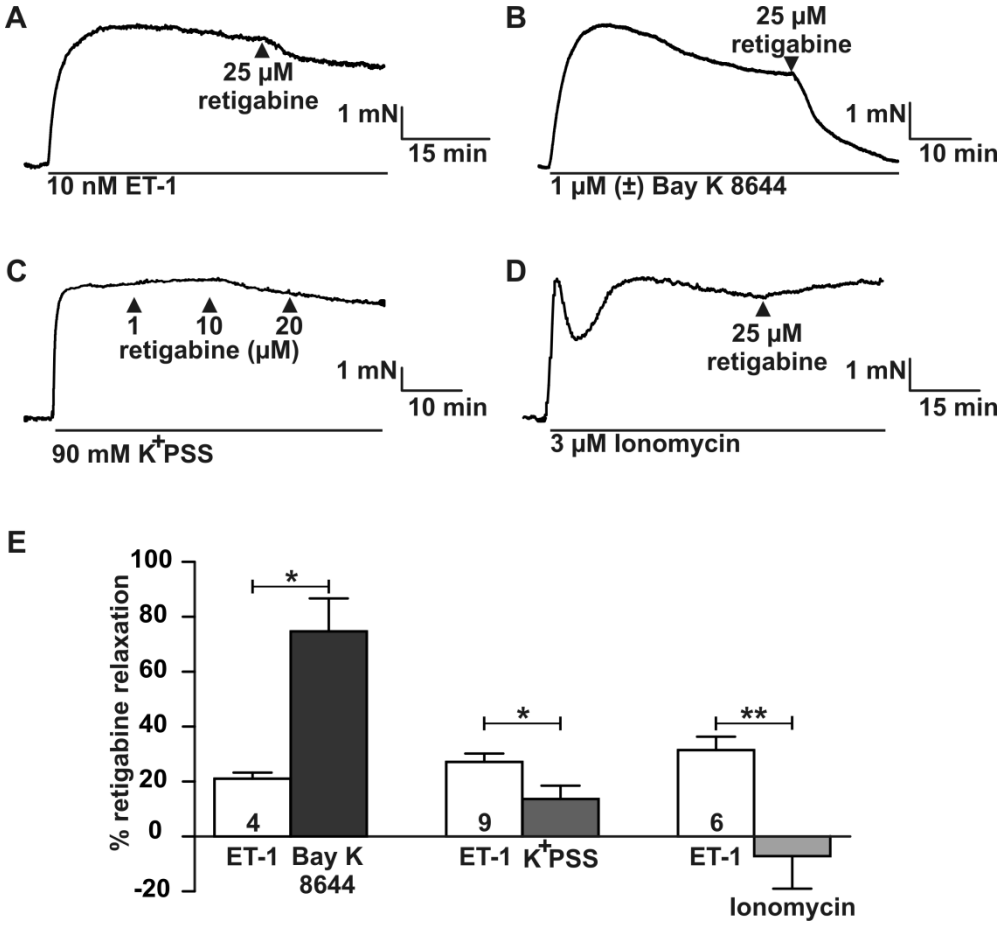

Figure 2.13: Retigabine relaxion of pulmonary artery smooth muscle varies with voltage-gated Ca^{2+} influx. Original records show the effect of retigabine on pulmonary artery tone when vessels were constricted with 10 nM ET-1 (A), Bay K 8644 (B), 90 mM K^+ PSS (C) or 3 µM ionomycin (D). Bar chart (E) depicts the mean relaxation produced by 25 µM retigabine in each of these conditions. Experiments were carried out on paired vessels to enable responses of Bay K 8644, ionomycin or K^+ stimulated vessels to be directly compared with ET-1 stimulated vessels. * paired t-test, P<0.5; **p<0.01.

2.5 Discussion

This study aimed to establish the profile of expression of the *KCNQ* K_V7 alpha subunit mRNA transcripts in human iPAs and to determine if K_V7 channel modulators alter human iPA tone. This is the first report demonstrating that K_V7 channel modulators can alter the tone of human iPAs The results suggest that K_V7 channels play a major role in regulating the membrane potential and Ca^{2+} signalling in human PA smooth muscle. The vasoconstriction caused by blockers of K_V7 channels, as well as its dependence on voltage-gated Ca^{2+} influx, implies that K_V7 channels are open at the RMP and contribute to the lack of tone in un-stimulated PAs. Unlike the situation in human systemic arteries (Ng et al., 2011), $K_V7.1$ channels appear to contribute at rest, such that blocking them selectively with the active isomer of chromanol 293B caused pronounced pulmonary vasoconstriction. However, there are also species differences since chromanol 293B did not constrict rat iPAs. Other K_V7 channel subtypes must also play a role, because vasodilation was induced by retigabine and ZnPy, neither of which activates $K_V7.1$. The mechanism of vasodilation involved inhibition of voltage-gated Ca^{2+} influx, consistent with the opening of K_V7 channels and membrane hyperpolarisation. The pharmacological differences between human pulmonary and systemic arteries, along with the potent vasodilating action of K_V7 channel activators, suggest that K_V7 channels could be exploited therapeutically for the treatment of PH.

2.5.1 K_V7 channels expressed in human iPAs

The expression of the *KCNQ* transcripts was primarily investigated using mRNA obtained from intact human iPAs. mRNA for all *KCNQ* transcripts, except *KCNQ2* was detected. The same *KCNQ* expression profile in mouse and rat iPAs was previously reported by Joshi et al. (2009). In this study the same *KCNQ* expression profile was obtained in the presence or absence of the adventitia and endothelium, thus *KCNQ* genes are expressed in PA smooth muscle. qRT-PCR was performed to determine the *KCNQ* expression levels in iPAs relative to heart, brain or omental arteries. Human iPAs contained approximately a quarter of the mRNA for *KCNQ1* relative to the heart sample. The iPA expression of *KCNQ3-5* were all higher relative to the brain sample used in the study. These results are similar to the relative expression of the *KCNQ* genes in rat iPAs compared with brain and heart. This compares to a 40% higher *KCNQ1* gene expression in rat heart than in iPA. *KCNQ4* and *KCNQ5* were both reported to have higher expression in rat iPAs compared to rat brain (Joshi et al., 2009). The level of expression in iPA, compared with other tissues where their

function has been established, is likely to be sufficiently high to provide physiologically active K_V7 channels.

Only one other study has reported expression of *KCNQ* mRNA transcripts in the human vasculature. Ng et al. (2010) demonstrated that all visceral adipose and mesenteric arteries investigated robustly expressed *KCNQ4*, however the expression of all other *KCNQ* transcripts was not consistently detected. In order of decreasing frequency *KCNQ3*, *KCNQ1* and *KCNQ5* were detected, whereas *KCNQ2* was not expressed in any human systemic artery tested. In the current study, neither human iPAs nor omental arteries were found to express *KCNQ2* mRNA. The absence of *KCNQ2* mRNA in four different human vascular beds, suggests that it may not be widely expressed in the human vasculature.

Ng et al., (2010) concluded that similar amounts of all the *KCNQ* genes, except *KCNQ*2, were expressed in human systemic arteries, since the relative abundance of all the transcripts were similar. Using the same reasoning, Joshi et al., 2009 concluded that *KCNQ4* was the most abundant *KCNQ* transcript in rat iPAs. There are potential pitfalls when qRT-PCR is used to determine relative amounts of different genes within a tissue (ie *KCNQ1* vs *KCNQ4* in PA). This is because the amount of each gene detected during PCR is affected by the chemistry used during cDNA synthesis and the position of the primers used to detect a gene during PCR. For example, the PCR primers used to detect one gene may bind in close proximity to the annealing site of the random hexamers and / or primers against the poly-A-tail during cDNA synthesis, while the PCR primers used to detect another gene bind further away. In this scenario, the cDNA synthesis reaction would be considerably more efficient for the former gene, thus any difference in the gene expression levels detected by PCR could be attributed to the cDNA synthesis reaction. Therefore the conclusions on *KCNQ* mRNA expression from these two papers may be flawed.

Since different housekeeping genes were used, it is not possible to compare the expression of the *KCNQ* transcripts in the systemic arteries investigated by Ng et al., (2010) to the vessels in this study. The expression profile of the *KCNQ* transcripts in human omental artery does, however, appear similar to that in human iPAs, except for *KCNQ5*, which may be more abundant in iPAs. Statistical analysis was limited by the low N number for the omental arteries. This finding resembles the data by Joshi et al., (2009), who showed a similar expression profile of *KCNQ* transcripts in rat iPAs compared to mesenteric arteries, except that *KCNQ4* appeared to be more abundant in rat iPA.

2.5.2 KCNE expression

All *KCNE* subunits were found to be expressed in all four human iPA samples tested, except *KCNE4* which was undetected in one iPA sample. This is the only study to demonstrate the expression of *KCNE* transcripts in the human vasculature. All *KCNE* transcripts were detected in mouse aorta, carotid and femoral arteries with the relative expression of each transcript varying between the arteries (Yeung et al., 2007). This difference in expression could dramatically alter the function of the K_V7 channels within the arteries, since the *KCNE* transcripts can drastically alter the electrophysiological and pharmacological properties of K_V7 channels.

2.5.3 Preliminary western blot

A preliminary attempt at detecting the presence of the $K_V7.4$ α-subunit protein in human iPA was positive, in that a band of the correct molecular weight was detected in one of the three human iPA lysates tested. The band was, however, only faintly stained. The positive lysate was the only one of the human samples that stained positively for α-actin and it also gave the darkest ponceau stain out of the three human iPA lysates. Thus it contained more protein than the negative lysates. This suggests that human iPAs do express the $K_V7.4$ α-subunit protein, which can be detected if sufficient total protein is present. None of the human iPA lysates gave rise to the expected band for β-tubulin, suggesting that there was limited protein even in the sample that was positive for $K_V7.4$. Moreover, the smudged appearance of the ponceau stain in the human iPA lysates could be due to protein in the samples being degraded. Although the BCA assay was used to ensure the same amount of total protein was added to the gel for each sample, it does not provide any information on the integrity of the protein present as it detects proteins as small as tripeptides. The iPA samples used for western blot had not been tested in a myograph, so their functional integrity was unknown. As the delay between surgery and dissection of arteries from the lung can be several hours, the human samples may have been less well preserved than the freshly isolated rat samples, which showed clear $K_V7.4$ bands on the western blot

Although preliminary, this is the first study to detect $K_V7.4$ protein in a human iPA by western blot. Immuno-staining showing localisation of $K_V7.1$, $K_V7.3$, $K_V7.4$ and $K_V7.5$ in the muscle layer of human systemic artery sections has been reported (Ng et al., 2011). There

was, however, a lack of convincing controls to rule out non-specific binding of the antibodies to the tissue. The expression pattern of K_V7 subunits in vascular tissue and the relative expression in pulmonary *versus* systemic arteries therefore remains to be determined.

2.5.4 Pharmacology

Two lines of pharmacological evidence support a functional role for K_V7 channels in human iPAs. First, the K_V7 channel blockers linopridine, XE991 and chromanol 293B all caused marked constriction of human iPAs. Secondly, the K_V7 channel activators, flupirtine, retigabine and ZnPy all induced relaxation of pre-constricted human iPAs. The effects of the K_V7 channel blockers and activators used in this study occurred at concentrations considered selective for the K_V7 channels (Robbins 2001).

2.5.4.1 K_V7 channel block evoked pulmonary vasoconstriction

The selectivity of linopirdine and XE991 are usually reported by comparing their effects with those on I_{KM} and heterologously expressed K_V7 channels. The EC_{50} values for linopirdine and XE991 (1-3 µM) inducing human iPA constriction were similar to IC_{50} values previously reported to block I_{KM} in rat neurons. Linopirdine inhibited I_{KM} in rat superior cervical sympathetic ganglion cells with an IC_{50} value of 3-7 µM (Costa and Brown., 1997; Lamas et al., 1997), while XE991 inhibited currents with an IC_{50} of 0.98 µM (Wang et al., 1998). The EC_{50} of linopirdine and XE991 in the current study are likely to be sufficient to block heterologously expressed K_V7 channels. Linopirdine inhibits current from heterologously expressed $K_V7.1$, $K_V7.2$ and $K_V7.2/K_V7.3$ channels with IC_{50} values of 8.9, 4.8 and 4.0 µM respectively (Robbins 2001). XE991 is more potent at inhibiting current from heterologously expressed $K_V7.1$, $K_V7.2$ and $K_V7.2/K_V7.3$ channels with IC_{50} values of 0.75, 0.71 and 0.6 µM, respectively. IC_{50} values higher than the EC_{50} values obtained for both linopirdine and XE991 in the current study have been reported for heterologously expressed $K_V7.4$ and $K_V7.5$ channels. Linopirdine blocks current from heterologously expressed $K_V7.4$ and $K_V7.5$ channels with IC_{50} values of 14 µM and 51 µM respectively, while XE991 blocks the same channels with IC_{50} values of 5.5 µM and 65 µM, respectively (Schroeder et al., 2000a; Søgaard et al., 2001). Of the K_V7 channels found to be expressed in human iPA, the potencies of linopirdine and XE991 at inducing constriction suggest a role for $K_V7.1$ channels along with $K_V7.4$ and $K_V7.5$.

Chromanol 293B is a $K_V7.1$ blocker, which abolishes $K_V7.1$ current at concentrations having little effects on other K_V7 channels (Lerche et al., 2007). Chromanol 293B is usually reported by comparing its effects on the system of interest with those on the cardiac I_{Ks} ($K_V7.1$/KCNE1) and/or heterologously expressed $K_V7.1$ channels. The EC_{50} for chromanol 293B-induced human iPA constriction (1.8 μM) is comparable to the IC_{50} reported to block I_{Ks} in guinea pig ventricular myocytes (2.1 μM) or *Xenopus* oocytes (6.2 μM) (Busch et al., 1996). Given its selectivity for $K_V7.1$ channels, the potent effect of chromanol 293B on human iPA suggests that $K_V7.1$ channels may be important for maintaining low tone in the human vessels, a role that was not apparent in rat iPA. This may be a PA specific effect, because chromanol 293B also failed to affect the tone of human systemic arteries (Ng et al, 2011).

Although the K_V7 channel blockers tested on human iPAs caused constriction, a loss of constriction was often observed at concentrations at or above 10 μM. This is unlikely to be due to an action on the endothelium, because a similar loss of tone at high linopirdine and XE991 concentrations in rat PA was found to be unaffected by removing the endothelium (Joshi et al, 2006). A similar pattern has been reported in brain slices, where 100 μM linopirdine decreased acetylcholine release despite enhancing release at lower concentrations (Zaczek et al 1997). This action was not investigated further since it only occurred at a high concentrations, where the potential for off target effects is increased.

The vasoconstrictor effects of K_V7 blockers are due to a direct effect on the smooth muscle cells in the vessel wall (Joshi et al, 2006). PASMCs contain various channels and transporters, including K^+, Cl^- and Ca^{2+} ion channels. It is plausible that linopirdine, XE991 or chromanol 293B may have interacted with one of these ion channels to cause the constriction observed. Lamas et al. (1997) reported that linopirdine was less effective at inhibiting other K_V currents in rat superior cervical sympathetic ganglia, including the delayed rectifier (IC_{50} 63 μM) and transient outward current (IC_{50} 69 μM), and produced no detectable inhibition of Ca^{2+}-activated K^+ currents. These observations concur with other studies where linopirdine and XE991 were found to be significantly more potent at blocking K_V7 channels compared to $K_V1.2$, $K_V1.5$, $K_V10.1$, $K_V11.1$, $K_V11.3$ and $K_V12.1$ channels heterologously expressed under similar conditions (Wang et al, 1988). Both linopirdine and XE991 (10 μM) were shown to cause a 10% reduction in current amplitude in HEK cells overexpressing the $K_V2.1$ channel (Wladyka and Kunze, 2006). Heteromeric $K_V1.2/K_V1.5$ and $K_V2.1/K_V9.3$ currents were also blocked by 10 μM XE991 with approximately 27% and 40%

inhibition at 0 mV, respectively. This is, however, smaller than the block of $K_V7.4$ currents (approximately 55%) at the same potential (Zhong et al., 2010). Thus 10 µM XE991 could affect other heterotetrameric Kv channels expressed in PASMCs, raising the possibility that the constriction observed upon the addition of XE991 to human iPA could be due to inhibition of heteromeric $K_V1.2/K_V1.5$ and/or $K_V2.1/K_V9.3$ currents. On the other hand, these currents were not affected by 1 µM linopirdine, which blocks $K_V7,4$ by approximately 27% at 0 mV (Zhong et al., 2010). Since linopirdine and XE991 both caused constriction of human iPA, K_V7 inhibiton is therefore the more likely mechanism. This is particularly important since these channels have been proposed to be open at RMP in PASMCs (Jeong et al., 2013; Moudgil et al., 2006; Patel et al., 1997). Linopirdine was also reported recently to activate TRPV1 channels, although no increase in current at concentrations lower than 10 µM was observed (Neacsu and Babes, 2010), the concentration that induced the maximum constriction in human iPA. Therefore, it is unlikely that Ca^{2+} influx through TRPV1 channels contributed to human iPA constriction. Experiments demonstrated (-)chromanol 293B to have negligible effects on guinea pig I_{kr} and no significant effect on $K_V11.1$ (hERG) channels (Busch et al., 1996). Moveover, 30 µM (-)chromanol 293B blocked $K_V7.1$/KCNE1 current by 90 %, $K_V1.5$ by 52 % and $K_V4.3$ by 37 % (Yang et al., 2000). Negligible effects on these channels would be expected at the concentrations of (-)chromanol 293B that evoked constriction of iPA. These reports all support the idea that the actions of linopirdine, XE991 and (-)chromanol 293B observed in the current study were mediated via blockade of K_V7 channels, especially at the lower concentrations used. Combined with the mRNA expression data obtained in this study, it is likely that $K_V7.1$ and also $K_V7.4$ and $K_V7.5$, is responsible for the constriction observed in the presence of the three blockers used. Although *KCNQ3* mRNA was shown to be expressed, and linopirdine blocks $K_V7.3$ channels with an IC_{50} in the appropriate concentration range, the involvement of these channels is unlikely to be major as they relatively insensitive to both XE991 and (-)chromanol 293B (Robbins, 2001). As *KCNQ2* mRNA was not expressed, $K_V7.2$ channels do not play a significant role in PASMCs.

2.5.4.2 K_V7 channel activation evoked pulmonary vasodilatation

The K_V7 channel activators flupirtine, retigabine and ZnPy all produced concentration-dependent relaxation of agonist pre-constricted human iPAs. The concentrations required for dilation by all three drugs lay within the concentration range expected for K_V7 channel activation. Flupirtine relaxed with an EC_{50} of 13 µM, which is similar to the EC_{50} of 10-20 µM

for activation of I_{KM} in rat nodose neurons (Wladyka and Kunze, 2006). Information is limited on the concentration-current relationship of flupirtine on heterologously expressed K_V7 channels, although Martire et al., (2004) demonstrated that 10 μM flupirtine caused a hyperpolarizing shift in the voltage-dependence of activation of *KCNQ2* subunits transfected in CHO cells, with maximal current enhancement observed at potentials around -65 mV.

Retigabine relaxed human iPAs with an EC_{50} between 4 and 10 μM, depending on what agonist was used to pre-constrict the arteries. These values are quite close to previously reported EC_{50} values for retigabine on the I_{KM} and heterologously expressed K_V7 channels. Retigabine prevented neurotransmitter release in rat hippocampal and cortical synaptosomes with an EC_{50} value of 1 μM (Martire et al., 2004). It activated homomeric and heteromeric K_V7 channels with EC_{50} values ranging from 0.3 to 5.2 μM, with the following order of potency (EC_{50}) reported by Tatulian et al (2001): $K_V7.3$ (0.6 μM) , $K_V7.2/3$ (1.9 μM), $K_V7.2$ and $K_V7.5$ (2.5 μM), $K_V7.4$ (5.2 μM) (Dupuis et al., 2002; Rundfeldt and Netzer, 2000b; Tatulian et al., 2001; Wickenden et al., 2000). Tatulian et al (2001) also reported that the maximum hyperpolarizing shift in the voltage dependence of activation was induced by 100 μM retigabine in all K_V7 channels investigated, except $K_V7.4$ which required 300 μM retigabine. The maximum hyperpolarizing shift was of the following order: $K_V7.3$ (-42.8 mV), $K_V7.2/3$ (-30.4 mV), $K_V7.4$ (-24.6 mV), $K_V7.2$ (-24.2 mV) (Tatulian et al., 2001). Given that retigabine and flupirtine are ineffective at activating $K_V7.1$ channels, these channels are not required for the vasodilation to K_V7 activators. The higher potency of retigabine at $K_V7.3$ channels, compared with PA, suggests these are not the major K_V7 channels mediating vasodilation. Thus $K_V7.4$ and/or $K_V7.5$ channels are likely to be the main channels mediating the dilation to K_V7 activators in human iPA.

Human iPAs relaxed in the presence of ZnPy with an EC_{50} around 1 μM. ZnPy (10 μM) has been shown to double I_{KM} in rat dorsal root ganglian neurons, while activating recombinant $K_V7.2$ and $K_V7.2/K_V7.3$ with EC_{50} values of 1.5 and 2.4 μM respectively (Xiong et al., 2007, 2008b). At 10 μM, ZnPy potentiated homotetramers of all K_V7 subunits, except $K_V7.3$ (Xiong et al., 2007), confirming that $K_V7.3$ channels are not required for vasodilation in response to K_V7 activators. The drug caused an almost 80-fold increase in the amplitude of $K_V7.4$ current at -30 mV and converted barely detectable $K_V7.5$ currents into large, robust currents, consistent with the involvement of $K_V7.4$ and/or $K_V7.5$ channels in ZnPy vasodilation. A role

for $K_V7.1$ in the dilation cannot be ruled out, because 10 μM ZnPy caused a 4-fold enhancement of homomeric $K_V7.1$ currents (Xiong et al, 2007).

The differences between IC_{50} values on heterologously expressed K_V7 channels and the EC_{50} values obtained in this study may be explained by the different electrophysiological properties and pharmacology of each K_V7 homomer and heteromer. Furthermore, the KCNE auxiliary subunits can also dramatically alter the properties of homomer and heteromer K_V7 channels. Since the subunit composition of the K_V7 channels in human iPAs is unknown, it is not possible to compare the artery to one particular K_V7 homomer. Also, most electrophysiology experiments are performed at room temperature while experiments investigating vessel tone are carried out at 37 °C. An increase in temperature to 37 °C has been reported to cause an increase in magnitude of the I_{Ks} ($K_V7.1$/KCNE1) tail current (Dong et al., 2006). Further understanding of K_V7 channel subtypes in PASMC will require an electophysiological approach, to identify the biophysical properties of the channels in human PASMC that are targeted by the K_V7 modulating drugs.

2.5.4.3 K_V7 channel modulators indirectly alter calcium influx via L-type calcium channels

The constrictions evoked by XE991 and linopirdine were abolished by nifedipine, whether it was applied before the K_V7 channel blocker or after the constriction induced by the blocker was established. Since linopirdine (30 μM) has been shown to have no effect on currents recorded from endogenous VGCCs in bovine chromaffin cells (Dzhura et al., 2006), it seems unlikely that linopirdine or XE991 caused Ca^{2+} influx by directly opening VGCC in PASMCs. A Ca^{2+} entry mechanism via VGCCs is expected if the drugs blocked a K^+ channel that was constitutively open at the RMP. The result of blocking efflux of K^+ through these channels would be to cause membrane depolarisation and activation of nifedipine-sensitive, L-type VGCCs (Clapp and Gurney, 1991b).

Similar findings were reported for rat mesenteric, aorta and pulmonary arteries, using the L-type VGCC blockers verapamil (10 μM), nicardipine (1 μM) and nifedipine (1 μM), respectively (Joshi et al., 2009; Mackie et al., 2008; Yeung et al., 2007). In the current study, the low concentration of nifedipine required to prevent human iPA constriction to linopirdine or XE991 underlies the importance of indirect activation of VGCC for constriction induced by K_V7 channel blockers. Gurney and co-workers demonstrated that 5

μM XE991 consistently reduced the K^+ outward current in freshly isolated human PASMCs (Katie Smith, personal communication). Furthermore, linopirdine (10 μM) and XE991 (5 μM) have previously been shown to cause membrane depolarisation in freshly isolated rat PASMCs (Joshi et al., 2009).

The pulmonary vasodilator effect of retigabine was likely to be due to inhibition of voltage-gated Ca^{2+} entry, based on several findings. Firstly, when tested on vessels pre-constricted with Bay K 8644, retigabine (25 μM) caused 75% relaxation, nearly 4-fold larger than the response in vessels pre-constricted with ET-1 (20% relaxation). ET-1 contracts smooth muscle by raising cell Ca^{2+} via multiple pathways, including IP_3-induced Ca^{+2} release, Ca^{+2} oscillations maintained by Ca^{+2} influx and Ca^{2+} sensitisation (Perez-Zoghbi and Sanderson, 2007). In contrast, the nifedipine analogue, Bay K 8644, directly activates L-type VGCC, resulting in Ca^{2+} influx and contraction (Preuss et al., 1985; Schramm et al., 1983). The action of Bay K 8644 is voltage-dependent, with greater current amplitudes recorded at depolarised potentials compared to hyperpolarised potentials. Thus, membrane hyperpolarisation evoked by retigabine would indirectly reduce the Ca^{2+} influx through the L-type VGCCs activated by Bay K 8644 and therefore cause relaxation. In contrast, retigabine would not be capable of having such a pronounced effect on the constriction induced by ET-1 as only part of the contraction is dependent on the activation of VGCCs (Goto et al., 1989). The Ca^{2+} ionophore, ionomycin, mediates voltage-independent Ca^{2+} influx into smooth muscle cells (Liu and Hermann, 1978). The addition of retigabine to vessels pre-constricted by ionomycin failed to cause relaxation, but instead produced a slight enhancement of the constriction. As the Ca^{2+} influx caused by ionomycin is independent of voltage, it would not be suppressed by membrane hypepolarisation. In fact, hyperpolarisation increases the electrochemical gradient for Ca^{2+}, thereby promoting further Ca^{2+} influx, which could explain the small contractile effect of retigabine in these conditions.

The role of K^+ channels in the response to retigabine was investigated by constricting the vessels with external solution containing 90 mM K^+. With external $[K^+]$ raised to 90 mM the cell membrane will depolarise to around -15 mV, which results in Ca^{2+} influx and contraction (Casteels et al., 1977a, 1977b) and E_K would be shifted from around -90 mV to -27 mV.. At such positive membrane potentials, the electrochemical gradient for K^+ would be virtually abolished, preventing K^+ channel openers from inducing hyperpolarisation. Therefore, a drug acting solely via K^+ channel activation should not cause relaxation of

vessels pre-constricted with 90 mM K^+PSS. The K_{ATP} channel activators cromakalim and pinacidil were previously observed to be unable to induce hyperpolarisation in arteries pre-constricted with 80 mM K^+ (Hamilton and Weston, 1989). When tested on arteries constricted with 90 mM K^+, retigabine was significantly less effective at causing dilation when compared with ET-1 contractions, consistent with K^+ channel activation contributing to the response. Nevertheless, the dilator effect was not abolished, implying that retigabine has additional actions that contribute to its effect. A recent study showed that at 10 μM, retigabine had a direct inhibitory action on cerebral artery smooth muscle Ca^{2+} channels (Mani et al., 2013). This could explain the dilation that remains in the presence of high K^+, where voltage-gated Ca^{2+} entry mediates the contraction. Direct suppression of Ca^{2+} influx cannot be the only action of retigabine, because that would predict a greater effect at suppressing responses to 90 mM K^+, due entirely to VGCCs, than ET-1, where VGCC provide only one of the pathways leading to contraction. Thus taken together, the results suggest that retigabine dilates human iPA by two synergistic mechanisms: activation of K_V7 channels, leading to smooth muscle membrane hyperpolarisation, and suppression of Ca^{2+} influx and inhibition of Ca^{2+} influx directly. It could be hypothesised, that, by combining K^+ channel activation and membrane hyperpolarisation with Ca^{2+} antagonism, retigabine could have advantages over Ca^{2+} antagonists that are currently used in the treatment of PAH.

2.5.5 Comparison of pulmonary and systemic arteries

In studies of human systemic vessels, Ng et al., (2010) demonstrated that 10 μM linopirdine or 10 μM XE991 caused constriction of visceral adipose and mesenteric arteries. Clinical trials of linopirdine did not, however, find any evidence for adverse effects on the cardiovascular or gastrointestinal systems (Pieniaszek et al., 1995). Linopirdine (10 μM) appears equally effective in three types of human artery (Table 2.4), although XE991 (10 μM) may be more effective at constricting human iPAs compared to either of the systemic vessels investigated (Table 2.4). This difference could be due to the relative potency of linopirdine at blocking different homomeric or heteromeric combinations of K_V7 channels with or without KCNE subunits. Alternatively it could reflect a more prominent role for K_V7 channels in setting RMP and maintaining low tone in iPAs.

Human artery type	10 µM linopirdine constriction (% KCl)	10 µM XE991 constriction (% KCl)
visceral adipose tissue	60	40
Mesenteric	70	40
Intra-pulmonary	60	80

Table 2.4: Comparison of K_V7 channel blocker effects on human systemic and pulmonary arteries. Magnitude of constriction reported for K_V7 channel blockers when tested at 10 µM, as % of the response to 60 mM (visceral adipose and mesenteric arteries) or 50 mM (iPA) KCl. Systemic data from Ng et al., (2010).

Although human systemic arteries constricted in response to XE991 (Table 2.4), they were unresponsive to chromanol 293B (Ng et al., 2011). Thus although $K_V7.1$ channels may contribute to the maintenance of low resting tone in human iPAs, they do not appear to serve this function in the human systemic vessels. This may represent a functional difference between pulmonary and systemic arteries that could be exploited for drug discovery. Interestingly, in rat aorta, pulmonary and mesenteric arteries, drugs claimed to activate $K_V7.1$ channels selectively caused vasodilation, which was reversed by $K_V7.1$-selective blockers, despite the blockers having no effect on resting tone (Chadha et al., 2012). Although not tested in human vessels, these findings suggest that $K_V7.1$ channels could play additional roles in counteracting vasoconstriction, in both pulmonary and systemic arteries.

The K_V7 channel activators, retigabine and ZnPy, dilated ET-1 constricted pulmonary and omental arteries with similar EC_{50} values, in the range 3-10 µM, but omental arteries responded with a larger maximal relaxation in each case. This is probably not due to different functional roles of K_V7 channels in the vessels, but more likely reflects different relative contributions of voltage-gated Ca^{2+} entry to muscle contraction. Endothelin-1 constricts human omental arteries mainly by activating ET_A receptors (Riezebos et al., 1994), but employs both ET_B and ET_A receptors in human pulmonary artery (McCulloch et al., 1996). ET_A receptors signal through Gq/11 and Gs proteins, whereas ET_B receptors signal through Gq/11 and Gi/o proteins (Alexander et al., 2011). The signalling pathways giving rise to smooth muscle contraction in each vessel may therefore employ different

proportions of voltage-gated Ca^{2+} influx. Contraction that is heavily dependent on Ca^{2+} influx through VGCC is predicted to be most sensitive to membrane hyperpolarisation brought about by K^+ channel activators. Consistent with this idea, the K_{ATP} channel activator, levcromakalim, dilated rat PA by no more than 50% (Clapp et al., 1993), close to the maximum response of human PA to retigabine, but fully relaxed human omental artery (Kinoshita et al., 2004), as seen here with retigabine.

The contribution of K_V7 channels to vascular tone has been studied in more detail in rodents. Gurney and co-workers previously showed that mouse and rat iPAs were constricted by linopirdine or XE991 as effectively as by 50 mM KCl, with EC_{50} values of 1.3 and 0.4 μM, respectively (Joshi et al., 2006). Linopirdine (1 μM) and XE991 (10 μM) have also been reported to constrict rat cerebral arteries (Mani et al., 2013; Zhong et al., 2010). Byron and co-workers reported that rat mesenteric arteries constrict by 35% in the presence of a maximum concentration (10 μM) of linopirdine (Mackie et al., 2008), but two independent labs reported that 1 μM XE991, when applied at rest, caused only slight constriction of rat mesenteric arteries (Joshi et al., 2009; Yeung et al., 2007). Mouse thoracic aorta constricted in the presence of 1-10 μM linopirdine or XE991 when they were applied to vessels at rest, albeit causing only 30% of the contraction produced by 60 mM KCl (Yeung et al., 2007). Greenwood et al., (2007) demonstrated that rat carotid and femoral arteries constricted in the presence of 10 μM XE991, whereas Joshi et al (2006) reported 1 μM XE991 to be ineffective in the same arteries. One possible reason for this discrepancy, besides the concentrations used, is the presence of phenylephrine to induce pre-tone in the Greenwood et al., (2007) study. Joshi et al (2006) also demonstrated rat coronary, renal and tail arties do not constrict in the presence of 1 μM XE991 although the effect of XE991 in the presence of pre-tone has not been investigated in these vessels. Although there is incomplete agreement about the sensitivities of different vascular preparations to K_V7 blockers, it is clear that rat iPAs constrict in the absence of pre-tone, but that other vessels may be sensitised to the effects of K_V7 blockers in the presence of pre-existing tone. This may reflect differential contributions of K_V7 channels to the resting potential and resting tone in different vascular beds.

2.5.6 Species differences

In all species studied to date, drugs that block K_V7 channels have been found to evoke concentration-dependent pulmonary vasoconstriction, while K_V7 channel activators caused concentration-dependent vasodilatation. But species differences are apparent. Whereas rodent arteries express the *KCNQ1*, *4* and *5* subunit isoforms (Joshi et al., 2009), we found that human arteries additionally express *KCNQ3* mRNA, in agreement with a recent study on arteries from human visceral adipose tissue (Ng et al., 2011). We also found differences between human and rodent PAs in their sensitivities to K_V7 channel modulators. The K_V7 channel blocker XE991 was around 10-fold more potent than linopirdine at evoking constriction of rat PA (Joshi et al., 2006), but the drugs were equipotent in human vessels. Their EC_{50} values in human vessels (3 and 1 μM respectively) were close to that reported for linopirdine in rat PA (1.3 μM; Joshi et al., 2006). Furthermore, human iPAs constricted in response to (-)chromanol 293B, which had no effect on rat iPAs.

Species variation in sensitivity to K_V7 channel activators appear less marked. The EC_{50} for retigabine-induced dilation of rat PAs has not been reported, but it suppressed 50% of the phenylephrine-induced tone at 13 μM and was 5-fold more potent than flupirtine (Joshi et al., 2009). With EC_{50} values of 5 μM and 12.5 μM, respectively, retigabine was also more potent than flupirtine in human iPAs, although both produced the same maximum response.

Caution must be taken when comparing rat and human iPAs. The rat iPAs used by Joshi et al., (2006) were all from healthy, interbred, male Sprague Dawley rats and fed the same diet. Human iPAs were from patients with quite varied demographics. The patients included both sexes, over a wide range of ages, with various diets, and all had lung cancer. This was apparent in the considerable variability seen with all the drugs tested on human iPAs and apparent in the standard error of the means. This experimental variability may contribute to the differences in drug potency seen between rat and human iPAs.

2.6 Conclusion

Human pulmonary and systemic arteries express similar *KCNQ* subunit profiles and both dilate in response to K_V7 channel activators, which show similar potency on each vessel. The K_V7 channels targeted by these drugs likely play a similar functional role in pulmonary and systemic resistance arteries. Exactly which K_V7 subunits make up the functional

channels is not yet clear. Gene knockdown studies on rat renal arteries suggest that $K_V7.4$ channels play a major role (Chadha et al., 2012), but $K_V7.5$ channels have also been implicated, especially in the vasoconstrictor response to vasopressin (Mackie and Byron, 2008). Our work suggests an additional contribution from $K_V7.1$ channels in human iPA. By being open at rest and contributing to the smooth muscle cell RMP, these channels may consequently play a major role in the maintenance of low vascular tone in the pulmonary circulation.

The finding that K_V7 channel activators were equally effective on pulmonary and systemic resistance arteries may seem to argue against their use as pulmonary vasodilators. But despite the *in vitro* effects of these drugs on systemic vessels, clinical studies have shown no effect on blood pressure. The only reported vascular side effect of retigabine appears to be headache (French et al., 2011). Since *in vitro* studies of K_V7 channel activators require the vessel to be pre-constricted, the dilator effect of the drugs may only become apparent *in vivo* under conditions of raised tone. A pulmonary selective effect may therefore be possible in PAH, where the PAs have raised tone, are more depolarised and thus have a greater driving force on K^+ flux. This possibility is strengthened by the different pharmacological profiles of human pulmonary and systemic arteries revealed by the effects of chromanol 293B. Indeed, with an apparent dual effect of K_V7 channel activation and VGCC inhibition, these drugs might provide benefits over and above those provided by traditional Ca^{2+} antagonists. The latter currently provide the mainstay of treatment for PAH patients showing a favourable response to acute vasodilator testing (Galiè et al., 2009). By hyperpolarising smooth muscle, K_V7 channel activators should cause similar suppression of voltage-gated Ca^{2+} influx, but they would additionally reverse the depolarization that is characteristic of the disease and raises Ca^{2+} influx (Yuan et al., 1998a). This should be beneficial due to the disruptive effect of depolarization on electrogenic ion transporters, such as the Na^+/Ca^{2+} exchanger (Läuger, 1987), which normally removes Ca^{2+} from the smooth muscle cell. Thus K_V7 channel activators have the potential to correct and protect against the deregulated Ca^{2+} signalling that underlies vasoconstriction and cell proliferation in pulmonary hypertensive disease.

2.7 Acknowledgements

Professor Dave Singh and Dr Jonathan Plumb, the University Hospital of South Manchester, provided the lung samples. Dr Mark Wareing, Manchester Maternal and Fetal Health

Research Centre Biobank, provided omentum samples. Dr Nikita Gamper, University of Leeds, provided the *KCNQ4* cDNA.

2.8 References

Brueggemann, L.I., Mackie, A.R., Martin, J.L., Cribbs, L.L., and Byron, K.L. (2011). Diclofenac distinguishes among homomeric and heteromeric potassium channels composed of KCNQ4 and KCNQ5 subunits. Molecular Pharmacology. *79*, 10-23

Busch, A.E., Suessbrich, H., Waldegger, S., Sailer, E., Greger, R., Lang, H., Lang, F., Gibson, K.J., and Maylie, J.G. (1996). Inhibition of I_{Ks} in guinea pig cardiac myocytes and guinea pig IsK channels by the chromanol 293B. Pflügers Archiv: European Journal of Physiology *432*, 1094–1096Cai, S.-Q., Park, K.H., and Sesti, F. (2006). An evolutionarily conserved family of accessory subunits of K+ channels. Cell Biochem. Biophys. *46*, 91–99.

Casteels, R., Kitamura, K., Kuriyama, H., and Suzuki, H. (1977a). Excitation-contraction coupling in the smooth muscle cells of the rabbit main pulmonary artery. The Journal of Physiology *271*, 63–79.

Casteels, R., Kitamura, K., Kuriyama, H., and Suzuki, H. (1977b). The membrane properties of the smooth muscle cells of the rabbit main pulmonary artery. The Journal of Physiology *271*, 41–61.

Chadha, P.S., Zunke, F., Zhu, H.-L., Davis, A.J., Jepps, T.A., Olesen, S.P., Cole, W.C., Moffatt, J.D., and Greenwood, I.A. (2012). Reduced *KCNQ4*-encoded voltage-dependent potassium channel activity underlies impaired β-adrenoceptor-mediated relaxation of renal arteries in hypertension. Hypertension *59*, 877–884.

Charpentier, F., Mérot, J., Loussouarn, G., and Baró, I. (2010). Delayed rectifier K^+ currents and cardiac repolarization. Journal of Molecular and Cellular Cardiology *48*, 37–44.

Clapp, L.H., Davey, R., and Gurney, A.M. (1993). ATP-sensitive K^+ channels mediate vasodilation produced by lemakalim in rabbit pulmonary artery. The American Journal of Physiology *264*, H1907–15.

Costa, A.M., and Brown, B.S. 1997. Inhibition of M-current in cultured rat superior cervical ganglia by linopirdine: mechanism of action studies. Neuropharmacology *36*, 1747–1753.

Devulder, J. (2010). Flupirtine in pain management: pharmacological properties and clinical use. CNS Drugs *24*, 867–881.

Dheda, K., Huggett, J.F., Bustin, S.A., Johnson, M.A., Rook, G., and Zumla, A. (2004). Validation of housekeeping genes for normalizing RNA expression in real-time PCR. BioTechniques *37*, 112–114, 116, 118–119.

Dupuis, D.S., Schrøder, R.L., Jespersen, T., Christensen, J.K., Christophersen, P., Jensen, B.S., and Olesen, S.P. (2002). Activation of KCNQ5 channels stably expressed in HEK293 cells by BMS-204352. European Journal of Pharmacology *437*, 129–137.

Dzhura, E. V, He, W., and Currie, K.P.M. (2006). Linopirdine modulates calcium signaling and stimulus-secretion coupling in adrenal chromaffin cells by targeting M-type K^+ channels and nicotinic acetylcholine receptors. The Journal of Pharmacology and Experimental Therapeutics *316*, 1165–1174.

Eskesen, K., János, T., Tibor, H., Délia, S., László, V., and Edvinsson, L. (2007). Unaltered mRNA expression of calcitonin-like receptor and receptor activity modifying proteins in human arteries in stroke and myocardial infarction. Ideggyógyászati Szemle *60*, 459–466.

Fleige, S., and Pfaffl, M.W. (2006). RNA integrity and the effect on the real-time qRT-PCR performance. Molecular Aspects of Medicine *27*, 126–139.

Fleige, S., Walf, V., Huch, S., Prgomet, C., Sehm, J., and Pfaffl, M.W. (2006). Comparison of relative mRNA quantification models and the impact of RNA integrity in quantitative real-time RT-PCR. Biotechnology Letters *28*, 1601–1613..

Foss, D.L., Baarsch, M.J., and Murtaugh, M.P. (1998). Regulation of hypoxanthine phosphoribosyltransferase, glyceraldehyde-3-phosphate dehydrogenase and beta-actin mRNA expression in porcine immune cells and tissues. Animal Biotechnology *9*, 67–78.

French, J.A., Abou-Khalil, B.W., Leroy, R.F., Yacubian, E.M.T., Shin, P., Hall, S., Mansbach, H., and Nohria, V. (2011). Randomized, double-blind, placebo-controlled trial of ezogabine (retigabine) in partial epilepsy. Neurology *76*, 1555–1563.

Galiè, N., Hoeper, M.M., Humbert, M., Torbicki, A., Vachiery, J.-L., Barbera, J.A., Beghetti, M., Corris, P., Gaine, S., Gibbs, J.S., et al. (2009a). Guidelines for the diagnosis and treatment of pulmonary hypertension: the Task Force for the Diagnosis and Treatment of Pulmonary Hypertension of the European Society of Cardiology (ESC) and the European Respiratory Society (ERS), endorsed by the International Society of Heart and Lung Transplantation (ISHLT). European Heart Journal *30*, 2493–2537.

Glare, E.M., Divjak, M., Bailey, M.J., and Walters, E.H. (2002). beta-Actin and GAPDH housekeeping gene expression in asthmatic airways is variable and not suitable for normalising mRNA levels. Thorax *57*, 765–770.

Goto, K., Kasuya, Y., Matsuki, N., Takuwa, Y., Kurihara, H., Ishikawa, T., Kimura, S., Yanagisawa, M., and Masaki, T. (1989). Endothelin activates the dihydropyridine-sensitive, voltage-dependent Ca^{2+} channel in vascular smooth muscle. PNAS *86*, 3915–3918.

Greenwood, I.A., and Ohya, S. (2009). New tricks for old dogs: KCNQ expression and role in smooth muscle. British Journal of Pharmacology *156*, 1196–1203.

Hamilton, T.C., and Weston, A.H. (1989). Cromakalim, nicorandil and pinacidil: novel drugs which open potassium channels in smooth muscle. General Pharmacology *20*, 1–9.

Imbeaud, S., Graudens, E., Boulanger, V., Barlet, X., Zaborski, P., Eveno, E., Mueller, O., Schroeder, A., and Auffray, C. (2005). Towards standardization of RNA quality assessment using user-independent classifiers of microcapillary electrophoresis traces. Nucleic Acids Research *33*, e56.

Jensen, H.S., Callø, K., Jespersen, T., Jensen, B.S., and Olesen, S.-P. (2005). The KCNQ5 potassium channel from mouse: a broadly expressed M-current like potassium channel modulated by zinc, pH, and volume changes. Brain Research. Molecular Brain Research *139*, 52–62

Jeong, I., Choi, B.H., and Hahn, S.J. (2013). Pergolide block of the cloned K_V1.5 potassium channels. Naunyn-Schmiedeberg's Archives of Pharmacology *386*, 125–133.

Joshi, S., Sedivy, V., Hodyc, D., Herget, J., and Gurney, A.M. (2009). KCNQ modulators reveal a key role for KCNQ potassium channels in regulating the tone of rat pulmonary artery smooth muscle. The Journal of Pharmacology and Experimental Therapeutics *329*, 368–376.

Karamsetty, M.R., Klinger, J.R., and Hill, N.S. (2001). Phytoestrogens restore nitric oxide-mediated relaxation in isolated pulmonary arteries from chronically hypoxic rats. Journal of Pharmacology and Experimental Therapeutics. *297*, 968–974.

Kubisch, C., Schroeder, B.C., Friedrich, T., Lütjohann, B., El-Amraoui, A., Marlin, S., Petit, C., and Jentsch, T.J. (1999). KCNQ4, a novel potassium channel expressed in sensory outer hair cells, is mutated in dominant deafness. Cell *96*, 437–446.

Lamas, J.A., Selyanko, A.A., and Brown, D.A. (1997). Effects of a cognition-enhancer, linopirdine (DuP 996), on M-type potassium currents (I_{KM}) and some other voltage- and ligand-gated membrane currents in rat sympathetic neurons. The European Journal of Neuroscience *9*, 605–616.

Läuger, P. (1987). Voltage dependence of sodium-calcium exchange: predictions from kinetic models. The Journal of Membrane Biology *99*, 1–11.

Lerche, C., Bruhova, I., Lerche, H., Steinmeyer, K., Wei, A.D., Strutz-Seebohm, N., Lang, F., Busch, A.E., Zhorov, B.S., and Seebohm, G. (2007). Chromanol 293B binding in KCNQ1 (K_V7.1) channels involves electrostatic interactions with a potassium ion in the selectivity filter. Molecular Pharmacology *71*, 1503–1511.

Lundquist, A.L., Manderfield, L.J., Vanoye, C.G., Rogers, C.S., Donahue, B.S., Chang, P.A., Drinkwater, D.C., Murray, K.T., and George, A.L. (2005). Expression of multiple KCNE genes in human heart may enable variable modulation of I(Ks). Journal of Molecular and Cellular Cardiology *38*, 277–287.

Mani, B.K., O'Dowd, J., Kumar, L., Brueggemann, L.I., Ross, M., and Byron, K.L. (2013). Vascular KCNQ (K_V7) potassium channels as common signaling intermediates and therapeutic targets in cerebral vasospasm. Journal of Cardiovascular Pharmacology *61*, 51–62.

Martire, M., Castaldo, P., D'Amico, M., Preziosi, P., Annunziato, L., and Taglialatela, M. (2004). M channels containing KCNQ2 subunits modulate norepinephrine, aspartate, and GABA release from hippocampal nerve terminals. The Journal of Neuroscience *24*, 592–597.

McCulloch, K.M., Docherty, C.C., Morecroft, I., and MacLean, M.R. (1996). EndothelinB receptor-mediated contraction in human pulmonary resistance arteries. British Journal of Pharmacology *119*, 1125–1130.

Morecroft, I., Murray, A., Nilsen, M., Gurney, A.M., and MacLean, M.R. (2009). Treatment with the K_V7 potassium channel activator flupirtine is beneficial in two independent mouse models of pulmonary hypertension. British Journal of Pharmacology *157*, 1241–1249.

Moudgil, R., Michelakis, E.D., and Archer, S.L. (2006). The role of K^+ channels in determining pulmonary vascular tone, oxygen sensing, cell proliferation, and apoptosis: implications in hypoxic pulmonary vasoconstriction and pulmonary arterial hypertension. Microcirculation *13*, 615–632.

Mueller, O., Hahnenberger, K., Dittmann, M., Yee, H., Dubrow, R., Nagle, R., and Ilsley, D. (2000). A microfluidic system for high-speed reproducible DNA sizing and quantitation. Electrophoresis *21*, 128–134.

Mulvany M.J. (1988). Procedures for investigation of small vessels using small vessel myograph. Danish Myo Technology, 2004. Available at: http://www.dmt.dk/files/manualer/procedures_for_investigation.pdf (Accessed 28th September 2013)

Neacsu, C., and Babes, A. (2010). The M-channel blocker linopirdine is an agonist of the capsaicin receptor TRPV1. Journal of Pharmacological Sciences *114*, 332–340.

Ng, F.L., Davis, A.J., Jepps, T.A., Harhun, M.I., Yeung, S.Y., Wan, A., Reddy, M., Melville, D., Nardi, A., Khong, T.K., Greenwood I.A. (2011). Expression and function of the K^+ channel KCNQ genes in human arteries. British Journal of Pharmacology *162*, 42–53.

Norel, X., Walch, L., Costantino, M., Labat, C., Gorenne, I., Dulmet, E., Rossi, F., and Brink, C. (1996). M1 and M3 muscarinic receptors in human pulmonary arteries. British Journal of Pharmacology. *119*, 149–157.

Osipenko, O.N., Alexander, D., MacLean, M.R., and Gurney, A.M. (1998). Influence of chronic hypoxia on the contributions of non-inactivating and delayed rectifier K currents to the resting potential and tone of rat pulmonary artery smooth muscle. British Journal of Pharmacology *124*, 1335–1337.

Patel, A.J., Lazdunski, M., and Honoré, E. (1997). $K_V2.1/K_V9.3$, a novel ATP-dependent delayed-rectifier K^+ channel in oxygen-sensitive pulmonary artery myocytes. The EMBO Journal *16*, 6615–6625.

Perez-Zoghbi, J.F., and Sanderson, M.J. (2007). Endothelin-induced contraction of bronchiole and pulmonary arteriole smooth muscle cells is regulated by intracellular Ca^{2+}

oscillations and Ca^{2+} sensitization. American Journal of Physiology-Lung Cellular and Molecular Physiology *293*, L1000–11.

Pfaffl, M.W. (2001). A new mathematical model for relative quantification in real-time RT-PCR. Nucleic Acids Research *29*, e45.

Pfaffl, M.W., Tichopad, A., Prgomet, C., and Neuvians, T.P. (2004). Determination of stable housekeeping genes, differentially regulated target genes and sample integrity: BestKeeper--Excel-based tool using pair-wise correlations. Biotechnology Letters *26*, 509–515.

Pieniaszek, H.J., Fiske, W.D., Saxton, T.D., Kim, Y.S., Garner, D.M., Xilinas, M., and Martz, R. (1995). Single-dose pharmacokinetics, safety, and tolerance of linopirdine (DuP 996) in healthy young adults and elderly volunteers. Journal of Clinical Pharmacology *35*, 22–30.

Preuss, K.C., Gross, G.J., Brooks, H.L., and Warltier, D.C. (1985). Slow channel calcium activators, a new group of pharmacological agents. Life Sciences *37*, 1271–1278.

Riezebos, J., Watts, I.S., and Vallance, P.J. (1994). Endothelin receptors mediating functional responses in human small arteries and veins. British Journal of Pharmacology *111*, 609–615.

Rundfeldt, C., and Netzer, R. (2000a). Investigations into the mechanism of action of the new anticonvulsant retigabine. Interaction with GABAergic and glutamatergic neurotransmission and with voltage-gated ion channels. Arzneimittelforschung *50*, 1063–1070.

Rundfeldt, C., and Netzer, R. (2000b). The novel anticonvulsant retigabine activates M-currents in Chinese hamster ovary-cells tranfected with human KCNQ2/3 subunits. Neuroscience Letters *282*, 73–76.

Schmittgen, T.D., and Zakrajsek, B.A. (2000). Effect of experimental treatment on housekeeping gene expression: validation by real-time, quantitative RT-PCR. Journal of Biochemical and Biophysical Methods *46*, 69–81.

Schramm, M., Thomas, G., Towart, R., and Franckowiak, G. Novel dihydropyridines with positive inotropic action through activation of Ca^{2+} channels. Nature *303*, 535–537.

Schroeder, A., Mueller, O., Stocker, S., Salowsky, R., Leiber, M., Gassmann, M., Lightfoot, S., Menzel, W., Granzow, M., and Ragg, T. (2006). The RIN: an RNA integrity number for assigning integrity values to RNA measurements. BMC Molecular Biology *7*, 3.

Schroeder, B.C., Hechenberger, M., Weinreich, F., Kubisch, C., and Jentsch, T.J. (2000a). KCNQ5, a novel potassium channel broadly expressed in brain, mediates M-type currents. The Journal of Biological Chemistry *275*, 24089–24095.

Shimoda, L.A., and Laurie, S.S. (2013). Vascular remodeling in pulmonary hypertension. Journal of Molecular Medicine (Berlin, Germany) *91*, 297–309.

Smirnov, S. V, Robertson, T.P., Ward, J.P., and Aaronson, P.I. (1994). Chronic hypoxia is associated with reduced delayed rectifier K^+ current in rat pulmonary artery muscle cells. The American Journal of Physiology *266*, H365–70.

Søgaard, R., Ljungstrøm, T., Pedersen, K.A., Olesen, S.P., and Jensen, B.S. (2001). KCNQ4 channels expressed in mammalian cells: functional characteristics and pharmacology. American Journal of Physiology- Cell Physiology *280*, C859–66.

Stenmark, K.R., Meyrick, B., Galie, N., Mooi, W.J., and McMurtry, I.F. (2009). Animal models of pulmonary arterial hypertension: the hope for etiological discovery and pharmacological cure. American Journal of Physiology- Lung Cellular and Molecular Physiology *297*, L1013–32.

Suzuki, H., and Twarog, B.M. (1982). Membrane properties of smooth muscle cells in pulmonary hypertensive rats. The American Journal of Physiology *242*, H907–15.

Suzuki, T., Higgins, P.J., and Crawford, D.R. (2000). Control selection for RNA quantitation. BioTechniques *29*, 332–337.

Szelenyi, I. (2013). Flupirtine, a re-discovered drug, revisited. Inflammation Research *62*, 251–258

Tatulian, L., Delmas, P., Abogadie, F.C., and Brown, D.A. (2001). Activation of expressed KCNQ potassium currents and native neuronal M-type potassium currents by the anti-convulsant drug retigabine. The Journal of Neuroscience *21*, 5535–5545.

Thellin, O., Zorzi, W., Lakaye, B., De Borman, B., Coumans, B., Hennen, G., Grisar, T., Igout, A., and Heinen, E. (1999). Housekeeping genes as internal standards: use and limits. Journal of Biotechnology *75*, 291–295.

Tinel, N., Lauritzen, I., Chouabe, C., Lazdunski, M., and Borsotto, M. (1998). The KCNQ2 potassium channel: splice variants, functional and developmental expression. Brain localization and comparison with KCNQ3. FEBS Letters *438*, 171–176.

Tricarico, C., Pinzani, P., Bianchi, S., Paglierani, M., Distante, V., Pazzagli, M., Bustin, S.A., and Orlando, C. (2002). Quantitative real-time reverse transcription polymerase chain reaction: normalization to rRNA or single housekeeping genes is inappropriate for human tissue biopsies. Analytical Biochemistry *309*, 293–300.

Vandesompele, J., De Preter, K., Pattyn, F., Poppe, B., Van Roy, N., De Paepe, A., and Speleman, F. (2002). Accurate normalization of real-time quantitative RT-PCR data by geometric averaging of multiple internal control genes. Genome Biology *3*, research0034.

Wang, H.S., Pan, Z., Shi, W., Brown, B.S., Wymore, R.S., Cohen, I.S., Dixon, J.E., and McKinnon, D. (1998). KCNQ2 and KCNQ3 potassium channel subunits: molecular correlates of the M-channel. Science *282*, 1890–1893.

Wickenden, A.D., Yu, W., Zou, A., Jegla, T., and Wagoner, P.K. (2000). Retigabine, a novel anti-convulsant, enhances activation of KCNQ2/Q3 potassium channels. Molecular Pharmacology *58*, 591–600.

Wladyka, C.L., and Kunze, D.L. (2006). KCNQ/M-currents contribute to the resting membrane potential in rat visceral sensory neurons. The Journal of Physiology *575*, 175–189.

World Medical Association. (2013). World Medical Association Declaration of Helsinki: ethical principles for medical research involving human subjects. Journal of the American Medical Association *310*, 2191–2194

Wu, D.-M., Jiang, M., Zhang, M., Liu, X.-S., Korolkova, Y. V, and Tseng, G.-N. (2006). KCNE2 is colocalized with KCNQ1 and KCNE1 in cardiac myocytes and may function as a negative modulator of I_{Ks} current amplitude in the heart. Heart Rhythm *3*, 1469–1480.

Xiong, Q., Sun, H., and Li, M. (2007). Zinc pyrithione-mediated activation of voltage-gated KCNQ potassium channels rescues epileptogenic mutants. Nature Chemical Biology *3*, 287–296.

Xiong, Q., Gao, Z., Wang, W., and Li, M. (2008b). Activation of K_V7 (KCNQ) voltage-gated potassium channels by synthetic compounds. Trends in Pharmacological Sciences *29*, 99–107.

Yamaguchi, T., Rodman, D., O'Brien, R., and McMurtry, I. (1989). Modulation of pulmonary artery contraction by endothelium-derived relaxing factor. European Journal of Pharmacology. *161*, 259–262.

Yang, I.C., Scherz, M.W., Bahinski, A., Bennett, P.B., and Murray, K.T. (2000). Stereoselective interactions of the enantiomers of chromanol 293B with human voltage-gated potassium channels. The Journal of Pharmacology and Experimental Therapeutics *294*, 955–962.

Yeung, S.Y.M., Pucovský, V., Moffatt, J.D., L, Saldanha, L., Schwake, M., Ohya, S., and Greenwood, I.A. (2007). Molecular expression and pharmacological identification of a role for K_V7 channels in murine vascular reactivity. British Journal of Pharmacology *151*, 758–770.

Yuan, J.X., Aldinger, A.M., Juhaszova, M., Wang, J., Conte, J. V, Gaine, S.P., Orens, J.B., and Rubin, L.J. (1998a). Dysfunctional voltage-gated K^+ channels in pulmonary artery smooth muscle cells of patients with primary pulmonary hypertension. Circulation *98*, 1400–1406.

Yuan, X.J., Tod, M.L., Rubin, L.J., and Blaustein, M.P. (1990). Contrasting effects of hypoxia on tension in rat pulmonary and mesenteric arteries. The American Journal of Physiology *259*, H281–9.

Zaczek, R., Chorvat, R.J., Brown, B.S. (1997) Linopirdine: Pharmacology of a neurotransmitter release enhancer. CNS Drug reviews 3 pp 103-119

Zhong, X.Z., Harhun, M.I., Olesen, S.P., Ohya, S., Moffatt, J.D., Cole, W.C., and Greenwood, I.A. (2010). Participation of KCNQ (K_V7) potassium channels in myogenic control of cerebral arterial diameter. The Journal of Physiology *588*, 3277–3293.

Chapter 3 : Loss of K_V7 channel expression and function in proliferating human pulmonary artery smooth muscle cells

Katie Smith[1], Sean Brennan, Neil Bodagh, Paolo Tammaro[2], Alison M Gurney*

Faculty of Life Sciences

University of Manchester

Manchester

M13 9NT

[1]Current address:

UCL Ear Institute, University College London, Gower Street, London WC1E 6BT

[2]Current address:

Department of Pharmacology, University of Oxford, Mansfield Road, Oxford OX1 3QT

Intended journal: Pulmonary Circulation

*Author for correspondence

3.1. Abstract

Pulmonary arterial hypertension (PAH) is characterised by vascular remodelling, in which pulmonary artery smooth muscle cells (PASMCs) become highly proliferative and migrate within and from the medial layer of the artery. Proliferation and migration are associated with altered Ca^{2+} handling, which may be a consequence of altered membrane potential. Following recent observations linking K_V7 potassium channels to the control of membrane potential in PASMC, the aim of this study was to determine if K_V7 channels play any role in the events that underlie smooth muscle proliferation and migration. Freshly isolated human PASMC displayed non-inactivating, voltage-gated K^+ currents, recorded by whole-cell patch-clamp electrophysiology. They also expressed mRNA transcripts for $K_V7.1$, $K_V7.3$, $K_V7.4$ and $K_V7.5$ channel subunits, as measured by RT-PCR. The voltage-gated currents and all transcripts, except for $K_V7.5$, disappeared before the first passage when PASMC were cultured and were not recovered by growth arresting cells in low serum medium. Cell proliferation was measured in cultured cells by DNA uptake of 5-bromo-2'-deoxy-uridine (BrdU) and immunostaining for the Ki67 antigen, while migration was assessed as the repopulation of a scratched area in a confluent layer of PASMC. A range of drugs that block or activate K_V7 channels had no effect on either the proliferation or migration of PASMC. It is concluded that although $K_V7.5$ channel transcripts are preserved in proliferating PASMC, the functional channels play no role in the proliferation or migration of these cells. The expression of $K_V7.1$, $K_V7.3$ and $K_V7.4$ is limited to contractile PASMC, where their loss may be important for the differentiation of PASMC from a contractile into a proliferative phenotype.

3.2 Introduction

PAH is characterised by a mean PA pressure above 25 mmHg at rest and has a poor prognosis. It is a progressive disease in which pulmonary vascular resistance increases due to vasoconstriction and remodelling of the small PAs. The processes involved in remodelling include the proliferation and migration of PASMCs, along with smooth muscle hyperplasia and muscularisation of normally non-muscular arteries (Shimoda and Laurie, 2013). In the healthy vessel wall, mature PASMCs regulate contraction and proliferate at an extremely low rate. They appear to lose contractility in PAH and show an increased rate of proliferation. In fact after isolation and culture, PASMC from PAH patients show higher rates of proliferation compared with PASMC from patients without PAH (Falcetti et al., 2010; Ikeda et al., 2010; Marcos et al., 2004).

A key event in PASMC contraction, proliferation and migration is a rise in $[Ca^{2+}]_i$, with a higher resting $[Ca^{2+}]_i$ found in proliferating cells compared with quiescent cells (Golovina, 1999; Kuhr et al., 2012; Leggett et al., 2012; Mandegar et al., 2004; Platoshyn et al., 2000). An important factor in the regulation of $[Ca^{2+}]_i$ is the PASMC membrane potential. The high permeability of the membrane to K^+ relative to other ions in contractile cells results in a steady efflux of K^+, which polarises the membrane at around -50 mV (Evans et al., 1996; Osipenko et al., 1998). This stops VGCCs from opening, thereby limiting Ca^{2+} influx (Clapp and Gurney, 1991a). PASMC are depolarised in PAH, both in animal models and humans (Osipenko et al., 1998; Smirnov et al., 1994; Suzuki and Twarog, 1982; Yuan et al., 1998c) and the depolarisation is an early event in disease progression (Hong et al., 2005). Proliferating PASMC are also more depolarised than growth arrested cells (Platoshyn et al., 2000), implying a link between depolarisation and the switch from predominantly contractile to proliferating cells in PAH. Such a link between membrane potential and cell differentiation and proliferation has been reported for many cell types (Sundelacruz et al., 2009), suggesting a universally important mechanism. The finding that PASMC proliferation could be inhibited by activating K_{ATP} channels and hyperpolarising the membrane (Zhu et al., 2008) suggests a causative role for depolarisation.

The depolarisation of PASMC in PAH reflects a loss of expression and activity of K^+ channels (Osipenko et al., 1998; Smirnov et al., 1994; Yuan et al., 1998c). A number of distinct K^+ channels have been proposed as mediators of the resting K^+ efflux and membrane potential, although there is lack of agreement on which predominate (Gurney and Joshi,

2006; Gurney et al., 2002). It is likely that several K^+ channels contribute and the inhibition of any one of them would lead to depolarisation. We have identified a role for K_V7 channels, encoded by the *KCNQ1-5* genes, in regulating the membrane potential of rodent and human PASMC (Brennan et al., 2011; Joshi et al., 2009). This family of K^+ channels is of particular interest, because they are good pharmacological targets. Indeed the K_V7 channel activator, retigabine, was recently approved for the treatment of epilepsy, due to its enhancement of the neuronal I_{KM} mediated by $K_V7.2/7.3$ channels (Amabile and Vasudevan, 2013). Tissue specificity is also a possibility due to the amenability of K_V7 channels to the development of subunit-selective drugs for $K_V7.1$, $K_V7.2$ and $K_V7.4$ channels (Boehlen et al., 2013; Lerche et al., 2007; Yu et al., 2013). K_V7 channel activators hyperpolarise PASMCs and evoke vasodilatation, while blockers of these channels have the opposite effects (Brennan et al., 2011; Joshi et al., 2006, 2009).

Since membrane potential influences PASMC proliferation and migration, we hypothesised that these activities would also be inhibited by K_V7 channel activators and suppressed by K_V7 channel blockers. There is precedence for this in skeletal muscle, where $K_V7.5$ channels were found to be up regulated during progression of the cell cycle (Roura-Ferrer et al., 2008) and the K_V7 channel activator, retigabine, reduced proliferation (Iannotti et al., 2010). In contrast, the mature differentiated muscle displayed high levels of $K_V7.1$, $K_V7.3$ and $K_V7.4$ transcripts and retigabine suppressed differentiation (Iannotti et al., 2010). We therefore investigated the expression of K_V7 transcripts in quiescent and proliferating human PASMC and investigated their roles in proliferation and migration using K_V7 modulating drugs to interfere with channel activity.

3.3 Methods

3.3.1 Human Tissue samples

The use of human tissue for this study was approved by the South Manchester Research Ethics Committee (reference 03/SM/396). Samples were collected with informed consent in compliance with the Helsinki Declaration.

Lung samples were obtained from patients undergoing surgical resection for suspected or confirmed lung cancer and stored at 4°C until collection. Tissue was transferred to the laboratory on ice and placed in cold physiological salt solution (PSS) containing 122 mM NaCl, 5 mM KCl, 1 mM $MgCl_2$, 0.5 mM NaH_2PO_4, 0.5 mM KH_2PO_4, 10 mM HEPES, 11 mM glucose, and 1.8 mM $CaCl_2$, pH 7.3. Distal PAs were dissected from lung samples within 24 h of tumour resection. Some were cut open longitudinally, then into small segments and stored in RNA*later*® solution (Invitrogen, UK), according to the manufacturer's instructions. The remaining vessels were carefully denuded of endothelium by rubbing the intimal surface with filter paper and the adventitial layer carefully removed. The remaining smooth muscle layer was used to isolate PASMC and generate primary cultures.

3.3.2 Cell isolation and culture

Muscle strips from human PA (2-4 mm long), were washed in dissociation medium (DM) of the following composition: 110 mM NaCl, 5 mM KCl, 10 mM HEPES, 0.5 mM KH_2PO_4, 0.5 mM NaH_2PO_4, 10 mM $NaHC0_3$, 10 mM taurine, 0.5 mM EDTA, 160 µM $CaCl_2$, 2 mM $MgCl_2$, 30 µM phenol Red, pH 7.0. Smooth muscle cells were then enzymatically isolated from the tissue as previously described (Clapp and Gurney, 1991a) and washed in DM. Some were used immediately for electrophysiology experiments. Drops of remaining cell suspension were placed on the bottom of a 35 mm culture dish and left for around 15 min at room temperature to adhere to the surface. Smooth muscle growth medium (2 ml), prepared by adding smooth muscle growth supplement to smooth muscle basal medium (PromoCell GmbH, Heidelberg, Germany), was then added and the dish transferred to a humidified incubator at 37°C, with 5% CO_2. The cells were washed with fresh medium every 2 days until a confluent layer formed and they were passaged into a 25 cm^2 culture flask. Human PASMCs isolated from a healthy 17 year-old female were also purchased from PromoCell (Cat #: C-12521) for comparison.

PASMCs from both sources were sub-cultured in smooth muscle growth medium, containing 5% (v/v) foetal calf serum, 0.5 ng/ml epidermal growth factor, 2 ng/ml basic fibroblast growth factor and 5 µg/ml insulin. Cells were passaged after 80-90% confluence using the Promocell DetachKit, following the manufacturer's instructions. Cell growth was inhibited when required by replacing the complete medium with medium containing low (0.1%) foetal calf serum for 24 h. Cells were used for experiments between passages 4 and 6, when no changes in cell morphology were noted.

3.3.3 *KCNQ* mRNA Expression

Total RNA was isolated using an RNeasy Micro or Mini kit (Qiagen, UK). Genomic DNA was removed using an RNase-free DNase kit (Qiagen, UK). First strand cDNA was synthesised from the total RNA using SuperScript® III (Invitrogen, UK) with random hexameric oligonucleotides (Invitrogen, UK). A reaction mix omitting reverse transcriptase was used as a negative control (RT-).

The primers used in RT-PCR to amplify mRNAs coding for the subunits of K_V7 channels are listed in (Table 3.1). The primers for *KCNQ2*, *KCNQ4* and *KCNQ5* were from Primer Design, UK. Primers for *KCNQ1* and *KCNQ3* were designed using Primer 3 software (v.0.4.0; Whitehead Institute and Howard Hughes Medical Institute, http://primer3.sourceforge.net/) to amplify intron-spanning sequences. First-strand cDNA (38 ng), or its respective negative control, was used as the template in a 25 µl PCR reaction including forward and reverse primers (MWG Biotech, Ebersberg, Germany, 0.5 µM each) and 12.5 µl Hotstart Taq polymerase mastermix (Qiagen). The reaction mix was heated to 95°C for 15 min followed by 35 repetitions of the following cycle: denaturation (94°C, 45 s), annealing (50 °C, 45 s) and extension (72°C, 1 min). PCR products were analysed using 1.5% agarose gel electrophoresis and visualised with ethidium bromide under ultraviolet illumination, using a GelDoc2000 system to capture the images (Bio-Rad, Hercules, CA, USA).

Gene	Accession Number	Primer (5'-3')	Product length (bp)
*KCNQ*1	NM_000218	For: ATTCGACGCATGCAGTACTT	122
		Rev: AACCTCATGGTGCGCATCAA	
*KCNQ*2	NM_172107	For: CCACCATCAAGGAGTATGAGAAG	102
		Rev: TACTTCGTGCGGATCTGGG	
*KCNQ*3	NM_004519	For: AGGTGGATGCACAAGGAGAG	159
		Rev: AGGTGGATGCACAAGGAGAG	
*KCNQ*4	NM_004700	For: CGCCTCCTTCCTGGTCTAC	104
		Rev: ATTACATTGACAACCATCGGCT	
*KCNQ*5	NM_019842	For: AGCAGAACATGAGACCACCAGA	124
		Rev: CATCTATCAACAGGTCCTTCGG	

Table 3.1:*KCNQ1-5* Primers for PCR. Forward (For) and reverse (Rev) primers for genes with the indicated accession numbers were used to amplify transcripts with the base pair (bp) length indicated.

3.3.4 Electrophysiology

Cultured PASMC were detached from a culture dish using the Promocell DetachKit and re-suspended in complete medium. Drops of a cell suspension were placed on coverslips in a 35 mm culture dish and allowed to adhere to the glass overnight in an incubator. The coverslips were placed on the bottom of the recording chamber for electrophysiology experiments.

Cells were continually superfused with PSS and the whole-cell patch-clamp technique was used to measure membrane currents and membrane potential as previously described (Osipenko et al., 1998), using an Axopatch 200A amplifier (Axon CNS, Molecular Devices, Sunnyvale, CA, USA). Borosilicate glass pipettes (3-4 MΩ) were filled with the following solution (in mM): KCl 130, HEPES 20, EGTA 1, $MgCl_2$, Na_2GTP 0.5; pH adjusted to 7.2 with KOH. The uncompensated series resistance when recording from freshly isolated or

cultured PASMC was 11 ± 1 MΩ (n=43) and 10 ± 1 MΩ (n=9), respectively. The largest current recorded in this study (408 pA), from freshly isolated PASMCs at 60 mV, would be associated with the largest voltage error of 4.5 mV. Resting membrane potential was measured as the zero current potential under current-clamp conditions and was not corrected for the liquid junction potential. To record K^+ currents under voltage clamp, cells were clamped at -80 mV and 2.5 s steps applied in 10 mV increments to between -70 and +40 mV. Voltage and current commands were generated with the Whole-Cell Analysis Program V3.6.6 data acquisition software (John Dempster, University of Strathclyde, Glasgow, UK) through a BNC 2090 interface (National Instruments Corporation, Newbury, UK). Current amplitudes were normalised to the membrane capacitance in each cell and reported in units of pA/pF. Mean capacitance, calculated by integrating the area under the capacity transient evoked at the start of a -10 mV voltage steps, was 27 ± 1 pF (n=40) in freshly isolated PASMC and 50 ± 7 pF (n=9) in cultured cells. Currents were not leak subtracted.

3.3.5 PASMC proliferation

Cell counting is a common method used to evaluate changes in the rate of proliferation. However, whilst it can indicate changes in the total number of cells, it does not distinguish whether such changes reflect altered rates of proliferation and/or apoptosis. Moreove, since PASMCs in culture grow slowly compared to other cell types, it can be difficult to obtain sufficient increases in cell number to give reliable data (Goncharova et al., 2006). For this reason, two different methods were used to assess PASMC proliferation. The first measured 5-bromo-2'-deoxy-uridine (BrdU) uptake into DNA using a monoclonal anti-BrdU antibody with a BrdU labelling and detection kit I (Roche Applied Science, Burgess Hill, UK), following the manufacturer's instructions. PASMC were grown to 30% confluence on poly-d-lysine coated glass coverslips in 24-well plates with complete smooth muscle growth medium. Low-serum medium was substituted for 24 h before experiments began, in order to inhibit cell growth. Proliferation was then stimulated by re-introducing the complete growth medium, with or without the addition of drug or vehicle. Proliferation was allowed to continue for 24 h and BrdU (10 μM) added to the medium for the last 4 h. Coverslips were then washed and exposed for 30 min to a fixative solution prepared by mixing 70% ethanol and 50 mM glycine in a 7:3 ratio. The fixed cells were incubated with the anti-BrdU antibody for 30min at 37˚C, followed by anti-mouse-Ig-fluorescein for 30min at 37°C in the

dark. The second assay employed a rabbit monoclonal antibody (Abcam, Cambridge, UK; ab16667) directed against the Ki67 antigen, expressed preferentially during the late G_1, S, G_2 and M phases of the cell cycle, but not in quiescent (G_0) cells. PASMCs were prepared, growth inhibited and stimulated to proliferate for 24 h as in the BrdU assay, but were then fixed with 4% paraformaldehyde in phosphate buffered saline (PBS) for 20 min followed by permeabilisation with 0.1% Triton X100 in PBS for 5 min at room temperature. Cells were then incubated at room temperature with blocking solution (10 % FCS in PBS) for 30 min, followed by the anti-Ki67 antibody (1:100 dilution) for 1 h and then a tetramethylrhodamine isothiocyanate (TRITC)-labelled goat anti-rabbit IgG (Abcam ab6718) for 1 h.

Coverslips were mounted on slides for fluorescence imaging using Vectashield mounting medium (Vector laboratories, Peterborough, UK) containing the nuclear marker 4',6-diamidino-2-phenylindole (DAPI, 1.5 µg/ml). Fluorescent images were captured with MetaVue Software (Molecular Devices) and a Coolsnap ES camera (Photometrics) mounted on an Olympus wide field BX51 upright microscope, using a 10x/ 0.30 Plan fluorescence objective. Excitation and detection wavelengths were selected using filter sets for DAPI, fluorescein and TRITC. Images were processed and analysed using Image J (http://rsb.info.nih.gov/ij) to count the total number of cells, indicated by DAPI staining, and proliferating cells. Data are presented as the percentage of cells staining positively for BrdU or Ki67.

3.3.6 PASMC scratch wound assay

PASMCs were grown to 100% confluence on 12-well plates with compete growth medium then growth was inhibited for 24 h in low serum (0.1%) medium. A sterile pipette tip was used to scratch a 0.5 mm wide wound in each well. The cells were washed with low serum medium to remove debris then fresh low serum medium containing drug or control was added to each well. The 12-well plate was mounted on the incubated (37°C, 5% CO_2) stage of an AS MDW live cell imaging system (Leica Microsystems, Wetzlar, Germany). A series of brightfield images was acquired, at the same positions, every 10 min for up to 24 h, using a 5x/ 0.15 Plan Fluotar objective, a Coolsnap HQ CCD camera (Photometrics, Tucson, AZ) and Image Pro 6.3 imaging software (Media Cybernetics Inc, Rockville, MD, USA). Point visiting was used to allow multiple positions to be imaged each time and three fields were imaged in each well. ImageJ 1.6 was used to assess repopulation of the scratch by cells in each field.

The percentage of the scratched area that was re-covered at each time point was measured as the average from the three fields in each well.

3.4 Results

3.4.1 Pulmonary artery smooth muscle cell phenotype

In order to ensure the cells used were PASMCs and not endothelium or fibroblasts, two markers of the smooth muscle phenotype were used. The smooth muscle phenotype was confirmed by positive immunofluorescence staining with antibodies directed against smooth muscle myosin and smooth muscle α–actin (Figure 3.1).

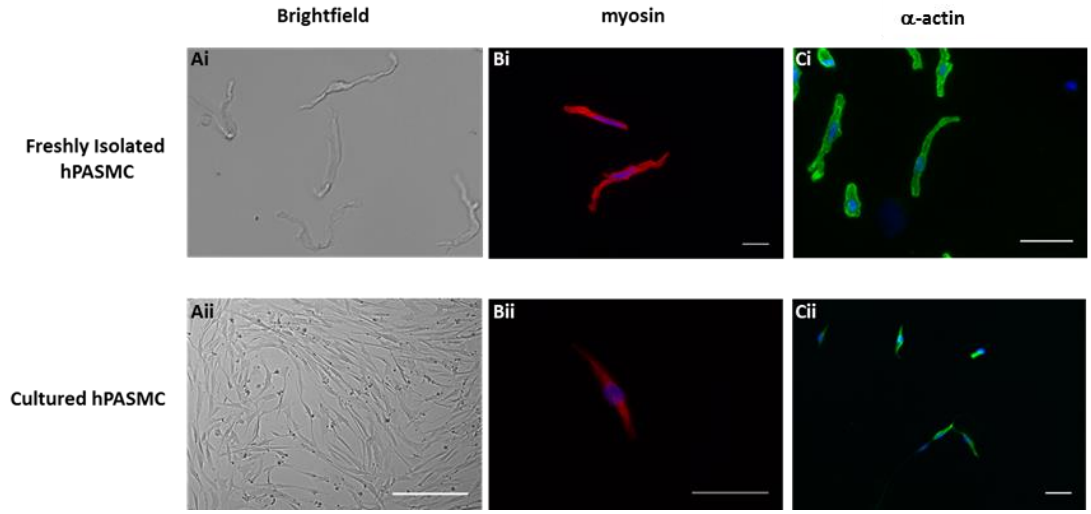

Figure 3.1: Representative images of freshly isolated and cultured PASMCs. Brightfield images (left panels) show freshly isolated (Ai) and cultured (Aii) PASMCs. Fluorescence images show smooth muscle myosin (red; middle panels) and α-actin staining (green; right panel) in freshly isolated (Bi and Bii) and cultured (Ci and Cii) PASMCs. Nuclear staining with DAPI shown in blue. Scale bar is 20 µm. Immunofluorescence staining conducted by the post-doctoral researcher Katie Smith.

3.4.2 Expression of K_V7 channel genes

We recently reported that human PA expresses mRNA transcribed from the *KCNQ1*, *KCNQ3*, *KCNQ4* and *KCNQ5* genes, but not *KCNQ2* (Brennan et al., 2011). When mRNA expression was investigated in cultured human PASMCs, either in cells sourced commercially (Figure 3.2A) or isolated and cultured in-house (Figure 3.2B), only *KCNQ5* was convincingly present.

As the absence of the other transcripts could reflect down-regulation during the switch from the contractile to proliferative phenotype, we re-assessed expression after growth arresting cells by reducing the serum from 5 to 0.1 % for 20 h. As shown in Figure 3.2C, the same expression profile was apparent. To address concerns that in measurements of whole artery the transcripts might not have arisen from the smooth muscle cells, we isolated mRNA from muscle strips that had been carefully denuded of both endothelium and adventitia. Some of the same muscle strips were used to prepare cultured PASMC and expression was compared in the muscle at the time of cell isolation and in the cultured cells after the first passage (P1). Figure 3.2D shows that mRNAs for *KCNQ1*, *KCNQ3*, *KCNQ4* and *KCNQ5* were all present at the time of PASMC isolation, but all except *KCNQ5* had disappeared by P1. To determine how early the down-regulation occurred, we also assessed expression when the cells first reached confluence and before they were passaged (P0). Even at that early time, *KCNQ1*, *KCNQ3* and *KCNQ4* transcripts were barely detectable (Figure 3.2D). These data show that mRNA expression of the *KCNQ* genes was reduced in cultured PASMCs.

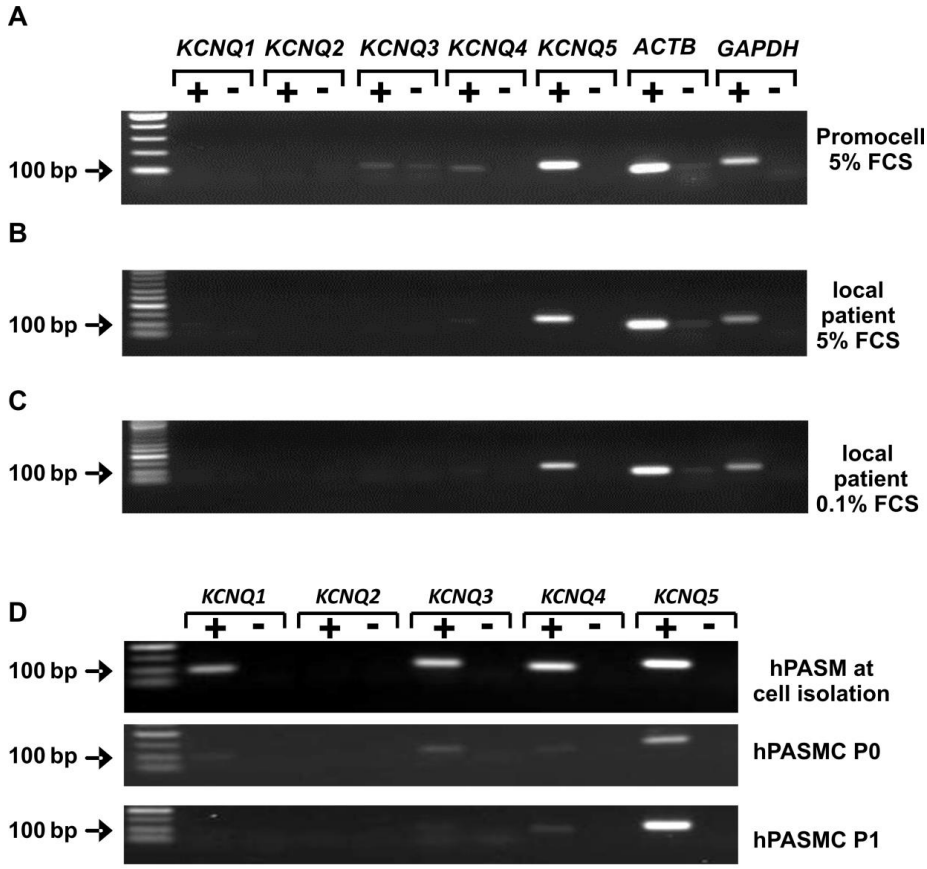

Figure 3.2: K_V7 subunit expression in human PASMC. End point RT-PCR analysis of KCNQ1-5 transcripts in cultured human PASMC from a commercial source (A), prepared in-house and maintained in 5% foetal calf serum (FCS) in short term culture (B) or growth arrested in 0.1 % FCS (C). D, Expression compared in PASMC from a single human iPA at the time of isolation, when the cells first became confluent (P0) and following the first passage (P1). Negative controls (-) employed the same reactions, but without reverse transcriptase. Expected sizes of PCR products: *KCNQ1* 122 bp; *KCNQ2* 102 bp; *KCNQ3* 159 bp: *KCNQ4* 104 bp; *KCNQ5* 124 bp. Size markers in left hand lanes show 100 bp (A) or 50 bp (B and C) ladder. The band corresponding to 100 bp is indicated alongside each ladder. Genes *ACTB* and *GAPDH* provide positive controls. End-point PCR experiments were done by the post-doctoral researcher K. Smith, using primers optimised by S. Brennan.

3.4.3 Functional expression of K_V7 channels

To assess the importance of K_V7 channels in the proliferation and migration of cultured PAMSCs the expression profile of these channels was investigated. K_V7 channel currents are typically slow to activate and are non-inactivating during sustained depolarisation. To

activate these channels in PASMC we therefore applied voltage steps of 2.5 s duration, from a holding potential of -80 mV, to gradually more depolarised potentials. Figure 3.3A shows typical records of currents activated in freshly isolated human PASMCs with this protocol. Currents were outwardly rectifying and at positive potentials they activated fully within 500 ms. The current-voltage relationship is typical of outwardly rectifying K^+ channels with activation apparent at potentials more positive than -50 mV (Figure 3.3C). In contrast, the currents recorded from cultured PASMC were small and showed no time-dependent activation during voltage steps (Figure 3.3B). The current-voltage relationship shows a linear change in current with depolarisation (Figure 3.3C).

The mean RMP of freshly isolated human PASMCs was -41 ± 1.6 mV (n = 27). In contrast, the mean RMP of cultured human PASMCs was -10 ± 2.2 mV (n = 6) consistent with an absence of outward K^+ currents in these cells (Figure 3.3D). Thus culturing PASMC led to a loss of both voltage-gated K^+ current and membrane potential.

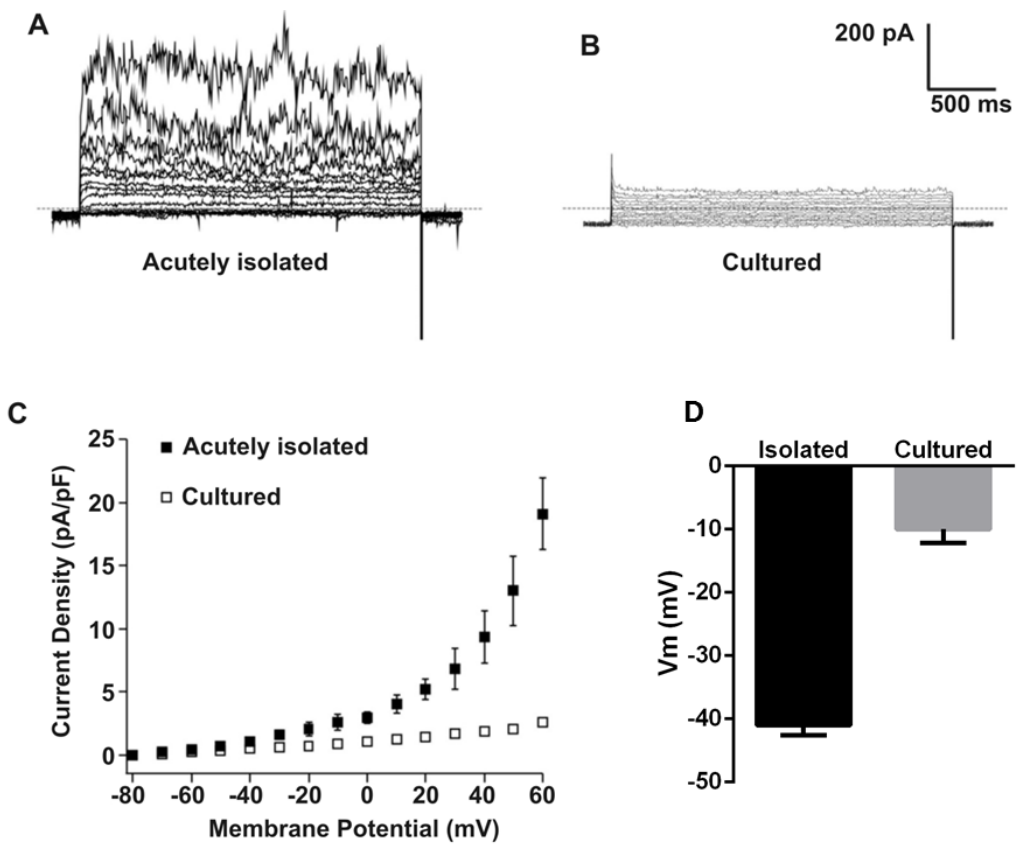

Figure 3.3: Voltage-gated K^+ currents recorded from human PASMCs. Original records from an acutely isolated PASMC (A) and a PASMC maintained in short term culture (B).

Dotted line indicates zero current. C, Mean current density versus voltage relationships for acutely isolated (n=4) and cultured (n=3) PASMC. Voltage protocol: -80 mV holding potential, 2.5 s steps in 10mV increments to +60 mV at 5 s intervals. D, mean resting membrane potential measurements from freshly isolated (n=27) and cultured PAMCs (n=6). Electrophysiology experiments were done by the post-doctoral researcher K. Smith, using cells isolated by S. Brennan.

3.4.4 PASMC proliferation

Proliferation was assessed from the ratio of cells staining positively for BrdU uptake to the total number of cells indicated by DAPI. Figure 3.4 shows fluorescence images of BrDU and DAPI staining of control cells when incubated in the absence of any K_V7 modulator. Each dot in the image represents a cell. Images are shown when cells were quiescent in low (0.1%) serum or stimulated to proliferate with 5% serum, with or without the addition of vehicle controls (water or DMSO). In each case the number of proliferating cells, identified by BrdU-stained nuclei, was less than the total number of cells identified by DAPI staining of DNA. The stimulating effect of serum on proliferation was apparent in the larger number of BrdU-positive cells present after incubation with 5% serum, compared with 0.1% serum. Figure 3.5 shows representative images of BrdU and DAPI staining of cells incubated in the presence of K_V7 channel activators for 24 h, while Figure 3.6 displays similar images of cells incubated for 24 h with K_V7 channel blockers. To quantify proliferation, the ratio of BrdU-positive cells to DAPI-positive cells was calculated for each condition and the results are summarised in Figure 3.7A.

To investigate the role of K_V7 channels in PASMC proliferation, K_V7 channel modulators were used to alter channel function. PASMC proliferation was measured in the absence and presence of XE991 or linopirdine to block all K_V7 channels (Robbins, 2001), retigabine or flupirtine to activate $K_V7.2$-5 channels (Tatulian et al., 2001; Wickenden et al., 2001) or zinc pyrithione (ZnPy) to activate all K_V7 channels except $K_V7.3$ (Xiong et al., 2007). The drugs were tested at concentrations known to modulate PA tone (Chapter 2). As can be seen in Figure 3.7 none of the drugs had a significant effect on PASMC proliferation. Similar results were obtained using the Ki67 antigen as a marker for proliferation. Antibody binding to Ki67 gives rise to fluorescent staining of the nuclei in proliferating cells, similar to that seen with BrdU. Figure 3.7B shows the proportion of cells that stained positive for Ki67 when they were exposed to additional blockers or activators of K_V7 channels. UCL2077 blocks

$K_V7.1$ and $K_V7.2$ channels (Soh and Tzingounis, 2010), BMS-204352 activates $K_V7.4$ and $K_V7.5$ (Dupuis et al., 2002; Schrøder et al., 2001) and L-364,373 selectively activates $K_V7.1$ (Salata et al., 1998; Seebohm et al., 2003). When applied at concentrations known to modulate these K_V7 channels, none of the drugs had a significant effect on proliferation. These results suggest that K_V7 channels are not involved in the proliferation of PASMCs.

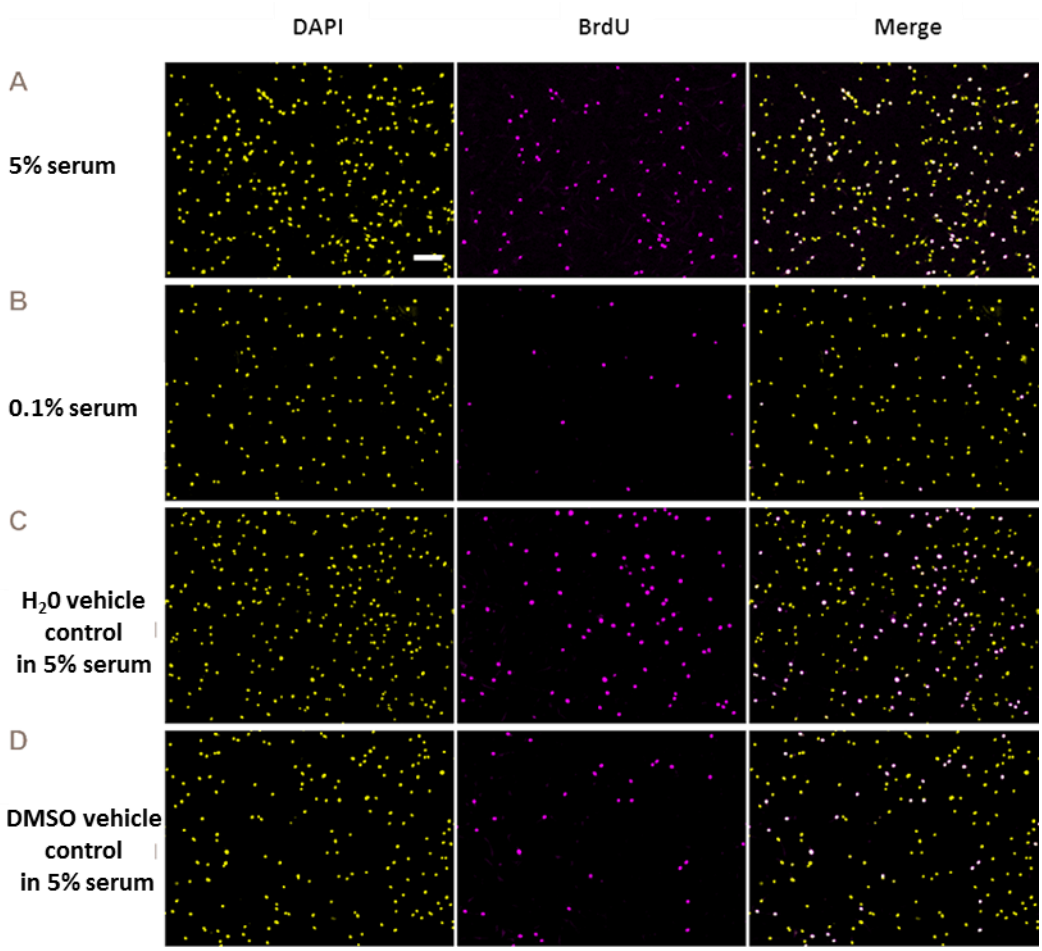

Figure 3.4: Representative fluorescence images of PASMCs used in the BrdU proliferation assay. PASMC nuclei were co-stained for DAPI (yellow, left) and BrdU (magenta, middle), with merged images shown on the right. PASMC were cultured in 5% (A) or 0.1% serum (A) Drug vehicle controls, water (C) or DMSO (D) were added to cultures stimulated with 5% serum . Scale bar= 40 µm.

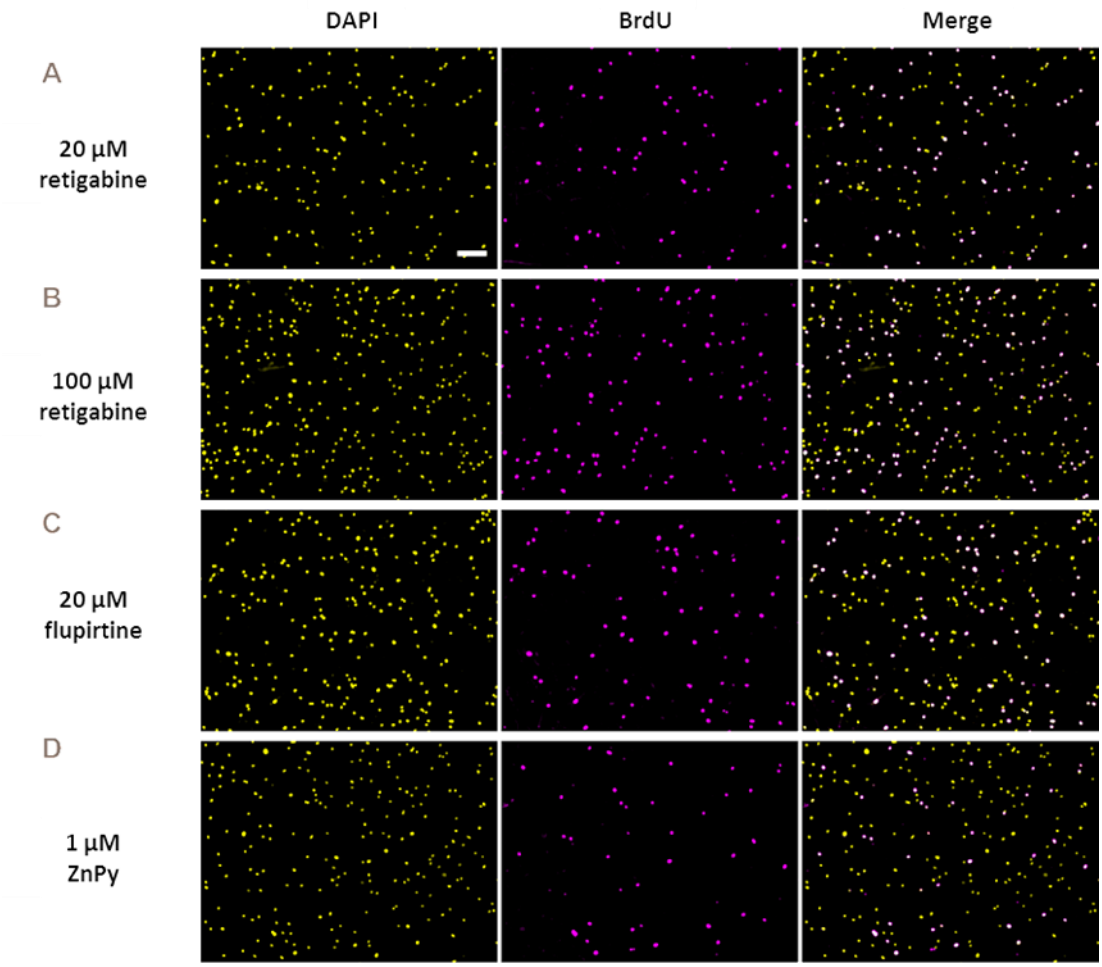

Figure 3.5: Representative fluorescence images of DAPI and BrdU staining in PASMCs exposed to K_V7 channel activators. PASMC nuclei were co-stained for DAPI (yellow, left) and BrdU (magenta, middle), with merged images shown on the right. PASMC were cultured for 24 h in the presence of 5% serum and 20 µM retigabine (A), 100 µM retigabine (B), 20 µM flupirtine (C) or 1 µM ZnPy (D). scale bar= 40 µm. Control images of cells treated in the same way, but not exposed to drugs are shown in Figure 3.4.

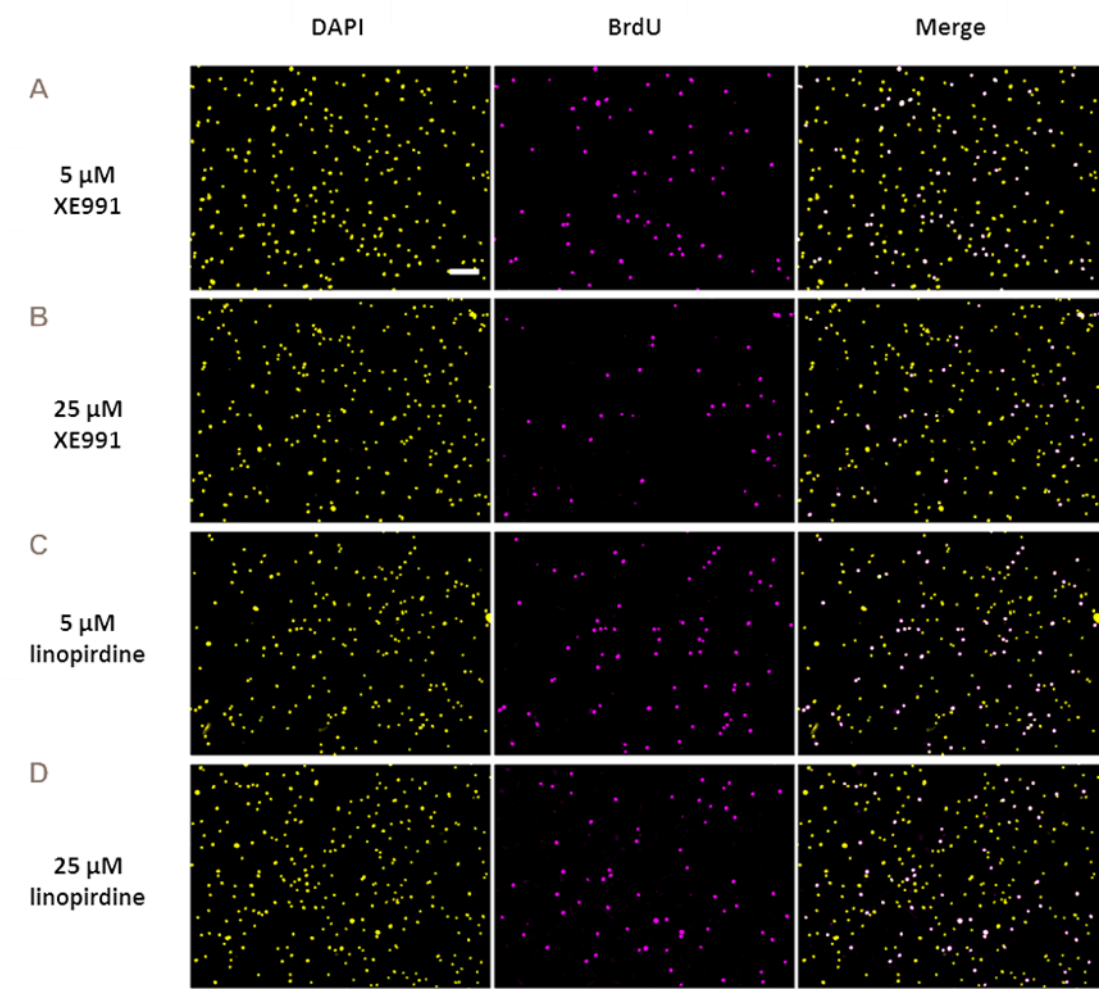

Figure 3.6: Representative fluorescence images of DAPI and BrdU staining in PASMCs exposed to K_V7 channel blockers. PASMC nuclei were co-stained for DAPI (yellow, left) and BrdU (magenta, middle), with merged images shown on the right. PASMC were cultured for 24 h in the presence of 5% serum and 5 µM XE991 (A), 25 µM XE991 (B), 5 µM linopirdine (C) or 25 µM linopirdine (D). scale bar= 40 µm. Control images of cells treated in the same way, but not exposed to drugs are shown in Figure 3.4.

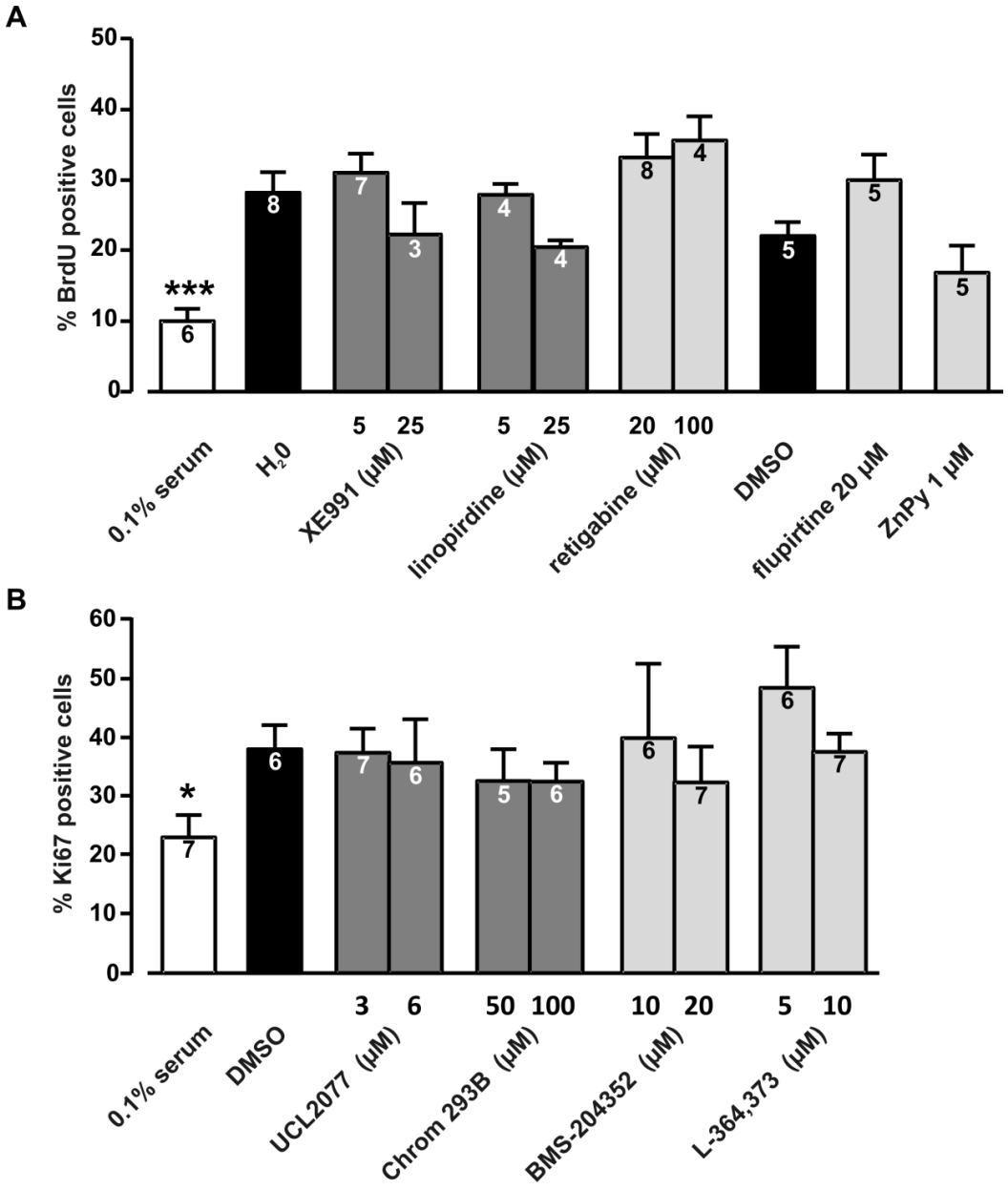

Figure 3.7: Human PASMC proliferation is unaffected by K_V7 channel modulators. Cell proliferation was measured as the percent of cells taking up BrdU (A) or staining positively for the Ki67 antigen (B). Proliferation was measured in cells where growth was inhibited in 0.1% serum (open bars) or stimulated to proliferate with 5% serum (all other bars) in the presence of drug or appropriate vehicle (1% H_2O or DMSO, black bars). K_V7 channel blockers (medium grey bars) and K_V7 channel activators (light grey bars) are displayed to the right of the associated vehicle. Number of repeats is shown within bars. *p<0.05, ***p<0.001 vs all measurements at 5% serum (ANOVA with Bonferroni post-test) K. Smith and N. Bodagh contributed to the data shown.

3.4.5 PASMC migration

PASMC migration was assessed by the scratch wound assay. After the removal of PASMCs using a pipette tip, cells gradually repopulated the area within 24 hr. As illustrated in Figure 3.8 which shows representative images taken during wound closure, cells started to migrate into the cleared area within 4h and by 8h covered almost half of the wound. The addition of water or DMSO, in volumes used for drug dilution, had no effect on wound closure (Figure 3.8). Representative images were taken every 10 min for 24 hr during the scratch wound assay. Cultured PASMCs incubated in the presence of K_V7 channel blockers or K_V7 channel activators are shown in Figure 3.9 and Figure 3.10, respectively. The scratched area was imaged over 24 h, by which time the wound had closed, but by 10h the edge of the migrating cells usually became indistinct and could not be detected reliably by the software. The first 10 h of migration was therefore quantified as an increasing % reduction in the scratch area over time. Figure 3.11 shows the repopulation of a scratched area in a confluent layer of PASMC over time, in the absence (vehicle control) and presence of K_V7 channel modulating drugs. Incubation in 5 μM XE991 (Figure 3.11A), 20 μM retigabine (Figure 3.11B) or 20 μM flupirtine (Figure 3.11C) had no effect on the migration rate of human PASMCs. At 1 μM, ZnPy caused a slowing of cell migration (Figure 3.11D). Its main effect was to delay the onset of migration for around 2 h. After about 4 h, migration then proceeded in parallel with control. At 10 μM, ZnPy appeared to shrink the cells, while the cells pulled on each other making the scratch wound larger rather than smaller over time (Figure 3.10). It was also noted that after 24 h with 10 μM ZnPy, most of cells had detached from the culture dish. Thus, overall, it appears that increasing or decreasing the activity of K_V7 channels had no consistent effect on PASMC migration. These data suggest that K_V7 channels are not involved in cultured PASMC migration although a role for these channels in vivo cannot be ruled out.

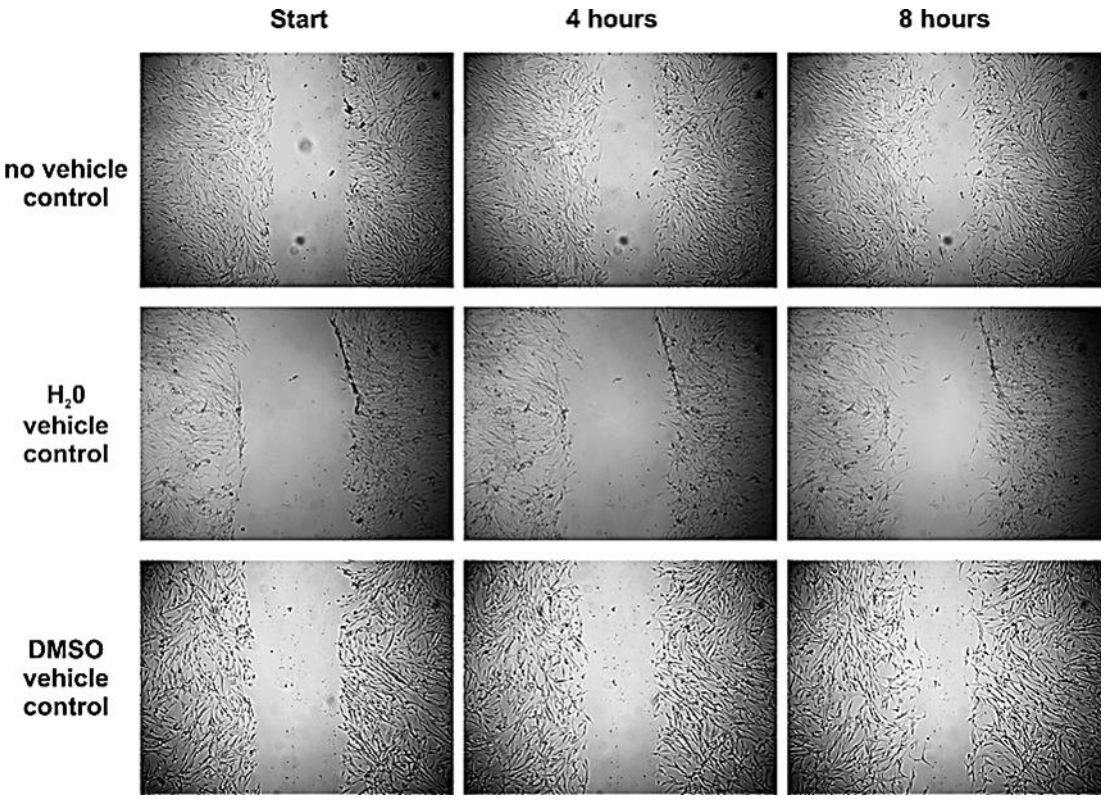

Figure 3.8: Representative images of PASMCs in control conditions during a scratch wound assay. PASMC migration over a cell free area in low serum was measured for 24 h in the presence of no vehicle (top), 1% water vehicle control (middle) or 1% DMSO control (bottom). The representative images display the position of the PASMCs at 0, 4 and 8 hr after applying the scratch, indicated by the empty area through the middle of the cells, for each condition.

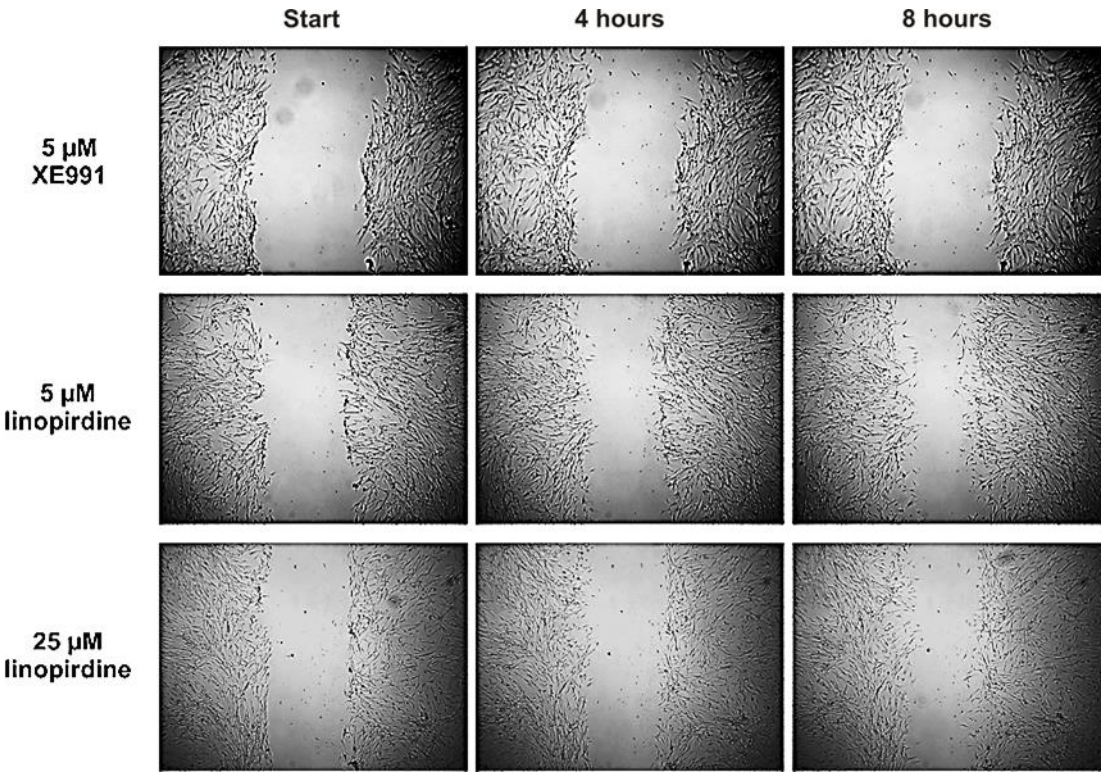

Figure 3.9:: Representative images displaying migration of PASMCs in the presence of K_V7 channel blockers. PASMC migration over a cell free area in low serum was measured in the presence of either 5 µM XE991 (top), 5 µM linopirdine (middle) or 25 µM linopirdine (bottom). The representative images display the position of the PASMCs at 0, 4 and 8 hr for each drug concentration tested.

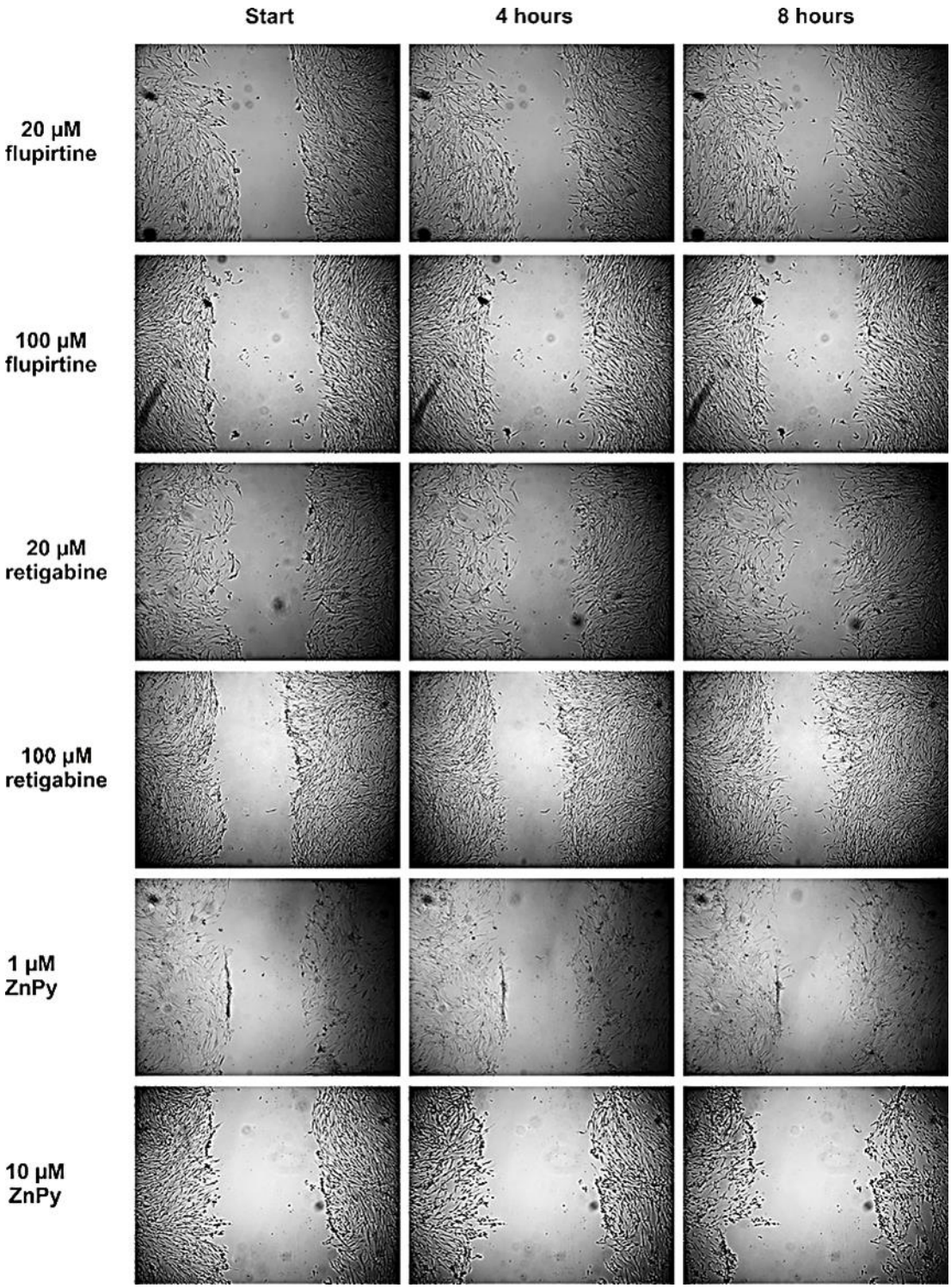

Figure 3.10: Representative images displaying migration of PASMCs in the presence of K_V7 channel activators. PASMC migration over a cell free area in low serum was measured in the presence of either flupirtine (top, 20 or 100 µM), retigabine (middle, 20 or 100 µM) or ZnPy (bottom, 1µM or 10µM). The representative images display the position of the PASMCs at 0, 4 and 8 hr for each drug concentration tested.

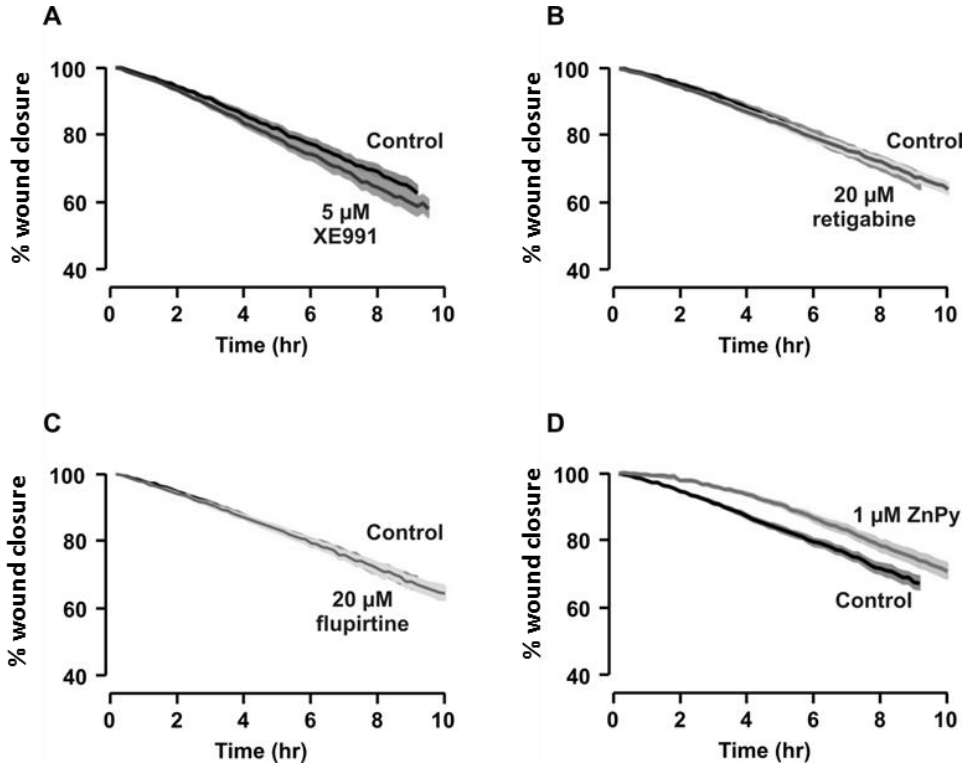

Figure 3.11: K_V7 channel modulators and human PASMC migration. A confluent layer of PASMC was scratched to remove cells and the repopulation of the scratched area measured as the percent of wound closure as a function of time. Experiments were performed in the absence (vehicle control) and presence of 5 µM XE991 (A), 20 µM retigabine (B), 20 µM flupirtine (C) or 1 µM ZnPy (D). Each experiment was performed in duplicate with cells from three independent human PASMC cultures. K. Smith contributed to data shown.

3.5 Discussion

The aims of the current study were 2-fold. Firstly, to reveal the expression profile of the *KCNQ* mRNA transcripts in cultured PASMCs. Secondly, to determine if K_V7 channel modulators alter the rate of human PASMCs proliferation and/or migration. This study has shown that when cultured, human PASMCs almost completely lose the mRNA transcripts encoding $K_V7.1$, $K_V7.3$ and $K_V7.4$ channel α-subunits, but continue to express mRNA for the $K_V7.5$ α-subunit. The K_V current was also essentially abolished in cultured cells compared to freshly isolated cells and this was associated with the RMP in cultured PASMCs being more depolarised than freshly isolated cells. Drugs that modulate K_V7 channel activity had no effect on the rate of proliferation or migration of these cells in culture. These results argue against a role of functional $K_V7.5$ channels in the proliferation or migration of PASMC, but

suggest that K_V7 channels are a characteristic of contractile cells and their down regulation could perhaps play a part in phenotypic modulation.

3.5.1 PASMC Differentiation

All *KCNQ* transcripts, except *KCNQ2*, were found to be expressed in intact human PASMCs, where K_V7 channel modulators have potent and pronounced effects on contraction and vessel tone (Brennan et al., 2011). The expression profile of the transcripts in cultured PASMC was markedly different, with mRNA detected only for $K_V7.5$ by end-point RT-PCR. This loss of expression was an early event during the switch of contractile cells into a proliferative phenotype, as it was complete following the first passage of cells in culture. Indeed, the expression of *KCNQ1*, *KCNQ3* and *KCNQ4* transcripts was barely detectable in confluent cells even before the first passage, the earliest time point at which we could assess expression in cultured cells. As growth inhibition of the cultured cells in low serum medium failed to recover the pattern of mRNA expression seen in freshly isolated PASMCs, $K_V7.1$, $K_V7.3$ and $K_V7.4$ subunits may be specific to the fully mature, contractile smooth muscle cell. In low serum, 10-20% of the cells were in the quiescent, G_0 stage of the cell cycle, as evidenced by BrdU incorporation and Ki67 staining, both of which increased markedly upon return of the cells to 5% serum. The expression of K_V7 subunits in human PASMC appears therefore to be independent of the cell cycle, but to be linked to differentiation.

The loss of K_V7 subunit expression when PASMCs were grown in culture was mirrored by a loss of outward K^+ current with characteristics of K_V7 channels, i.e. voltage-gated currents that did not inactivate during prolonged depolarisation (Joshi et al., 2009; Mani et al., 2013). This agrees with previous reports of small K_V currents in cultured human PASMC (Platoshyn et al., 2000; Ciu et al., 200). The amplitude of outward current measured here (2 pA/pF at 60 mV) was similar to that reported for cultured cells deprived of serum for less than 8h (2.5 pA/pF at 60 mV), and small compared with cells cultured in low serum for >48h (11 pA/pF at 60 mV), when recorded under similar conditions (Ciu et al, 2002). Also as found here, cultured human PASMC were previously found to have a more depolarised RMP (-15 to -20 mV), but after 48 h of serum deprivation this was restored to around -40 mV (Platoshyn et al., 2000; Ciu et al., 200). Interestingly, when deprived of serum for 24h, as used here to inhibit cell growth, the amplitude of K_V current (~4 pA/pF at 60 mV) and the RMP (~-25 mV) were closer to the values seen after 8h of serum removal than >48h (Ciu et

al., 2002), suggesting that 24h of serum deprivation may not have been sufficient to induce a fully differentiated phenotype. The cells may not become fully differentiated even after 48h of serum deprivation, because the K_V current amplitude reported under these conditions (Ciu et al., 2002) was less than half of that seen in the freshly isolated PASMC. Unfortunately, in our hands the cells became detached from the culture dish after 24 h in low serum medium, precluding studies beyond this time point.

PAs express many K_V channels and some have been reported to be down regulated in culture, resulting in a reduction in outward K^+ current in cultured PASMCs (Yuan et al., 1993b). The expression of mRNA for TASK-1, K_V1.5 and K_V2.1 K^+ channels were all shown to be significantly down regulated in cells from organ-cultured rat iPA (Manoury et al., 2009). As seen with the human cells, cultured rat PASMCs have also been reported to be more depolarised and display a reduction in the amplitude of I_{KV} and I_{KN}, compared to freshly isolated PASMCs (Platoshyn et al., 2000; Manoury et al., 2009). This could have important consequences for Ca^{2+} signalling, which has been implicated, along with changes in membrane potential, in the phenotypic modulation of vascular smooth muscle cells (Cheong et al., 2006; Landsberg and Yuan, 2004; Neylon et al., 1994). Therefore, K_V7 channel activity may be one of several signals that regulate membrane potential and may contribute to the modulation of cell phenotype. A similar role for voltage-gated Na^+ channels in PASMCs was proposed previously (Firth et al., 2011), since voltage-gated Na^+ currents were only readily detected in cultured vascular smooth muscle cells (Choby et al., 2000; James et al., 1995; Quignard et al., 1997). The expression of functional Na^+ channels in cultured cells may be a trigger for differentiation and/ or proliferation, by increasing $[Ca^{2+}]_i$. This increase in $[Ca^{2+}]_i$ could occur due to opening of T-type VGCCs (Rodman et al., 2005), as a consequence of membrane depolarisation caused by an influx of Na^+ or by the Na^+/Ca^{2+} exchanger operating in reverse mode (Arnon et al., 2000; Boccara et al., 1999; Pluteanu and Cribbs., 2011).

K_V7.1, K_V7.3 and K_V7.4 have been reported to display a marked increase in expression during the transition of C_2C_{12} skeletal myoblasts into myotubes, which go on to form mature muscle fibres (Iannotti et al., 2010). The marker of differentiation, myogenin, was up-regulated by retigabine in an XE991-sensitive manner, suggesting that K_V7 channels regulate skeletal muscle differentiation (Iannotti et al., 2010). Perhaps K_V7 channels play a similar role in human PASMCs. Although any or all of the K_V7 subunits expressed in PASMC might be involved, it is of interest that K_V7.1 has been implicated in the differentiation of

rat germ cells (Tsevi et al., 2005). It is likely that K_V7 channel expression is altered when the PASMC phenotype changes from a contractile to proliferative phenotype, thus the channels could be markers of PASMC phenotype/diferentiation. The proliferative phenotype does not appear to require functional K_V7 channels, as the small current remaining in cultured cells was voltage-independent and K_V7 modulators had no effect on proliferation. This does not exclude a role for these subunits as part of a signalling complex, such as with $K_V1.3$, hERG and EAG channels (Cidad et al., 2012; Pier et al., 2014; Ouadid-Ahidouch and Ahidouch, 2013).

3.5.2 Proliferation

Since $K_V7.5$ channels have been implicated in proliferation in other cell types, their role in human PASMC proliferation was investigated in this study, to investigate their potential as a therapeutic target for PAH. Briefly, we find that approximately 25% of the serum-stimulated PASMCs stained for BrdU in control conditions, after a 4 h exposure. It is common to starve cells of serum for 48 h in order to synchronize them in the G_0/G_1 phase of the cell cycle (Platoshyn et al., 2000; Cui et al, 2002; Goncharova et al., 2006). However, in our hands, cells did not survive for 48 h without serum. If this had been possible, fewer proliferating cells may have been detected in the low serum cultures, allowing for a greater increase upon stimulation with serum. Unlike the findings in skeletal muscle, none of the K_V7 modulators tested altered the rate of serum-induced proliferation of human PASMCs. Thus although these cells express $K_V7.5$ mRNA transcripts, the channels do not appear to contribute to proliferation and cannot be recruited to oppose proliferation either. This may reflect an absence of functional $K_V7.5$ channels in the plasma membrane, because no currents with the characteristics of K_V7 channels in the cultured PASMC were detected. On the other hand, heterologous expression studies have shown that even when $K_V7.5$ channel protein is present in the plasma membrane, homomeric channels may not give rise to measurable current (Xiong et al. 2007). As ZnPy was able to induce current through these silent K_V7 channels (Xiong et al, 2007), the drug could be used with electrophysiology in the future to test for the presence of functional $K_V7.5$ channels in proliferating human PASMC.

A role for $K_V7.5$ channels in skeletal myoblast proliferation has been proposed due to enhanced expression occurring over time in conditions encouraging proliferation. Furthermore, the application of 100 μM linopirdine significantly reduced the rate of myoblast proliferation by 60% (Roura-Ferrer et al., 2008). Compared with $K_V7.1$ and $K_V7.3$

channels, homomeric $K_V7.5$ channels have a relatively low affinity for linopirdine (IC_{50} >10 μM (Robbins, 2001), so the need for high concentrations to interfere with proliferation could reflect an action on $K_V7.5$ channels. However, the effects of linopirdine at this high concentration are more likely to result from non-specific effects unrelated to K_V7 channels (Lamas et al., 1997; Wang et al., 1998; Wladyka and Kunze, 2006. Furthermore, they conflict with another report, where retigabine (10 μM) was found to inhibit proliferation (Iannotti et al., 2010), despite having the opposite effect to linopirdine on K_V7 channels. In that study, 10 μM XE991 had no effect on skeletal myoblast proliferation by itself, but prevented the reduction in proliferation caused by retigabine. It is unclear whether the effect described above, reflects pharmacological or physiological antagonism by XE991, because in the absence of drugs 100% of the cells were already in a proliferative state. Thus a direct stimulatory effect of XE991 might not be detected, but could counteract the inhibitory effect of retigabine. These reports show that the role of K_V7 channles in cell proliferation remains unclear and requires further investigation. The findings from this study are limited by the reduction in mRNA for the K_V7 channels in cultured PASMC. This reduction may be due to culture conditions and so perhaps not occur *in vivo*.

3.5.3 Migration

The pathophysiological changes that take place in hypertensive PAs include the migration of PASMC from the medial to intimal layer (Aiello et al., 2003; Jones et al., 1997; Sarkar et al., 2010). Hypoxia-induced PASMC migration is inhibited by blockers of voltage-gated Ca^{2+} entry, implicating the membrane potential in its control (Leggett et al., 2012). Nevertheless, we found no evidence for the involvement of K_V7 channels in the regulation of migration.

The role of K_V7 channels in PASMC migration was pharmacologically investigated using the *in vitro* scratch wound assay. The rate of closure of the gap was unaffected by a range of K_V7 modulators, both activators and inhibitors. Only ZnPy (1 μM) had an effect on migration, however, raising the ZnPy concentration to 10 μM revealed a toxic effect on the cells, suggesting a non-specific effect unrelated to K_V7 channel activation. Given the lack of effect on migration of the well-established K_V7 channel activators, flupirtine and retigabine, it is unlikely that the delay in PASMC migration caused by 1 μM ZnPy was due to K_V7 channel activation. Overall, our data argue against a role for K_V7 channels, including $K_V7.5$, in PASMC migration. As $K_V7.1$-4 channels were not detected in cultured PASMC, we cannot

exclude the possibility that one or more of these subtypes, expressed in contractile but not cultured cells, acts to inhibit migration.

3.5.4 Drug concentrations

The drug concentrations used for the proliferation and migration experiments were based on EC_{50} values for the effects of the modulators on heterologously expressed K_V7 channels (Robbins 2001), as well as for evoking human iPA constriction or relaxation. By using a concentration close to the EC_{50} value for each drug, it was hoped that any effect on PASMC proliferation or migration could be quantified, while avoiding potential non-selective effects of the modulators. As the K_V7 modulators did not significantly alter the rate of proliferation or migration of PASMCs, it was concluded that K_V7 channels play no role in either process. It has been reported, however, that the concentration of channel modulator needed to alter cell growth is sometimes higher than the EC_{50} for the activity (Felipe et al., 2006; Wonderlin and Strobl, 1996). This finding could be explained in two ways. Firstly, in order to stimulate proliferation via K^+ channel modulation, a larger and/or prolonged elevation of $[Ca^{2+}]_i$ may be required to activate the downstream signalling pathways. Secondly, this could potentially be attributed to the drug binding to the serum contained in the tissue culture medium and/or metabolism of the drug during prolonged (24 h) exposure (Wonderlin and Strobl, 1996), both of which would reduce the concentration at binding sites on the channel. In comparison, when investigating the effects of the K_V7 modulators by whole-cell patch clamping or myography, drug exposure is usually only a few minutes and no proteins are present in the PSS to bind the drug. Since linopirdine, XE991 and retigabine also failed to affect PASMC proliferation when tested at concentrations 5-20 fold higher than their EC_{50}s for modulating K_V7 channels, it is unlikely that a lowered effective concentration was responsible. This conclusion is strengthened by the reports of 10 µM retigabine and XE991 influencing myoblast proliferation in the presence of 10 % serum (Iannotti et al., 2010), which compares with 5% serum in the present study.

3.6 Conclusion

Overall the data support a role for K_V7 channels in maintaining the contractile phenotype of PASMC. Although *KCNQ5* mRNA is retained in cultured cells, we did not detect a functional role for $K_V7.5$ channels, either in mediating K_V currents in PASMC or in regulating PASMC proliferation or migration. No specific role for $K_V7.1$, $K_V7.3$ or $K_V7.4$ was identified, it is

possible that their disappearance when cells were cultured implies a role in phenotypic modulation but this requires further investigation. One or more K_V7 channels may be involved in preventing contractile PASMC from developing a proliferative phenotype or migrating in the vessel wall.

3.7 Acknowledgments

The Bioimaging Facility microscopes used in this study were purchased with grants from the Biotechnology and Biological Sciences Research Council, Wellcome Trust and the University of Manchester Strategic Fund. We are grateful to Peter March, Roger Meadows and Steve Marsden for their help with the microscopy.

3.8 References

Aiello, V.D., Gutierrez, P.S., Chaves, M.J.F., Lopes, A.A.B., Higuchi, M.L., and Ramires, J.A.F. (2003). Morphology of the internal elastic lamina in arteries from pulmonary hypertensive patients: a confocal laser microscopy study. Modern Pathology *16*, 411–416.

Amabile, C.M., and Vasudevan, A. (2013). Ezogabine: a novel antiepileptic for adjunctive treatment of partial-onset seizures. Pharmacotherapy *33*, 187–194.

Arnon, A., Hamlyn, J.M., and Blaustein, M.P. (2000). Na^+ entry via store-operated channels modulates Ca^{2+} signaling in arterial myocytes. American Journal of Physiology- Cell Physiology *278*, C163–73.

Boccara, G., Choby, C., Frapier, J.M., Quignard, J.F., Nargeot, J., Dayanithi, G., and Richard, S. (1999). Regulation of Ca^{2+} homeostasis by atypical Na^+ currents in cultured human coronary myocytes. Circulation Research *85*, 606–613

Boehlen, A., Schwake, M., Dost, R., Kunert, A., Fidzinski, P., Heinemann, U., and Gebhardt, C. (2013). The new KCNQ2 activator 4-Chlor-N-(6-chlor-pyridin-3-yl)-benzamid displays anticonvulsant potential. British Journal of Pharmacology *168*, 1182–1200.

Brennan, S., Oliveira, R., Gurney, A. (2011). Effects of KV7 potassium channel modulators on human intra-pulmonary artery. Proceedings of The Physiological Society 25, C15 and PC15.

Busch, A.E., Suessbrich, H., Waldegger, S., Sailer, E., Greger, R., Lang, H., Lang, F., Gibson, K.J., and Maylie, J.G. (1996). Inhibition of I_{Ks} in guinea pig cardiac myocytes and guinea pig IsK channels by the chromanol 293B. Pflügers Archiv: European Journal of Physiology *432*, 1094–1096.

Cheong, A., Wood, I.C., and Beech, D.J. (2006). Less REST, more vascular disease? Regulation of cell cycle and migration of vascular smooth muscle cells. Cell Cycle *5*, 129–131.

Choby, C., Mangoni, M.E., Boccara, G., Nargeot, J., and Richard, S. (2000). Evidence for tetrodotoxin-sensitive sodium currents in primary cultured myocytes from human, pig and rabbit arteries. Pflügers Archiv : European Journal of Physiology *440*, 149–152.

Cidad, P., Jiménez-Pérez, L., García-Arribas, D., Miguel-Velado, E., Tajada, S., Ruiz-McDavitt, C., López-López, J.R., and Pérez-García, M.T. (2012). Kv1.3 channels can modulate cell proliferation during phenotypic switch by an ion-flux independent mechanism. Arteriosclerosis, Thrombosis, and Vascular Biology *32*, 1299–1307.

Cui, Y., Tran, S., Tinker, A., and Clapp, L.H. (2002). The molecular composition of K(ATP) channels in human pulmonary artery smooth muscle cells and their modulation by growth. American Journal of Respiratory Cell and Molecular Biology *26*, 135–143.

Evans, A., Osipenko, O., and Gurney, A. (1996). Properties of a novel K^+ current that is active at resting potential in rabbit pulmonary artery smooth muscle cells. The Journal of Physiology *496*, 407.

Falcetti, E., Hall, S.M., Phillips, P.G., Patel, J., Morrell, N.W., Haworth, S.G., and Clapp, L.H. (2010). Smooth muscle proliferation and role of the prostacyclin (IP) receptor in idiopathic pulmonary arterial hypertension. American Journal of Respiratory and Critical Care Medicine *182*, 1161–1170.

Felipe, A., Vicente, R., Villalonga, N., Roura-Ferrer, M., Martínez-Mármol, R., Solé, L., Ferreres, J.C., and Condom, E. (2006). Potassium channels: new targets in cancer therapy. Cancer Detection and Prevention *30*, 375–385.

Firth, A.L., Remillard, C. V, Platoshyn, O., Fantozzi, I., Ko, E.A., and Yuan, J.X.-J. (2011). Functional ion channels in human pulmonary artery smooth muscle cells: Voltage-dependent cation channels. Pulmonary Circulation *1*, 48–71.

Golovina, V.A. (1999). Cell proliferation is associated with enhanced capacitative Ca^{2+} entry in human arterial myocytes. The American Journal of Physiology *277*, C343–9.

Goncharova, E.A., Lim, P., Goncharov, D.A., Eszterhas, A., Panettieri, R.A., and Krymskaya, V.P. (2006). Assays for in vitro monitoring of proliferation of human airway smooth muscle (ASM) and human pulmonary arterial vascular smooth muscle (VSM) cells. Nature Protocols *1*, 2905–2908

Gurney, A.M., and Joshi, S. (2006). The role of twin pore domain and other K^+ channels in hypoxic pulmonary vasoconstriction. Novartis Foundation Symposium *272*, 218–28; discussion 228–33, 274–9.

Gurney, A.M., Osipenko, O.N., MacMillan, D., and Kempsill, F.E.J. (2002). Potassium channels underlying the resting potential of pulmonary artery smooth muscle cells. Clinical and Experimental Pharmacology & Physiology *29*, 330–333.

Hong, Z., Weir, E.K., Varghese, A., and Olschewski, A. (2005). Effect of normoxia and hypoxia on K^+ current and resting membrane potential of fetal rabbit pulmonary artery smooth muscle. Physiological Research *54*, 175–184.

Iannotti, F.A., Panza, E., Barrese, V., Viggiano, D., Soldovieri, M.V., and Taglialatela, M. (2010). Expression, localization, and pharmacological role of K_V7 potassium channels in skeletal muscle proliferation, differentiation, and survival after myotoxic insults. The Journal of Pharmacology and Experimental Therapeutics *332*, 811–820.

Ikeda, T., Nakamura, K., Akagi, S., Kusano, K.F., Matsubara, H., Fujio, H., Ogawa, A., Miura, A., Miura, D., Oto, T., Yamanaka, R., Otsuka, F., Date, H., Ohe, T., Ito, H. (2010). Inhibitory effects of simvastatin on platelet-derived growth factor signaling in pulmonary artery smooth muscle cells from patients with idiopathic pulmonary arterial hypertension. Journal of Cardiovascular Pharmacology *55*, 39–48.

James, A.F., Okada, T., and Horie, M. (1995). A fast transient outward current in cultured cells from human pulmonary artery smooth muscle. The American Journal of Physiology *268*, H2358–65.

Jones, P.L., Cowan, K.N., and Rabinovitch, M. (1997). Tenascin-C, proliferation and subendothelial fibronectin in progressive pulmonary vascular disease. The American Journal of Pathology *150*, 1349–1360.

Joshi, S., Balan, P., and Gurney, A.M. (2006). Pulmonary vasoconstrictor action of KCNQ potassium channel blockers. Respiratory Research *7*, 31.

Joshi, S., Sedivy, V., Hodyc, D., Herget, J., and Gurney, A.M. (2009). KCNQ modulators reveal a key role for KCNQ potassium channels in regulating the tone of rat pulmonary artery smooth muscle. The Journal of Pharmacology and Experimental Therapeutics *329*, 368–376.

Kuhr, F.K., Smith, K.A., Song, M.Y., Levitan, I., and Yuan, J.X.-J. (2012). New mechanisms of pulmonary arterial hypertension: role of Ca^{2+} signaling. American Journal of Physiology. Heart and Circulatory Physiology *302*, H1546–62.

Lamas, J.A., Selyanko, A.A., and Brown, D.A. (1997). Effects of a cognition-enhancer, linopirdine (DuP 996), on M-type potassium currents (I_{KM}) and some other voltage- and ligand-gated membrane currents in rat sympathetic neurons. The European Journal of Neuroscience *9*, 605–616.

Landsberg, J.W., and Yuan, J.X.-J. (2004). Calcium and TRP channels in pulmonary vascular smooth muscle cell proliferation. Physiology *19*, 44–50.

Leggett, K., Maylor, J., Undem, C., Lai, N., Lu, W., Schweitzer, K., King, L.S., Myers, A.C., Sylvester, J.T., Sidhaye, V., Shimoda, L.A. (2012). Hypoxia-induced migration in pulmonary arterial smooth muscle cells requires calcium-dependent upregulation of aquaporin 1. American Journal of Physiology-Lung Cellular and Molecular Physiology *303*, L343–53.

Lerche, C., Bruhova, I., Lerche, H., Steinmeyer, K., Wei, A.D., Strutz-Seebohm, N., Lang, F., Busch, A.E., Zhorov, B.S., and Seebohm, G. (2007). Chromanol 293B binding in KCNQ1

(K_V7.1) channels involves electrostatic interactions with a potassium ion in the selectivity filter. Molecular Pharmacology *71*, 1503–1511.

Liang, C.-C., Park, A.Y., and Guan, J.-L. (2007). In vitro scratch assay: a convenient and inexpensive method for analysis of cell migration in vitro. Nature Protocols *2*, 329–333.

Mandegar, M., Fung, Y.-C.B., Huang, W., Remillard, C. V, Rubin, L.J., and Yuan, J.X.-J. (2004). Cellular and molecular mechanisms of pulmonary vascular remodeling: role in the development of pulmonary hypertension. Microvascular Research *68*, 75–103.

Mani, B.K., O'Dowd, J., Kumar, L., Brueggemann, L.I., Ross, M., and Byron, K.L. (2013). Vascular KCNQ (K_V7) potassium channels as common signaling intermediates and therapeutic targets in cerebral vasospasm. Journal of Cardiovascular Pharmacology *61*, 51–62.

Manoury, B., Etheridge, S.L., Reid, J., and Gurney, A.M. (2009). Organ culture mimics the effects of hypoxia on membrane potential, K^+ channels and vessel tone in pulmonary artery. British Journal of Pharmacology *158*, 848–861.

Marcos, E., Fadel, E., Sanchez, O., Humbert, M., Dartevelle, P., Simonneau, G., Hamon, M., Adnot, S., and Eddahibi, S. (2004). Serotonin-induced smooth muscle hyperplasia in various forms of human pulmonary hypertension. Circulation Research *94*, 1263–1270.

Neacsu, C., and Babes, A. (2010). The M-channel blocker linopirdine is an agonist of the capsaicin receptor TRPV1. Journal of Pharmacological Sciences *114*, 332–340.

Neylon, C.B., Avdonin, P. V, Dilley, R.J., Larsen, M.A., Tkachuk, V.A., and Bobik, A. (1994). Different electrical responses to vasoactive agonists in morphologically distinct smooth muscle cell types. Circulation Research *75*, 733–741.

Osipenko, O.N., Alexander, D., MacLean, M.R., and Gurney, A.M. (1998). Influence of chronic hypoxia on the contributions of non-inactivating and delayed rectifier K currents to the resting potential and tone of rat pulmonary artery smooth muscle. British Journal of Pharmacology *124*, 1335–1337.

Ouadid-Ahidouch, H., and Ahidouch, A. (2013). K(+) channels and cell cycle progression in tumor cells. Frontiers in Physiology. *4*, 220.

Pier, D.M., Shehatou, G.S.G., Giblett, S., Pullar, C.E., Trezise, D.J., Pritchard, C.A., Challiss, R.A.J., and Mitcheson, J.S. (2014). Long-term channel block is required to inhibit cellular transformation by human ether-à-go-go-related gene (hERG1) potassium channels. Molecular Pharmacology. *86*, 211–221

Platoshyn, O., Golovina, V.A., Bailey, C.L., Limsuwan, A., Krick, S., Juhaszova, M., Seiden, J.E., Rubin, L.J., and Yuan, J.X.-J. (2000). Sustained membrane depolarization and pulmonary artery smooth muscle cell proliferation. American Journal of Physiology- Cell Physiology *279*, C1540–9.

Pluteanu, F., and Cribbs, L.L. (2011). Regulation and function of Cav3.1 T-type calcium channels in IGF-I-stimulated pulmonary artery smooth muscle cells. American Journal of Physiology - Cell Physiology. *300*, C517–25.

Quignard, J.F., Ryckwaert, F., Albat, B., Nargeot, J., and Richard, S. (1997). A novel tetrodotoxin-sensitive Na^+ current in cultured human coronary myocytes. Circulation Research *80*, 377–382.

Roura-Ferrer, M., Solé, L., Martínez-Mármol, R., Villalonga, N., and Felipe, A. (2008). Skeletal muscle K_V7 (KCNQ) channels in myoblast differentiation and proliferation. Biochemical and Biophysical Research Communications *369*, 1094–1097.

Salata, J.J., Jurkiewicz, N.K., Wang, J., Evans, B.E., Orme, H.T., and Sanguinetti, M.C. (1998). A novel benzodiazepine that activates cardiac slow delayed rectifier K^+ currents. Molecular Pharmacology *54*, 220–230.

Sarkar, J., Gou, D., Turaka, P., Viktorova, E., Ramchandran, R., and Raj, J.U. (2010). MicroRNA-21 plays a role in hypoxia-mediated pulmonary artery smooth muscle cell proliferation and migration. American Journal of Physiology- Lung Cellular and Molecular Physiology *299*, L861–71.

Schrøder, R.L., Jespersen, T., Christophersen, P., Strøbaek, D., Jensen, B.S., and Olesen, S.P. (2001). KCNQ4 channel activation by BMS-204352 and retigabine. Neuropharmacology *40*, 888–898.

Seebohm, G., Pusch, M., Chen, J., and Sanguinetti, M.C. (2003). Pharmacological activation of normal and arrhythmia-associated mutant KCNQ1 potassium channels. Circulation Research *93*, 941–947.

Smirnov, S. V, Robertson, T.P., Ward, J.P., and Aaronson, P.I. (1994). Chronic hypoxia is associated with reduced delayed rectifier K^+ current in rat pulmonary artery muscle cells. The American Journal of Physiology *266*, H365–70.

Soh, H., and Tzingounis, A. V (2010). The specific slow afterhyperpolarization inhibitor UCL2077 is a subtype-selective blocker of the epilepsy associated KCNQ channels. Molecular Pharmacology *78*, 1088–1095.

Sundelacruz, S., Levin, M., and Kaplan, D.L. (2009). Role of membrane potential in the regulation of cell proliferation and differentiation. Stem Cell Reviews *5*, 231–246.

Suzuki, H., and Twarog, B.M. (1982). Membrane properties of smooth muscle cells in pulmonary hypertensive rats. The American Journal of Physiology *242*, H907–15.

Tatulian, L., Delmas, P., Abogadie, F.C., and Brown, D.A. (2001). Activation of expressed KCNQ potassium currents and native neuronal M-type potassium currents by the anti-convulsant drug retigabine. The Journal of Neuroscience *21*, 5535–5545.

Tsevi, I., Vicente, R., Grande, M., López-Iglesias, C., Figueras, A., Capellà, G., Condom, E., and Felipe, A. (2005). KCNQ1/KCNE1 channels during germ-cell differentiation in the rat: expression associated with testis pathologies. Journal of Cellular Physiology *202*, 400–410.

Wang, H.S., Pan, Z., Shi, W., Brown, B.S., Wymore, R.S., Cohen, I.S., Dixon, J.E., and McKinnon, D. (1998). KCNQ2 and KCNQ3 potassium channel subunits: molecular correlates of the M-channel. Science *282*, 1890–1893.

Wickenden, A.D., Zou, A., Wagoner, P.K., and Jegla, T. (2001). Characterization of KCNQ5/Q3 potassium channels expressed in mammalian cells. British Journal of Pharmacology *132*, 381–384.

Wladyka, C.L., and Kunze, D.L. (2006). KCNQ/M-currents contribute to the resting membrane potential in rat visceral sensory neurons. The Journal of Physiology *575*, 175–189.

Wonderlin, W.F., and Strobl, J.S. (1996). Potassium channels, proliferation and G1 progression. The Journal of Membrane Biology *154*, 91–107.

Xiong, Q., Sun, H., and Li, M. (2007). Zinc pyrithione-mediated activation of voltage-gated KCNQ potassium channels rescues epileptogenic mutants. Nature Chemical Biology *3*, 287–296.

Yu, J., Taylor, L., Wilson, J., Comhair, S., Erzurum, S., and Polgar, P. (2013). Altered expression and signal transduction of endothelin-1 receptors in heritable and idiopathic pulmonary arterial hypertension. Journal of Cellular Physiology *228*, 322–329.

Yuan, X.J., Goldman, W.F., Tod, M.L., Rubin, L.J., and Blaustein, M.P. (1993b). Ionic currents in rat pulmonary and mesenteric arterial myocytes in primary culture and subculture. The American Journal of Physiology *264*, L107–15.

Yuan, X.J., Wang, J., Juhaszova, M., Gaine, S., and Rubin, L. (1998c). Attenuated K channel gene transcription in primary pulmonary hypertension. The Lancet *351*, 726–727.

Zhu, Y., Zhang, S., Xie, W., Li, Q., Zhou, Y., and Wang, H. (2008). Iptakalim inhibited endothelin-1-induced proliferation of human pulmonary arterial smooth muscle cells through the activation of K_{ATP} channel. Vascular Pharmacology *48*, 92–99.

Chapter 4 : Mechanisms of vasodilation by the K_V7 channel activator zinc pyrithione

Sean Brennan, Basma Eid and A M Gurney[1]

Faculty of Life Sciences, University of Manchester, 46 Grafton Street, Manchester M13 9NT

Intended journal: British Journal of Pharmacology.

[1]Author for correspondence:

4.1 Abstract

K_V7 channels are implicated as regulators of vascular smooth muscle membrane potential and tone. Studies on rodent models of pulmonary arterial hypertension (PAH) suggest that K_V7 channel activation could provide a therapeutic strategy. Zinc pyrithione (ZnPy) is a newly discovered K_V7 channel activator with a selectivity profile and mechanism of action distinct from the classical activator, retigabine. This study aimed to establish if, like retigabine, ZnPy is a pulmonary vasodilator, and if so, to elucidate the mechanism. The effects of ZnPy (0.01– 100 μM) were investigated on pre-constricted isolated rat iPAs using wire myography. ZnPy evoked concentration-dependent inhibition of phenylephrine-constricted arteries by up to 85%, with an EC_{50} of 1 μM. It was equally effective on intact and endothelium-denuded vessels and against constriction induced by the Ca^{2+} channel agonist, BAY K 8644. However, below 10 μM, ZnPy did not inhibit constriction induced by the Ca^{2+} ionophore, ionomycin. The ZnPy concentration-response relationship was unaffected by the K^+ channel blockers 4-aminopyridine, tetraethylammonium ions, iberiotoxin, paxilline or glibenclamide. However, compared to control (absence of drug), the EC_{50} was shifted to higher concentrations from 5.4 ± 0.3 (n=5) to 4.9 ± 0.1 (n=6, one-way ANOVA with Dunn's post-test $p<0.0419$) by the K_V7 channel blocker, XE991 (100 nM). These data suggest that ZnPy caused relaxation by activating K_V7 channels. However, ZnPy also dilated vessels pre-constricted with 90 mK^+, which prevented K^+ flux across the membrane, or 1 μM XE991, so it appears to have an additional action, possibly inhibition of voltage-gated Ca^{2+} channels. Since ZnPy also reduced constriction to phenylephrine in the absence of extracellular Ca^{2+} by about 20%, it may have an intracellular action.

These data suggest ZnPy-induced dilation was in part caused by K_V7 channel activation, however, additional mechanisms also contributed. Although ZnPy is an effective tool for studies on isolated K_V7 channels and cells, its usefulness as a probe for K_V7 channels in intact tissues may be limited by effects that are inconsistent with an action on K_V7 channels.

4.2 Introduction

K_V7 channels, encoded by the *KCNQ* genes, are attracting increasing interest as regulators of the membrane potential in vascular smooth muscle (Gurney et al., 2010; Jepps et al., 2013; Mani et al., 2013). In PASMCs, K_V7 channels appear to contribute to the RMP and drugs that alter their activity have profound effects on pulmonary vascular tone (Brennan et al, 2013; Joshi et al, 2006; 2009). Flupirtine, a drug that activates K_V7 channels, was found to prevent the development of PAH in two mouse models and to reverse pre-existing disease (Morecroft et al., 2009). Thus K_V7 channels are potential molecular targets for therapeutic pulmonary vasodilator drugs. Three of the five *KCNQ* genes (*KCNQ1*, *KCNQ4* and *KCNQ5*) are expressed in rodent PASMC, but it is not yet known which subunits form the functional channels (Joshi et al., 2009). The evidence points towards $K_V7.4$ being a key α-subunit (Joshi et al, 2009; Sedivy et al, 2014). Knockdown of $K_V7.4$ expression by RNA interference was found to impair β-adrenergic vasodilation in an isolated systemic artery (Chadha et al., 2012), implying that channels containing $K_V7.4$ α-subunits are also functionally important in the systemic circulation. On the other hand, knockdown of $K_V7.5$ by RNA interference reduced K^+ current and prevented its inhibition by the vasoconstrictor, vasopressin, in rat aorta A7r5 smooth muscle cells (Brueggemann et al., 2007). Thus, $K_V7.4$ and $K_V7.5$ subunits could both contribute to the regulation of artery tone. Using the same RNA interference methods, Gurney and co-workers have been unable to reliably knock down K_V7 channel expression in PAs (unpublished observations). Therefore, alternative approaches are required to ascertain the roles of the different K_V7 subunits expressed in PAs.

A number of drug molecules can selectively activate or inhibit K_V7 channels (Robbins, 2001; Miceli et al., 2008; Xiong et al., 2008) and two activators have been approved for clinical use. Retigabine, also known as ezogabine and marketed as Trobalt (USA) or Potiga (Europe), was recently approved for treating epilepsy, while flupirtine, a structural analogue, has been used as an analgesic since the 1980s (Szelenyi, 2013). These drugs activate $K_V7.2$ to $K_V7.5$, but not $K_V7.1$ channels, and cause a hyperpolarizing shift of the current *versus* voltage relationship (Dupuis et al., 2002; Schrøder et al., 2001; Tatulian et al., 2001). Both drugs enhance K^+ current in PASMC, evoke hyperpolarisation and promote vasodilation (Brennan et al., 2011; Joshi et al., 2009; Sedivy et al, 2014). New drug molecules that activate K_V7 channels with different subunit selectivity and mechanisms are being

developed (Mattmann et al., 2012; Wickenden et al., 2008; Xiong et al., 2008; Yu et al, 2011;), thus enabling a pharmacological approach to investigating the roles of different K_V7 α-subunits.

Zinc pyrithione, a small molecule commonly used to treat dandruff and psoriasis, was recently reported to act as an activator of K_V7 channels, with several properties distinguishing it from retigabine and flupirtine (Xiong et al., 2007; 2008). It activates all K_V7 isoforms in heterologous expression systems, except $K_V7.3$, but is most potent at $K_V7.4$ and $K_V7.5$ channels (order of potency $K_V7.5 > K_V7.4 > K_V7.2 > K_V7.1$). This contrasts with retigabine, which is around 10-fold more potent at homomeric $K_V7.3$ channels compared with $K_V7.4$ (Tatulian et al., 2001). Like retigabine, ZnPy causes a hyperpolarizing shift in the current-voltage relationship, but it also causes a marked increase in current amplitude at all potentials. These differences reflect distinct binding sites for retigabine and ZnPy on the channels, shown by site-directed mutagenesis (Xiong et al., 2007, 2008), and make ZnPy a unique molecular probe for investigating K_V7 channel function. The potency of ZnPy at $K_V7.4$ and $K_V7.5$ channels makes it particularly attractive for investigating the roles of these subunits in the regulation of pulmonary artery tone. This study therefore investigated whether ZnPy could act as a pulmonary vasodilator by activating K_V7 channels. The results demonstrate that ZnPy dilates pre-constricted rat intra-pulmonary arteries by an endothelium-independent mechanism. Part of the relaxation observed could be accounted for by K_V7 channel activation, but additional mechanisms, independent of K^+ channel activation, are also involved.

4.3 Methods

4.3.1 Rat pulmonary arteries

This investigation was carried out under regulations dictated by the UK Scientific Procedures (Animals) Act 1986 and conforms to the Guide for the Care and Use of Laboratory Animals published by the National Institutes of Health (NIH Publication No. 85-23, revised 1996). Male Sprague Dawley rats (200–250 g) were sacrificed by cervical dislocation. Intra-PAs were dissected from the lungs once they were excised into physiological salt solution (PSS) containing (mM): NaCl 120; KCl 5; $MgCl_2$ 1; NaH_2PO_4 0.5; KH_2PO_4 0.5; glucose 11; $CaCl_2$ 1.8; pH 7.4 with NaOH.

4.3.2 Myography

Intra-PAs with external diameters in the region of 300 to 600 μm were dissected free of connective tissue and mounted in a small vessel myograph (Danish Myo Technology, Aarhus, Denmark; Mulvany, 1988). Vessel wall tension was measured as described for human vessels in chapter 2 section 2.3.5.2. Vessels were submerged in pre-warmed physiological salt solution and maintained at 37°C for the entire experiment. A basal tension of 4 mN was applied to the vessels before allowing them to equilibrate for 30 min, washing every 15 min. Where indicated, endothelial function was disrupted by gently rubbing the vessel lumen with a roughened wire and adding both 300 μM N(G)-nitro-L-arginine methyl ester (L-NAME), a nitric oxide synthase inhibitor, and 10 μM indomethacin, a cyclooxygenase inhibitor, to the myograph chamber. By using these drugs, it was possible to determine if ZnPy caused relaxation by an endothelium-dependent or independent mechanism.

4.3.3 Experimental protocols

At the start of each experiment, vessels were challenged three times with 50 mM KCl for 5-6 min to check vessel integrity. Following washout, the α_1-adrenoceptor agonist phenylephrine (1 μM) was applied to provide a sustained level of tension, against which the ability of ZnPy to cause dilation could be tested. ZnPy was applied cumulatively at concentrations from 10 nM to 100 μM and the response measured as percent inhibition of the phenylephrine-induced tone. In some experiments ZnPy was replaced with sodium pyrithione or $ZnCl_2$ at the same concentrations. This was to determine if pyrithione or Zn^{2+} could cause relaxation independently or whether both chemical entities were required for relaxation. To investigate the effects of ZnPy in the absence of extracellular Ca^{2+}, responses to phenylephrine (10 μM) were evoked in Ca^{2+}-free PSS, where Ca^{2+} was omitted from the normal PSS and 1 mM EGTA added, with the pH adjusted to 7.4 with NaOH. Using a previously described protocol (Gurney and Allam, 1995), vessels were bathed in Ca^{2+}-free PSS for 10 min before and during the application of phenylephrine, followed by re-introduction of normal Ca^{2+} PSS to refill the Ca^{2+} stores. The protocol was repeated three times, with ZnPy (5 μM) added 10 min before the second phenylephrine application.

In separate experiments, the abilities of K^+ channel blocking drugs to interfere with the effects of ZnPy were tested. The drugs used were 4-aminopyridine (1 mM),

tetraethylammonium ions (TEA, 10 mM), paxilline (1 μM), iberiotoxin (50 nM), glibenclamide (10 μM) and XE991 (1-100 nM). Each drug was applied for 10 min before and during the addition of phenylephrine and subsequent application of ZnPy. An alternative approach was to pre-constrict vessels with 1 μM XE991 in place of phenylephrine. The mechanism of vasodilation was also assessed by creating conditions predicted to interfere with or promote the actions of a drug that opens K^+ channels. The K^+ electrochemical gradient was virtually abolished by pre-constricting vessels with PSS containing 90 mM K^+ in place of phenylephrine. To prevent changes in osmolarity, the solution was prepared by equimolar substitution of KCl for NaCl. To generate contraction due to voltage-gated Ca^{2+} entry, phenylephrine was replaced with the L-type VGCC channel activator Bay K 8644 (1 μM). To generate contraction mediated by voltage-independent Ca^{2+} influx, phenylephrine was replaced with the Ca^{2+} ionophore, ionomycin (3 μM). As ionomycin also acts on the endothelium to cause the release of endothelium-derived relaxing factors (Kemp et al., 1995), all experiments with ionomycin were carried out on endothelium-denuded vessels treated with L-NAME plus indomethacin.

4.3.4 Data Analysis

Data handling and statistical analyses were performed with Microsoft Excel and GraphPad Prism 6 (GraphPad Software Inc., La Jolla, CA, USA) software. Results are represented as mean ± standard error of the mean. Concentrations causing 50% of the maximum effect (EC_{50}) were determined from fits of the Hill equation with a variable slope to concentration-response curves. Normality of data was evaluated using the Shapiro-Wilk test and parametric (student t-test) or non-parametric (Mann-Whitney U) statistical tests applied appropriately when comparing two groups of data. One or two way analysis of variance (ANOVA) with Bonferroni post tests were used for comparison of multiple groups, as indicated. Differences between means were considered significant if $P<0.05$.

4.3.5 Drugs

Phenylephrine hydrochloride, L-NAME, ZnPy, Na pyrithione (NaPy), $ZnCl_2$, 4-AP, TEA chloride (TEA), glibenclamide, ionomycin, EGTA and dimethylsulphoxide (DMSO) were purchased from Sigma-Aldrich (Poole, UK). (±)Bay K 8664 was supplied by R&D Systems Europe (Abingdon, UK). XE991, paxilline and iberiotoxin were from Tocris Bioscience (Bristol, UK). Drugs were dissolved in water or DMSO to provide 10 or 100 mM stock

solutions, which were stored as frozen aliquots. Working solutions were prepared fresh each day by serial dilution of the stock in PSS. The vehicle concentration did not exceed 1%.

4.4 Results

4.4.1 Zinc pyrithione dilates rat intra-pulmonary arteries

The aim of this study was to ascertain whether ZnPy could act as a pulmonary vasodilator agent and the mechanism responsible for this effect. To investigate the pulmonary vasodilaton induced by ZnPy, rat iPAs mounted on a myograph were pre-constricted with phenylephrine. Once the phenylephrine-induced constriction reached a plateau, usually within 30-40 min, this was maintained for at least two hours. When ZnPy was applied to intact rat iPA constricted with phenylephrine, after a plateau was reached, it caused concentration-dependent relaxation (Figure 4.1A). The response developed slowly, sometimes taking 30 min or longer to reach steady state. Dilation was first detected at concentrations between 100 nM and 1 μM. The maximum effect, amounting to 85% inhibition of the phenylephrine-induced constriction, was apparent at 10 μM ZnPy. Higher concentrations occasionally produced further transient relaxation, but the predominant effect at ≥100 μM ZnPy was a delayed increase in tension, which could be substantial. Figure 4.1D shows the mean concentration-response curve obtained from 5 vessels, which gave a pEC_{50} (negative log of the half maximal effective molar concentration) of 6.0 ± 0.1 (n=5). Relaxation at 100 μM ZnPy was taken as the lowest tension value before constriction developed.

To determine if the endothelium played a role in ZnPy dilation, vessels were denuded of endothelium and exposed to 300 μM L-NAME and 10 μM indomethacin for the duration of the experiment to prevent nitric oxide or prostacyclin release, respectively. Under these conditions, ZnPy produced similar concentration-dependent dilation (Figure 4.1B). Comparison of the concentration-response curves in the presence and absence of endothelium showed no significant effect of removing the endothelium (Figure 4.1D). The absence of endothelium did not significantly alter the pEC_{50} (6.4 ± 0.3, n=5) compared to intact vessels.

The complexed form of ZnPy, comprising one Zn atom and two pyrithione moieties, is responsible for its interaction with K_V7 channels and is not mimicked by the Na salt (Xiong et al., 2007). To determine if the ZnPy complex was responsible for its actions on rat iPA, we

compared the effects of ZnPy with NaPy and $ZnCl_2$ applied separately over the same concentration range (Figure 4.1E). $ZnCl_2$ had essentially no effect on PAs at concentrations up to 100 μM. The effects of NaPy were highly variable. In 3 of 13 experiments it enhanced constriction at concentrations ≤10 μM, but varying degrees of dilation were observed in other vessels. The average effect measured from 13 vessels was a concentration-dependent dilation that reached maximum at 10 μM NaPy, where it reduced the phenylephrine constriction by around 40%. This effect was less than half the response to ZnPy at the same concentration (P=0.01). These data suggest that the complexed form of ZnPy, rather than Zn^{2+} or pyrithione, was responsible for the endothelium-independent dilation observed, thus, possibly suggesting a role for K_V7 channels in the dilation.

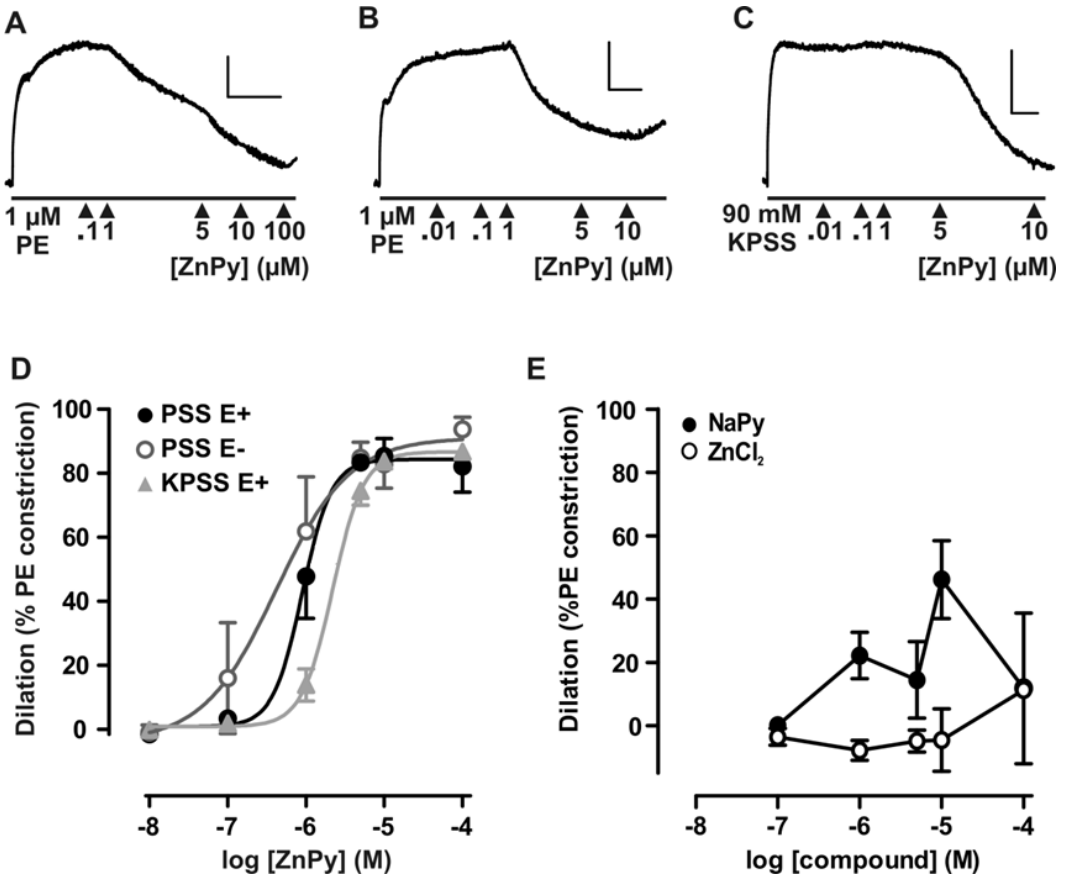

Figure 4.1: ZnPy dilates agonist pre-constricted rat intra-pulmonary arteries. Original records show concentration-dependent dilation induced by ZnPy of intact (A) and endothelium denuded (B) arteries pre-constricted with 1 μM phenylephrine (PE) and arteries pre-constricted with 90 mM K^+ PSS (C). Calibration bars are 2 mN (vertical) and 30 min (horizontal). D) Concentration-response curves for ZnPy dilation of phenylephrine-constricted vessels in the presence (E+, n=5) or absence (E-, n=5) of endothelium, or vessels constricted with 90 mM K^+ PSS (n=5). E) Concentration-response curves for dilation

measured in response to 0.1 – 100 μM NaPy (n=13) or $ZnCl_2$ (n=4) applied to vessels pre-constricted with phenylephrine (1 μM). Dilation measured as the percent loss of the tension induced by phenylephrine and plotted as mean ± S.E.M. Professor A. Gurney and B. Eid conducted experiments in part E.

4.4.2 K^+ channels and zinc pyrithione dilation

If the relaxation caused by ZnPy was due to activating K^+ channels, reducing the trans-membrane K^+ concentration gradient should inhibit the response. Vessels were therefore pre-constricted by increasing $[K^+]_o$ from 5.5 to 90 mM. Under these conditions ZnPy caused concentration-dependent relaxation, but substantial relaxation was not apparent until 5 μM (Figure 4.1C). Comparing the concentration-effect curve with that measured when vessels were pre-stimulated with phenylephrine shows a shift to higher concentrations (Figure 4.1D). The pEC_{50} for ZnPy dilation of K^+-constricted vessels was 5.6 ± 0.04 (n=5), which was significantly ($p< 0.01$) lower than measured in phenylephrine-constricted vessels.

The effects of a range of K^+ channel blocking drugs were tested on the ZnPy relaxation of phenylephrine (10 μM) constricted vessels. The drugs and concentrations were selected for their ability to inhibit particular types of K^+ channel (Alexander et al., 2011; Coetzee et al., 1999; Knaus et al., 1994). In each case the blocker was present throughout the experiment and, by themselves none of the drugs had any measurable effect on baseline tension (Figure 4.2). Original records show that ZnPy continued to evoke relaxation in the presence of 50 nM iberiotoxin, 10 mM TEA or 1 μM paxilline (Figure 4.3A-C), all of which block BK_{Ca} channels, while TEA additionally inhibits some voltage-gated K^+ channels. ZnPy also evoked relaxation in vessels treated with 1mM 4-AP (Figure 4.3D), a broad spectrum blocker of several voltage-gated K^+ channels, and 10 μM glibenclamide (Figure 4.3E), which inhibits K_{ATP} channels. Figure 4.3F compares the mean concentration-response curves for ZnPy dilation measured under control conditions and in the presence of each of these K^+ channel blockers. None of the drugs had a significant effect on the concentration-effect curve for ZnPy. The pEC_{50} values for ZnPy in the presence of each of the drugs were: iberiotoxin = 5.38 ± 0.07 (N=5); TEA = 5.4 ± 0.1 (n=6); paxilline = 5.6 ± 0.3 (N=6); 4-AP = 5.7 ± 0.2 (n=5); glibenclamide = 5.2 ± 0.1 (n=6). These data suggest that the ZnPy-induced dilation did not occur via activation of K^+ channels other than K_V7 channels .

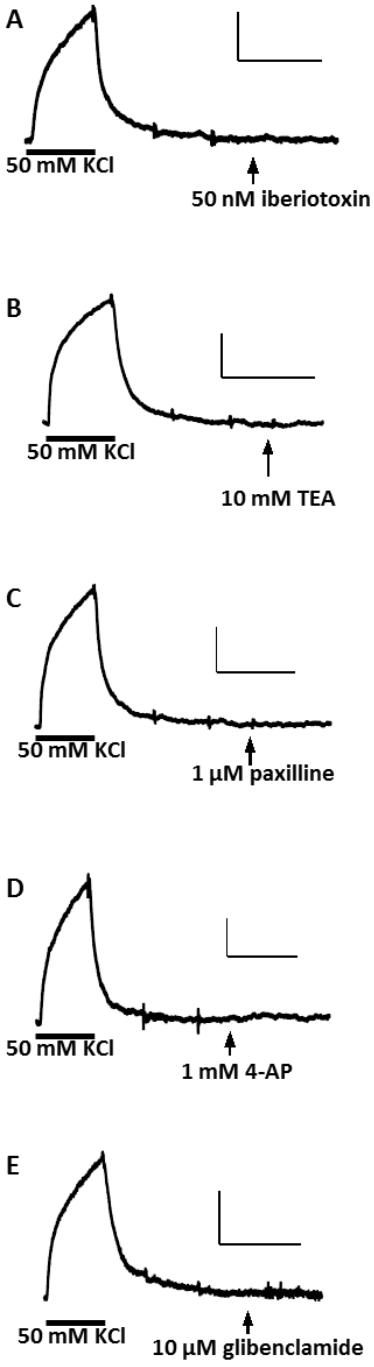

Figure 4.2: Classical K^+ channel blockers do not alter rat intra-pulmonary artery tone. Original records show rat iPA constriction to 50 mm KCl followed by washout and the subsequent addition of 50 nM iberiotoxin (A), 10 mM TEA (B), 1 μM paxilline (C), 1 mM 4-AP (D) or 10 μM glibenclamide (E). Calibration bars are 2 mN (vertical) and 500 s

(horizontal). B. Eid conducted the experiments in Figure 4.3 which use the same recordings in these example traces. Figure was constructed by S. Brennan.

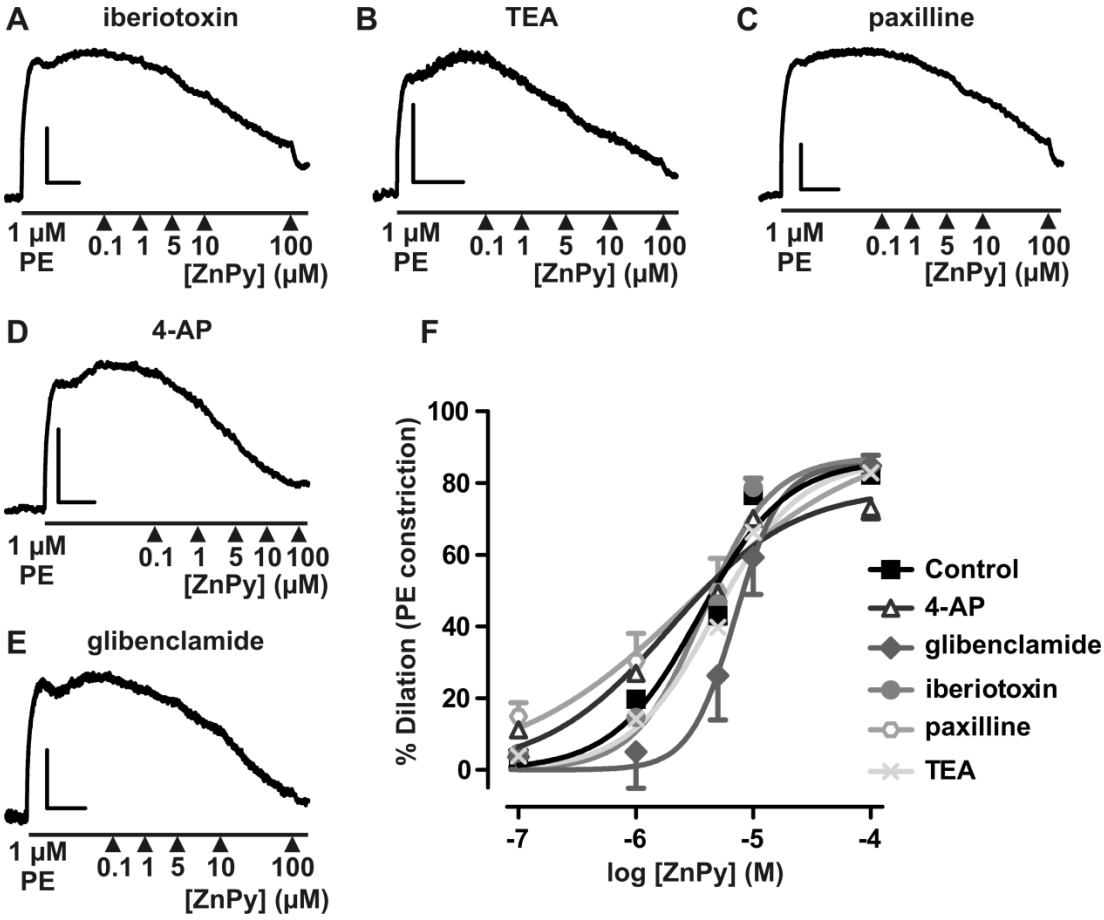

Figure 4.3: ZnPy relaxation is unaffected in the presence of K^+ channel blockers. Original records show ZnPy-induced dilation of rat iPA pre-constricted by 10 µM PE in the continued presence of 50 nM iberiotoxin (A), 10 mM TEA (B), 1 µM paxilline (C), 1 mM 4-AP (D) or 10 µM glibenclamide (E). Calibration bars are 2 mN (vertical) and 15 min (horizontal). F) Concentration-response curves for the dilator effect of ZnPy on vessels constricted with phenylephrine under control conditions and in the presence of each of the above drugs. Relaxation was measured in each vessel as a percentage of the constriction induced by phenylephrine. Data plotted as mean ± S.E.M of 5-6 observations. S. Brennan conducted the initial experiments in this series and they were completed by B. Eid. S. Brennan analysed the data and constructed the figure.

Similar experiments with inhibitors of K_V7 channels are complicated by the fact that these drugs are pulmonary vasoconstrictors at EC_{50} concentrations for blocking K_V7 channels (Joshi et al., 2006). The nature of the constriction developed by phenylephrine plus a K_V7 channel blocker would therefore differ from that induced by phenylephrine alone, thus invalidating comparisons. The relationship between membrane potential and constriction is, however, non-linear (Casteels et al., 1977a) due to the need to raise the membrane potential to the threshold for Ca^{2+} channel activation before Ca^{2+} can enter the cell and trigger contraction. With this in mind we tested concentrations of the K_V7 channel blocker, XE991, that were below or close to the threshold for activating contraction. When used at 100 nM, a threshold level for constriction (Joshi et al., 2006), XE991 had little effect on baseline tone, enabling constriction to be developed largely in response to phenylephrine. In these conditions ZnPy continued to cause relaxation, albeit at higher concentrations (Figure 4.4A). The concentration-response curve for ZnPy in the presence of 100 nM XE991 is compared in Figure 4.4B with 1 nM XE991, a concentration that had no effect on artery tone and little effect on K_V7 channels. In the presence of 1 nM XE991, ZnPy produced concentration-dependent dilation similar to that seen in its absence, beginning between 0.1 and 1 μM ZnPy (pEC_{50} = 5.4 ± 0.3, n=5). When the XE991 concentration was raised to 100 nM the concentration-response curve for ZnPy was shifted to the right, giving a pEC_{50} (4.9 ± 0.1, n=6) significantly lower than measured from control preparations in the absence of the drug (one-way ANOVA with Dunn's post-test $p< 0.0419$). To test if a sufficiently high concentration of XE991 could block the response to ZnPy we tested the ability of ZnPy to dilate vessels pre-constricted with 1 μM XE991 (Figure 4.4B), which evoked constriction amounting to 61 ± 6% (n=3) of the response to 50 mM KCl. Under these conditions ZnPy evoked concentration-dependent dilation with pEC_{50} = 5.64 ± 0.06 (n=4) and a maximum dilation of 73 ± 2% at 10 μM (Figure 4.4D), similar to the values measured for relaxation of phenylephrine-constricted vessels. Thus although the ZnPy relaxation was antagonised by XE991, but not other K^+ channel blockers, it could still relax iPAs at high concentrations of XE991, which cause sufficient block of K_V7 channels to evoke near maximum vasoconstriction (Joshi et al., 2006). These data suggest that the ZnPy-induced dilation was only partly caused by K_V7 channel activation and other mechanisms are likely also responsible.

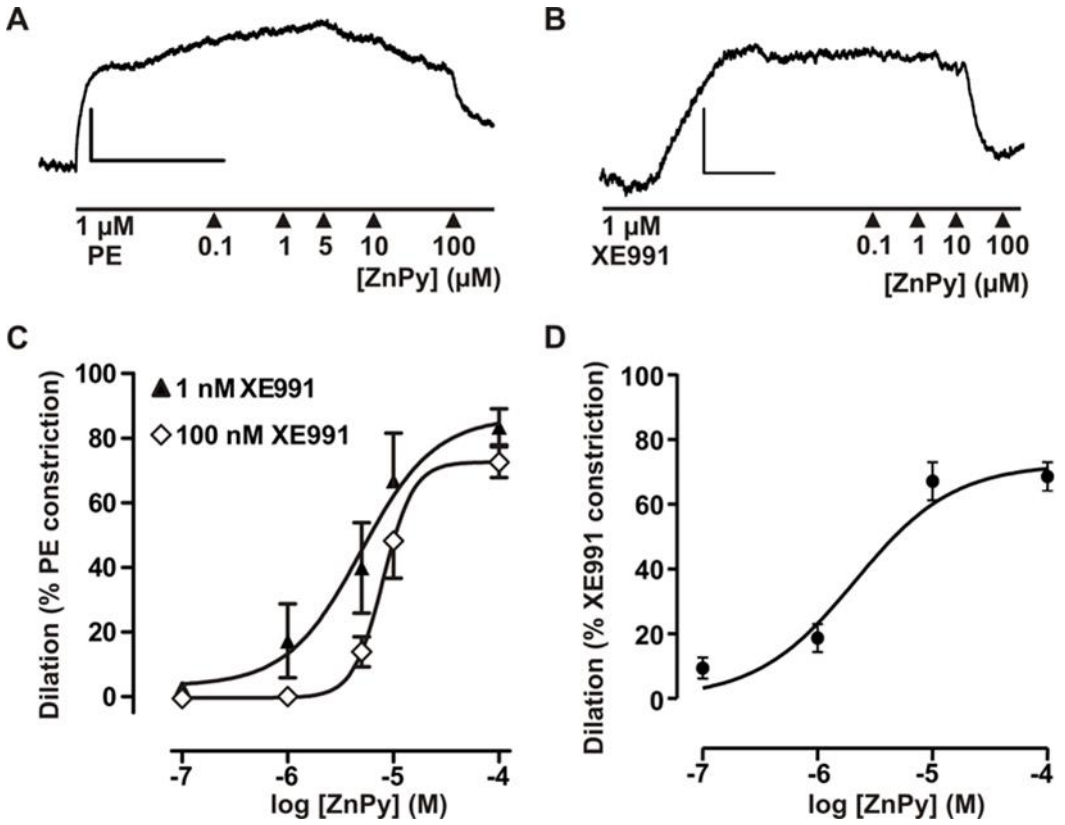

Figure 4.4: Effect of XE991 on ZnPy-induced relaxation. Orginal records show the effects of adding 0.1 -100 µM ZnPy to rat iPAs constricted with 1 µM phenylephrine in the continued presence of 100 nM XE991 (A) or 1 µM XE991 (B). Calibration bars are 2 mN (A) and 0.5 mN (C) (vertical) and 30 min (A) and 20 min (B) (horizontal). B) Concentration-response curves for ZnPy-induced relaxation of vessels constricted with 1 µM phenylephrine in the presence of 1 nM (n=5) or 100 nM (n=6) XE991. D, Concentration-response curve for ZnPy-induced relaxation of vessels constricted with 1 mM XE991 (n=3). Relaxation was measured in each vessel as a percentage of the tension developed by the constricting agent. Data expressed as mean ± S.E.M. B. Eid and Prof A. Gurney conducted experiments shown in this figure. S. Brennan carried out the initial experiments, analysed the data and constructed the figure.

4.4.3 Effects of zinc pyrithione on Ca^{2+} homeostasis

If the relaxation caused by ZnPy involved activation of smooth muscle K_V7 channels, this would in turn give rise to inhibition of Ca^{2+} entry through VGCCs in the smooth muscle cell membrane. The involvement of voltage-gated Ca^{2+} influx in the relaxant action of ZnPy was tested by investigating its ability to relax vessels constricted by agents that raise $[Ca^{2+}]_i$ in smooth muscle via different routes.

Bay K 8644 is an L-type VGCC agonist that directly increases smooth muscle $[Ca^{2+}]_i$ by increasing the channel open probability and shifting its activation curve to more hyperpolarised potentials, so that Ca^{2+} influx occurs at the resting potential (Hering et al., 1993). At 1 μM, Bay K 8644 induced sustained constriction (1.6 ± 0.4 mN, n=6) that was about 30% of the response to 1 μM phenylephrine (4.6 ± 0.7 mN, n=6; $p<0.01$) in paired vessels. The response to Bay K 8644 was reduced by the subsequent application of ZnPy at 5 μM and almost abolished at 10 μM (Figure 4.5A).

As a Ca^{2+} ionophore, ionomycin also directly increases smooth muscle $[Ca^{2+}]_i$, but by a voltage-independent mechanism that is not inhibited by membrane hyperpolarisation. As shown in Figure 4.5B, 3 μM ionomycin induced sustained constriction (6.1 ± 1.2 mN, n=6) that was not significantly different in amplitude from the response to phenylephrine. When applied to ionomycin constricted vessels, 5 μM ZnPy did not evoke relaxation, but when the concentration was raised to 10 μM it did. There was, however, a delay of 16 ± 3 min before the relaxation began, compared with only 0.9 ± 0.1 min for the response in phenylephrine-constricted vessels and 3.0 ± 0.8 min when Bay K 8644 was used. In the latter two conditions the response delay did not differ significantly. Figure 4.5C compares the mean amplitudes of responses to ZnPy (5 and 10 μM) when vessels were pre-constricted with phenylephrine, Bay K 8644 or ionomycin. At 5 μM, ZnPy was equally effective at dilating vessels constricted with Bay K 8644 or phenylephrine, but unable to relax vessels constricted with ionomycin, even causing a small, but significant constriction (5.1 ± 0.6% of the ionomycin-induced tone, 2-way ANOVA P=0.0038). Responses to 10 μM ZnPy were of a similar magnitude regardless of the pre-constricting agent, however between the two concentrations of ZnPy used the was a significant difference in the relaxation observed (2-way ANOVA $P<0.0001$).

The vasoconstriction evoked by phenylephrine arises due to the release of Ca^{2+} from stores in the sarcoplasmic reticulum of smooth muscle cells as well as from Ca^{2+} influx (Hamada et

al., 1997). When extracellular Ca^{2+} is removed, the store provides the sole source of Ca^{2+} for smooth muscle contraction. To determine if the ZnPy relaxation could involve an effect on store-released Ca^{2+}, we investigated the effects of the drug on constriction evoked by phenylephrine in Ca^{2+}-free solution. In the absence of extracellular Ca^{2+}, 10 μM phenylephrine evoked constriction that was short lived, reflecting depletion of the store. The amplitude of the constriction was 54 ± 6 % (n=4) of the response observed in normal PSS. The response to phenylephrine recorded in the absence of extracellular Ca^{2+} was further reduced by 36 ± 8 % (n=4, $p<0.01$) in the presence of 5 μM ZnPy, the effects of which were reversible upon washout (Figure 4.5D). In summary, ZnPy was most effective against constriction that depended on voltage-gated Ca^{2+} influx, but it also inhibited constriction that developed independently of Ca^{2+} influx and at 10 μM became equally effective regardless of the source of Ca^{2+}. Together, these data would suggest that K_V7 channel activation is unlikely to be the only mechanism by which ZnPy-induced dilation occurs.

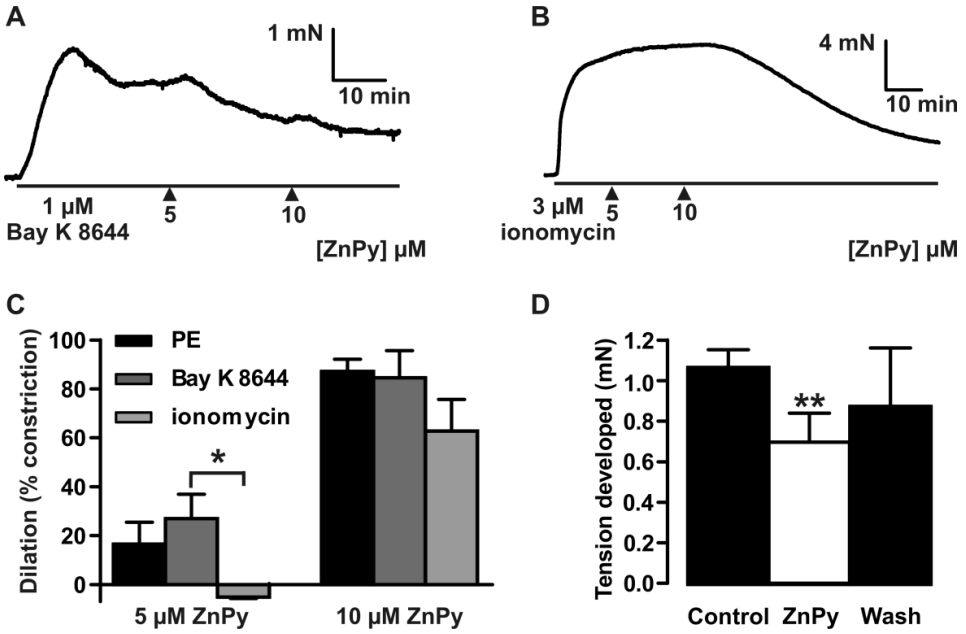

Figure 4.5: Sources of Ca^{2+} affected by ZnPy. Original records show the effect of ZnPy on the tension developed by arteries in response to the continued application of 1 μM BayK8644 (A) or 3 μM ionomycin (B). C) Bar chart comparing mean relaxation in response to 5 or 10 μM ZnPy when applied to vessels pre-constricted with 1 μM phenylephrine (n=6), Bay K 8644 (n=6) or ionomycin (n=6). *$p<0.05$. D) Tension developed in Ca^{2+}-free conditions in response to 10 μM phenylephrine before (control) and during exposure to 5 μM ZnPy and following washout of ZnPy (n=4). **$p<0.01$ versus control. Values plotted in C and D

are mean ± S.E.M. B. Eid contributed to experiments shown in this figure. S. Brennan designed the experiments, analysed the data and constructed the figure.

4.4 Discussion

Due to its different pharmacological profile from retigabine and flupirtine, including K_V7 subunit selectivity and mechanism of activation, ZnPy offered a new tool for probing the role of K_V7 channels in the pulmonary circulation. We have shown that, like the previously studied K_V7 channel activators, ZnPy relaxes iPAs and its mechanism involves K_V7 channel activation. Unfortunately, the results show that, in addition to indirectly suppressing Ca^{2+} channel activity by K_V7 channel activation and smooth muscle cell hyperpolarisation, ZnPy may also directly inhibit the voltage-dependent Ca^{2+} influx pathway. There is also evidence to suggest that ZnPy can inhibit voltage-independent Ca^{2+} influx at high concentrations and that it interferes with cellular pathways linking stored Ca^{2+} to smooth muscle contraction. These findings suggest that ZnPy may not be a good K_V7 channel activator for experiments using whole tissue samples.

ZnPy was found to act as a potent dilator of rat iPAs. Since the endothelium is capable of inducing vasorelaxation by releasing chemical mediators, such as nitric oxide, in a paracrine manner, the ability of ZnPy to induce relaxation in endothelium-denuded iPAs was measured and compared to intact iPAs (Ignarro et al., 1987; McCormack, 1990). The removal of the endothelium did not significantly alter the potency or efficacy of ZnPy, indicating that this effect was mediated by a direct action on the smooth muscle cells of the vessel wall. When vessels were constricted with 1 μM phenylephrine, relaxation in response to ZnPy occurred with an EC_{50} of 1 μM and showed a steep dependence on concentration, reaching maximum at around 10 μM. This is in accord with the EC_{50} concentrations of 3.5 μM, 1.5 μM and 2.4 μM reported for activation of heterologously expressed $K_V7.1$, $K_V7.2$ or $K_V7.2/7.3$ channels, respectively (Gao et al., 2008; Xiong et al., 2007). Since homomeric $K_V7.4$ and $K_V7.5$ channels displayed more pronounced activation than other K_V7 channels in response to 10 μM ZnPy (Xiong et al., 2007), any of the K_V7 channels expressed in rat PA ($K_V7.1$, $K_V7.4$, $K_V7.5$) could account for the drug's vasodilator effects. Several additional observations support activation of K_V7 channels as a mechanism contributing to ZnPy vasodilation. These include the ability of ZnPy to dilate vessels pre-constricted with Bay K 8644 and its reduced potency when vessels were exposed to a low concentration of the K_V7 channel blocker, XE991, or, pre-constricted with 90 mM K^+ or

ionomycin. On the other hand, ZnPy retained the ability to dilate vessels pre-constricted with 1 μM XE991 or stimuli that act independently of voltage-gated Ca^{2+} influx, implying that additional mechanisms must be involved in mediating the effect.

The reduced potency of ZnPy in the presence of XE991 provides the strongest evidence that K_V7 channel activation was involved in the dilator response. XE991 caused inhibition of the ZnPy-induced relaxation at a low concentration (100 nM), which had no effect by itself and is below the reported EC_{50} of 400 nM for evoking constriction of rat pulmonary artery (Joshi et al., 2006). At this threshold concentration, it is likely that XE991 blocked a proportion of K_V7 channels, but not enough to depolarise the membrane to a level that activates a sufficient number of L-type VGCCs to cause contraction. Moreover, 100 nM XE991 is expected to be selective for K_V7 channels. Although its selectivity has not been widely tested, XE991 is 3 orders of magnitude more potent at K_V7 than a range of other voltage-gated K^+ channels (Wang et al., 1998). Moreover, its potency on $K_V7.1$ channels is reduced 10-fold when they also contain the KCNE1 auxiliary subunit (Wang et al., 1998). Consistent with it acting via K_V7 channels, XE991 was the only one of several blockers, targeted against a range of K^+ channels, to inhibit responses to ZnPy. The lack of effect of 10 mM TEA on the ZnPy dilation is interesting, because at that concentration it is expected to suppress the activity of homomeric $K_V7.1$ (EC_{50}=5 mM) and $K_V7.4$ (EC_{50}=3 mM) channels (Hadley et al., 2000), but not $K_V7.5$, which is an order of magnitude less sensitive (Lerche et al., 2000a; Schroeder et al., 2000a). Thus the K_V7 channels contributing to the dilator action of ZnPy are most likely to be $K_V7.5$.

The effectiveness of ZnPy at relaxing vessels constricted with Bay K 8644 lends further support to the involvement of K^+ channel activation. Whereas smooth muscle contraction evoked by phenylephrine is initiated by Ca^{2+} from several sources and involves Ca^{2+} sensitisation of the contractile machinery, constriction to Bay K 8644 depends entirely on the influx of Ca^{2+} through L-type VGCCs (Su et al., 1964). Bay K 8644 enhances channel activation at the resting potential, but hyperpolarising the cell is expected to oppose the activation (Hering et al., 1993). If ZnPy directly inhibited L-type VGCCs, it would however, have the same effect.

Raising the extracellular K^+ concentration to 90 mM depolarises the membrane potential of pulmonary artery smooth muscle close to 0 mV, thus activating L-type VGCCs to cause contraction (Casteels et al., 1977a). At the same time it reduces the trans-membrane K^+

gradient, thereby preventing K^+ flux through open K^+ channels. Indeed, the K_{ATP} channel activator, cromakalim, failed to hyperpolarise smooth muscle when $[K^+]_o$ was raised above 40 mM (Nakao et al., 1988). The shift in the ZnPy concentration-effect curve to higher concentrations in vessels pre-constricted with 90 mM K^+, compared with phenylephrine, is consistent with a role for K^+ channel activation in the response. On the other hand, the failure of high $[K^+]_o$ to abolish the effect of ZnPy, as well as the pronounced dilation in response to ZnPy that is seen in vessels stimulated with 1 μM XE991, indicate that K^+ channel activation cannot fully account for the effects of ZnPy. Since the contractions stimulated by high $[K^+]_o$, Bay K 8644 and XE991 all depend exclusively on voltage-gated Ca^{2+} entry, direct inhibition of L-type VGCCs is likely to contribute as well.

As ionomycin contracts smooth muscle by activating voltage-independent Ca^{2+} entry, the inability of 5 μM ZnPy to reverse ionomycin-induced contraction is consistent with ZnPy mechanisms involving K^+ channel activation, membrane hyperpolarisation and L-type VGCC inhibition. In fact, the small constriction to ZnPy observed in the presence of ionomycin is consistent with an increased driving force for Ca^{2+} entry, an expected consequence of hyperpolarisation. The undiminished dilation in response to 10 μM ZnPy in the presence of ionomycin is, however, inconsistent with K^+ channel activation or Ca^{2+} channel inhibition and implies that additional mechanisms contribute at high ZnPy concentrations. It is notable that relaxation in response to 10 μM ZnPy occurred with a long time delay (> 15 min). A possible explanation is that K^+ channel activation and Ca^{2+} channel inhibition predominated at low concentrations of ZnPy and during the onset of dilation at higher concentrations, but other mechanisms took over as the dilation developed. This interpretation is consistent with the apparently greater inhibition of the dilation by XE991 seen at low ZnPy concentrations, resulting in a non-parallel shift in the concentration-effect curve. The ability of ZnPy to inhibit constrictor responses to phenylephrine in the absence of extracellular Ca^{2+} provides further evidence for an action that is independent of plasma membrane K^+ or Ca^{2+} channels. To inhibit these responses ZnPy must have acted within the cell, although the experiments reported here do not distinguish between targets affecting the release or accumulation of stored Ca^{2+}, or subsequent responses to the released Ca^{2+}.

ZnPy is an ionophore of zinc (Kim et al., 1999; Magda et al., 2008), thus zinc ions will follow down their chemical gradient in the presence of ZnPy. Zinc is known to be an important cofactor for over 2000 proteins (Andreini et al., 2006). For example, Zinc finger protein 191

has been reported to be required for vascular smooth muscle cell proliferation and migration after endovascular arterial injury (Lv et al., 2014). It could be argued that, as zinc was absent from the PSS solution used, intracellular zinc would diffuse out of the artery cells in the presence of ZnPy. This may help to explain why high concentrations of ZnPy appeared toxic.

4.5 Conclusion

ZnPy is a pulmonary vasodilator. Activation of K_V7 channels, most likely $K_V7.5$, is probably involved in mediating its effects. Additional mechanisms, independent of K_V7 channel activation, do however contribute. These mechanisms may involve inhibition of voltage-gated Ca^{2+} channels, as well as an action on intracellular signalling pathways. This lack of selectivity means that the usefulness of ZnPy for studies on intact arteries, and possibly other tissues, is limited. It may, however, provide a more effective tool for studying K_V7 channels in isolated myocytes or cell lines, where channel activity can be directly measured.

4.6 Acknowledgments

SB was supported by an MRC studentship. BE was supported by a scholarship from the Saudi Arabian government.

4.7 References

Alexander, S.P.H., Mathie, A., and Peters, J.A. (2011). Guide to Receptors and Channels (GRAC), 5th edition. British Journal of Pharmacology *164 Suppl* , S1–324.

Brennan, S., Oliveira, R., Gurney, A. (2011). Effects of KV7 potassium channel modulators on human intra-pulmonary artery. Proceedings of the Physiological Society 25, C15 and PC15.

Brueggemann, L.I., Moran, C.J., Barakat, J.A., Yeh, J.Z., Cribbs, L.L., and Byron, K.L. (2007). Vasopressin stimulates action potential firing by protein kinase C-dependent inhibition of KCNQ5 in A7r5 rat aortic smooth muscle cells. American Journal of Physiology. Heart and Circulatory Physiology *292*, H1352–63.

Casteels, R., Kitamura, K., Kuriyama, H., and Suzuki, H. (1977a). Excitation-contraction coupling in the smooth muscle cells of the rabbit main pulmonary artery. The Journal of Physiology *271*, 63–79.

Chadha, P.S., Zunke, F., Zhu, H.-L., Davis, A.J., Jepps, T.A., Olesen, S.P., Cole, W.C., Moffatt, J.D., and Greenwood, I.A. (2012). Reduced *KCNQ4*-encoded voltage-dependent potassium

channel activity underlies impaired β-adrenoceptor-mediated relaxation of renal arteries in hypertension. Hypertension *59*, 877–884.

Coetzee, W.A., Amarillo, Y., Chiu, J., Chow, A., Lau, D., McCormack, T., Moreno, H., Nadal, M.S., Ozaita, A., Pountney, D., Saganich, M., Vega-Saenz de Miera E., Rudy B. (1999). Molecular diversity of K^+ channels. Annals of the New York Academy of Sciences *868*, 233–285.

Dupuis, D.S., Schrøder, R.L., Jespersen, T., Christensen, J.K., Christophersen, P., Jensen, B.S., and Olesen, S.P. (2002). Activation of KCNQ5 channels stably expressed in HEK293 cells by BMS-204352. European Journal of Pharmacology *437*, 129–137.

Gao, Z., Xiong, Q., Sun, H., and Li, M. (2008). Desensitization of chemical activation by auxiliary subunits: convergence of molecular determinants critical for augmenting KCNQ1 potassium channels. The Journal of Biological Chemistry *283*, 22649–22658.

Gurney, A.M., and Allam, M. (1995). Inhibition of calcium release from the sarcoplasmic reticulum of rabbit aorta by hydralazine. British Journal of Pharmacology *114*, 238–244.

Gurney, A.M., Joshi, S., and Manoury, B. (2010). KCNQ potassium channels: new targets for pulmonary vasodilator drugs? Advances in Experimental Medicine and Biology *661*, 405–417.

Hadley, J.K., Noda, M., Selyanko, A.A., Wood, I.C., Abogadie, F.C., and Brown, D.A. (2000). Differential tetraethylammonium sensitivity of KCNQ1-4 potassium channels. British Journal of Pharmacology *129*, 413–415.

Hamada, H., Damron, D.S., Hong, S.J., Van Wagoner, D.R., and Murray, P.A. (1997). Phenylephrine-induced Ca^{2+} oscillations in canine pulmonary artery smooth muscle cells. Circulation Research *81*, 812–823.

Hering, S., Hughes, A.D., Timin, E.N., and Bolton, T.B. (1993). Modulation of calcium channels in arterial smooth muscle cells by dihydropyridine enantiomers. The Journal of General Physiology *101*, 393–410.

Ignarro, L.J., Byrns, R.E., Buga, G.M., and Wood, K.S. (1987). Endothelium-derived relaxing factor from pulmonary artery and vein possesses pharmacologic and chemical properties identical to those of nitric oxide radical. Circulation Research *61*, 866–879.

Jepps, T.A., Chadha, P.S., Davis, A.J., Harhun, M.I., Cockerill, G.W., Olesen, S.P., Hansen, R.S., and Greenwood, I.A. (2011). Downregulation of $K_V7.4$ channel activity in primary and secondary hypertension. Circulation *124*, 602–611..

Joshi, S., Balan, P., and Gurney, A.M. (2006). Pulmonary vasoconstrictor action of KCNQ potassium channel blockers. Respiratory Research *7*, 31.

Joshi, S., Sedivy, V., Hodyc, D., Herget, J., and Gurney, A.M. (2009). KCNQ modulators reveal a key role for KCNQ potassium channels in regulating the tone of rat pulmonary artery smooth muscle. The Journal of Pharmacology and Experimental Therapeutics *329*, 368–376.

Kemp, B.K., Smolich, J.J., Ritchie, B.C., and Cocks, T.M. (1995). Endothelium-dependent relaxations in sheep pulmonary arteries and veins: resistance to block by NG-nitro-L-arginine in pulmonary hypertension. British Journal of Pharmacology *116*, 2457–2467.

Knaus, H.G., McManus, O.B., Lee, S.H., Schmalhofer, W.A., Garcia-Calvo, M., Helms, L.M., Sanchez, M., Giangiacomo, K., Reuben, J.P., and Smith, A.B. (1994). Tremorgenic indole alkaloids potently inhibit smooth muscle high-conductance calcium-activated potassium channels. Biochemistry *33*, 5819–5828.

Lerche, C., Scherer, C.R., Seebohm, G., Derst, C., Wei, A.D., Busch, A.E., and Steinmeyer, K. (2000a). Molecular cloning and functional expression of KCNQ5, a potassium channel subunit that may contribute to neuronal M-current diversity. The Journal of Biological Chemistry *275*, 22395–22400.

Mani, B.K., O'Dowd, J., Kumar, L., Brueggemann, L.I., Ross, M., and Byron, K.L. (2013). Vascular KCNQ (K_V7) potassium channels as common signaling intermediates and therapeutic targets in cerebral vasospasm. Journal of Cardiovascular Pharmacology *61*, 51–62.

Mattmann, M.E., Yu, H., Lin, Z., Xu, K., Huang, X., Long, S., Wu, M., McManus, O.B., Engers, D.W., Le, U.M., Li, M., Lindsley, C.W., Hopkins, C.R. (2012). Identification of (R)-N-(4-(4-methoxyphenyl)thiazol-2-yl)-1-tosylpiperidine-2-carboxamide, ML277, as a novel, potent and selective $K_V7.1$ (KCNQ1) potassium channel activator. Bioorganic & Medicinal Chemistry Letters *22*, 5936–5941.

McCormack, D. (1990). Endothelium-derived relaxing factors and the human pulmonary circulation. Lung *168 Suppl*, 35–42.

Miceli, F., Soldovieri, M.V., Martire, M., and Taglialatela, M. (2008). Molecular pharmacology and therapeutic potential of neuronal K_V7-modulating drugs. Current Opinion in Pharmacology *8*, 65–74.

Morecroft, I., Murray, A., Nilsen, M., Gurney, A.M., and MacLean, M.R. (2009). Treatment with the K_V7 potassium channel activator flupirtine is beneficial in two independent mouse models of pulmonary hypertension. British Journal of Pharmacology *157*, 1241–1249.

Mulvany M.J. (1988). Procedures for investigation of small vessels using small vessel myograph. Danish Myo Technology, 2004. Available at: http://www.dmt.dk/files/manualer/procedures_for_investigation.pdf (Accessed 28th September 2013)

Nakao, K., Okabe, K., Kitamura, K., Kuriyama, H., and Weston, A.H. (1988). Characteristics of cromakalim-induced relaxations in the smooth muscle cells of guinea-pig mesenteric artery and vein. British Journal of Pharmacology *95*, 795–804.

Robbins, J. (2001). KCNQ potassium channels: physiology, pathophysiology, and pharmacology. Pharmacology & Therapeutics *90*, 1–19.

Schrøder, R.L., Jespersen, T., Christophersen, P., Strøbaek, D., Jensen, B.S., and Olesen, S.P. (2001). KCNQ4 channel activation by BMS-204352 and retigabine. Neuropharmacology *40*, 888–898.

Schroeder, B.C., Hechenberger, M., Weinreich, F., Kubisch, C., and Jentsch, T.J. (2000a). KCNQ5, a novel potassium channel broadly expressed in brain, mediates M-type currents. The Journal of Biological Chemistry *275*, 24089–24095.

Sedivy, V., Joshi, S., Ghaly, Y., Mizera, R., Zaloudikova, M., Brennan, S., Novotna, J., Herget, J., and Gurney, A.M. (2014). Role of Kv7 channels in responses of the pulmonary circulation to hypoxia. The American Journal of Physiology - Lung Cellular and Molecular Physiology.ajplung.00362.2013.

Su, C., Bevan, J.A., and Ursillo, R.C. (1964). Electrical quiescence of pulmonary artery smooth muscle during sympathomimetic stimulation. Circulation Research *15*, 26–27.

Szelenyi, I. (2013). Flupirtine, a re-discovered drug, revisited. Inflammation Research *62*, 251–258.

Tatulian, L., Delmas, P., Abogadie, F.C., and Brown, D.A. (2001). Activation of expressed KCNQ potassium currents and native neuronal M-type potassium currents by the anti-convulsant drug retigabine. The Journal of Neuroscience *21*, 5535–5545.

Wang, H.S., Pan, Z., Shi, W., Brown, B.S., Wymore, R.S., Cohen, I.S., Dixon, J.E., and McKinnon, D. (1998). KCNQ2 and KCNQ3 potassium channel subunits: molecular correlates of the M-channel. Science *282*, 1890–1893.

Wickenden, A.D., Krajewski, J.L., London, B., Wagoner, P.K., Wilson, W.A., Clark, S., Roeloffs, R., McNaughton-Smith, G., and Rigdon, G.C. (2008). N-(6-chloro-pyridin-3-yl)-3,4-difluoro-benzamide (ICA-27243): a novel, selective KCNQ2/Q3 potassium channel activator. Molecular Pharmacology. *73*, 977–986.

Xiong, Q., Sun, H., and Li, M. (2007). Zinc pyrithione-mediated activation of voltage-gated KCNQ potassium channels rescues epileptogenic mutants. Nature Chemical Biology *3*, 287–296.

Xiong, Q., Sun, H., Zhang, Y., and Nan, F. (2008a). Combinatorial augmentation of voltage-gated KCNQ potassium channels by chemical openers. Proceedings of The *105*, 3128–3133.

Xiong, Q., Gao, Z., Wang, W., and Li, M. (2008b). Activation of K_V7 (KCNQ) voltage-gated potassium channels by synthetic compounds. Trends in Pharmacological Sciences *29*, 99–107.

Yu, H., Zou, B., Wu, M., McManus, O.B., Le Engers, J., Cheung, Y.Y., Salovich, J.M., Hopkins, C.R., Lindsley, C.W., Li, M. (2013). Identification of a novel, small molecule inhibitor of KCNQ2 channels. Probe Reports from the NIH Molecular Libraries Program [Internet].

Chapter 5 : General Discussion

5.1 Main findings

Previous findings in the literature suggest that K_V7 channels are expressed and play a functional role in regulating the tone of rodent iPAs, by indirectly altering Ca^{2+} influx through VGCCs in PASMCs (Joshi et al, 2006; 2009). Furthermore, activators of K_V7 channels suppressed PAH in mouse models of the disease (Morecroft et al, 2009), which involves the proliferation and migration of PASMCs in addition to pulmonary vasoconstriction. Since K^+ channels are involved in regulating the rate of proliferation and migration in a range of cell types, this led to the hypothesis that K_V7 channel activators could provide an effective treatment for PAH, by inhibiting PASMC contraction, proliferation and migration. In order to assess whether the beneficial effects of K_V7 activators might be translated to humans, this study set out to determine the expression and physiological role of these channels in modulating vessel tone, PASMC proliferation and migration in healthy human iPA. Briefly, the present study has demonstrated that *KCNQ* mRNA is expressed in human iPA. Moreover, K_V7 channel modulators were found to alter the tone of human iPA by indirectly changing calcium influx. Although calcium influx is also important for PASMC proliferation and migration, the K_V7 modulators did not appear to alter the rates of either of these cellular processes in cultured PASMCs, presumably because of the down regulation of K_V7 channels in culture.

This is the first study to provide evidence for a functional role of K_V7 channels in human iPAs. RT-PCR showed that human iPA expresses a similar profile of *KCNQ* genes to iPA in other species, that is *KCNQ1, KCNQ4* and *KCNQ5*. Human iPA additionally expressed mRNA for *KCNQ3*. Preliminary western blot suggests that the $K_V7.4$ is also expressed at the protein level. The expression of all the above *KCNQ* genes in iPA was unaffected by the removal of the endothelium and adventitia, suggesting that the *KCNQ* transcripts are expressed in the medial layer of the artery. RT-qPCR demonstrated that the *KCNQ* transcripts were expressed in the arteries at levels comparable to either heart (*KCNQ1*) or brain (*KCNQ3-5*).

Myography experiments revealed that the K_V7 channel blockers linopirdine and XE991 both caused concentration-dependent constriction of human iPAs. Although not therapeutically useful to treat PAH, K_V7 channel blockers provided insight into the physiological role of the K_V7 channels within this vascular bed. The vasoconstriction caused by the K_V7 channel

blockers is consistent with the idea that functional K_V7 channels are open at rest. If the K_V7 channels were not expressed or functional then a blocker of the channels would not be expected to alter resting tone. This is consistent with previous findings that demonstrated that linopirdine and XE991, which constrict rat iPAs (Joshi et al., 2006), also cause membrane depolarisation and reduce the amplitude of I_{KN} in rat PASMCs (Joshi et al., 2009). The $K_V7.1$ channel blocker, chromanol 293B, when applied as the active stereoisomer, also caused concentration-dependent constriction of human iPAs. This demonstrates a potential species difference in the subunit-composition of functional K_V7 channels between rat and human iPAs, since chromanol 293B did not alter rat iPA tone. The widely used K_V7 activators, flupirtine and retigabine, both caused concentration-dependent relaxation of agonist pre-constricted human iPAs. Experiments investigating the mechanism of action of the K_V7 blockers and activators supported the idea that they indirectly caused an alteration in the opening probability of VGCC and hence Ca^{2+} influx. This is consistent with the drugs acting on K^+ channels and with previous work on rat pulmonary and systemic vessels, which demonstrated that VGCC block prevents a rise in vascular tone in the presence of a K_V7 channel blocker (Joshi et al., 2009; Mackie et al., 2008; Yeung et al., 2007).

From the findings of this work, it was hypothesised that K_V7 channels may play a role in human PASMC proliferation and/or migration, processes that are also implicated in PAH. This is because, like iPA vasoconstriction, PASMC proliferation and migration require membrane depolarisation and calcium influx to occur (Golovina, 1999; Kuhr et al., 2012; Leggett et al., 2012; Mandegar et al., 2004; Platoshyn et al., 2000). Since the K_V7 modulators indirectly altered $[Ca^{2+}]_i$ and human iPA tone, presumably by altering PASMC membrane potential, as shown in rat (Joshi et al., 2006;2009), it is reasonable to hypothesise that the K_V7 channels may also alter the rate at which PASMC proliferate and/or migrate through the same mechanism. These properties were studied in PASMC in culture, where the cells develop a proliferative phenotype. Initial experiments revealed that the expression of the *KCNQ* transcripts, except *KCNQ5*, was virtually abolished as soon as cultures were established. This could mean that K_V7 channels are involved in the transition of PASMCs from a contractile to a proliferative phenotype during culture. Although the *KCNQ5* transcript was still expressed in PASMC during culture, it did not appear to play a role in the regulation of cell proliferation or migration, as drugs that modulate its activity had no effect on these properties. This contrasts with reports that K_V7 channels inhibit the proliferation of skeletal muscle myoblasts (Roura-Ferrer et al., 2008; Iannotti et al., 2010).

Indeed, a number of K_V channel α-subunits, including K_V1.3, hERG and EGA1, have been implicated in the regulation of proliferation in various cell types (Cidad et al., 2012; Pier et al., 2014; Ouadid-Ahidouch and Ahidouch, 2013). Since the mRNA expression of the K_V7.1, K_V7.3 and K_V7.4 α-subunits was down regulated in cultured PASMCs, it is unclear if any of them could affect the rate of proliferation or migration. The possibility that K_V7.1, K_V7.3 and K_V7.4 α-subunits play a role in proliferation or migration cannot be ruled out on the basis of these data. This loss of expression observed in this study may not occur in PASMCs in vivo, thus they could still potentially play a role.

In terms of a potential treatment target for PAH, one advantage of the K_V7 channel family, with respect to other K^+ channels, is that there are drugs currently available with reasonable selectivity towards the K_V7 channels, and they are safe enough for use in humans (Saletu et al., 1989; Pieniaszek et al., 1995; Hermann et al., 2003; Deeks, 2011). Thus, the K_V7 channels are a good starting point for exploring K^+ channel activation as a potential treatment. One drawback of these drugs is the lack of selectivity among members of the K_V7 channel family. This makes it difficult to determine which K_V7 subtype is responsible for any effect observed. Drugs selective for one K_V7 sub-family member over others would help in future studies aiming to identify the physiological role of particular K_V7 channels. Furthermore, such a drug would potentially have reduced side effects should it be used therapeutically.

ZnPy provided us with a K_V7 activator that differs in 2 main ways from retigabine (Xiong et al., 2007, 2008). First, ZnPy has a different selectivity profile among the K_V7 channel sub-family members. Second, ZnPy can potentiate the current amplitude through single K_V7 channels, whereas retigabine does not. Similarly to other K_V7 activators, ZnPy relaxed pre-constricted iPAs in a concentration-dependent manner. The finding that a low concentration (100 nM) of XE991 shifted the ZnPy concentration-response curve to the right, suggested that at least part of the relaxation could be attributed to K_V7 channel activation. On the other hand, the ability of ZnPy to cause relaxation of rat iPA when the K^+ electrochemical gradient was virtually abolished, implies that its effects could not be solely attributed to K^+ channel activation. The effects of ZnPy in the proliferation and migration assays also indicate that the drug lacks selectivity for K_V7 channels. At 10 µM, a concentration causing near maximal relaxation of the intact artery, ZnPy appeared to be toxic to PASMCs. Thus at the end of the proliferation assay, the majority of PASMCs had become detached from the cell culture dish. Moreover in the scratch-wound migration

assay, time-lapse imaging showed that PASMCs moved away from the scratch and clumped together. Also, when the ZnPy concentration was raised to 100 µM, its relaxing effect on iPA was reversed and the vessels routinely remained contracted even after prolonged periods of washing. Therefore, although ZnPy may be an effective tool for studying K_V7 channels in electrophysiological experiments, where channel activity can be directly measured, its use on whole tissues is complicated by these unpredicted, and apparently toxic effects.

5.2 Clinical implications

The K_V7 channel blocker, linopirdine, was developed as a cognition-enhancing drug and has been shown to enhance the performance of laboratory animals in learning and memory paradigms (Brioni et al., 1993; Cook et al., 1990). There is also evidence that linopridine has vigilance-enhancing properties in humans (Saletu et al., 1989). The drug is generally well tolerated in humans, with the most common side effect being headache, most likely due to cerebral vasospasm (Pieniaszek et al., 1995; Saletu et al., 1989). Healthy young male volunteers administered with a dose of 55 mg linopirdine had a peak plasma concentration of 1.56 µM within 40 minutes (Pieniaszek et al., 1995). In the present study, this concentration produced over 40 % (of KCl response) constriction in human iPA. This implies that at the concentrations used in clinical trials, PA constriction may occur. This would be unlikely to be noticed as PA pressure is not commonly investigated during clinical trials. The half-life of linopirdine is approximately 2 hours, suggesting that iPA constriction could be maintained for a long period of time. This means constriction of the iPAs, and hence pulmonary hypertension, is a potential side effect of cognition enhancers acting by blocking K_V7 channels.

The K_V7 channel activator retigabine was recently approved as a treatment for epilepsy by the European Medicines Agency and the United States Food and Drug Administration, with the respective trade names of Trobalt® and Potiga®. Table 5.1 shows the mean plasma concentrations of retigabine reached in human subjects after different retigabine regimens. (Deeks, 2011; Hermann et al., 2003). Human iPAs pre-constricted with either PE, ET-1 or 5-HT relaxed by over 20% in the presence of 5 µM retigabine. Thus, following even the lowest dose of retigabine tested in man, plasma concentrations were reached that produced pulmonary dilation in the current study. Although dilation would probably only occur at the high plasma concentrations, however, this has not been measured. In the clinical trials for

epilepsy, retigabine was generally well tolerated in adults with partial-onset seizures, with most adverse events being of mild or moderate severity. The most common side effects in patients receiving 1200 mg retigabine per day were dizziness (26%), somnolence (19%) and fatigue (10%).

The dilation of human iPAs induced by retigabine, demonstrated in the present study, would probably not be a cause of adverse effects in healthy volunteers or patients prescribed the drug for epilepsy, since the PA is normally a low tone system with little or no intrinsic tone (Ducret et al., 2010). Human iPA tone was unaffected by retigabine when applied to a vessel at basal tone (not shown). This was also shown previously to be the case in rat iPAs (Joshi et al., 2009). Thus unless the artery tone was raised (e.g. if PH was present) retigabine would be unlikely to cause dilation. However, in PAH where tone is abnormally raised, retigabine could provide relief at the doses approved for treating epilepsy.

Study participants	Dose mg	C_{max} (μM)	T_{max} (hours)
Healthy males[1]	Single 200	2.4	2.2
Adults with epilepsy[2]	600 per day	3.1	1
	900 per day	3.3	1
	1200 per day	6.1	2.3

Table 5.1: Retigabine pharmacokinetic parameters measured in healthy and epileptic subjects. C_{max}, peak plasma concentration of retigabine; t_{max}, time to reach Cmax. Data from [1] Hermann et al., 2003 and [2] Deeks, 2011.

5.3 Future work

The work presented in this thesis has furthered the understanding of the physiological role of K_V7 channels in human iPAs. However, as well as answering many questions there are still areas that require more research.

Part of the rationale for this study was to determine if K_V7 channels could be a novel target in the treatment of PAH. The hypothesis was that K_V7 channels will be expressed and functional in human iPA and play an important role in pulmonary artery smooth muscle contraction, proliferation and migration. The main findings are consistent with the hypothesis. Unfortunately, none of the human lung samples collected for this study were from patients diagnosed with PH. Therefore, whether K_V7 channel modulators will affect iPA tone in PAH arteries is still unknown. This is important considering a report demonstrating the reduced ability of the K_V7 modulators to alter iPA tone in animal models

of PAH (Morecroft et al., 2009). Linopirdine was found to be less potent and effective at constricting iPA from mice with PAH, induced by over expression of the serotonin transporter ($SERT^+$), compared to control animals. Flupirtine was also less potent at relaxing iPAs from $SERT^+$ mice compared to wild-type mice. This could be due to a loss of *KCNQ* expression in the iPA of $SERT^+$ mice, as a reduction in *KCNQ4* expression has been reported in rats with PAH due to chronic exposure to hypoxia (Sedivy et al, 2014). Furthermore, $K_V7.4$ expression was reduced in rodent models of primary and secondary systemic hypertension, in association with a loss of sensitivity to K_V7 modulators (Jepps et al., 2011). Yet despite the potential down-regulation of *KCNQ* transcripts, treatment with flupirtine was beneficial in the hypoxic and $SERT^+$ models of PAH (Morecroft et al., 2009). Hence, it is important to investigate K_V7 channel expression and the effect of K_V7 channel modulators on iPAs from patients diagnosed with PH, although such vessels are not readily available.

Gene deletion experiments could provide an alternative way to identify the roles of K_V7 channels in iPA. These could include the use of *KCNQ* knockout mice for *in vivo* studies or small interfering RNA (siRNA) to investigate intact cells or vessels. The latter approach was used to demonstrate that $K_V7.4$ channels mediate β-adrenergic relaxation in systemic arteries (Chadha et al., 2012). Unfortunately, the Gurney laboratory has been unable to knock down K_V7 channel expression in rodent iPAs (R. Oliveira-unpublished observations) and it has not been attempted in human vessels. Transfection of cultured PASMCs may be more reliable and could be used with patch-clamp experiments to determine the contributions of different K_V7 channel subunits to I_{KN} and also in setting the RMP. If the membrane potential was found to be more depolarised in siRNA-treated PASMCs compared to control PASMCs, this would strongly support the hypothesis of K_V7 channels setting the membrane potential. It would also be helpful to determine the effects on cultured PASMCs of re-introducing the lost *KCNQ* genes. Such an approach could determine if increasing K_V7 channel expression returns the cells to a differentiated phenotype in terms of RMP and K^+ currents.

Physiological studies on K_V7 channels would be helped by having more subunit-selective modulator dugs. From a therapeutic and clinical perspective, a subunit-specific drug might also lead to fewer side effects. Recently a number of K_V7 subunit-selective drugs were reported, which could be beneficial, at least experimentally. A binding assay panel of 68 G-protein coupled receptors, ion channels and transporters, screened with a range of compounds, revealed ML252 as a potent blocker of $K_V7.2$ channels with an IC_{50} of 69 nM.

$K_V7.1$, $K_V7.2/3$ and $K_V7.4$ channels were blocked, but the IC_{50} values were all reported to be above 1 μM. The only other significant target that ML252 interacted with was the melatonin-1 receptor, where it caused 61% inhibition of radio ligand binding at 10 μM (Yu et al., 2013). Compound ML277 was shown to be a potent activator of $K_V7.1$ channels, with an EC_{50} of 260 nM, while it also increased the $K_V7.1$ current by 266% at +40 mV (Yu et al., 2013). ML213 is a potent activator of $K_v7.2$ and $K_v7.4$ channels, with EC_{50} values of 230 nM and 510 nM, respectively (Yu H et al., 2013). The selectivity of ML213 for K_V7 channel activation was also tested in the 68 binding assays described above and was found not to bind significantly with any of the channels, receptors or transporters tested. The development of these new drugs that can differentiate among K_V7 channel subunits raises the possibility of testing more thoroughly the physiological role and therapeutic potential of individual K_V7 channel subunits. Given the lack of reported *KCNQ2* and $K_V7.2$ expression in vascular smooth muscle, ML213 could be used as a specific $K_V7.4$ activator to elucidate the vascular role of $K_V7.4$.

5.4 Concluding remarks

This thesis presents the first in depth study of the physiological role of K_V7 channels in human iPAs. Messenger RNAs for *KCNQ1-5*, except *KCNQ2*, were expressed in human iPAs, while a preliminary Western blot detected $K_V7.4$ protein in human iPA. The K_V7 blockers linopirdine, XE991 and even the $K_V7.1$ selective blocker, chromanol 293B, caused concentration-dependent constriction of human iPA in myography experiments. The presence of just 100 nM nifedipine, a VGCC blocker, prevented the K_V7 blocker induced constriction, indicating that Ca^{2+} influx through VGCC is required. Conversely, the K_V7 activators retigabine and flupirtine relaxed vessels that were pre-constricted. The mechanism of action of retigabine was shown to be consistent with K^+ channel activation, but also Ca^{+2} channel block. The recently reported K_V7 activator, ZnPy, also relaxed iPAs of both rat and human. Only part of the ZnPy effect could be attributed, however, to K_V7 channel activation, while concentrations above 10 μM seemed to be toxic to cultured human PASMCs. None of the K_V7 modulators altered the rate of cultured PASMC proliferation or migration. This rules out a possible role for $K_V7.5$ channels, as these were the only K_V7 channels to be robustly expressed in cultured PASMCs. A role for other K_V7 channels cannot be ruled out as their expression may not be altered in proliferating cells *in vivo*. Overall this research has demonstrated that the K_V7 channels do play a role in

regulating human iPA tone and that activators of these channels might potentially be useful in the treatment of PAH.

References

Aaronson, P.I., Robertson, T.P., and Ward, J.P.T. (2002). Endothelium-derived mediators and hypoxic pulmonary vasoconstriction. Respiratory Physiology & Neurobiology *132*, 107–120.

Abbott, G.W., and Goldstein, S.A.N. (2002). Disease-associated mutations in KCNE potassium channel subunits (MiRPs) reveal promiscuous disruption of multiple currents and conservation of mechanism. The FASEB Journal *16*, 390–400.

Aiello, V.D., Gutierrez, P.S., Chaves, M.J.F., Lopes, A.A.B., Higuchi, M.L., and Ramires, J.A.F. (2003). Morphology of the internal elastic lamina in arteries from pulmonary hypertensive patients: a confocal laser microscopy study. Modern Pathology *16*, 411–416.

Albarwani, S., Robertson, B.E., Nye, P.C., and Kozlowski, R.Z. (1994). Biophysical properties of Ca^{2+}- and Mg-ATP-activated K^{+} channels in pulmonary arterial smooth muscle cells isolated from the rat. Pflügers Archiv : European Journal of Physiology *428*, 446–454.

Alexander, S.P.H., Mathie, A., and Peters, J.A. (2011). Guide to Receptors and Channels (GRAC), 5th edition. British Journal of Pharmacology *164 Suppl* , S1–324.

Amabile, C.M., and Vasudevan, A. (2013). Ezogabine: a novel antiepileptic for adjunctive treatment of partial-onset seizures. Pharmacotherapy *33*, 187–194.

Ammälä, C., Moorhouse, A., Gribble, F., Ashfield, R., Proks, P., Smith, P.A., Sakura, H., Coles, B., Ashcroft, S.J., and Ashcroft, F.M. (1996). Promiscuous coupling between the sulphonylurea receptor and inwardly rectifying potassium channels. Nature *379*, 545–548.

Andreini, C., Banci, L., Bertini, I., and Rosato, A. (2006). Counting the zinc-proteins encoded in the human genome. Journal of Proteome Research. *5*, 196–201.

Applied Biosystems. (1997). User Bulletin #2 ABI PRISM 7700 Sequence Detection System. Available at: http://www3.appliedbiosystems.com/cms/groups/mcb_support/documents/generaldocuments/cms_040980.pdf (Accessed 28th September 2013)

Archer, S.L. (1996). Diversity of phenotype and function of vascular smooth muscle cells. The Journal of Laboratory and Clinical Medicine *127*, 524–529.

Archer, S.L., Huang, J.M., Reeve, H.L., Hampl, V., Tolarová, S., Michelakis, E., and Weir, E.K. (1996). Differential distribution of electrophysiologically distinct myocytes in conduit and resistance arteries determines their response to nitric oxide and hypoxia. Circulation Research *78*, 431–442.

Archer, S.L., Souil, E., Dinh-Xuan, A.T., Schremmer, B., Mercier, J.C., El Yaagoubi, A., Nguyen-Huu, L., Reeve, H.L., and Hampl, V. (1998). Molecular identification of the role of voltage-gated K^+ channels, $K_V1.5$ and $K_V2.1$, in hypoxic pulmonary vasoconstriction and control of resting membrane potential in rat pulmonary artery myocytes. The Journal of Clinical Investigation *101*, 2319–2330.

Arnon, A., Hamlyn, J.M., and Blaustein, M.P. (2000). Na+ entry via store-operated channels modulates Ca^{2+} signaling in arterial myocytes. American Journal of Physiology- Cell Physiology *278*, C163–73.

Badesch, D.B., Raskob, G.E., Elliott, C.G., Krichman, A.M., Farber, H.W., Frost, A.E., Barst, R.J., Benza, R.L., Liou, T.G., Turner, M., Giles, S., Feldkircher, K., Miller, D.P., McGoon, M.D. (2010). Pulmonary arterial hypertension: baseline characteristics from the REVEAL Registry. Chest *137*, 376–387.

Bading, H., Hardingham, G.E., Johnson, C.M., and Chawla, S. (1997). Gene regulation by nuclear and cytoplasmic calcium signals. Biochemical and Biophysical Research Communications *236*, 541–543.

Barhanin, J., Lesage, F., Guillemare, E., Fink, M., Lazdunski, M., and Romey, G. (1996). KVLQT1 and lsK (minK) proteins associate to form the I_{Ks} cardiac potassium current. Nature *384*, 78–80.

Barnes, P.J., and Liu, S.F. (1995). Regulation of pulmonary vascular tone. Pharmacological Reviews *47*, 87–131.

Beisel, K.W., Rocha-Sanchez, S.M., Morris, K.A., Nie, L., Feng, F., Kachar, B., Yamoah, E.N., and Fritzsch, B. (2005). Differential expression of KCNQ4 in inner hair cells and sensory neurons is the basis of progressive high-frequency hearing loss. The Journal of Neuroscience *25*, 9285–9293.

Bendahhou, S., Marionneau, C., Haurogne, K., Larroque, M.-M., Derand, R., Szuts, V., Escande, D., Demolombe, S., and Barhanin, J. (2005). In vitro molecular interactions and distribution of KCNE family with KCNQ1 in the human heart. Cardiovascular Research *67*, 529–538.

Berridge, M.J. (1993). Inositol trisphosphate and calcium signalling. Nature *361*, 315–325.

Bialecki, R.A., Kulik, T.J., and Colucci, W.S. (1992). Stretching increases calcium influx and efflux in cultured pulmonary arterial smooth muscle cells. The American Journal of Physiology *263*, L602–6.

Bjornsson, J., and Edwards, W.D. (1985). Primary pulmonary hypertension: a histopathologic study of 80 cases. Mayo Clinic Proceedings. *60*, 16–25.

Blackburn-Munro, G., Dalby-Brown, W., Mirza, N.R., Mikkelsen, J.D., and Blackburn-Munro, R.E. (2005). Retigabine: chemical synthesis to clinical application. CNS Drug Reviews *11*, 1–20.

Boccara, G., Choby, C., Frapier, J.M., Quignard, J.F., Nargeot, J., Dayanithi, G., and Richard, S. (1999). Regulation of Ca^{2+} homeostasis by atypical Na^{+} currents in cultured human coronary myocytes. Circulation Research *85*, 606–613.

Boe, J., and Simonsson, B.G. (1980). Adrenergic receptors and sympathetic agents in isolated human pulmonary arteries. European Journal of Respiratory Diseases *61*, 195–202.

Boehlen, A., Schwake, M., Dost, R., Kunert, A., Fidzinski, P., Heinemann, U., and Gebhardt, C. (2013). The new KCNQ2 activator 4-Chlor-N-(6-chlor-pyridin-3-yl)-benzamid displays anticonvulsant potential. British Journal of Pharmacology *168*, 1182–1200.

Bowman, C.L., Gottlieb, P.A., Suchyna, T.M., Murphy, Y.K., and Sachs, F. (2007). Mechanosensitive ion channels and the peptide inhibitor GsMTx-4: history, properties, mechanisms and pharmacology. Toxicon *49*, 249–270.

Brayden, J.E., and Nelson, M.T. (1992). Regulation of arterial tone by activation of calcium-dependent potassium channels. Science *256*, 532–535.

Brennan, S., Oliveira, R., Gurney, A. (2011). Effects of KV7 potassium channel modulators on human intra-pulmonary artery. Proceedings of The Physiological Society 25, C15 and PC15.

Brioni, J.D., Curzon, P., Buckley, M.J., Arneric, S.P., and Decker, M.W. (1993). Linopirdine (DuP996) facilitates the retention of avoidance training and improves performance of septal-lesioned rats in the water maze. Pharmacology, Biochemistry, and Behavior *44*, 37–43.

Brown, D.A. (2008). K_V7 (KCNQ) potassium channels that are mutated in human diseases. The Journal of Physiology *586*, 1781–1783.

Brown, D.A., and Adams, P.R. (1980). Muscarinic suppression of a novel voltage-sensitive K^{+} current in a vertebrate neurone. Nature *283*, 673–676.

Brueggemann, L.I., Moran, C.J., Barakat, J.A., Yeh, J.Z., Cribbs, L.L., and Byron, K.L. (2007). Vasopressin stimulates action potential firing by protein kinase C-dependent inhibition of KCNQ5 in A7r5 rat aortic smooth muscle cells. American Journal of Physiology. Heart and Circulatory Physiology *292*, H1352–63.

Brueggemann, L.I., Mackie, A.R., Martin, J.L., Cribbs, L.L., and Byron, K.L. (2011). Diclofenac distinguishes among homomeric and heteromeric potassium channels composed of KCNQ4 and KCNQ5 subunits. Molecular Pharmacology. *79*, 10-23

Brueggemann, L.I., Mackie, A.R., Cribbs, L.L., Freda, J., Tripathi, A., Majetschak, M., and Byron, K.L. (2014). Differential protein kinase C-dependent modulation of Kv7.4 and Kv7.5 subunits of vascular Kv7 channels. The Journal of Biological Chemistry. *289*, 2099–2111

Burg, E.D., Remillard, C. V, and Yuan, J.X.-J. (2008). Potassium channels in the regulation of pulmonary artery smooth muscle cell proliferation and apoptosis: pharmacotherapeutic implications. British Journal of Pharmacology *153 Suppl* , S99–S111.

Busch, A.E., Suessbrich, H., Waldegger, S., Sailer, E., Greger, R., Lang, H., Lang, F., Gibson, K.J., and Maylie, J.G. (1996). Inhibition of I_{Ks} in guinea pig cardiac myocytes and guinea pig IsK channels by the chromanol 293B. Pflügers Archiv: European Journal of Physiology *432*, 1094–1096.

Cai, S.-Q., Park, K.H., and Sesti, F. (2006). An evolutionarily conserved family of accessory subunits of K^+ channels. Cell Biochemistry and Biophysics *46*, 91–99.

Carstairs, J.R., Nimmo, A.J., and Barnes, P.J. (1985). Autoradiographic visualization of beta-adrenoceptor subtypes in human lung. The American Review of Respiratory Disease *132*, 541–547.

Casteels, R., Kitamura, K., Kuriyama, H., and Suzuki, H. (1977a). Excitation-contraction coupling in the smooth muscle cells of the rabbit main pulmonary artery. The Journal of Physiology *271*, 63–79.

Casteels, R., Kitamura, K., Kuriyama, H., and Suzuki, H. (1977b). The membrane properties of the smooth muscle cells of the rabbit main pulmonary artery. The Journal of Physiology *271*, 41–61.

Cernacek, P., and Stewart, D.J. (1989). Immunoreactive endothelin in human plasma: marked elevations in patients in cardiogenic shock. Biochemical and Biophysical Research Communications *161*, 562–567.

Chadha, P.S., Jepps, T.A., Carr, G., Stott, J.B., Zhu, H.-L., Cole, W.C., and Greenwood, I.A. (2014). Contribution of kv7.4/kv7.5 heteromers to intrinsic and calcitonin gene-related peptide-induced cerebral reactivity. Arteriosclerosis, Thrombosis, and Vascular Biology. 34, 887–893

Chadha, P.S., Zunke, F., Zhu, H.-L., Davis, A.J., Jepps, T.A., Olesen, S.P., Cole, W.C., Moffatt, J.D., and Greenwood, I.A. (2012). Reduced *KCNQ4*-encoded voltage-dependent potassium channel activity underlies impaired β-adrenoceptor-mediated relaxation of renal arteries in hypertension. Hypertension *59*, 877–884.

Chalmers, S., Olson, M.L., MacMillan, D., Rainbow, R.D., and McCarron, J.G. (2007). Ion channels in smooth muscle: regulation by the sarcoplasmic reticulum and mitochondria. Cell Calcium *42*, 447–466.

Chao, T.S., Byron, K.L., Lee, K.M., Villereal, M., and Rosner, M.R. (1992). Activation of MAP kinases by calcium-dependent and calcium-independent pathways. Stimulation by thapsigargin and epidermal growth factor. The Journal of Biological Chemistry *267*, 19876–19883.

Charpentier, F., Mérot, J., Loussouarn, G., and Baró, I. (2010). Delayed rectifier K^+ currents and cardiac repolarization. Journal of Molecular and Cellular Cardiology *48*, 37–44.

Chen, S.J., Chen, Y.F., Meng, Q.C., Durand, J., Dicarlo, V.S., and Oparil, S. (1995). Endothelin-receptor antagonist bosentan prevents and reverses hypoxic pulmonary hypertension in rats. Journal of Applied Physiology *79*, 2122–2131.

Cheong, A., Wood, I.C., and Beech, D.J. (2006). Less REST, more vascular disease? Regulation of cell cycle and migration of vascular smooth muscle cells. Cell Cycle *5*, 129–131.

Choby, C., Mangoni, M.E., Boccara, G., Nargeot, J., and Richard, S. (2000). Evidence for tetrodotoxin-sensitive sodium currents in primary cultured myocytes from human, pig and rabbit arteries. Pflügers Archiv : European Journal of Physiology *440*, 149–152.

Christman, B.W., McPherson, C.D., Newman, J.H., King, G.A., Bernard, G.R., Groves, B.M., and Loyd, J.E. (1992). An imbalance between the excretion of thromboxane and prostacyclin metabolites in pulmonary hypertension. The New England Journal of Medicine *327*, 70–75.

Cidad, P., Jiménez-Pérez, L., García-Arribas, D., Miguel-Velado, E., Tajada, S., Ruiz-McDavitt, C., López-López, J.R., and Pérez-García, M.T. (2012). Kv1.3 channels can modulate cell proliferation during phenotypic switch by an ion-flux independent mechanism. Arteriosclerosis, Thrombosis, and Vascular Biology *32*, 1299–1307.

Clapp, L.H., and Gurney, A.M. (1991a). Outward currents in rabbit pulmonary artery cells dissociated with a new technique. Experimental Physiology *76*, 677–693.

Clapp, L.H., and Gurney, A.M. (1991b). Modulation of calcium movements by nitroprusside in isolated vascular smooth muscle cells. Pflügers Archiv: European Journal of Physiology *418*, 462–470.

Clapp, L.H., and Gurney, A.M. (1992). ATP-sensitive K^+ channels regulate resting potential of pulmonary arterial smooth muscle cells. The American Journal of Physiology *262*, H916–20.

Clapp, L.H., Davey, R., and Gurney, A.M. (1993). ATP-sensitive K^+ channels mediate vasodilation produced by lemakalim in rabbit pulmonary artery. The American Journal of Physiology *264*, H1907–15.

Clapp, L.H., Finney, P., Turcato, S., Tran, S., Rubin, L.J., and Tinker, A. (2002). Differential effects of stable prostacyclin analogs on smooth muscle proliferation and cyclic AMP generation in human pulmonary artery. American Journal of Respiratory Cell and Molecular Biology *26*, 194–201.

Coetzee, W.A., Amarillo, Y., Chiu, J., Chow, A., Lau, D., McCormack, T., Moreno, H., Nadal, M.S., Ozaita, A., Pountney, D., Saganich, M., Vega-Saenz de Miera E., Rudy B. (1999). Molecular diversity of K^+ channels. Annals of the New York Academy of Sciences *868*, 233–285.

Coleman, R.A., Smith, W.L., and Narumiya, S. (1994). International Union of Pharmacology classification of prostanoid receptors: properties, distribution, and structure of the receptors and their subtypes. Pharmacological Reviews *46*, 205–229.

Constanti, A., and Brown, D.A. (1981). M-Currents in voltage-clamped mammalian sympathetic neurones. Neuroscience Letters *24*, 289–294.

Cook, L., Nickolson, V.J., Steinfels, G.F., Rohrbach, K.W., Denoble, V.J. (1990) .Cognition enhancement by the acetylcholine releaser DuP 996. *19*, 301-314.

Corbin, J.D., Beasley, A., Blount, M.A., and Francis, S.H. (2005). High lung PDE5: a strong basis for treating pulmonary hypertension with PDE5 inhibitors. Biochemical and Biophysical Research Communications *334*, 930–938.

Cornfield, D.N., Stevens, T., McMurtry, I.F., Abman, S.H., and Rodman, D.M. (1993). Acute hypoxia increases cytosolic calcium in fetal pulmonary artery smooth muscle cells. The American Journal of Physiology *265*, L53–6.

Costa, A.M., and Brown, B.S. 1997. Inhibition of M-current in cultured rat superior cervical ganglia by linopirdine: mechanism of action studies. Neuropharmacology *36*, 1747–1753.

Cui, Y., Tran, S., Tinker, A., and Clapp, L.H. (2002). The molecular composition of K(ATP) channels in human pulmonary artery smooth muscle cells and their modulation by growth. American Journal of Respiratory Cell and Molecular Biology *26*, 135–143.

D'Alonzo, G.E., Barst, R.J., Ayres, S.M., Bergofsky, E.H., Brundage, B.H., Detre, K.M., Fishman, A.P., Goldring, R.M., Groves, B.M., and Kernis, J.T. (1991). Survival in patients with primary pulmonary hypertension. Results from a national prospective registry. Annals of Internal Medicine *115*, 343–349.

Dalle Lucca, S.L., Dalle Lucca, J.J., Borges, A.C., Ihara, S.S., and Paiva, T.B. (2000). Abnormal proliferative response of the carotid artery of spontaneously hypertensive rats after angioplasty may be related to the depolarized state of its smooth muscle cells. Brazilian Journal of Medical and Biological Research *33*, 919–927.

Davie, N., Haleen, S.J., Upton, P.D., Polak, J.M., Yacoub, M.H., Morrell, N.W., and Wharton, J. (2002). ET_A and ET_B receptors modulate the proliferation of human pulmonary artery smooth muscle cells. American Journal of Respiratory and Critical Care Medicine *165*, 398–405.

Davies, A.R., and Kozlowski, R.Z. (2001). K_V channel subunit expression in rat pulmonary arteries. Lung *179*, 147–161.

Day, R.M., Agyeman, A.S., Segel, M.J., Chévere, R.D., Angelosanto, J.M., Suzuki, Y.J., and Fanburg, B.L. (2006). Serotonin induces pulmonary artery smooth muscle cell migration. Biochemical Pharmacology *71*, 386–397.

Deeks, E.D. (2011). Retigabine (ezogabine): in partial-onset seizures in adults with epilepsy. CNS Drugs *25*, 887–900.

Demiryurek, A.T., Wadsworth, R.M., and Kane, K.A. (1991). Effects of hypoxia on isolated intrapulmonary arteries from the sheep. Pulmonary Pharmacology *4*, 158–164.

Devulder, J. (2010). Flupirtine in pain management: pharmacological properties and clinical use. CNS Drugs *24*, 867–881.

Dheda, K., Huggett, J.F., Bustin, S.A., Johnson, M.A., Rook, G., and Zumla, A. (2004). Validation of housekeeping genes for normalizing RNA expression in real-time PCR. BioTechniques *37*, 112–114, 116, 118–119.

Doi, S., Damron, D.S., Horibe, M., and Murray, P.A. (2000). Capacitative Ca^{2+} entry and tyrosine kinase activation in canine pulmonary arterial smooth muscle cells. American Journal of Physiology- Lung Cellular and Molecular Physiology *278*, L118–30.

Dong, M.-Q., Lau, C.-P., Gao, Z., Tseng, G.-N., and Li, G.-R. (2006). Characterization of recombinant human cardiac KCNQ1/KCNE1 channels (I (Ks)) stably expressed in HEK 293 cells. The Journal of Membrane Biology *210*, 183–192.

Ducret, T., El Arrouchi, J., Courtois, A., Quignard, J.-F., Marthan, R., and Savineau, J.-P. (2010). Stretch-activated channels in pulmonary arterial smooth muscle cells from normoxic and chronically hypoxic rats. Cell Calcium *48*, 251–259.

Duggal, P., Vesely, M.R., Wattanasirichaigoon, D., Villafane, J., Kaushik, V., and Beggs, A.H. (1998). Mutation of the gene for IsK associated with both Jervell and Lange-Nielsen and Romano-Ward forms of Long-QT syndrome. Circulation *97*, 142–146.

Dumas, J.P., Bardou, M., Goirand, F., and Dumas, M. (1999). Hypoxic pulmonary vasoconstriction. General Pharmacology *33*, 289–297.

Duprat, F., Lesage, F., Fink, M., Reyes, R., Heurteaux, C., and Lazdunski, M. (1997). TASK, a human background K^+ channel to sense external pH variations near physiological pH. The EMBO Journal *16*, 5464–5471.

Dupuis, D.S., Schrøder, R.L., Jespersen, T., Christensen, J.K., Christophersen, P., Jensen, B.S., and Olesen, S.P. (2002). Activation of KCNQ5 channels stably expressed in HEK293 cells by BMS-204352. European Journal of Pharmacology *437*, 129–137.

Durmowicz, A.G., Frid, M.G., Wohrley, J.D., and Stenmark, K.R. (1996). Expression and localization of tropoelastin mRNA in the developing bovine pulmonary artery is dependent on vascular cell phenotype. American Journal of Respiratory Cell and Molecular Biology *14*, 569–576.

Dzhura, E. V, He, W., and Currie, K.P.M. (2006). Linopirdine modulates calcium signaling and stimulus-secretion coupling in adrenal chromaffin cells by targeting M-type K^+ channels and nicotinic acetylcholine receptors. The Journal of Pharmacology and Experimental Therapeutics *316*, 1165–1174.

Eddahibi, S., Raffestin, B., Braquet, P., Chabrier, P.E., and Adnot, S. (1991). Pulmonary vascular reactivity to endothelin-1 in normal and chronically pulmonary hypertensive rats. Journal of Cardiovascular Pharmacology *17 Suppl 7*, S358–61.

Ellis, F.H., Grindlay, J.H., and Edwards, J.E. (1952). The bronchial arteries. III. Structural changes after division of the rat's left pulmonary artery. The American Journal of Pathology *28*, 89–103.

Enyedi, P., and Czirják, G. (2010). Molecular background of leak K^+ currents: two-pore domain potassium channels. Physiological Reviews. *90*, 559–605.

Eskesen, K., János, T., Tibor, H., Délia, S., László, V., and Edvinsson, L. (2007). Unaltered mRNA expression of calcitonin-like receptor and receptor activity modifying proteins in human arteries in stroke and myocardial infarction. Ideggyógyászati Szemle *60*, 459–466.

Evans, A., Osipenko, O., and Gurney, A. (1996). Properties of a novel K^+ current that is active at resting potential in rabbit pulmonary artery smooth muscle cells. The Journal of Physiology *496*, 407.

Evans, A.M., Osipenko, O.N., Haworth, S.G., and Gurney, A.M. (1998). Resting potentials and potassium currents during development of pulmonary artery smooth muscle cells. The American Journal of Physiology *275*, H887–99.

Falcetti, E., Hall, S.M., Phillips, P.G., Patel, J., Morrell, N.W., Haworth, S.G., and Clapp, L.H. (2010). Smooth muscle proliferation and role of the prostacyclin (IP) receptor in idiopathic pulmonary arterial hypertension. American Journal of Respiratory and Critical Care Medicine *182*, 1161–1170.

Felipe, A., Vicente, R., Villalonga, N., Roura-Ferrer, M., Martínez-Mármol, R., Solé, L., Ferreres, J.C., and Condom, E. (2006). Potassium channels: new targets in cancer therapy. Cancer Detection and Prevention *30*, 375–385.

Feng, X., Cai, Y., Dawes, K.E., and Laurent, G.J. (1996). Endothelin-1 induces chemotaxis of pulmonary artery smooth muscle cells. Zhongguo Yi Xue Ke Xue Yuan Xue Bao. Acta Academiae Medicinae Sinicae *18*, 338–342.

Finley, M.R., Li, Y., Hua, F., Lillich, J., Mitchell, K.E., Ganta, S., Gilmour, R.F., and Freeman, L.C. (2002). Expression and coassociation of ERG1, KCNQ1, and KCNE1 potassium channel proteins in horse heart. American Journal of Physiology. Heart and Circulatory Physiology *283*, H126–38.

Firth, A.L., Remillard, C. V, Platoshyn, O., Fantozzi, I., Ko, E.A., and Yuan, J.X.-J. (2011). Functional ion channels in human pulmonary artery smooth muscle cells: Voltage-dependent cation channels. Pulmonary Circulation *1*, 48–71.

Fleige, S., and Pfaffl, M.W. (2006). RNA integrity and the effect on the real-time qRT-PCR performance. Molecular Aspects of Medicine *27*, 126–139.

Fleige, S., Walf, V., Huch, S., Prgomet, C., Sehm, J., and Pfaffl, M.W. (2006). Comparison of relative mRNA quantification models and the impact of RNA integrity in quantitative real-time RT-PCR. Biotechnology Letters *28*, 1601–1613.

Foss, D.L., Baarsch, M.J., and Murtaugh, M.P. (1998). Regulation of hypoxanthine phosphoribosyltransferase, glyceraldehyde-3-phosphate dehydrogenase and beta-actin mRNA expression in porcine immune cells and tissues. Animal Biotechnology *9*, 67–78.

Freeman, W.K., Rorie, D.K., and Tyce, G.M. (1981). Effects of 5-hydroxytryptamine on neuroeffector junction in human pulmonary artery. Journal of Applied Physiology: Respiratory, Environmental and Exercise Physiology *51*, 693–698.

French, J.A., Abou-Khalil, B.W., Leroy, R.F., Yacubian, E.M.T., Shin, P., Hall, S., Mansbach, H., and Nohria, V. (2011). Randomized, double-blind, placebo-controlled trial of ezogabine (retigabine) in partial epilepsy. Neurology *76*, 1555–1563.

Frid, M.G., Printesva, O.Y., Chiavegato, A., Faggin, E., Scatena, M., Koteliansky, V.E., Pauletto, P., Glukhova, M.A., and Sartore, S. (1993). Myosin heavy-chain isoform composition and distribution in developing and adult human aortic smooth muscle. Journal of Vascular Research *30*, 279–292.

Frid, M.G., Moiseeva, E.P., and Stenmark, K.R. (1994). Multiple phenotypically distinct smooth muscle cell populations exist in the adult and developing bovine pulmonary arterial media in vivo. Circulation Research *75*, 669–681.

Frid, M.G., Aldashev, A.A., Dempsey, E.C., and Stenmark, K.R. (1997). Smooth muscle cells isolated from discrete compartments of the mature vascular media exhibit unique phenotypes and distinct growth capabilities. Circulation Research *81*, 940–952.

Fröhlich, H., Boini, K.M., Seebohm, G., Strutz-Seebohm, N., Ureche, O.N., Föller, M., Eichenmüller, M., Shumilina, E., Pathare, G., Singh, A.K., et al. (2011). Hypothyroidism of gene-targeted mice lacking KCNQ1. Pflügers Archiv : European Journal of Physiology *461*, 45–52.

Fukuroda, T., Kobayashi, M., Ozaki, S., Yano, M., Miyauchi, T., Onizuka, M., Sugishita, Y., Goto, K., and Nishikibe, M. (1994). Endothelin receptor subtypes in human versus rabbit pulmonary arteries. Journal of Applied Physiology *76*, 1976–1982.

Gaine, S.P., and Rubin, L.J. (1998). Primary pulmonary hypertension. Lancet *352*, 719–725.

Galiè, N., Ghofrani, H.A., Torbicki, A., Barst, R.J., Rubin, L.J., Badesch, D., Fleming, T., Parpia, T., Burgess, G., Branzi, A., et al. (2005). Sildenafil citrate therapy for pulmonary arterial hypertension. The New England Journal of Medicine *353*, 2148–2157.

Galiè, N., Hoeper, M.M., Humbert, M., Torbicki, A., Vachiery, J.-L., Barbera, J.A., Beghetti, M., Corris, P., Gaine, S., Gibbs, J.S., et al. (2009a). Guidelines for the diagnosis and treatment of pulmonary hypertension: the Task Force for the Diagnosis and Treatment of Pulmonary Hypertension of the European Society of Cardiology (ESC) and the European Respiratory Society (ERS), endorsed by the International Society of Heart and Lung Transplantation (ISHLT). European Heart Journal *30*, 2493–2537.

Galiè, N., Hoeper, M.M., Humbert, M., Torbicki, A., Vachiery, J.-L., Barbera, J.A., Beghetti, M., Corris, P., Gaine, S., Gibbs, J.S., et al. (2009b). Guidelines for the diagnosis and treatment of pulmonary hypertension. European Respiratory Journal. *34*, 1219–1263.

Gao, Z., Xiong, Q., Sun, H., and Li, M. (2008). Desensitization of chemical activation by auxiliary subunits: convergence of molecular determinants critical for augmenting KCNQ1 potassium channels. The Journal of Biological Chemistry *283*, 22649–22658.

Gardener, M.J., Johnson, I.T., Burnham, M.P., Edwards, G., Heagerty, A.M., and Weston, A.H. (2004). Functional evidence of a role for two-pore domain potassium channels in rat mesenteric and pulmonary arteries. British Journal of Pharmacology *142*, 192–202.

Geraci, M.W., Gao, B., Shepherd, D.C., Moore, M.D., Westcott, J.Y., Fagan, K.A., Alger, L.A., Tuder, R.M., and Voelkel, N.F. (1999). Pulmonary prostacyclin synthase overexpression in transgenic mice protects against development of hypoxic pulmonary hypertension. The Journal of Clinical Investigation *103*, 1509–1515.

Gerthoffer, W.T. (2007). Mechanisms of vascular smooth muscle cell migration. Circulation Research *100*, 607–621.

Ghofrani, H.A., Wiedemann, R., Rose, F., Olschewski, H., Schermuly, R.T., Weissmann, N., Seeger, W., and Grimminger, F. (2002). Combination therapy with oral sildenafil and inhaled iloprost for severe pulmonary hypertension. Annals of Internal Medicine *136*, 515–522.

Giaid, A., and Saleh, D. (1995). Reduced expression of endothelial nitric oxide synthase in the lungs of patients with pulmonary hypertension. The New England Journal of Medicine *333*, 214–221.

Giuriato, L., Scatena, M., Chiavegato, A., Tonello, M., Scannapieco, G., Pauletto, P., and Sartore, S. (1992). Non-muscle myosin isoforms and cell heterogeneity in developing rabbit vascular smooth muscle. Journal of Cell Science *101 (Pt 1*): 233–246.

Glare, E.M., Divjak, M., Bailey, M.J., and Walters, E.H. (2002). beta-Actin and GAPDH housekeeping gene expression in asthmatic airways is variable and not suitable for normalising mRNA levels. Thorax *57*, 765–770.

Gofman, Y., Shats, S., Attali, B., Haliloglu, T., and Ben-Tal, N. (2012). How does KCNE1 regulate the K_V7.1 potassium channel? Model-structure, mutations, and dynamics of the K_V7.1-KCNE1 complex. Structure *20*, 1343–1352.

Golovina, V.A. (1999). Cell proliferation is associated with enhanced capacitative Ca^{2+} entry in human arterial myocytes. The American Journal of Physiology *277*, C343–9.

Goncharova, E.A., Lim, P., Goncharov, D.A., Eszterhas, A., Panettieri, R.A., and Krymskaya, V.P. (2006). Assays for in vitro monitoring of proliferation of human airway smooth muscle (ASM) and human pulmonary arterial vascular smooth muscle (VSM) cells. Nature Protocols *1*, 2905–2908.

Gönczi, M., Szentandrássy, N., Johnson, I.T., Heagerty, A.M., and Weston, A.H. (2006). Investigation of the role of TASK-2 channels in rat pulmonary arteries; pharmacological and functional studies following RNA interference procedures. British Journal of Pharmacology *147*, 496–505.

González, C., Baez-Nieto, D., Valencia, I., Oyarzún, I., Rojas, P., Naranjo, D., and Latorre, R. (2012). K^+ channels: function-structural overview. Comprehensive Physiology. *2*, 2087–2149.

Goto, K., Kasuya, Y., Matsuki, N., Takuwa, Y., Kurihara, H., Ishikawa, T., Kimura, S., Yanagisawa, M., and Masaki, T. (1989). Endothelin activates the dihydropyridine-sensitive, voltage-dependent Ca^{2+} channel in vascular smooth muscle. PNAS *86*, 3915–3918.

Greenwood, I.A., and Ohya, S. (2009). New tricks for old dogs: KCNQ expression and role in smooth muscle. British Journal of Pharmacology *156*, 1196–1203.

Greenwood, I.A., Yeung, S., Schwake, M., and Pucovský, V. (2008). Bimodal effects of the K_V7 channel activator retigabine on vascular K^+ currents. British Journal of Pharmacology *155*, 62–72.

Gruetter, C.A., Ignarro, L.J., Hyman, A.L., and Kadowitz, P.J. (1981). Contractile effects of 5-hydroxytryptamine in isolated intrapulmonary arteries and veins. Canadian Journal of Physiology and Pharmacology *59*, 157–162.

Grunnet, M., Jespersen, T., Rasmussen, H.B., Ljungstrøm, T., Jorgensen, N.K., Olesen, S.-P., and Klaerke, D.A. (2002). KCNE4 is an inhibitory subunit to the KCNQ1 channel. The Journal of Physiology *542*, 119–130.

Grunnet, M., Olesen, S.-P., Klaerke, D.A., and Jespersen, T. (2005). hKCNE4 inhibits the hKCNQ1 potassium current without affecting the activation kinetics. Biochemical and Biophysical Research Communications *328*, 1146–1153.

Guibert, C., Marthan, R., and Savineau, J.P. (1996). Angiotensin II-induced Ca^{2+}-oscillations in vascular myocytes from the rat pulmonary artery. The American Journal of Physiology *270*, L637–42.

Guibert, C., Ducret, T., and Savineau, J.-P. (2008). Voltage-independent calcium influx in smooth muscle. Progress in Biophysics and Molecular Biology *98*, 10–23.

Gunthorpe, M.J., Large, C.H., and Sankar, R. (2012). The mechanism of action of retigabine (ezogabine), a first-in-class K+ channel opener for the treatment of epilepsy. Epilepsia *53*, 412–424.

Gümüşel, B., Orhan, D., Tolunay, O., and Uma, S. (2001). The role of nitric oxide in mediating nonadrenergic, noncholinergic relaxation in rat pulmonary artery. Nitric Oxide , 296–301.

Gurney, A.M. (2002). Multiple sites of oxygen sensing and their contributions to hypoxic pulmonary vasoconstriction. Respiratory Physiology & Neurobiology *132*, 43–53.

Gurney, A.M., and Allam, M. (1995). Inhibition of calcium release from the sarcoplasmic reticulum of rabbit aorta by hydralazine. British Journal of Pharmacology *114*, 238–244.

Gurney, A.M., and Joshi, S. (2006). The role of twin pore domain and other K^+ channels in hypoxic pulmonary vasoconstriction. Novartis Foundation Symposium *272*, 218–28; discussion 228–33, 274–9.

Gurney, A.M., Osipenko, O.N., MacMillan, D., and Kempsill, F.E.J. (2002). Potassium channels underlying the resting potential of pulmonary artery smooth muscle cells. Clinical and Experimental Pharmacology & Physiology *29*, 330–333.

Gurney, A.M., Osipenko, O.N., MacMillan, D., McFarlane, K.M., Tate, R.J., and Kempsill, F.E.J. (2003). Two-pore domain K channel, TASK-1, in pulmonary artery smooth muscle cells. Circulation Research *93*, 957–964.

Gurney, A.M., Joshi, S., and Manoury, B. (2010). KCNQ potassium channels: new targets for pulmonary vasodilator drugs? Advances in Experimental Medicine and Biology *661*, 405–417.

Hadley, J.K., Noda, M., Selyanko, A.A., Wood, I.C., Abogadie, F.C., and Brown, D.A. (2000). Differential tetraethylammonium sensitivity of KCNQ1-4 potassium channels. British Journal of Pharmacology *129*, 413–415.

Haitin, Y., and Attali, B. (2008). The C-terminus of K_V7 channels: a multifunctional module. The Journal of Physiology *586*, 1803–1810.

Hall, S.M., Davie, N., Klein, N., and Haworth, S.G. (2011). Endothelin receptor expression in idiopathic pulmonary arterial hypertension: effect of bosentan and epoprostenol treatment. European Respiratory Journal. *38*, 851–860.

Hamada, H., Damron, D.S., Hong, S.J., Van Wagoner, D.R., and Murray, P.A. (1997). Phenylephrine-induced Ca^{2+} oscillations in canine pulmonary artery smooth muscle cells. Circulation Research *81*, 812–823.

Hamilton, T.C., and Weston, A.H. (1989). Cromakalim, nicorandil and pinacidil: novel drugs which open potassium channels in smooth muscle. General Pharmacology *20*, 1–9.

Heitzmann, D., and Warth, R. (2007). No potassium, no acid: K^+ channels and gastric acid secretion. Physiology *22*, 335–341.

Hering, S., Hughes, A.D., Timin, E.N., and Bolton, T.B. (1993). Modulation of calcium channels in arterial smooth muscle cells by dihydropyridine enantiomers. The Journal of General Physiology *101*, 393–410.

Hermann, R., Knebel, N.G., Niebch, G., Richards, L., Borlak, J., and Locher, M. (2003). Pharmacokinetic interaction between retigabine and lamotrigine in healthy subjects. European Journal of Clinical Pharmacology *58*, 795–802.

Herner, S.J., and Mauro, L.S. (1999). Epoprostenol in primary pulmonary hypertension. The Annals of Pharmacotherapy *33*, 340–347.

Higenbottam, T., Wheeldon, D., Wells, F., and Wallwork, J. (1984). Long-term treatment of primary pulmonary hypertension with continuous intravenous epoprostenol (prostacyclin). Lancet *1*, 1046–1047.

Hillier, S.C., Graham, J.A., Hanger, C.C., Godbey, P.S., Glenny, R.W., and Wagner, W.W. (1997). Hypoxic vasoconstriction in pulmonary arterioles and venules. Journal of Applied Physiology *82*, 1084–1090.

Hirata, Y., Emori, T., Eguchi, S., Kanno, K., Imai, T., Ohta, K., and Marumo, F. (1993). Endothelin receptor subtype B mediates synthesis of nitric oxide by cultured bovine endothelial cells. The Journal of Clinical Investigation *91*, 1367–1373.

Hislop, A., and Reid, L. (1978). Normal structure and dimensions of the pulmonary arteries in the rat. Journal of Anatomy *125*, 71–83.

Holden, W.E., and McCall, E. (1984). Hypoxia-induced contractions of porcine pulmonary artery strips depend on intact endothelium. Experimental Lung Research *7*, 101–112.

Holzmann, S., Kukovetz, W.R., and Schmidt, K. (1980). Mode of action of coronary arterial relaxation by prostacyclin. Journal of Cyclic Nucleotide Research *6*, 451–460.

Hong, Z., Weir, E.K., Nelson, D.P., and Olschewski, A. (2004). Subacute hypoxia decreases voltage-activated potassium channel expression and function in pulmonary artery myocytes. American Journal of Respiratory Cell and Molecular Biology *31*, 337–343.

Hong, Z., Weir, E.K., Varghese, A., and Olschewski, A. (2005). Effect of normoxia and hypoxia on K^+ current and resting membrane potential of fetal rabbit pulmonary artery smooth muscle. Physiological Research *54*, 175–184.

Houghton, J., and Phillips, E.M. (1973). The pharmacology of human isolated pulmonary vascular tissue. British Journal of Pharmacology *47*, 676P–677P.

Housley, G.D., and Ashmore, J.F. (1992). Ionic currents of outer hair cells isolated from the guinea-pig cochlea. The Journal of Physiology *448*, 73–98.

Howard, R.J., Clark, K.A., Holton, J.M., and Minor, D.L. (2007). Structural insight into KCNQ (K_V7) channel assembly and channelopathy. Neuron *53*, 663–675.

Hulme, J.T., Coppock, E.A., Felipe, A., Martens, J.R., and Tamkun, M.M. (1999). Oxygen sensitivity of cloned voltage-gated K^+ channels expressed in the pulmonary vasculature. Circulation Research *85*, 489–497.

Humbert, M., Sitbon, O., Chaouat, A., Bertocchi, M., Habib, G., Gressin, V., Yaici, A., Weitzenblum, E., Cordier, J.-F., Chabot, F., Dromer, C., Pison, C., Reynaud-Gaubert, M., Haloun, A., Laurent, M., Hachulla, E., Simonneau, G. (2006). Pulmonary arterial hypertension in France: results from a national registry. American Journal of Respiratory and Critical Care Medicine *173*, 1023–1030.

Iannotti, F.A., Panza, E., Barrese, V., Viggiano, D., Soldovieri, M.V., and Taglialatela, M. (2010). Expression, localization, and pharmacological role of K_V7 potassium channels in skeletal muscle proliferation, differentiation, and survival after myotoxic insults. The Journal of Pharmacology and Experimental Therapeutics *332*, 811–820.

Ichida, F., Uese, K., Tsubata, S., Hashimoto, I., Hamamichi, Y., Fukahara, K., Murakami, A., and Miyawaki, T. (1997). Additive effect of beraprost on pulmonary vasodilation by inhaled nitric oxide in children with pulmonary hypertension. The American Journal of Cardiology *80*, 662–664.

Ignarro, L.J., Byrns, R.E., Buga, G.M., and Wood, K.S. (1987). Endothelium-derived relaxing factor from pulmonary artery and vein possesses pharmacologic and chemical properties identical to those of nitric oxide radical. Circulation Research *61*, 866–879.

Ikeda, T., Nakamura, K., Akagi, S., Kusano, K.F., Matsubara, H., Fujio, H., Ogawa, A., Miura, A., Miura, D., Oto, T., Yamanaka, R., Otsuka, F., Date, H., Ohe, T., Ito, H. (2010). Inhibitory effects of simvastatin on platelet-derived growth factor signaling in pulmonary artery smooth muscle cells from patients with idiopathic pulmonary arterial hypertension. Journal of Cardiovascular Pharmacology *55*, 39–48.

Imbeaud, S., Graudens, E., Boulanger, V., Barlet, X., Zaborski, P., Eveno, E., Mueller, O., Schroeder, A., and Auffray, C. (2005). Towards standardization of RNA quality assessment using user-independent classifiers of microcapillary electrophoresis traces. Nucleic Acids Research *33*, e56.

Jabr, R.I., Toland, H., Gelband, C.H., Wang, X.X., and Hume, J.R. (1997). Prominent role of intracellular Ca^{2+} release in hypoxic vasoconstriction of canine pulmonary artery. British Journal of Pharmacology *122*, 21–30.

James, A.F., Okada, T., and Horie, M. (1995). A fast transient outward current in cultured cells from human pulmonary artery smooth muscle. The American Journal of Physiology *268*, H2358–65.

Janiak, R., Wilson, S.M., Montague, S., and Hume, J.R. (2001). Heterogeneity of calcium stores and elementary release events in canine pulmonary arterial smooth muscle cells. American Journal of Physiology- Cell Physiology *280*, C22–33.

Jasmin, J.F., Lucas, M., Cernacek, P., and Dupuis, J. (2001). Effectiveness of a nonselective ET(A/B) and a selective ET_A antagonist in rats with monocrotaline-induced pulmonary hypertension. Circulation *103*, 314–318.

Jenkinson, D.H. (2006). Potassium channels--multiplicity and challenges. British Journal of Pharmacology *147 Suppl* , S63–71.

Jensen, H.S., Callø, K., Jespersen, T., Jensen, B.S., and Olesen, S.-P. (2005). The KCNQ5 potassium channel from mouse: a broadly expressed M-current like potassium channel modulated by zinc, pH, and volume changes. Brain Research. Molecular Brain Research *139*, 52–62.

Jeong, I., Choi, B.H., and Hahn, S.J. (2013). Pergolide block of the cloned K_V1.5 potassium channels. Naunyn-Schmiedeberg's Archives of Pharmacology *386*, 125–133.

Jepps, T.A., Greenwood, I.A., Moffatt, J.D., Sanders, K.M., and Ohya, S. (2009). Molecular and functional characterization of K_V7 K^+ channel in murine gastrointestinal smooth muscles. American Journal of Physiology. Gastrointestinal and Liver Physiology *297*, G107–15.

Jepps, T.A., Chadha, P.S., Davis, A.J., Harhun, M.I., Cockerill, G.W., Olesen, S.P., Hansen, R.S., and Greenwood, I.A. (2011). Downregulation of K_V7.4 channel activity in primary and secondary hypertension. Circulation *124*, 602–611.

Jiang, Z., Wallner, M., Meera, P., and Toro, L. (1999). Human and rodent MaxiK channel beta-subunit genes: cloning and characterization. Genomics *55*, 57–67.

Jin, N., Packer, C.S., and Rhoades, R.A. (1992). Pulmonary arterial hypoxic contraction: signal transduction. The American Journal of Physiology *263*, L73–8.

Jindal, H.K., Folco, E.J., Liu, G.X., and Koren, G. (2008). Posttranslational modification of voltage-dependent potassium channel K_V1.5: COOH-terminal palmitoylation modulates its biological properties. American Journal of Physiology. Heart and Circulatory Physiology *294*, H2012–21.

Jones, P.L., Cowan, K.N., and Rabinovitch, M. (1997). Tenascin-C, proliferation and subendothelial fibronectin in progressive pulmonary vascular disease. The American Journal of Pathology *150*, 1349–1360.

Joshi, S., Balan, P., and Gurney, A.M. (2006). Pulmonary vasoconstrictor action of KCNQ potassium channel blockers. Respiratory Research *7*, 31.

Joshi, S., Sedivy, V., Hodyc, D., Herget, J., and Gurney, A.M. (2009). KCNQ modulators reveal a key role for KCNQ potassium channels in regulating the tone of rat pulmonary artery smooth muscle. The Journal of Pharmacology and Experimental Therapeutics *329*, 368–376.

Kang, T.M., Park, M.K., and Uhm, D.-Y. (2003). Effects of hypoxia and mitochondrial inhibition on the capacitative calcium entry in rabbit pulmonary arterial smooth muscle cells. Life Sciences *72*, 1467–1479.

Karamsetty, M.R., Klinger, J.R., and Hill, N.S. (2001). Phytoestrogens restore nitric oxide-mediated relaxation in isolated pulmonary arteries from chronically hypoxic rats. Journal of Pharmacology and Experimental Therapeutics. *297*, 968–974.

Kaukinen, S., Ylitalo, P., Pessi, T., and Vapaatalo, H. (1984). Hemodynamic effects of iloprost, a prostacyclin analog. Clinical Pharmacology and Therapeutics *36*, 464–469.

Kemp, B.K., Smolich, J.J., Ritchie, B.C., and Cocks, T.M. (1995). Endothelium-dependent relaxations in sheep pulmonary arteries and veins: resistance to block by NG-nitro-L-arginine in pulmonary hypertension. British Journal of Pharmacology *116*, 2457–2467.

Kharkovets, T., Hardelin, J.P., Safieddine, S., Schweizer, M., El-Amraoui, A., Petit, C., and Jentsch, T.J. (2000). KCNQ4, a K^+ channel mutated in a form of dominant deafness, is expressed in the inner ear and the central auditory pathway. PNAS *97*, 4333–4338.

Kim, S.J., and Greger, R. (1999). Voltage-dependent, slowly activating K^+ current (I_{Ks}) and its augmentation by carbachol in rat pancreatic acini. Pflügers Archiv: European Journal of Physiology *438*, 604–611.

Kim, C.H., Kim, J.H., Moon, S.J., Chung, K.C., Hsu, C.Y., Seo, J.T., and Ahn, Y.S. (1999). Pyrithione, a zinc ionophore, inhibits NF-kappaB activation. Biochem. Biochemical and Biophysical Research Communications. *259*, 505–509.

Kinoshita, H., Azma, T., Nakahata, K., Iranami, H., Kimoto, Y., Dojo, M., Yuge, O., and Hatano, Y. (2004). Inhibitory effect of high concentration of glucose on relaxations to activation of ATP-sensitive K+ channels in human omental artery. Arterioscler. Thromb. Vasc. Biol. 24, 2290–2295.

Kirber, M.T., Ordway, R.W., Clapp, L.H., Walsh, J. V, and Singer, J.J. (1992). Both membrane stretch and fatty acids directly activate large conductance Ca^{2+}-activated K^+ channels in vascular smooth muscle cells. FEBS letters. 297, 24–28.

Klinger, F., Geier, P., Dorostkar, M.M., Chandaka, G.K., Yousuf, A., Salzer, I., Kubista, H., and Boehm, S. (2012). Concomitant facilitation of GABAA receptors and K_V7 channels by the non-opioid analgesic flupirtine. British Journal of Pharmacology *166*, 1631–1642.

Klinger, J.R., Abman, S.H., and Gladwin, M.T. (2013). Nitric oxide deficiency and endothelial dysfunction in pulmonary arterial hypertension. American Journal of Respiratory and Critical Care Medicine. *188*, 639–646.

Kloner, R.A. (2004). Cardiovascular effects of the 3 phosphodiesterase-5 inhibitors approved for the treatment of erectile dysfunction. Circulation *110*, 3149–3155.

Knaus, H.G., McManus, O.B., Lee, S.H., Schmalhofer, W.A., Garcia-Calvo, M., Helms, L.M., Sanchez, M., Giangiacomo, K., Reuben, J.P., and Smith, A.B. (1994). Tremorgenic indole alkaloids potently inhibit smooth muscle high-conductance calcium-activated potassium channels. Biochemistry *33*, 5819–5828.

Ko, E.A., Park, W.S., Ko, J.-H., Han, J., Kim, N., and Earm, Y.E. (2005). Endothelin-1 increases intracellular Ca^{2+} in rabbit pulmonary artery smooth muscle cells through phospholipase C. American Journal of Physiology. Heart and Circulatory Physiology *289*, H1551–9.

Kornhuber, J., Maler, M., Wiltfang, J., Bleich, S., Degner, D., and Rüther, E. (1999). Neuronal potassium channel opening with flupirtine. Fortschritte Der Neurologie-Psychiatrie *67*, 466–475.

Köttgen, M., Hoefer, A., Kim, S.J., Beschorner, U., Schreiber, R., Hug, M.J., and Greger, R. (1999). Carbachol activates a K^+ channel of very small conductance in the basolateral membrane of rat pancreatic acinar cells. Pflügers Archiv : European Journal of Physiology *438*, 597–603.

Kovitz, K.L., Aleskowitch, T.D., Sylvester, J.T., and Flavahan, N.A. (1993). Endothelium-derived contracting and relaxing factors contribute to hypoxic responses of pulmonary arteries. The American Journal of Physiology *265*, H1139–48.

Krick, S., Platoshyn, O., McDaniel, S.S., Rubin, L.J., and Yuan, J.X. (2001a). Augmented K^+ currents and mitochondrial membrane depolarization in pulmonary artery myocyte apoptosis. American Journal of Physiology- Lung Cellular and Molecular Physiology *281*, L887–94.

Krick, S., Platoshyn, O., Sweeney, M., Kim, H., and Yuan, J.X. (2001b). Activation of K^+ channels induces apoptosis in vascular smooth muscle cells. American Journal of Physiology- Cell Physiology *280*, C970–9.

Kroigaard, C., Kudryavtseva, O., Dalsgaard, T., Wandall-Frostholm, C., Olesen, S.-P., and Simonsen, U. (2013). $K_{Ca}3.1$ channel downregulation and impaired endothelium-derived hyperpolarization-type relaxation in pulmonary arteries from chronically hypoxic rats. Experimental Physiology *98*, 957–969.

Kubisch, C., Schroeder, B.C., Friedrich, T., Lütjohann, B., El-Amraoui, A., Marlin, S., Petit, C., and Jentsch, T.J. (1999). KCNQ4, a novel potassium channel expressed in sensory outer hair cells, is mutated in dominant deafness. Cell *96*, 437–446.

Kuhr, F.K., Smith, K.A., Song, M.Y., Levitan, I., and Yuan, J.X.-J. (2012). New mechanisms of pulmonary arterial hypertension: role of Ca^{2+} signaling. American Journal of Physiology. Heart and Circulatory Physiology *302*, H1546–62.

LaDouceur, D.M., Flynn, M.A., Keiser, J.A., Reynolds, E., and Haleen, S.J. (1993). ET_A and ET_B receptors coexist on rabbit pulmonary artery vascular smooth muscle mediating contraction. Biochemical and Biophysical Research Communications *196*, 209–215.

Lal, H., Woodward, B., and Williams, K.I. (1996). Investigation of the contributions of nitric oxide and prostaglandins to the actions of endothelins and sarafotoxin 6c in rat isolated perfused lungs. British Journal of Pharmacology *118*, 1931–1938.

Lamas, J.A., Selyanko, A.A., and Brown, D.A. (1997). Effects of a cognition-enhancer, linopirdine (DuP 996), on M-type potassium currents (I_{KM}) and some other voltage- and ligand-gated membrane currents in rat sympathetic neurons. The European Journal of Neuroscience *9*, 605–616.

Landsberg, J.W., and Yuan, J.X.-J. (2004). Calcium and TRP channels in pulmonary vascular smooth muscle cell proliferation. Physiology *19*, 44–50.

Langer, S.Z. (1980). Presynaptic regulation of the release of catecholamines. Pharmacological Reviews *32*, 337–362.

Langer, S.Z., and Hicks, P.E. (1984). Alpha-adrenoreceptor subtypes in blood vessels: physiology and pharmacology. Journal of Cardiovascular Pharmacology *6 Suppl 4*, S547–58.

Läuger, P. (1987). Voltage dependence of sodium-calcium exchange: predictions from kinetic models. The Journal of Membrane Biology *99*, 1–11.

Leach, R.M., Robertson, T.P., Twort, C.H., and Ward, J.P. (1994). Hypoxic vasoconstriction in rat pulmonary and mesenteric arteries. The American Journal of Physiology *266*, L223–31.

Leggett, K., Maylor, J., Undem, C., Lai, N., Lu, W., Schweitzer, K., King, L.S., Myers, A.C., Sylvester, J.T., Sidhaye, V., Shimoda, L.A. (2012). Hypoxia-induced migration in pulmonary arterial smooth muscle cells requires calcium-dependent upregulation of aquaporin 1. American Journal of Physiology-Lung Cellular and Molecular Physiology *303*, L343–53.

Lerche, C., Scherer, C.R., Seebohm, G., Derst, C., Wei, A.D., Busch, A.E., and Steinmeyer, K. (2000a). Molecular cloning and functional expression of KCNQ5, a potassium channel subunit that may contribute to neuronal M-current diversity. The Journal of Biological Chemistry *275*, 22395–22400.

Lerche, C., Seebohm, G., Wagner, C.I., Scherer, C.R., Dehmelt, L., Abitbol, I., Gerlach, U., Brendel, J., Attali, B., and Busch, A.E. (2000b). Molecular impact of MinK on the enantiospecific block of I(Ks) by chromanols. British Journal of Pharmacology *131*, 1503–1506.

Lerche, C., Bruhova, I., Lerche, H., Steinmeyer, K., Wei, A.D., Strutz-Seebohm, N., Lang, F., Busch, A.E., Zhorov, B.S., and Seebohm, G. (2007). Chromanol 293B binding in KCNQ1 (K_V7.1) channels involves electrostatic interactions with a potassium ion in the selectivity filter. Molecular Pharmacology *71*, 1503–1511.

Lesage, F., and Lazdunski, M. (2000). Molecular and functional properties of two-pore-domain potassium channels. American Journal of Physiology. Renal Physiology *279*, F793–801.

Liang, C.-C., Park, A.Y., and Guan, J.-L. (2007). In vitro scratch assay: a convenient and inexpensive method for analysis of cell migration in vitro. Nature Protocols *2*, 329–333.

Limsuwan, A., Platoshyn, O., Yu, Y., Rubin, L.J., Rothman, A., and Yuan, J.X. (2001). Inhibition of K^+ channel activity in human pulmonary artery smooth muscle cells by serum from patients with pulmonary hypertension secondary to congenital heart disease. Pediatric Research *50*, 23–28.

Lopatin, A.N., and Nichols, C.G. (2001). Inward rectifiers in the heart: an update on I_{K1}. Journal of Molecular and Cellular Cardiology. *33*, 625–638.

Lundquist, A.L., Manderfield, L.J., Vanoye, C.G., Rogers, C.S., Donahue, B.S., Chang, P.A., Drinkwater, D.C., Murray, K.T., and George, A.L. (2005). Expression of multiple KCNE genes in human heart may enable variable modulation of I(Ks). Journal of Molecular and Cellular Cardiology *38*, 277–287.

Lv, L., Zhang, J., Wang, P., Meng, Q., Liang, W., and Zhang, L. (2014). Zinc finger protein 191 deficiency attenuates vascular smooth muscle cell proliferation, migration, and intimal hyperplasia after endovascular arterial injury. Journal of Vascular Surgery. *59*, 500–509.

Ma, L., Roman-Campos, D., Austin, E.D., Eyries, M., Sampson, K.S., Soubrier, F., Germain, M., Trégouët, D.-A., Borczuk, A., Rosenzweig, E.B., et al. (2013). A novel channelopathy in pulmonary arterial hypertension. The New England Journal of Medicine *369*, 351–361.

McCrossan, Z.A., and Abbott, G.W. (2004). The MinK-related peptides. Neuropharmacology 47, 787–821.

Mackie, A.R., and Byron, K.L. (2008). Cardiovascular KCNQ (K_V7) potassium channels: physiological regulators and new targets for therapeutic intervention. Molecular Pharmacology *74*, 1171.

Mackie, A.R., Brueggemann, L.I., Henderson, K.K., Shiels, A.J., Cribbs, L.L., Scrogin, K.E., and Byron, K.L. (2008). Vascular KCNQ potassium channels as novel targets for the control of mesenteric artery constriction by vasopressin, based on studies in single cells, pressurized arteries, and in vivo measurements of mesenteric vascular resistance. The Journal of Pharmacology and Experimental Therapeutics *325*, 475–483.

Madden, J.A., Dawson, C.A., and Harder, D.R. (1985). Hypoxia-induced activation in small isolated pulmonary arteries from the cat. Journal of Applied Physiology *59*, 113–118.

Madden, J.A., Vadula, M.S., and Kurup, V.P. (1992). Effects of hypoxia and other vasoactive agents on pulmonary and cerebral artery smooth muscle cells. The American Journal of Physiology *263*, L384–93.

Magda, D., Lecane, P., Wang, Z., Hu, W., Thiemann, P., Ma, X., Dranchak, P.K., Wang, X., Lynch, V., Wei, W., et al. (2008). Synthesis and anticancer properties of water-soluble zinc ionophores. Cancer Research. *68*, 5318–5325.

Main, M.J., Cryan, J.E., Dupere, J.R., Cox, B., Clare, J.J., and Burbidge, S.A. (2000). Modulation of KCNQ2/3 potassium channels by the novel anticonvulsant retigabine. Molecular Pharmacology *58*, 253–262.

Mandegar, M., and Yuan, J.X.J. (2002). Role of K^+ channels in pulmonary hypertension. Vascular Pharmacology *38*, 25–33.

Mandegar, M., Fung, Y.-C.B., Huang, W., Remillard, C. V, Rubin, L.J., and Yuan, J.X.-J. (2004). Cellular and molecular mechanisms of pulmonary vascular remodeling: role in the development of pulmonary hypertension. Microvascular Research *68*, 75–103.

Mani, B.K., O'Dowd, J., Kumar, L., Brueggemann, L.I., Ross, M., and Byron, K.L. (2013). Vascular KCNQ (K_V7) potassium channels as common signaling intermediates and therapeutic targets in cerebral vasospasm. Journal of Cardiovascular Pharmacology *61*, 51–62.

Manoury, B., Etheridge, S.L., Reid, J., and Gurney, A.M. (2009). Organ culture mimics the effects of hypoxia on membrane potential, K^+ channels and vessel tone in pulmonary artery. British Journal of Pharmacology *158*, 848–861.

Manoury, B., Lamalle, C., Oliveira, R., Reid, J., and Gurney, A.M. (2011). Contractile and electrophysiological properties of pulmonary artery smooth muscle are not altered in TASK-1 knockout mice. The Journal of Physiology. *589*, 3231–3246.

Marchand, P., Gilroy, J.C., and Wilson, V.H. (1950). An anatomical study of the bronchial vascular system and its variations in disease. Thorax *5*, 207–221.

Marcos, E., Fadel, E., Sanchez, O., Humbert, M., Dartevelle, P., Simonneau, G., Hamon, M., Adnot, S., and Eddahibi, S. (2004). Serotonin-induced smooth muscle hyperplasia in various forms of human pulmonary hypertension. Circulation Research *94*, 1263–1270.

Evans, A., and Ward, J.P.T. (2009). Hypoxic pulmonary vasoconstriction--invited article. Advances in Experimental Medicine and Biology *648*, 351–360.

Marrion, N. V, Smart, T.G., and Brown, D.A. (1987). Membrane currents in adult rat superior cervical ganglia in dissociated tissue culture. Neuroscience Letters *77*, 55–60.

Marshall, C., and Marshall, B.E. (1992). Hypoxic pulmonary vasoconstriction is not endothelium dependent. Proceedings of the Society for Experimental Biology and Medicine. Society for Experimental Biology and Medicine *201*, 267–270.

Martin, E., Dahan, D., Cardouat, G., Gillibert-Duplantier, J., Marthan, R., Savineau, J.-P., and Ducret, T. (2012). Involvement of TRPV1 and TRPV4 channels in migration of rat pulmonary arterial smooth muscle cells. Pflügers Archiv: European Journal of Physiology *464*, 261–272.

Martire, M., Castaldo, P., D'Amico, M., Preziosi, P., Annunziato, L., and Taglialatela, M. (2004). M channels containing KCNQ2 subunits modulate norepinephrine, aspartate, and GABA release from hippocampal nerve terminals. The Journal of Neuroscience *24*, 592–597.

Matos, J.E., Sausbier, M., Beranek, G., Sausbier, U., Ruth, P., and Leipziger, J. (2007). Role of cholinergic-activated KCa1.1 (BK), KCa3.1 (SK4) and K_V7.1 (KCNQ1) channels in mouse colonic Cl^- secretion. Acta Physiologica *189*, 251–258.

Mattmann, M.E., Yu, H., Lin, Z., Xu, K., Huang, X., Long, S., Wu, M., McManus, O.B., Engers, D.W., Le, U.M., Li, M., Lindsley, C.W., Hopkins, C.R. (2012). Identification of (R)-N-(4-(4-methoxyphenyl)thiazol-2-yl)-1-tosylpiperidine-2-carboxamide, ML277, as a novel, potent and selective K_V7.1 (KCNQ1) potassium channel activator. Bioorganic & Medicinal Chemistry Letters *22*, 5936–5941.

McCormack, D. (1990). Endothelium-derived relaxing factors and the human pulmonary circulation. Lung *168 Suppl*, 35–42.

McCulloch, K.M., Docherty, C.C., Morecroft, I., and MacLean, M.R. (1996). EndothelinB receptor-mediated contraction in human pulmonary resistance arteries. British Journal of Pharmacology *119*, 1125–1130.

McCulloch, K.M., Kempsill, F.E., Buchanan, K.J., and Gurney, A.M. (2000). Regional distribution of potassium currents in the rabbit pulmonary arterial circulation. Experimental Physiology *85*, 487–496.

McDaniel, S.S., Platoshyn, O., Wang, J., Yu, Y., Sweeney, M., Krick, S., Rubin, L.J., and Yuan, J.X. (2001). Capacitative Ca^{2+} entry in agonist-induced pulmonary vasoconstriction. American Journal of Physiology- Lung Cellular and Molecular Physiology *280*, L870–80.

McKay, M.C., and Worley, J.F. (2001). Linoleic acid both enhances activation and blocks $K_V1.5$ and $K_V2.1$ channels by two separate mechanisms. American Journal of Physiology. Cell Physiol. *281*, C1277–84.

McLaughlin, V. V, Archer, S.L., Badesch, D.B., Barst, R.J., Farber, H.W., Lindner, J.R., Mathier, M.A., McGoon, M.D., Park, M.H., Rosenson, R.S., Rubin, L.J., Tapson, V.F., Varga, J., Harrington, R.A., Anderson, J.L., Bates, E.R., Bridges, C.R., Eisenberg, M.J., Ferrari, V.A., Grines, C.L., Hlatky, M.A., Jacobs, A.K., Kaul, S., Lichtenberg, R.C., Lindner, J.R., Moliterno, D.J., Mukherjee, D., Pohost, G.M., Rosenson, R.S., Schofield, R.S., Shubrooks, S.J., Stein, J.H., Tracy, C.M., Weitz, H.H., Wesley, D.J.; ACCF/AHA. (2009). ACCF/AHA 2009 expert consensus document on pulmonary hypertension: a report of the American College of Cardiology Foundation Task Force on Expert Consensus Documents and the American Heart Association: developed in collaboration with the American College of Chest Physicians, American Thoracic Society, Inc., and the Pulmonary Hypertension Association. Circulation *119*, 2250–2294.

McLaughlin, V. V, Davis, M., and Cornwell, W. (2011). Pulmonary arterial hypertension. Current Problems in Cardiology *36*, 461–517.

Meoli, D.F., and White, R.J. (2010). Endothelin-1 induces pulmonary but not aortic smooth muscle cell migration by activating ERK1/2 MAP kinase. Canadian Journal of Physiology and Pharmacology. *88*, 830–839.

Meyrick, B., Hislop, A., and Reid, L. (1978). Pulmonary arteries of the normal rat: the thick walled oblique muscle segment. Journal of Anatomy *125*, 209–221.

Miceli, F., Cilio, M.R., Taglialatela, M., and Bezanilla, F (2009). Gating currents from neuronal $K_V7.4$ channels: general features and correlation with the ionic conductance. Channels *3*, 274–283.

Miceli, F., Soldovieri, M.V., Martire, M., and Taglialatela, M. (2008). Molecular pharmacology and therapeutic potential of neuronal K_V7-modulating drugs. Current Opinion in Pharmacology *8*, 65–74.

Migneault, A., Sauvageau, S., Villeneuve, L., Thorin, E., Fournier, A., Leblanc, N., and Dupuis, J. (2005). Chronically elevated endothelin levels reduce pulmonary vascular reactivity to nitric oxide. American Journal of Respiratory and Critical Care Medicine *171*, 506–513.

Mikkelsen, E.O., Sakr, A.M., and Jespersen, L.T. (1983) Effects of nifedipine on contractile responses to potassium, histamine, and 5-hydroxytryptamine in isolated human pulmonary vessels. Journal of Cardiovascular Pharmacology *5*, 317–320.

Milara, J., Ortiz, J.L., Juan, G., Guijarro, R., Almudever, P., Martorell, M., Morcillo, E.J., and Cortijo, J. (2010). Cigarette smoke exposure up-regulates endothelin receptor B in human

pulmonary artery endothelial cells: molecular and functional consequences. British Journal of Pharmacology *161*, 1599–1615.

Mironov, A.A., Rekhter, M.D., Kolpakov, V.A., Andreeva, E.R., Polishchuk, R.S., Bannykh, S.I., Filippov, S. V, Peretjatko, L.P., Kulida, L. V, and Orekhov, A.N. (1995). Heterogeneity of smooth muscle cells in embryonic human aorta. Tissue & Cell *27*, 31–38.

Morecroft, I., Murray, A., Nilsen, M., Gurney, A.M., and MacLean, M.R. (2009). Treatment with the K_V7 potassium channel activator flupirtine is beneficial in two independent mouse models of pulmonary hypertension. British Journal of Pharmacology *157*, 1241–1249.

Morokuma, J., Blackiston, D., and Levin, M. (2008). KCNQ1 and KCNE1 K^+ channel components are involved in early left-right patterning in Xenopus laevis embryos. Cellular Physiology and Biochemistry : International Journal of Experimental Cellular Physiology, Biochemistry, and Pharmacology *21*, 357–372.

Moudgil, R., Michelakis, E.D., and Archer, S.L. (2006). The role of K^+ channels in determining pulmonary vascular tone, oxygen sensing, cell proliferation, and apoptosis: implications in hypoxic pulmonary vasoconstriction and pulmonary arterial hypertension. Microcirculation *13*, 615–632.

Mueller, O., Hahnenberger, K., Dittmann, M., Yee, H., Dubrow, R., Nagle, R., and Ilsley, D. (2000). A microfluidic system for high-speed reproducible DNA sizing and quantitation. Electrophoresis *21*, 128–134.

Mulvany M.J. (1988). Procedures for investigation of small vessels using small vessel myograph. Danish Myo Technology, 2004. Available at: http://www.dmt.dk/files/manualer/procedures_for_investigation.pdf (Accessed 28th September 2013)

Murray, T.R., Chen, L., Marshall, B.E., and Macarak, E.J. (1990). Hypoxic contraction of cultured pulmonary vascular smooth muscle cells. American Journal of Respiratory Cell and Molecular Biology *3*, 457–465.

Nakao, K., Okabe, K., Kitamura, K., Kuriyama, H., and Weston, A.H. (1988). Characteristics of cromakalim-induced relaxations in the smooth muscle cells of guinea-pig mesenteric artery and vein. British Journal of Pharmacology *95*, 795–804.

Narumiya, S., Sugimoto, Y., and Ushikubi, F. (1999). Prostanoid receptors: structures, properties, and functions. Physiological Reviews *79*, 1193–1226.

Neacsu, C., and Babes, A. (2010). The M-channel blocker linopirdine is an agonist of the capsaicin receptor TRPV1. Journal of Pharmacological Sciences *114*, 332–340.

Nelson, M.T., and Quayle, J.M. (1995). Physiological roles and properties of potassium channels in arterial smooth muscle. Am. J. Physiol. Cell Physiology. *268*, C799.

Neylon, C.B., Avdonin, P. V, Dilley, R.J., Larsen, M.A., Tkachuk, V.A., and Bobik, A. (1994). Different electrical responses to vasoactive agonists in morphologically distinct smooth muscle cell types. Circulation Research *75*, 733–741.

Neyroud, N., Tesson, F., Denjoy, I., Leibovici, M., Donger, C., Barhanin, J., Fauré, S., Gary, F., Coumel, P., Petit, C., Schwartz, K., Guicheney, P. (1997). A novel mutation in the potassium channel gene K_VLQT1 causes the Jervell and Lange-Nielsen cardioauditory syndrome. Nature Genetics *15*, 186–189.

Ng, F.L., Davis, A.J., Jepps, T.A., Harhun, M.I., Yeung, S.Y., Wan, A., Reddy, M., Melville, D., Nardi, A., Khong, T.K., Greenwood I.A. (2011). Expression and function of the K^+ channel KCNQ genes in human arteries. British Journal of Pharmacology *162*, 42–53.

Ng, L.C., and Gurney, A.M. (2001). Store-operated channels mediate Ca^{2+} influx and contraction in rat pulmonary artery. Circulation Research. *89*, 923–929.

Ng, L.C., McCormack, M.D., Airey, J.A., Singer, C.A., Keller, P.S., Shen, X.-M., and Hume, J.R. (2009). TRPC1 and STIM1 mediate capacitative Ca^{2+} entry in mouse pulmonary arterial smooth muscle cells. The Journal of Physiology *587*, 2429–2442.

Ng, L.C., Ramduny, D., Airey, J.A., Singer, C.A., Keller, P.S., Shen, X.-M., Tian, H., Valencik, M., and Hume, J.R. (2010). Orai1 interacts with STIM1 and mediates capacitative Ca^{2+} entry in mouse pulmonary arterial smooth muscle cells. American Journal of Physiology. Cell Physiology *299*, C1079–90.

Nichols, C.G., and Lopatin, A.N. (1997). Inward rectifier potassium channels. Annual Review of Physiology. *59*, 171–191.

Nichols, C.G., Singh, G.K., and Grange, D.K. (2013). KATP channels and cardiovascular disease: suddenly a syndrome. Circulation Research. *112*, 1059–1072.

Noble, D., and Tsien, R.W. (1968). The kinetics and rectifier properties of the slow potassium current in cardiac Purkinje fibres. The Journal of Physiology *195*, 185–214.

Norel, X., Walch, L., Costantino, M., Labat, C., Gorenne, I., Dulmet, E., Rossi, F., and Brink, C. (1996). M1 and M3 muscarinic receptors in human pulmonary arteries. British Journal of Pharmacology *119*, 149–157.

Núñez, R., Sancho-Martínez, S.M., Novoa, J.M.L., and López-Hernández, F.J. (2010). Apoptotic volume decrease as a geometric determinant for cell dismantling into apoptotic bodies. Cell Death and Differentiation *17*, 1665–1671.

Ogawa, A., Firth, A.L., Smith, K.A., Maliakal, M. V, and Yuan, J.X.-J. (2012). PDGF enhances store-operated Ca^{2+} entry by upregulating STIM1/Orai1 via activation of Akt/mTOR in human pulmonary arterial smooth muscle cells. American Journal of Physiology- Cell Physiology *302*, C405–11.

Ohya, S., Asakura, K., Muraki, K., Watanabe, M., and Imaizumi, Y. (2002). Molecular and functional characterization of ERG, KCNQ, and KCNE subtypes in rat stomach smooth

muscle. American Journal of Physiology. Gastrointestinal and Liver Physiology *282*, G277–87.

Ohya, S., Sergeant, G.P., Greenwood, I.A., and Horowitz, B. (2003). Molecular variants of KCNQ channels expressed in murine portal vein myocytes: a role in delayed rectifier current. Circulation Research *92*, 1016.

Olschewski, A., Li, Y., Tang, B., Hanze, J., Eul, B., Bohle, R.M., Wilhelm, J., Morty, R.E., Brau, M.E., Weir, E.K., et al. (2006). Impact of TASK-1 in human pulmonary artery smooth muscle cells. Circulation Research *98*, 1072–1080.

Olschewski, H., Ghofrani, H.A., Walmrath, D., Schermuly, R., Temmesfeld-Wollbruck, B., Grimminger, F., and Seeger, W. (1999). Inhaled prostacyclin and iloprost in severe pulmonary hypertension secondary to lung fibrosis. American Journal of Respiratory and Critical Care Medicine *160*, 600–607.

Ortiz, J.L., Labat, C., Norel, X., Gorenne, I., Verley, J., and Brink, C. (1992). Histamine receptors on human isolated pulmonary arterial muscle preparations: effects of endothelial cell removal and nitric oxide inhibitors. The Journal of Pharmacology and Experimental Therapeutics *260*, 762–767.

Osborn, M., Caselitz, J., and Weber, K. (1981). Heterogeneity of intermediate filament expression in vascular smooth muscle: a gradient in desmin positive cells from the rat aortic arch to the level of the arteria iliaca communis. Differentiation *20*, 196–202.

Osipenko, O.N., Evans, A.M., and Gurney, A.M. (1997). Regulation of the resting potential of rabbit pulmonary artery myocytes by a low threshold, O_2-sensing potassium current. British Journal of Pharmacology *120*, 1461–1470.

Osipenko, O.N., Alexander, D., MacLean, M.R., and Gurney, A.M. (1998). Influence of chronic hypoxia on the contributions of non-inactivating and delayed rectifier K currents to the resting potential and tone of rat pulmonary artery smooth muscle. British Journal of Pharmacology *124*, 1335–1337.

Osipenko, O.N., Tate, R.J., and Gurney, A.M. (2000). Potential role for K_V3.1b channels as oxygen sensors. Circulation Research *86*, 534–540.

Ouadid-Ahidouch, H., and Ahidouch, A. (2013). K(+) channels and cell cycle progression in tumor cells. Frontiers in Physiology. *4*, 220.

Owens, G.K. (1995). Regulation of differentiation of vascular smooth muscle cells. Physiological Reviews *75*, 487–517.

Palevsky, H.I., Long, W., Crow, J., and Fishman, A.P. (1990). Prostacyclin and acetylcholine as screening agents for acute pulmonary vasodilator responsiveness in primary pulmonary hypertension. Circulation *82*, 2018–2026.

Palmer, M.J.M.J. (2009). Leads for the treatment of pulmonary hypertension. Expert Opinion on Therapeutic Patents *19*, 575–592.

Park, K.S., Lee, H.A., Earm, K.H., Ko, J.H., Earm, Y.E., and Kim, S.J. (2006). Differential distribution of mechanosensitive nonselective cation channels in systemic and pulmonary arterial myocytes of rabbits. Journal of Vascular Research *43*, 347–354.

Partanen, M., Laitinen, A., Hervonen, A., Toivanen, M., and Laitinen, L.A. (1982). Catecholamine- and acetylcholinesterase-containing nerves in human lower respiratory tract. Histochemistry *76*, 175–188.

Patel, A.J., Lazdunski, M., and Honoré, E. (1997). $K_V2.1/K_V9.3$, a novel ATP-dependent delayed-rectifier K^+ channel in oxygen-sensitive pulmonary artery myocytes. The EMBO Journal *16*, 6615–6625.

Patel, R., Aronow, W.S., Patel, L., Gandhi, K., Desai, H., Kaul, D., and Sahgal, S.P. (2012). Treatment of pulmonary hypertension. Medical Science Monitor *18*, RA31–9.

Pauvert, O., Salvail, D., Rousseau, E., Lugnier, C., Marthan, R., and Savineau, J.P. (2002). Characterisation of cyclic nucleotide phosphodiesterase isoforms in the media layer of the main pulmonary artery. Biochemical Pharmacology *63*, 1763–1772.

Pauvert, O., Lugnier, C., Keravis, T., Marthan, R., Rousseau, E., and Savineau, J.P. (2003). Effect of sildenafil on cyclic nucleotide phosphodiesterase activity, vascular tone and calcium signaling in rat pulmonary artery. British Journal of Pharmacology *139*, 513–522.

Pawson, A.J., Sharman, J.L., Benson, H.E., Faccenda, E., Alexander, S.P.H., Buneman, O.P., Davenport, A.P., McGrath, J.C., Peters, J.A., Southan, C., et al. (2014). The IUPHAR/BPS Guide to PHARMACOLOGY: an expert-driven knowledgebase of drug targets and their ligands. Nucleic Acids Research. 42, D1098–D1106.

Peacock, A.J., Murphy, N.F., McMurray, J.J. V, Caballero, L., and Stewart, S. (2007). An epidemiological study of pulmonary arterial hypertension. The European Respiratory Journal *30*, 104–109.

Peinado, V.I., París, R., Ramírez, J., Roca, J., Rodriguez-Roisin, R., and Barberà, J.A. (2008). Expression of BK_{Ca} channels in human pulmonary arteries: relationship with remodeling and hypoxic pulmonary vasoconstriction. Vascular Pharmacology *49*, 178–184.

Pepke-Zaba, J., Higenbottam, T.W., Dinh-Xuan, A.T., Ridden, C., and Kealey, T. (1993). Alpha-adrenoceptor stimulation of porcine pulmonary arteries. European Journal of Pharmacology *235*, 169–175.

Perez-Zoghbi, J.F., and Sanderson, M.J. (2007). Endothelin-induced contraction of bronchiole and pulmonary arteriole smooth muscle cells is regulated by intracellular Ca^{2+} oscillations and Ca^{2+} sensitization. American Journal of Physiology-Lung Cellular and Molecular Physiology *293*, L1000–11.

Pfaffl, M.W. (2001). A new mathematical model for relative quantification in real-time RT-PCR. Nucleic Acids Research *29*, e45.

Pfaffl, M.W., Tichopad, A., Prgomet, C., and Neuvians, T.P. (2004). Determination of stable housekeeping genes, differentially regulated target genes and sample integrity: BestKeeper--Excel-based tool using pair-wise correlations. Biotechnology Letters *26*, 509–515.

Pieniaszek, H.J., Fiske, W.D., Saxton, T.D., Kim, Y.S., Garner, D.M., Xilinas, M., and Martz, R. (1995). Single-dose pharmacokinetics, safety, and tolerance of linopirdine (DuP 996) in healthy young adults and elderly volunteers. Journal of Clinical Pharmacology *35*, 22–30.

Pier, D.M., Shehatou, G.S.G., Giblett, S., Pullar, C.E., Trezise, D.J., Pritchard, C.A., Challiss, R.A.J., and Mitcheson, J.S. (2014). Long-term channel block is required to inhibit cellular transformation by human ether-à-go-go-related gene (hERG1) potassium channels. Molecular Pharmacology. *86*, 211–221

Pietra, G.G., Edwards, W.D., Kay, J.M., Rich, S., Kernis, J., Schloo, B., Ayres, S.M., Bergofsky, E.H., Brundage, B.H., and Detre, K.M. (1989). Histopathology of primary pulmonary hypertension. A qualitative and quantitative study of pulmonary blood vessels from 58 patients in the National Heart, Lung, and Blood Institute, Primary Pulmonary Hypertension Registry. Circulation *80*, 1198–1206.

Plaster, N.M., Tawil, R., Tristani-Firouzi, M., Canún, S., Bendahhou, S., Tsunoda, A., Donaldson, M.R., Iannaccone, S.T., Brunt, E., Barohn, R., et al. (2001). Mutations in $K_{ir}2.1$ cause the developmental and episodic electrical phenotypes of Andersen's syndrome. Cell *105*, 511–519.

Platoshyn, O., Golovina, V.A., Bailey, C.L., Limsuwan, A., Krick, S., Juhaszova, M., Seiden, J.E., Rubin, L.J., and Yuan, J.X.-J. (2000). Sustained membrane depolarization and pulmonary artery smooth muscle cell proliferation. American Journal of Physiology- Cell Physiology *279*, C1540–9.

Platoshyn, O., Yu, Y., Golovina, V.A., McDaniel, S.S., Krick, S., Li, L., Wang, J.Y., Rubin, L.J., and Yuan, J.X. (2001). Chronic hypoxia decreases K_V channel expression and function in pulmonary artery myocytes. American Journal of Physiology- Lung Cellular and Molecular Physiology *280*, L801–12.

Platoshyn, O., Remillard, C. V, Fantozzi, I., Mandegar, M., Sison, T.T., Zhang, S., Burg, E., and Yuan, J.X.-J. (2004). Diversity of voltage-dependent K^+ channels in human pulmonary artery smooth muscle cells. American Journal of Physiology- Lung Cellular and Molecular Physiology *287*, L226–38.

Pluteanu, F., and Cribbs, L.L. (2011). Regulation and function of Cav3.1 T-type calcium channels in IGF-I-stimulated pulmonary artery smooth muscle cells. American Journal of Physiology - Cell Physiology. *300*, C517–25.

Post, J.M., Hume, J.R., Archer, S.L., and Weir, E.K. (1992). Direct role for potassium channel inhibition in hypoxic pulmonary vasoconstriction. The American Journal of Physiology *262*, C882–90.

Preuss, K.C., Gross, G.J., Brooks, H.L., and Warltier, D.C. (1985). Slow channel calcium activators, a new group of pharmacological agents. Life Sciences *37*, 1271–1278.

Prole, D.L., and Marrion, N. V (2004). Ionic permeation and conduction properties of neuronal KCNQ2/KCNQ3 potassium channels. Biophysical Journal *86*, 1454–1469.

Purtell, K., Paroder-Belenitsky, M., Reyna-Neyra, A., Nicola, J.P., Koba, W., Fine, E., Carrasco, N., and Abbott, G.W. (2012). The KCNQ1-KCNE2 K^+ channel is required for adequate thyroid I^- uptake. The FASEB Journal *26*, 3252–3259.

Quignard, J.F., Ryckwaert, F., Albat, B., Nargeot, J., and Richard, S. (1997). A novel tetrodotoxin-sensitive Na^+ current in cultured human coronary myocytes. Circulation Research *80*, 377–382.

Rabe, K.F., Tenor, H., Dent, G., Schudt, C., Nakashima, M., and Magnussen, H. (1994). Identification of PDE isozymes in human pulmonary artery and effect of selective PDE inhibitors. The American Journal of Physiology *266*, L536–43.

Reichenberger, F., Schauer, J., Kellner, K., Sack, U., Stiehl, P., and Winkler, J. (2001). Different expression of endothelin in the bronchoalveolar lavage in patients with pulmonary diseases. Lung *179*, 163–174.

Rensen, S.S.M., Doevendans, P.A.F.M., and van Eys, G.J.J.M. (2007). Regulation and characteristics of vascular smooth muscle cell phenotypic diversity. Netherlands Heart Journal *15*, 100–108.

Rhodes, C.J., Davidson, A., Gibbs, J.S.R., Wharton, J., and Wilkins, M.R. (2009). Therapeutic targets in pulmonary arterial hypertension. Pharmacology & Therapeutics *121*, 69–88.

Riezebos, J., Watts, I.S., and Vallance, P.J. (1994). Endothelin receptors mediating functional responses in human small arteries and veins. British Journal of Pharmacology *111*, 609–615.

Robbins, J. (2001). KCNQ potassium channels: physiology, pathophysiology, and pharmacology. Pharmacology & Therapeutics *90*, 1–19.

Robertson, B. (1997). The real life of voltage-gated K^+ channels: more than model behaviour. Trends in Pharmacological Sciences *18*, 474–483.

Rodman, D.M., Reese, K., Harral, J., Fouty, B., Wu, S., West, J., Hoedt-Miller, M., Tada, Y., Li, K.-X., Cool, C., et al. (2005). Low-voltage-activated (T-type) calcium channels control proliferation of human pulmonary artery myocytes. Circulation Research. 96, 864–872.

Rodrigues, M.A., Gomes, D.A., Leite, M.F., Grant, W., Zhang, L., Lam, W., Cheng, Y.-C., Bennett, A.M., and Nathanson, M.H. (2007). Nucleoplasmic calcium is required for cell proliferation. The Journal of Biological Chemistry *282*, 17061–17068.

Roepke, T.K., King, E.C., Reyna-Neyra, A., Paroder, M., Purtell, K., Koba, W., Fine, E., Lerner, D.J., Carrasco, N., and Abbott, G.W. (2009). Kcne2 deletion uncovers its crucial role in thyroid hormone biosynthesis. Nature Medicine *15*, 1186–1194.

Roura-Ferrer, M., Solé, L., Martínez-Mármol, R., Villalonga, N., and Felipe, A. (2008). Skeletal muscle K_V7 (KCNQ) channels in myoblast differentiation and proliferation. Biochemical and Biophysical Research Communications *369*, 1094–1097.

Roura-Ferrer, M., Solé, L., Oliveras, A., Villarroel, A., Comes, N., and Felipe, A. (2012). Targeting of $K_V7.5$ (KCNQ5)/KCNE channels to surface microdomains of cell membranes. Muscle & Nerve *45*, 48–54.

Rozkovec, A., Stradling, J.R., Shepherd, G., MacDermot, J., Oakley, C.M., and Dollery, C.T. (1988). Prediction of favourable responses to long term vasodilator treatment of pulmonary hypertension by short term administration of epoprostenol (prostacyclin) or nifedipine. British Heart Journal *59*, 696–705.

Rundfeldt, C., and Netzer, R. (2000a). Investigations into the mechanism of action of the new anticonvulsant retigabine. Interaction with GABAergic and glutamatergic neurotransmission and with voltage-gated ion channels. Arzneimittelforschung *50*, 1063–1070.

Rundfeldt, C., and Netzer, R. (2000b). The novel anticonvulsant retigabine activates M-currents in Chinese hamster ovary-cells tranfected with human KCNQ2/3 subunits. Neuroscience Letters *282*, 73–76.

Ruscic, K.J., Miceli, F., Villalba-Galea, C.A., Dai, H., Mishina, Y., Bezanilla, F., and Goldstein, S.A.N. (2013). I_{Ks} channels open slowly because KCNE1 accessory subunits slow the movement of S4 voltage sensors in KCNQ1 pore-forming subunits. PNAS *110*, E559–66.

Sadeghian, G., Ziaei, H., and Nilforoushzadeh, M.A. (2011). Treatment of localized psoriasis with a topical formulation of zinc pyrithione. Acta Dermatovenerologica APA *20*, 187–190.

Sahara, M., Sata, M., Morita, T., Hirata, Y., and Nagai, R. (2012). Nicorandil attenuates monocrotaline-induced vascular endothelial damage and pulmonary arterial hypertension. PLoS One. *7*, e33367.

Salata, J.J., Jurkiewicz, N.K., Wang, J., Evans, B.E., Orme, H.T., and Sanguinetti, M.C. (1998). A novel benzodiazepine that activates cardiac slow delayed rectifier K^+ currents. Molecular Pharmacology *54*, 220–230.

Saletu, B., Darragh, A., Salmon, P., and Coen, R. (1989). EEG brain mapping in evaluating the time-course of the central action of DUP 996--a new acetylcholine releasing drug. British Journal of Clinical Pharmacology *28*, 1–16.

Sandoval, J., Bauerle, O., Gomez, A., Palomar, A., Martínez Guerra, M.L., and Furuya, M.E. (1995). Primary pulmonary hypertension in children: clinical characterization and survival. Journal of the American College of Cardiology *25*, 466–474.

Sanguinetti, M.C., Curran, M.E., Zou, A., Shen, J., Spector, P.S., Atkinson, D.L., and Keating, M.T. (1996). Coassembly of KVLQT1 and minK (IsK) proteins to form cardiac I_{Ks} potassium channel. Nature *384*, 80–83.

Sarkar, J., Gou, D., Turaka, P., Viktorova, E., Ramchandran, R., and Raj, J.U. (2010). MicroRNA-21 plays a role in hypoxia-mediated pulmonary artery smooth muscle cell proliferation and migration. American Journal of Physiology- Lung Cellular and Molecular Physiology *299*, L861–71.

Sarzani, R., Pietrucci, F., Francioni, M., Salvi, F., Letizia, C., D'Erasmo, E., Dessì Fulgheri, P., and Rappelli, A. (2006). Expression of potassium channel isoforms mRNA in normal human adrenals and aldosterone-secreting adenomas. Journal of Endocrinological Investigation *29*, 147–153.

Schmittgen, T.D., and Zakrajsek, B.A. (2000). Effect of experimental treatment on housekeeping gene expression: validation by real-time, quantitative RT-PCR. Journal of Biochemical and Biophysical Methods *46*, 69–81.

Schramm, M., Thomas, G., Towart, R., and Franckowiak, G. Novel dihydropyridines with positive inotropic action through activation of Ca^{2+} channels. Nature *303*, 535–537.

Schrøder, R.L., Jespersen, T., Christophersen, P., Strøbaek, D., Jensen, B.S., and Olesen, S.P. (2001). KCNQ4 channel activation by BMS-204352 and retigabine. Neuropharmacology *40*, 888–898.

Schroeder, A., Mueller, O., Stocker, S., Salowsky, R., Leiber, M., Gassmann, M., Lightfoot, S., Menzel, W., Granzow, M., and Ragg, T. (2006). The RIN: an RNA integrity number for assigning integrity values to RNA measurements. BMC Molecular Biology *7*, 3.

Schroeder, B.C., Kubisch, C., Stein, V., and Jentsch, T.J. (1998). Moderate loss of function of cyclic-AMP-modulated KCNQ2/KCNQ3 K^+ channels causes epilepsy. Nature *396*, 687–690.

Schroeder, B.C., Hechenberger, M., Weinreich, F., Kubisch, C., and Jentsch, T.J. (2000a). KCNQ5, a novel potassium channel broadly expressed in brain, mediates M-type currents. The Journal of Biological Chemistry *275*, 24089–24095.

Schroeder, B.C., Waldegger, S., Fehr, S., Bleich, M., Warth, R., Greger, R., and Jentsch, T.J. (2000b). A constitutively open potassium channel formed by KCNQ1 and KCNE3. Nature *403*, 196–199.

Schwake, M., Pusch, M., Kharkovets, T., and Jentsch, T.J. (2000). Surface expression and single channel properties of KCNQ2/KCNQ3, M-type K^+ channels involved in epilepsy. The Journal of Biological Chemistry *275*, 13343–13348.

Schwartz, J.R., Bacon, R.A., Shah, R., Mizoguchi, H., and Tosti, A. (2013). Therapeutic efficacy of anti-dandruff shampoos: A randomized clinical trial comparing products based on potentiated zinc pyrithione and zinc pyrithione/climbazole. International Journal of Cosmetic Science.

Schwartz, S.M., Campbell, G.R., and Campbell, J.H. (1986). Replication of smooth muscle cells in vascular disease. Circulation Research *58*, 427–444.

Scott, J.A., Craig, I., and McCormack, D.G. (1996). Nonadrenergic noncholinergic relaxation of human pulmonary arteries is partially mediated by nitric oxide. American Journal of Respiratory and Critical Care Medicine *154*, 629–632.

Sedivy, V., Joshi, S., Ghaly, Y., Mizera, R., Zaloudikova, M., Brennan, S., Novotna, J., Herget, J., and Gurney, A.M. (2014). Role of Kv7 channels in responses of the pulmonary circulation to hypoxia. The American Journal of Physiology - Lung Cellular and Molecular Physiology.ajplung.00362.2013.

Seebohm, G., Lerche, C., Pusch, M., Steinmeyer, K., Brüggemann, A., and Busch, A.E. (2001). A kinetic study on the stereospecific inhibition of KCNQ1 and I_{Ks} by the chromanol 293B. British Journal of Pharmacology *134*, 1647–1654.

Seebohm, G., Pusch, M., Chen, J., and Sanguinetti, M.C. (2003). Pharmacological activation of normal and arrhythmia-associated mutant KCNQ1 potassium channels. Circulation Research *93*, 941–947.

Seino, S. (1999). ATP-sensitive potassium channels: a model of heteromultimeric potassium channel/receptor assemblies. Annual Review of Physiology. *61*, 337–362.

Selyanko, A.A., Hadley, J.K., Wood, I.C., Abogadie, F.C., Jentsch, T.J., and Brown, D.A. (2000). Inhibition of KCNQ1-4 potassium channels expressed in mammalian cells via M1 muscarinic acetylcholine receptors. The Journal of Physiology *522 Pt 3*, 349–355.

Seo, M., Kim, Y., Lee, Y.-I., Kim, S.-Y., Ahn, Y.-M., Kang, U.G., Roh, M.-S., Kim, Y.-S., and Juhnn, Y.-S. (2006). Membrane depolarization stimulates the proliferation of SH-SY5Y human neuroblastoma cells by increasing retinoblastoma protein (RB) phosphorylation through the activation of cyclin-dependent kinase 2 (Cdk2). Neuroscience Letters *404*, 87–92.

Shamgar, L., Haitin, Y., Yisharel, I., Malka, E., Schottelndreier, H., Peretz, A., Paas, Y., and Attali, B. (2008). KCNE1 constrains the voltage sensor of $K_V7.1$ K^+ channels. PloS One *3*, e1943.

Shapiro, M.S., Roche, J.P., Kaftan, E.J., Cruzblanca, H., Mackie, K., and Hille, B. (2000). Reconstitution of muscarinic modulation of the KCNQ2/KCNQ3 K^+ channels that underlie the neuronal M current. The Journal of Neuroscience *20*, 1710–1721.

Shi, W.-W., Yang, Y., Shi, Y., and Jiang, C. (2012). K_{ATP} channel action in vascular tone regulation: from genetics to diseases. Sheng Li Xue Bao *64*, 1–13.

Shimoda, L.A., and Laurie, S.S. (2013). Vascular remodeling in pulmonary hypertension. Journal of Molecular Medicine (Berlin, Germany) *91*, 297–309.

Shimoda, L.A., Sham, J.S., Shimoda, T.H., and Sylvester, J.T. (2000). L-type Ca^{2+} channels, resting $[Ca^{2+}]_i$, and ET-1-induced responses in chronically hypoxic pulmonary myocytes. American Journal of Physiology- Lung Cellular and Molecular Physiology *279*, L884–94.

Shirai, M., Sada, K., and Ninomiya, I. (1986). Effects of regional alveolar hypoxia and hypercapnia on small pulmonary vessels in cats. Journal of Applied Physiology (Bethesda, Md. : 1985) *61*, 440–448.

Simonneau, G., Galiè, N., Rubin, L.J., Langleben, D., Seeger, W., Domenighetti, G., Gibbs, S., Lebrec, D., Speich, R., Beghetti, M., et al. (2004). Clinical classification of pulmonary hypertension. Journal of the American College of Cardiology *43*, 5S–12S.

Simonneau, G., Robbins, I.M., Beghetti, M., Channick, R.N., Delcroix, M., Denton, C.P., Elliott, C.G., Gaine, S.P., Gladwin, M.T., Jing, Z.-C., et al. (2009). Updated clinical classification of pulmonary hypertension. Journal of the American College of Cardiology *54*, S43–54.

Simonneau, G., Gatzoulis, M.A., Adatia, I., Celermajer, D., Denton, C., Ghofrani, A., Gomez Sanchez, M.A., Krishna Kumar, R., Landzberg, M., Machado, R.F., et al. (2013). Updated clinical classification of pulmonary hypertension. Journal of the American College of Cardiology. *62*, D34–41.

Sims, S.M., Singer, J.J., and Walsh, J. V (1985). Cholinergic agonists suppress a potassium current in freshly dissociated smooth muscle cells of the toad. The Journal of Physiology *367*, 503–529.

Skalli, O., Ropraz, P., Trzeciak, A., Benzonana, G., Gillessen, D., and Gabbiani, G. (1986). A monoclonal antibody against alpha-smooth muscle actin: a new probe for smooth muscle differentiation. The Journal of Cell Biology *103*, 2787–2796.

Smirnov, S. V, Robertson, T.P., Ward, J.P., and Aaronson, P.I. (1994). Chronic hypoxia is associated with reduced delayed rectifier K^+ current in rat pulmonary artery muscle cells. The American Journal of Physiology *266*, H365–70.

Smirnov, S. V, Beck, R., Tammaro, P., Ishii, T., and Aaronson, P.I. (2002). Electrophysiologically distinct smooth muscle cell subtypes in rat conduit and resistance pulmonary arteries. The Journal of Physiology *538*, 867–878.

Smith, J.S., Iannotti, C.A., Dargis, P., Christian, E.P., and Aiyar, J. (2001). Differential expression of kcnq2 splice variants: implications to m current function during neuronal development. The Journal of Neuroscience *21*, 1096–1103.

Søgaard, R., Ljungstrøm, T., Pedersen, K.A., Olesen, S.P., and Jensen, B.S. (2001). KCNQ4 channels expressed in mammalian cells: functional characteristics and pharmacology. American Journal of Physiology- Cell Physiology *280*, C859–66.

Soh, H., and Tzingounis, A. V (2010). The specific slow afterhyperpolarization inhibitor UCL2077 is a subtype-selective blocker of the epilepsy associated KCNQ channels. Molecular Pharmacology *78*, 1088–1095.

Song, M.Y., Makino, A., and Yuan, J.X.-J. (2011). STIM2 Contributes to Enhanced Store-operated Ca Entry in Pulmonary Artery Smooth Muscle Cells from Patients with Idiopathic Pulmonary Arterial Hypertension. Pulmonary Circulation *1*, 84–94.

Starikova, A.M., Pogorelaya, N.C., and Kostyuk, P.G. (2000). Long-term depolarization changes morphological parameters of PC12 cells. Neuroscience *95*, 923–926.

Staub, N.C. (1985). Site of hypoxic pulmonary vasoconstriction. Chest *88*, 240S–245S.

Stenmark, K.R., Fagan, K.A., and Frid, M.G. (2006). Hypoxia-induced pulmonary vascular remodeling: cellular and molecular mechanisms. Circulation Research *99*, 675–691.

Stenmark, K.R., Meyrick, B., Galie, N., Mooi, W.J., and McMurtry, I.F. (2009). Animal models of pulmonary arterial hypertension: the hope for etiological discovery and pharmacological cure. American Journal of Physiology- Lung Cellular and Molecular Physiology *297*, L1013–32.

Stewart, D.J., Levy, R.D., Cernacek, P., and Langleben, D. (1991). Increased plasma endothelin-1 in pulmonary hypertension: marker or mediator of disease? Annals of Internal Medicine *114*, 464–469.

Strutz-Seebohm, N., Seebohm, G., Fedorenko, O., Baltaev, R., Engel, J., Knirsch, M., and Lang, F. (2006). Functional coassembly of KCNQ4 with KCNE-beta- subunits in Xenopus oocytes. Cellular Physiology and Biochemistry : International Journal of Experimental Cellular Physiology, Biochemistry, and Pharmacology *18*, 57–66.

Su, C., Bevan, J.A., and Ursillo, R.C. (1964). Electrical quiescence of pulmonary artery smooth muscle during sympathomimetic stimulation. Circulation Research *15*, 26–27.

Suchyna, T.M., Johnson, J.H., Hamer, K., Leykam, J.F., Gage, D.A., Clemo, H.F., Baumgarten, C.M., and Sachs, F. (2000). Identification of a peptide toxin from Grammostola spatulata spider venom that blocks cation-selective stretch-activated channels. The Journal of General Physiology *115*, 583–598.

Sugimoto, T., Tanabe, Y., Shigemoto, R., Iwai, M., Takumi, T., Ohkubo, H., and Nakanishi, S. (1990). Immunohistochemical study of a rat membrane protein which induces a selective potassium permeation: its localization in the apical membrane portion of epithelial cells. The Journal of Membrane Biology *113*, 39–47.

Sundelacruz, S., Levin, M., and Kaplan, D.L. (2009). Role of membrane potential in the regulation of cell proliferation and differentiation. Stem Cell Reviews *5*, 231–246.

Suzuki, H., and Twarog, B.M. (1982). Membrane properties of smooth muscle cells in pulmonary hypertensive rats. The American Journal of Physiology *242*, H907–15.

Suzuki, T., Higgins, P.J., and Crawford, D.R. (2000). Control selection for RNA quantitation. BioTechniques *29*, 332–337.

Szelenyi, I. (2013). Flupirtine, a re-discovered drug, revisited. Inflammation Research *62*, 251–258.

Takeo, S. (1992), Pharmacodynamics and Clinical Studies with Beraprost Sodium, a Drug for Peripheral Vascular Disease. Cardiovascular Drug Reviews *10*, 392–403.

Tanaka, Y., Koike, K., and Toro, L. (2004). MaxiK channel roles in blood vessel relaxations induced by endothelium-derived relaxing factors and their molecular mechanisms. Journal of Smooth Muscle Research. *40*, 125–153.

Tang, B., Li, Y., Nagaraj, C., Morty, R.E., Gabor, S., Stacher, E., Voswinckel, R., Weissmann, N., Leithner, K., Olschewski, H., et al. (2009). Endothelin-1 inhibits background two-pore domain channel TASK-1 in primary human pulmonary artery smooth muscle cells. American Journal of Respiratory Cell and Molecular Biology *41*, 476–483.

Tatulian, L., Delmas, P., Abogadie, F.C., and Brown, D.A. (2001). Activation of expressed KCNQ potassium currents and native neuronal M-type potassium currents by the anti-convulsant drug retigabine. The Journal of Neuroscience *21*, 5535–5545.

Thellin, O., Zorzi, W., Lakaye, B., De Borman, B., Coumans, B., Hennen, G., Grisar, T., Igout, A., and Heinen, E. (1999). Housekeeping genes as internal standards: use and limits. Journal of Biotechnology *75*, 291–295.

Thermo Scientific. T042 Technical Bulletin- Assessment of Nucleic Acid Purity. Available at: http://www.nanodrop.com/Library/T042-NanoDrop-Spectrophotometers-Nucleic-Acid-Purity-Ratios.pdf. (Accessed 28th September 2013).

Tinel, N., Lauritzen, I., Chouabe, C., Lazdunski, M., and Borsotto, M. (1998). The KCNQ2 potassium channel: splice variants, functional and developmental expression. Brain localization and comparison with KCNQ3. FEBS Letters *438*, 171–176.

Tinel, N., Diochot, S., Lauritzen, I., Barhanin, J., Lazdunski, M., and Borsotto, M. (2000a). M-type KCNQ2-KCNQ3 potassium channels are modulated by the KCNE2 subunit. FEBS Letters *480*, 137–141.

Tinel, N., Diochot, S., Borsotto, M., Lazdunski, M., and Barhanin, J. (2000b). KCNE2 confers background current characteristics to the cardiac KCNQ1 potassium channel. The EMBO Journal *19*, 6326–6330.

Toth, P.T., Marsboom, G., Hong, Z., Zhang, H., Bache-Wiig, P., Rehman, J., Archer, S.L. (2011). Sarcoplasmic Reticulum Calcium Buffering is Associated with Increased Cytosolic Calcium in Smooth Muscle Cells From Pulmonary Arterial Hypertension Patients. Circulation *124*, A12882.

Tricarico, C., Pinzani, P., Bianchi, S., Paglierani, M., Distante, V., Pazzagli, M., Bustin, S.A., and Orlando, C. (2002). Quantitative real-time reverse transcription polymerase chain reaction: normalization to rRNA or single housekeeping genes is inappropriate for human tissue biopsies. Analytical Biochemistry *309*, 293–300.

Tristani-Firouzi, M., and Sanguinetti, M.C. (1998). Voltage-dependent inactivation of the human K^+ channel K_VLQT1 is eliminated by association with minimal K^+ channel (minK) subunits. The Journal of Physiology *510 (Pt 1*, 37–45.

Tsevi, I., Vicente, R., Grande, M., López-Iglesias, C., Figueras, A., Capellà, G., Condom, E., and Felipe, A. (2005). KCNQ1/KCNE1 channels during germ-cell differentiation in the rat: expression associated with testis pathologies. Journal of Cellular Physiology *202*, 400–410.

Tuder, R.M., Marecki, J.C., Richter, A., Fijalkowska, I., and Flores, S. (2007). Pathology of pulmonary hypertension. Clinics in Chest Medicine *28*, 23–42, vii.

Turcato, S., and Clapp, L.H. (1999). Effects of the adenylyl cyclase inhibitor SQ22536 on iloprost-induced vasorelaxation and cyclic AMP elevation in isolated guinea-pig aorta. British Journal of Pharmacology *126*, 845–847.

Vallon, V., Grahammer, F., Richter, K., Bleich, M., Lang, F., Barhanin, J., Völkl, H., and Warth, R. (2001). Role of KCNE1-dependent K^+ fluxes in mouse proximal tubule. Journal of the American Society of Nephrology *12*, 2003–2011.

Vandesompele, J., De Preter, K., Pattyn, F., Poppe, B., Van Roy, N., De Paepe, A., and Speleman, F. (2002). Accurate normalization of real-time quantitative RT-PCR data by geometric averaging of multiple internal control genes. Genome Biology *3*, research0034.

Vicente, R., Escalada, A., Villalonga, N., Texidó, L., Roura-Ferrer, M., Martín-Satué, M., López-Iglesias, C., Soler, C., Solsona, C., Tamkun, M.M., et al. (2006). Association of $K_V1.5$ and $K_V1.3$ contributes to the major voltage-dependent K^+ channel in macrophages. The Journal of Biological Chemistry *281*, 37675–37685.

Wadsworth, R.M. (1994). Vasoconstrictor and vasodilator effects of hypoxia. Trends in Pharmacological Sciences *15*, 47–53.

Wallner, M., Meera, P., Ottolia, M., Kaczorowski, G.J., Latorre, R., Garcia, M.L., Stefani, E., and Toro, L. (1995). Characterization of and modulation by a beta-subunit of a human maxi KCa channel cloned from myometrium. Receptors Channels *3*, 185–199.

Wallner, M., Meera, P., and Toro, L. (1996). Determinant for beta-subunit regulation in high-conductance voltage-activated and Ca(2+)-sensitive K+ channels: an additional transmembrane region at the N terminus. Proceedings of the National Academy of Sciences. Sci. U. S. A. *93*, 14922–14927.

Wang, H.S., Pan, Z., Shi, W., Brown, B.S., Wymore, R.S., Cohen, I.S., Dixon, J.E., and McKinnon, D. (1998). KCNQ2 and KCNQ3 potassium channel subunits: molecular correlates of the M-channel. Science *282*, 1890–1893.

Wang, J., Juhaszova, M., Rubin, L.J., and Yuan, X.J. (1997). Hypoxia inhibits gene expression of voltage-gated K^+ channel alpha subunits in pulmonary artery smooth muscle cells. The Journal of Clinical Investigation *100*, 2347–2353.

Wang, J., Weigand, L., Wang, W., Sylvester, J.T., and Shimoda, L.A. (2005). Chronic hypoxia inhibits K_V channel gene expression in rat distal pulmonary artery. American Journal of Physiology- Lung Cellular and Molecular Physiology *288*, L1049–58.

Wang, Q., Curran, M.E., Splawski, I., Burn, T.C., Millholland, J.M., VanRaay, T.J., Shen, J., Timothy, K.W., Vincent, G.M., de Jager, T., et al. (1996). Positional cloning of a novel potassium channel gene: K_VLQT1 mutations cause cardiac arrhythmias. Nature Genetics *12*, 17–23.

Wang, W., Gao, X.-F., Xiao, L., Xiang, Z.-H., and He, C. (2011). K_V7/KCNQ channels are functionally expressed in oligodendrocyte progenitor cells. PloS One *6*, e21792.

Wang, Y., Coe, Y., Toyoda, O., and Coceani, F. (1995). Involvement of endothelin-1 in hypoxic pulmonary vasoconstriction in the lamb. The Journal of Physiology *482 (Pt 2*); 421–434.

Ward, J.P.T. (2007). Curiouser and curiouser: the perplexing conundrum of reactive oxygen species and hypoxic pulmonary vasoconstriction. Experimental Physiology *92*, 819–820.

Warth, R., Garcia Alzamora, M., Kim, J.K., Zdebik, A., Nitschke, R., Bleich, M., Gerlach, U., Barhanin, J., and Kim, S.J. (2002). The role of KCNQ1/KCNE1 K^+ channels in intestine and pancreas: lessons from the KCNE1 knockout mouse. Pflügers Archiv : European Journal of Physiology *443*, 822–828.

Wharton, J., Strange, J.W., Møller, G.M.O., Growcott, E.J., Ren, X., Franklyn, A.P., Phillips, S.C., and Wilkins, M.R. (2005). Antiproliferative effects of phosphodiesterase type 5 inhibition in human pulmonary artery cells. American Journal of Respiratory and Critical Care Medicine *172*, 105–113.

Wickenden, A.D., Yu, W., Zou, A., Jegla, T., and Wagoner, P.K. (2000). Retigabine, a novel anti-convulsant, enhances activation of KCNQ2/Q3 potassium channels. Molecular Pharmacology *58*, 591–600.

Wickenden, A.D., Zou, A., Wagoner, P.K., and Jegla, T. (2001). Characterization of KCNQ5/Q3 potassium channels expressed in mammalian cells. British Journal of Pharmacology *132*, 381–384.

Wiener, C.M., Dunn, A., and Sylvester, J.T. (1991). ATP-dependent K^+ channels modulate vasoconstrictor responses to severe hypoxia in isolated ferret lungs. The Journal of Clinical Investigation *88*, 500–504.

Wladyka, C.L., and Kunze, D.L. (2006). KCNQ/M-currents contribute to the resting membrane potential in rat visceral sensory neurons. The Journal of Physiology *575*, 175–189.

Wonderlin, W.F., and Strobl, J.S. (1996). Potassium channels, proliferation and G1 progression. The Journal of Membrane Biology *154*, 91–107.

World Medical Association. (2013). World Medical Association Declaration of Helsinki: ethical principles for medical research involving human subjects. Journal of the American Medical Association *310*, 2191–2194

Wu, D.-M., Jiang, M., Zhang, M., Liu, X.-S., Korolkova, Y. V, and Tseng, G.-N. (2006). KCNE2 is colocalized with KCNQ1 and KCNE1 in cardiac myocytes and may function as a negative modulator of I_{Ks} current amplitude in the heart. Heart Rhythm *3*, 1469–1480.

Wuttke, T. V, Seebohm, G., Bail, S., Maljevic, S., and Lerche, H. (2005). The new anticonvulsant retigabine favors voltage-dependent opening of the Kv7.2 (KCNQ2) channel by binding to its activation gate. Molecular Pharmacology. *67*, 1009–1017.

Xie, W., Wang, H., Wang, H., and Hu, G. (2004). Effects of iptakalim hydrochloride, a novel K_{ATP} channel opener, on pulmonary vascular remodeling in hypoxic rats. Life Sciences. *75*, 2065–2076.

Xiong, Q., Sun, H., and Li, M. (2007). Zinc pyrithione-mediated activation of voltage-gated KCNQ potassium channels rescues epileptogenic mutants. Nature Chemical Biology *3*, 287–296.

Xiong, Q., Sun, H., Zhang, Y., and Nan, F. (2008a). Combinatorial augmentation of voltage-gated KCNQ potassium channels by chemical openers. Proceedings of The *105*, 3128–3133.

Xiong, Q., Gao, Z., Wang, W., and Li, M. (2008b). Activation of K_V7 (KCNQ) voltage-gated potassium channels by synthetic compounds. Trends in Pharmacological Sciences *29*, 99–107.

Yamada, Y., Chen, X., Kobayashi, T., Kamada, Y., Nagashima, M., Tsutsuura, M., Seki, S., Yamakage, M., Namiki, A., and Tohse, N. (2002). A truncated splice variant of KCNQ1 cloned from rat heart. Biochemical and Biophysical Research Communications *294*, 199–204.

Yamaguchi, T., Rodman, D., O'Brien, R., and McMurtry, I. (1989). Modulation of pulmonary artery contraction by endothelium-derived relaxing factor. European Journal of Pharmacology. *161*, 259–262.

Yanagisawa, M., Kurihara, H., Kimura, S., Tomobe, Y., Kobayashi, M., Mitsui, Y., Yazaki, Y., Goto, K., and Masaki, T. (1988). A novel potent vasoconstrictor peptide produced by vascular endothelial cells. Nature *332*, 411–415.

Yang, I.C., Scherz, M.W., Bahinski, A., Bennett, P.B., and Murray, K.T. (2000). Stereoselective interactions of the enantiomers of chromanol 293B with human voltage-gated potassium channels. The Journal of Pharmacology and Experimental Therapeutics *294*, 955–962.

Yang, W.P., Levesque, P.C., Little, W.A., Conder, M.L., Shalaby, F.Y., and Blanar, M.A. (1997). K_VLQT1, a voltage-gated potassium channel responsible for human cardiac arrhythmias. Proceedings of the National Academy of Sciences of the United States of America *94*, 4017–4021.

Yang, W.P., Levesque, P.C., Little, W.A., Conder, M.L., Ramakrishnan, P., Neubauer, M.G., and Blanar, M.A. (1998). Functional expression of two K_VLQT1-related potassium channels responsible for an inherited idiopathic epilepsy. The Journal of Biological Chemistry *273*, 19419–19423.

Ye, C.L., and Rabinovitch, M. (1991). Inhibition of elastolysis by SC-37698 reduces development and progression of monocrotaline pulmonary hypertension. The American Journal of Physiology *261*, H1255–67.

Yeung, S.Y.M., and Greenwood, I.A. (2005). Electrophysiological and functional effects of the KCNQ channel blocker XE991 on murine portal vein smooth muscle cells. British Journal of Pharmacology *146*, 585–595.

Yeung, S.Y.M., Pucovský, V., Moffatt, J.D., L, Saldanha, L., Schwake, M., Ohya, S., and Greenwood, I.A. (2007). Molecular expression and pharmacological identification of a role for K_V7 channels in murine vascular reactivity. British Journal of Pharmacology *151*, 758–770.

Yeung, S.Y.M., Lange, W., Schwake, M., and Greenwood, I.A. (2008). Expression profile and characterisation of a truncated KCNQ5 splice variant. Biochemical and Biophysical Research Communications *371*, 741–746.

Yu, H., Lin, Z., Xu, K., Huang, X., Long, S., Wu, M., McManus, O.B., Le Engers, J., Mattmann, M.E., Engers, D.W., Le, U.M., Lindsley, C.W., Hopkins, C.R., Li, M. (2013). Identification of a novel, small molecule activator of KCNQ1 channels. Probe Reports from the NIH Molecular Libraries Program.

Yu, J., Taylor, L., Wilson, J., Comhair, S., Erzurum, S., and Polgar, P. (2013). Altered expression and signal transduction of endothelin-1 receptors in heritable and idiopathic pulmonary arterial hypertension. Journal of Cellular Physiology *228*, 322–329.

Yu H, Wu M, Hopkins C, Engers J, Townsend S, Lindsley C, McManus OB, L.M. (2013). A small molecule activator of KCNQ2 and KCNQ4 channels. Probe Reports from the NIH Molecular Libraries Program.

Yu, H., Zou, B., Wu, M., McManus, O.B., Le Engers, J., Cheung, Y.Y., Salovich, J.M., Hopkins, C.R., Lindsley, C.W., Li, M. (2013). Identification of a novel, small molecule inhibitor of KCNQ2 channels. Probe Reports from the NIH Molecular Libraries Program [Internet].

Yuan, X.J. (1995). Voltage-gated K^+ currents regulate resting membrane potential and $[Ca^{2+}]i$ in pulmonary arterial myocytes. Circulation Research *77*, 370–378.

Yuan, J.X., Aldinger, A.M., Juhaszova, M., Wang, J., Conte, J. V, Gaine, S.P., Orens, J.B., and Rubin, L.J. (1998a). Dysfunctional voltage-gated K^+ channels in pulmonary artery smooth muscle cells of patients with primary pulmonary hypertension. Circulation *98*, 1400–1406.

Yuan, X.J., Tod, M.L., Rubin, L.J., and Blaustein, M.P. (1990). Contrasting effects of hypoxia on tension in rat pulmonary and mesenteric arteries. The American Journal of Physiology *259*, H281–9.

Yuan, X.J., Goldman, W.F., Tod, M.L., Rubin, L.J., and Blaustein, M.P. (1993a). Hypoxia reduces potassium currents in cultured rat pulmonary but not mesenteric arterial myocytes. The American Journal of Physiology *264*, L116–23.

Yuan, X.J., Goldman, W.F., Tod, M.L., Rubin, L.J., and Blaustein, M.P. (1993b). Ionic currents in rat pulmonary and mesenteric arterial myocytes in primary culture and subculture. The American Journal of Physiology *264*, L107–15.

Yuan, X.J., Wang, J., Juhaszova, M., Golovina, V.A., and Rubin, L.J. (1998b). Molecular basis and function of voltage-gated K^+ channels in pulmonary arterial smooth muscle cells. The American Journal of Physiology *274*, L621–35.

Yuan, X.J., Wang, J., Juhaszova, M., Gaine, S., and Rubin, L. (1998c). Attenuated K channel gene transcription in primary pulmonary hypertension. The Lancet *351*, 726–727.

Zaczek, R., Chorvat, R.J., Brown, B.S. (1997) Linopirdine: Pharmacology of a neurotransmitter release enhancer. CNS Drug reviews 3 pp 103-119

Zaczek, R., Chorvat, R.J., Saye, J.A., Pierdomenico, M.E., Maciag, C.M., Logue, A.R., Fisher, B.N., Rominger, D.H., and Earl, R.A. (1998). Two new potent neurotransmitter release enhancers, 10,10-bis(4-pyridinylmethyl)-9(10H)-anthracenone and 10,10-bis(2-fluoro-4-pyridinylmethyl)-9(10H)-anthracenone: comparison to linopirdine. Journal of Pharmacology and Experimental Therapeutics. *285*, 724–730.

Zamora, M.A., Dempsey, E.C., Walchak, S.J., and Stelzner, T.J. (1993). BQ123, an ET_A receptor antagonist, inhibits endothelin-1-mediated proliferation of human pulmonary artery smooth muscle cells. American Journal of Respiratory Cell and Molecular Biology *9*, 429–433.

Zanellato, A.M., Borrione, A.C., Giuriato, L., Tonello, M., Scannapieco, G., Pauletto, P., and Sartore, S. (1990). Myosin isoforms and cell heterogeneity in vascular smooth muscle. I. Developing and adult bovine aorta. Developmental Biology *141*, 431–446.

Zhang, S., Yuan, J.X.-J., Barrett, K.E., and Dong, H. (2005). Role of Na^+/Ca^{2+} exchange in regulating cytosolic Ca^{2+} in cultured human pulmonary artery smooth muscle cells. American Journal of Physiology. Cell Physiology *288*, C245–52.

Zhang, S., Dong, H., Rubin, L.J., and Yuan, J.X.-J. (2007). Upregulation of Na^+/Ca^{2+} exchanger contributes to the enhanced Ca^{2+} entry in pulmonary artery smooth muscle cells from patients with idiopathic pulmonary arterial hypertension. American Journal of Physiology-Cell Physiology *292*, C2297–305.

Zhong, X.Z., Harhun, M.I., Olesen, S.P., Ohya, S., Moffatt, J.D., Cole, W.C., and Greenwood, I.A. (2010). Participation of KCNQ (K_V7) potassium channels in myogenic control of cerebral arterial diameter. The Journal of Physiology *588*, 3277–3293.

Zhu, Y., Zhang, S., Xie, W., Li, Q., Zhou, Y., and Wang, H. (2008). Iptakalim inhibited endothelin-1-induced proliferation of human pulmonary arterial smooth muscle cells through the activation of K_{ATP} channel. Vascular Pharmacology *48*, 92–99.